PhD in Biochemistry
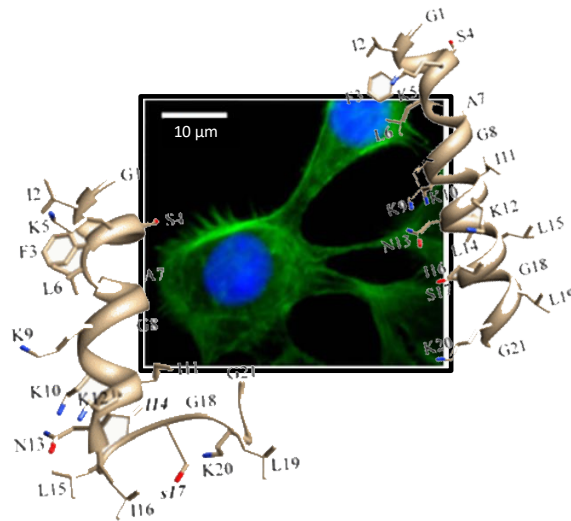
XXX Cycle (2014/2017)

Effects of two L- to D-amino acid substitutions on the structural and functional properties of the antimicrobial peptide esculentin-1a(1-21)

PhD student

Floriana Cappiello

Tutor

Prof. Maria Luisa Mangoni

Coordinator

Prof. Francesco Malatesta

Index

v

List of papers relevant for this thesis

- Loffredo MR, Ghosh A, Harmouche N, Casciaro B, Luca V, Bortolotti A, **Cappiello F**, Stella L, Bhunia A, Bechinger B, Mangoni ML. "Membrane perturbing activities and structural properties of the frog-skin derived peptide Esculentin-1a(1-21)NH$_2$ and its Diastereomer Esc(1-21)-1c: Correlation with their antipseudomonal and cytotoxic activity." *Biochim Biophys Acta.* 2017 Sep 12; 1859(12):2327-2339.

- **Cappiello F**, Di Grazia A, Segev-Zarko LA, Scali S, Ferrera L, Galietta L, Pini A, Shai Y, Di YP, Mangoni ML. "Esculentin-1a-derived peptides promote clearance of *Pseudomonas aeruginosa* internalized in bronchial cells of Cystic Fibrosis patients and lung cell migration: biochemical properties and a plausible mode of action." *Antimicrob Agents Chemother.* 2016 Nov 21; 60(12):7252-7262.

- Di Grazia A, **Cappiello F**, Cohen H, Casciaro B, Luca V, Pini A, Di YP, Shai Y, Mangoni ML. "D-Amino acids incorporation in the frog skin-derived peptide esculentin-1a(1-21)NH$_2$ is beneficial for its multiple functions." *Amino Acids.* 2015 Dec; 47(12):2505-19.

- Di Grazia A, **Cappiello F**, Imanishi A, Mastrofrancesco A, Picardo M, Paus R, Mangoni ML. "The Frog Skin-Derived Antimicrobial Peptide Esculentin-1a(1-21)NH$_2$ Promotes the Migration of Human HaCaT Keratinocytes in an EGF Receptor-Dependent Manner: A Novel Promoter of Human Skin Wound Healing?" *PLoS One.* 2015 Jun 12;10(6):e0128663.

List of other papers

- **Cappiello F**, Casciaro B, Mangoni ML. "A novel *in vitro* wound healing assay to evaluate cell migration." *J. Vis. Exp.* 2018; *in press.*

- Casciaro B, **Cappiello F**, Cacciafesta M, Mangoni ML. "Promising Approaches to Optimize the Biological Properties of the Antimicrobial Peptide Esculentin-1a(1-21)NH$_2$: Amino Acids Substitution and Conjugation to Nanoparticles." *Front Chem.* 2017 Apr 25; 5:26.

- Biondi B, Casciaro B, Di Grazia A, **Cappiello F**, Luca V, Crisma M, Mangoni ML. "Effects of Aib residues insertion on the structural-functional properties of the frog skin derived peptide Esculentin-1a(1-21)-NH$_2$." *Amino Acids.* 2017 Jan; 49(1):139-150.

- **Cappiello F**, Casciaro B, Kolar SS, Baidouri H, McDermott AM, Mangoni ML. "Methods for *In Vitro* Analysis of Antimicrobial Activity and Toxicity of Anti-keratitis Peptides: Bacterial Viability in Tears, MTT, and TNF-α Release Assays." *Methods Mol Biol.* 2017; 1548:395-409.

- Mangoni ML, Grazia AD, **Cappiello F**, Casciaro B, Luca V. "Naturally Occurring Peptides from *Rana temporaria*: Antimicrobial Properties and More." *Curr Top Med Chem.* 2016; 16(1):54-64.

Abstract

During the last years, the excessive and improper use of commercially available antibiotics has contributed to the development of resistant microbial pathogens, which represent a serious problem for the world public health. Among these microorganisms, the Gram-negative bacterium *Pseudomonas aeruginosa* is one of the most difficult to eradicate due to its ability to form sessile communities, named biofilms, which cause chronic infections, especially in the lungs of cystic fibrosis (CF) patients.

Naturally occurring antimicrobial peptides (AMPs), characterized by a different mechanism of action, represent a promising alternative to the commonly used drugs. AMPs are evolutionally conserved molecules produced by almost all living organisms as a first line of immune defense and amphibian skin is one of the richest sources.

The studies carried out in this thesis focused on two peptides:

Esculentin-1a(1-21)NH_2, [Esc(1-21) GIFSKLAGKKIKNLLISGLKG-NH_2], derived from the N-terminal region of the frog skin AMP esculentin-1a, and its diastereomer, Esc(1-21)-1c, containing two D-amino acids at positions 14 and 17 (i.e., D-Leu and D-Ser, respectively). This latter was designed with the purpose to reduce the peptide's cytotoxicity and to increase its stability to proteolytic enzymes.

The results achieved in this thesis have indicated that compared to Esc(1-21), the diastereomer is: i) significantly less toxic towards mammalian cells, in agreement with its lower α-helical structure, as determined by circular dichroism spectroscopy and nuclear magnetic resonance studies; ii) more effective against the biofilm form of *P. aeruginosa* (either reference or clinical isolates from CF patients) while maintaining high activity against the

3

free-living form of this pathogen; iii) more effective in killing *Pseudomonas* cells once internalized into bronchial cells expressing either the functional or the ΔF508 mutant of the CF transmembrane conductance regulator; iv) more resistant to bacterial and human elastases, which are abundant in CF lungs. In addition, the diastereomer was found (i) to have a higher activity than the all-L peptide in promoting migration of bronchial epithelial cells and presumably in favoring re-epithelialization of damaged lung tissue; (ii) to disaggregate and detoxify the bacterial lipopolysaccharide (LPS) and to inhibit cyclooxygenase-2 (COX-2) synthesis, albeit less than the wild-type peptide. Based on its interesting biological properties, Esc(1-21)-1c is a promising candidate for the development of a new drug that not only eliminates microbial pathogens, but also restores the integrity of a damaged tissue, such as the lung of CF patients, following *Pseudomonas* respiratory infections.

Abbreviations

AMP	Antimicrobial peptide
BrdU	Bromodeoxyuridine
CD	Circular dichroism
CF	Cystic Fibrosis
CFTR	Cystic Fibrosis Transmembrane Conductance Regulator
CFU	Colony-forming units
COX-2	Cyclooxygenase-2
CxF	Carboxyfluorescein
DMEMg	Dulbecco's modified Eagle's medium supplemented with 2 mM glutamine
DPC	Dodecylphosphocholine
EGFR	Epidermal Growth Factor Receptor
FBS	Fetal Bovine Serum
LB	Luria-Bertani broth
LPS	Lipopolysaccharide
MEMg	Minimum Essential Medium supplemented with 2 mM glutamine
MMP	Matrix metalloproteinase
MTT	3(4,5-Dimethylthiazol-2yl)2,5-diphenyltetrazolium bromide
NMR	Nuclear Magnetic Resonance
PBS	Phosphate buffered saline
POPC	1-palmitoyl-2-oleoyl-sn-glycero-3-phosphocholine
POPE	1-palmitoyl-2-oleoyl-sn-glycero-3-phosphoethanolamine
POPG	1-palmitoyl-2-oleoyl-sn-glycero-3-phosphoglycerol
RP-HPLC	Reversed-Phase High-Performance Liquid Chromatography
SDS	Sodium-dodecylsulfate
TNF-α	Tumor Necrosis Factor α

1. Introduction

1.1 Antibiotic resistance

An antibiotic is a natural or synthetic compound with antimicrobial activity, able to kill or block the growth of microorganisms. Antibiotics represent one of the most significant medical achievements of the twentieth century. In fact, the treatment of microbial infections with antibiotics has resulted in the reduction of human mortality, thus improving human health and increasing the life expectancy (WHO 2017; Nordqvist 2017).

However, since the discovery of antibiotics, over several decades, their excessive and indiscriminate use for clinical and veterinary purposes, has significantly contributed to the selection and spread of the so-called "superbugs", bacterial strains resistant to conventional antibiotics, e.g. β-lactams, aminoglycosides, tetracyclines and fluoroquinolones (WHO 2014; O'Neill 2016; Davies and Davies 2010; Livermore 2011; Schmieder and Edwards 2012). Nowadays, according to the latest World Health Organization reports, multidrug-resistant (MDR) bacterial infections are actually one of the most complex global health challenges, causing almost 50,000 deaths per year in Europe and in the US, a number expected to grow up to tenfold by 2050, killing more than cancer (O'Neill 2016) (Fig. 1).
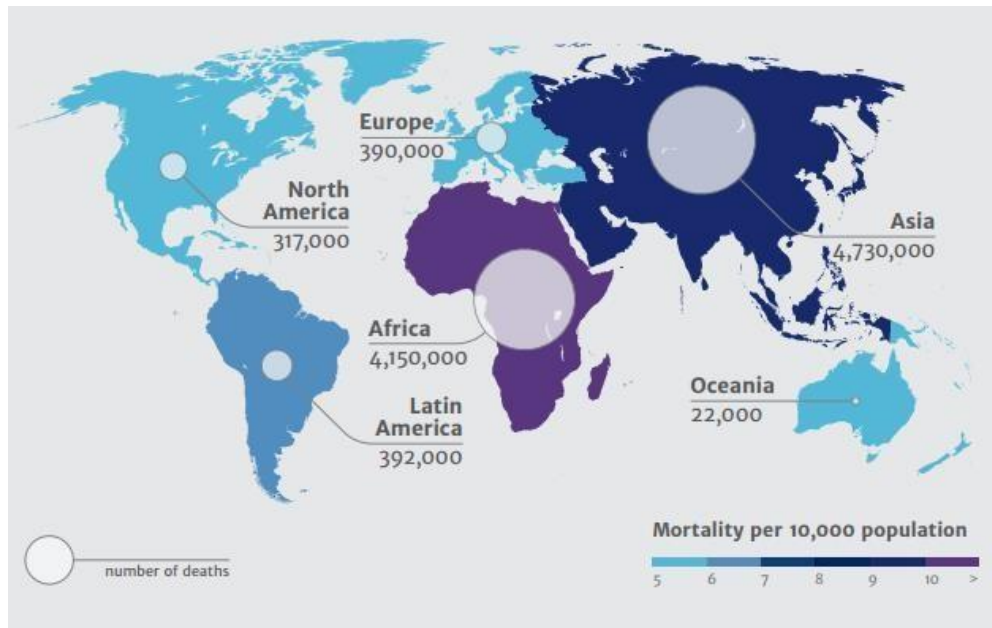
Fig. 1 Deaths attributable to antimicrobial resistance every year by 2050 (from O'Neill, 2014).

There are several mechanisms by which bacteria develop resistance to antibiotics. These mechanisms consist of biochemical modifications that alter bacterial cell properties that normally render the cell sensitive to drugs.

Antibiotic resistance can be classified into natural (intrinsic) and acquired resistance.

Intrinsic resistance refers to non-responsiveness to an antibiotic that has been acquired by the organism as a feature of its species. Each species is intrinsically resistant to a group of antibiotics. For example, Gram-negative bacteria are naturally resistant to vancomycin as it is unable to cross their outer membrane, while Gram-positive bacteria are resistant to β-lactam antibiotics (e.g. cephalosporins and penicillins), due to the production of β-lactamase or penicillin-binding proteins (PBP), enzymes involved in the

peptidoglycan synthesis of the bacterial cell wall, that have low affinity for penicillin binding (Chen et al. 2011).

Otherwise, the resistance may be acquired when deriving from mutations in existing genes (vertical evolution) or the acquisition of new genes (horizontal gene transfer) from other strains or microbial species by transferring of mobile genetic elements, such as phages, plasmids and transposons (Schmieder and Edwards 2012).

The main strategies by which bacteria counteract antibiotic activity include:

- diminished intracellular drug concentration by decreased cell permeability and increased efflux by both the cytoplasmic and the outer membrane
- drug inactivation for example by neutralization of the antimicrobial agent by enzymes (proteolytic cleavage)
- antibiotic modification by enzymes able of adding different chemical groups to antibiotics
- modification or complete elimination of the target by the creation of alternative metabolic pathways (Chen et al. 2011) (Fig. 2).
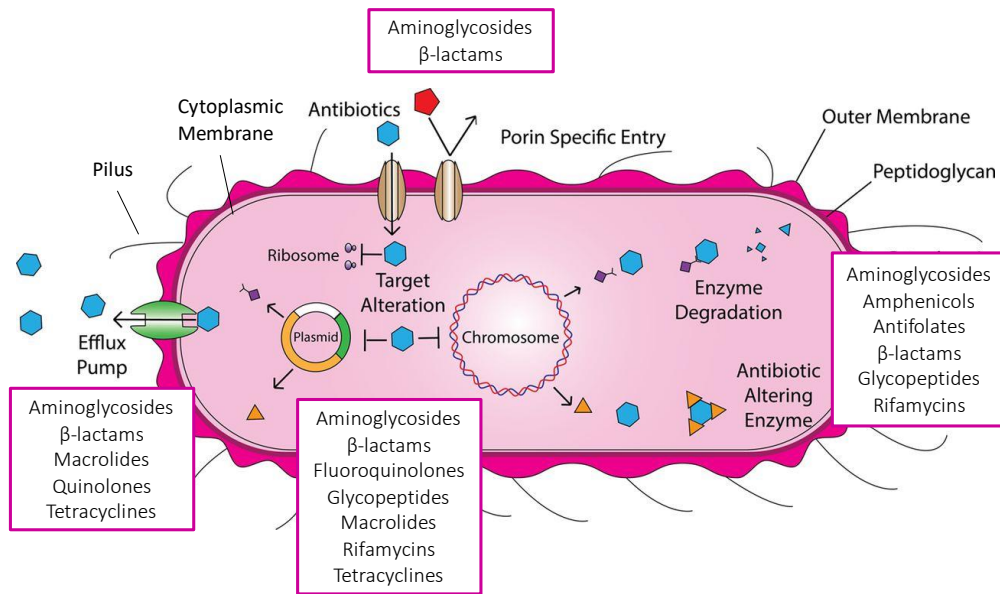
Fig. 2 Mechanisms of antibiotic resistance in bacteria. The classes of antibiotics affected by each of the mechanisms are listed in the boxes (modified by Mukerji et al. 2017 and Schmieder and Edwards 2012).

1.2 Antimicrobial peptides (AMPs) and innate immunity

The absence of antibiotics with new mechanisms of action that counteract the spread of MDR strains requires the development of new antimicrobial strategies. For this reason, especially in the last two decades, antimicrobial peptides (AMPs) have received the attention of the international scientific community, representing new possible compounds to be used for antimicrobial therapy (Mangoni 2011; Alba et al. 2012; Fjell et al. 2011).

AMPs, also called "host defense peptides" (HDP), are evolutionally conserved molecules widely distributed in almost all living species, including bacteria, fungi, insects, plants, amphibians as well as higher eukaryotes such as mammals (Ageitos et al. 2016).

A significant growth of AMP research started in the 1980s due to the discoveries of insect cecropins by Hans Boman, human α-defensins by Robert Lehrer and magainins by Michael Zasloff (Wang et al. 2016a).

According to the Antimicrobial Peptide Database (APD) (http://aps.unmc.edu/AP/main.php), the isolated and characterized AMPs so far are more than 2900.

AMPs have a protective function as a first line of immune defense against a wide range of infectious agents, such as Gram-positive and Gram-negative bacteria, viruses, fungi and some parasites, before the adaptive immune system is activated. While the innate immune system, which is present in all organisms, is rapid and does not change during repeated infections, the adaptive immune system, that evolved most recently in vertebrates, is highly specific for pathogens.

Specifically, in order to prevent colonization of host tissues by pathogens, AMPs are mainly secreted by tissues that form a barrier against the external environment, such as skin and mucous membranes. They are also stored in granules within the phagocytes, where they participate in the killing of phagocytized microorganisms (Boman 1991; Hancock and Diamond 2000; Zasloff 2002; Mangoni et al. 2016). AMPs can be produced constitutively or induced by microbial molecules and cytokines that trigger a signaling transduction cascade leading to the activation of NF-kB-controlled genes, including those encoding for AMPs (Thaiss et al. 2016).

Besides their antimicrobial activity, AMPs from higher eukaryotes have been found to have additional biological properties that are involved in the modulation of the host immune system: stimulation of chemotaxis (Mookherjee and Hancock 2007), suppression of proinflammatory cytokine

release (Afacan et al. 2012), immune cell differentiation (Davidson et al. 2004), promotion of angiogenesis and wound healing (Wu et al. 2010) (Fig. 3).
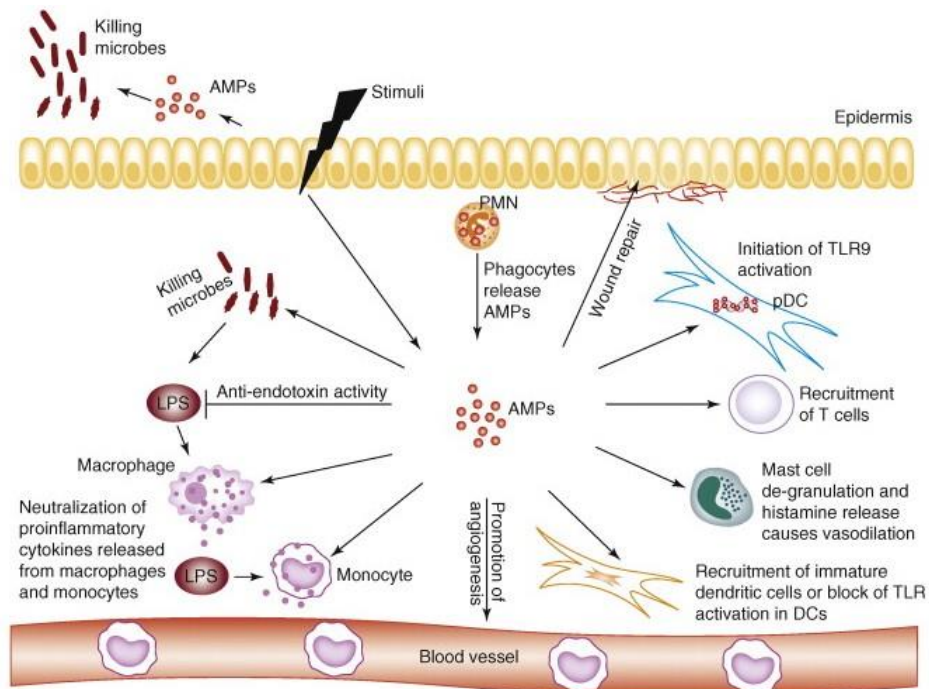
Fig. 3 Multiple functions of antimicrobial peptides in host defense.
Abbreviations: AMP, antimicrobial peptide; DC, dendritic cell; LPS, lipopolysaccharide; pDC, plasmacytoid dendritic cell; PMN, polymorphonucleocyte; TLR, Toll-like receptor (from Lai and Gallo 2009).

Innate immunity is activated when signal molecules, such as those of bacterial cells (e.g. lipopolysaccharide, LPS), are recognized by pattern recognition receptors (PRRs), including Toll-like receptors (TLRs), mainly expressed by mononuclear cells and macrophages. Following the interaction between LPS micelles (the biologically active form of the endotoxin) and the LPS-binding protein (LBP), the LPS–LBP complex interacts with the CD14, the primary receptor of LPS, and together they bind and activate the TLR4-

mediated intracellular signalling pathway, which activates the NF-kB transcription factor. This results in the production and secretion of pro-inflammatory cytokines (e.g., "tumor necrosis factor α", TNF-α). Some peptides can bind and disaggregate LPS micelles to smaller size particles, thus preventing the production of TNF-α (Fig. 4). If TNF-α is produced in high amounts because of a prolonged activation of the immune system, it can lead to a systemic inflammatory syndrome or sepsis, which, in extreme cases, leads to death (Hancock and Sahl 2006; Mangoni and Shai 2011; D'Este et al. 2012).
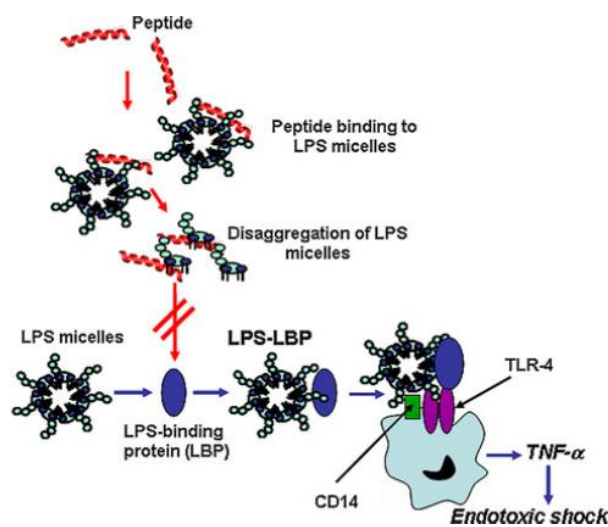
Fig. 4 Schematic representation of the LPS-neutralizing activity of AMPs (from Mangoni and Shai 2011).

1.3 AMPs: general features and classification

AMPs generally contain less than 100 amino acids (Ganz 2003). Unlike conventional antibiotics, synthesized by microorganisms through several steps, each one catalyzed by a different enzyme (Boman 1995), AMPs are encoded by genes and ribosomally synthesized as pre-propeptides of 60-170

amino acids, consisting of an N-terminal signal for endoplasmic reticulum, an anionic pro-segment and a C-terminal cationic peptide that acquires antimicrobial activity after its cleavage from the rest of the molecule by different kind of proteases (Bals 2000). Cationicity is an important feature for electrostatic interaction of AMPs with negatively charged membrane phospholipids of bacterial cells or other microorganisms (Yeaman and Yount 2003).

Pre-propeptides typically undergo some post-translational modifications, such as glycosylation, C-terminal amidation (a very common modification in linear AMPs from frog skin) (Mangoni et al. 2006; Nicolas and El Amri 2009), aminoacidic isomerization, halogenation, cyclization, N-terminal acetylation and hydroxylation, that modify their activity (Zasloff 2002; Wang 2012).

AMPs typically have a positive charge, at neutral pH, from +2 to +9 due to the presence of Lys and/or Arg residues, and a substantial portion ($\geq 30\%$) of hydrophobic residues that confers to the AMPs an amphipathic character (Zasloff 2002; Rinaldi 2002; Hancock and Sahl 2006). Following interaction with hydrophobic environments such as biological or artificial membranes, they often fold into amphipathic conformations (Powers and Hancock 2003).

According to their secondary structure, AMPs are generally classified into four families: peptides with α-helices, β-sheets, non-α- or β-structures (extended) and with a hairpin-loop structure (Fig. 5) (Mojsoska and Jenssen 2015).

- α-helical peptides (Fig. 5A) are often unstructured in aqueous solution, but they adopt an amphipathic helical structure in contact with biological

14

membranes (Yeaman and Yount 2003). Among them, some peptides are well known: the human cathelicidin LL-37, the frog skin magainins and the insects cecropins (Boman 1995; Zanetti et al. 2002; Mahlapuu et al. 2016; Huang et al. 2010).

- Peptides consisting of mixed structure made of β-sheets, connected by one or more intramolecular disulfide bridges (Fig. 5B), include defensins which are produced in neutrophils, macrophages and epithelial cells (Lai and Gallo 2009) and protegrins, first discovered in porcine leukocytes (Taylor et al. 2008). Due to their rigid structure, the β-sheet peptides are more ordered in aqueous solution and do not drastically change conformation as helical peptides upon membrane interaction (Yeaman and Yount 2003).

- Extended/random-coil linear peptides (Fig. 5C) often contain a high content of arginine, proline, tryptophan, and/or histidine residues. They fold into amphipathic structures after contact with a membrane (Takahashi et al. 2010; Nguyen et al. 2011). The best studied peptides in this group are indolicidin, produced by bovine leukocytes (Powers and Hancock 2003), and bactenecins.

- Peptides exhibiting a hairpin-loop structure (Fig. 5D) interconnected by at least one disulfide bridge include thanatin (Ma et al. 2016).
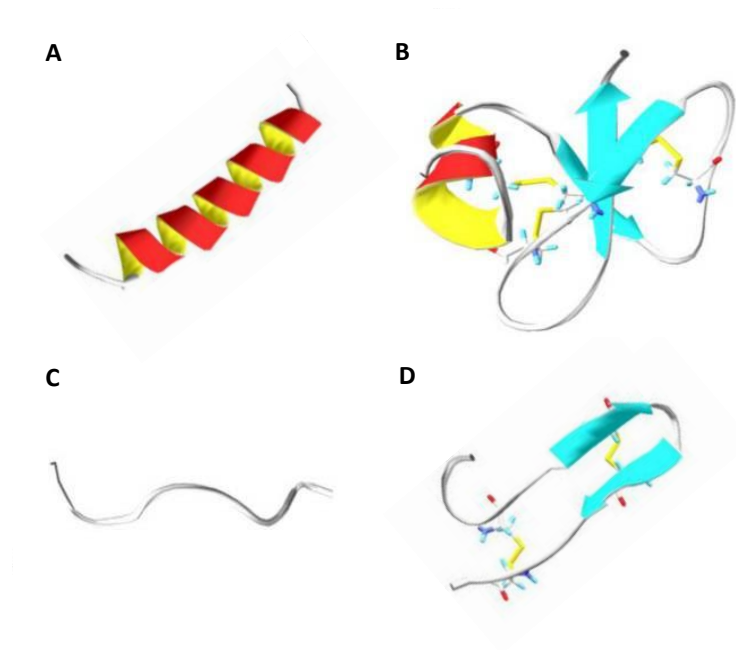
Fig. 5 Representative secondary structures of AMPs (modified by Mojsoska and Jenssen 2015).

1.4 AMPs: mechanism of action

Based on their mechanism of microbicidal activity, AMPs can be divided into two classes: membranolytic peptides and non-membrane active peptides.

Most AMPs are cationic molecules that adopt an amphipathic α-helical structure in membrane environments (Powers and Hancock 2003; Jenssen et al. 2006). Cationicity and amphipathicity are the two crucial chemical-physical factors, especially for the mechanism of action of α-helical AMPs, which is generally based on the perturbation of the target microbial membrane (Bechinger and Gorr 2017).

Before reaching the microbial membrane, the first event that occurs is the electrostatic interaction of the positively charged AMPs with the negatively

charged components of the microbial cell surface, such as the lipopolysaccharides (LPS), in the outer membrane of Gram-negative bacteria, or acidic polysaccharides (teichoic and teichuronic acids), in the peptidoglycan layer of Gram-positive bacteria (Brogden 2005) (Fig. 6).
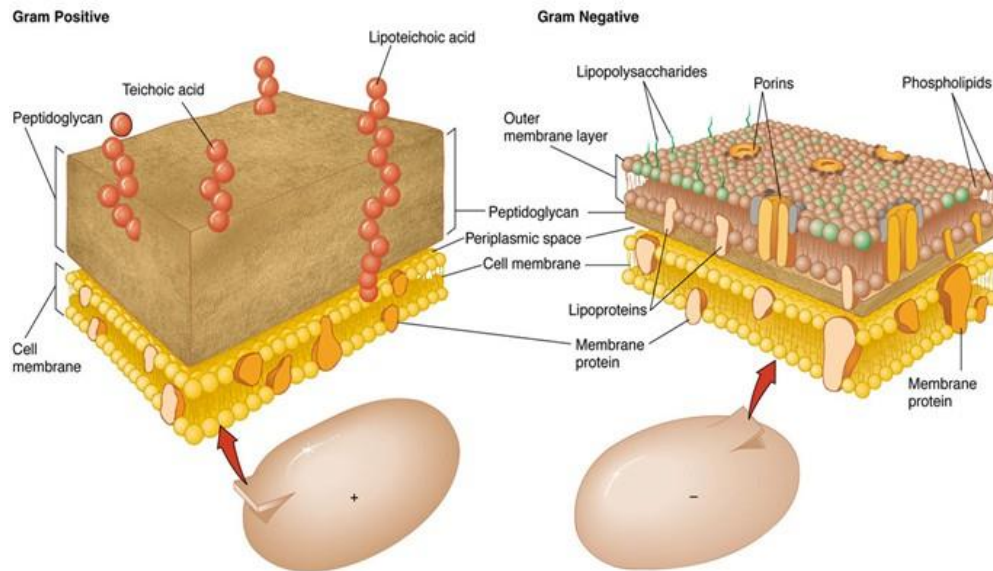
Fig. 6 Schematic representation of the cell wall of Gram-positive and Gram-negative bacteria.

The passage of AMPs through the outer membrane of Gram-negative bacteria occurs by a mechanism called "self-promoted uptake pathway" (Fig. 7). The cationic peptides interact with the binding sites of the bivalent ions Ca^{2+} and Mg^{2+} on the surface of the LPS and move them from their position. This results in the outer membrane damage and access of the peptides to the periplasmic space (Hancock 1997; Zasloff 2002).
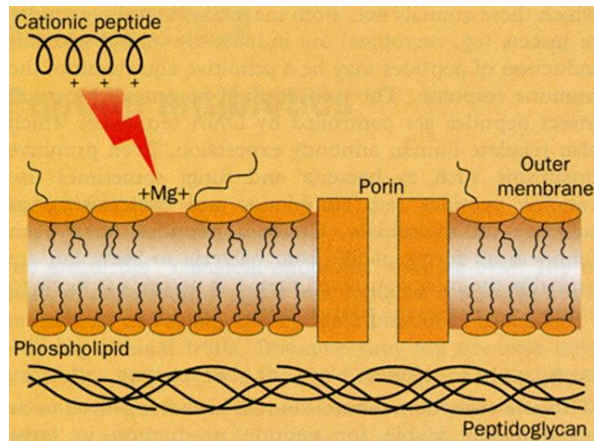
Fig. 7 Self-promoted uptake of cationic peptides across outer membranes of Gram-negative bacteria (from Hancock 1997).

Once reached the periplasmic space, AMPs target the plasma membrane. Peptide-membrane interaction is the most important step controlling the selectivity of AMPs toward microbial membranes, which are much richer in anionic phospholipids, such as phosphatidylglycerol, cardiolipin, and the electrically-neutral (zwitterionic) phosphatidylethanolamine, compared to those of mammalian cells mainly made of zwitterionic lipids, such as phosphatidylcholine, sphingomyelin and cholesterol (Lohner 2009) (Fig. 8).
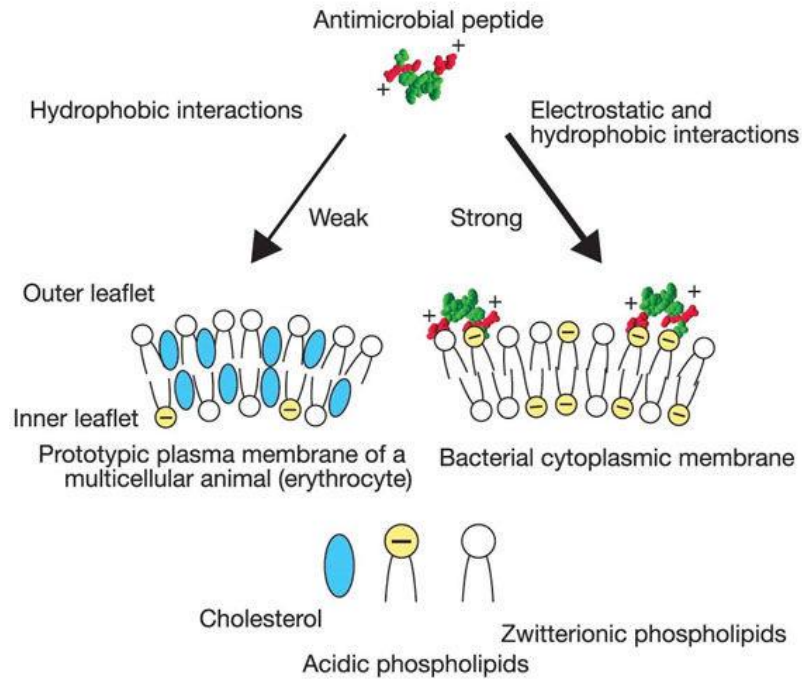
Fig. 8 Molecular basis of cell selectivity of AMPs. AMPs form amphipathic structures with a positively charged face (red) and a hydrophobic face (green). Electrostatic interaction between the positive charges of AMPs and negatively charged components (yellow) at the eukaryotic cell surface (left) and bacterial surface (right) is the major driving force for cellular association (from Zasloff 2002).

In addition, the transmembrane potential of bacteria, ranging from -130 to -150 mV, contributes to the increasing attraction of positively charged peptides and to their insertion into the membrane or their translocation in the cytoplasm, unlike mammalian cells which exhibit a difference in membrane potential between -90 and -110 mV (Powers and Hancock 2003; Yeaman and Yount 2003).

Nevertheless, different studies revealed that not only peptide charge and amphipathicity are essential factors for antimicrobial activity and mechanism

of action of AMPs, but also several other features such as the size, the primary structure, the conformation and the hydrophobicity of the peptide (Guilhelmelli et al. 2013).

Moreover, the peptides ability to traverse the lipid bilayer can be influenced by the concentration of the peptide itself, its tendency to self-assemble or to oligomerize, the phospholipid composition and the fluidity of the target membrane.

The permeabilization of the membrane is a fundamental step in the microbicidal activity of AMPs. Several models that explain membrane disruption by AMPs have been proposed:

- **Barrel-stave model** (Ehrenstein and Lecar 1977)

AMPs are inserted perpendicularly to the plane of the membrane bilayer forming a pore like a stave (Fig. 9). The hydrophobic surfaces of the helices interact with the fatty acid chains of the membrane phospholipids, while the hydrophilic surfaces point inward, producing a transmembrane pore. The recruitment of additional peptide monomers, before the insertion of AMPs in the membrane, leads to an increase of the pore size (Shai 1999). In this model, the membrane does not display significant curvature and the hydration of the membrane remains unchanged (Li et al. 2017). As few as three molecules are needed to form a transmembrane pore.

- **Toroidal pore model** (Ludtke et al. 1996; Matsuzaki et al. 1996)

Unlike the "barrel-stave" model, transmembrane pores are delimited by peptide molecules intercalated to membrane lipids. The peptides are always in contact with the polar heads of the membrane phospholipids, even when they are perpendicularly inserted into the lipid bilayer (Brogden 2005) (Fig.

20

9). The polar faces of the peptides associate with the polar head groups of the lipids. As the AMPs penetrate deeper into the membrane, the head groups of the lipids are dragged into the lipid tail region to form toroidal shaped pores while the lipid tails are packed away from the surface of the pore, resulting in significant lipid disorder and membrane curvature change. Toroidal pores are also accompanied by enhanced membrane hydration, as evidenced by significant water penetration into the membrane (Li et al. 2017). The pore is lined by both the peptides and the lipid head groups, which are likely to screen and mask cationic peptide charges.

- **Carpet-like model** (Shai 1999; Pouny et al. 1992)

Some AMPs, that not necessarily assume the amphipathic α-helix conformation, line parallel to the membrane surface via electrostatic interactions with the anionic heads of the membrane phospholipids. The peptide molecules cover the membrane surface in a "carpet"-like manner without being inserted into its hydrophobic core (Fig. 9). Afterwards, the peptides reorient themselves such that their hydrophobic face is toward the lipids and the hydrophilic face toward the phospholipid headgroups. When their surface concentrations reach a critical value, the AMPs cause a detergent-like solubilization of the lipid bilayer in micelles (Shai 2002).

- **Disordered toroidal pore model**

The pore formation is more stochastic and involves fewer peptides (Sengupta et al. 2008) (Fig. 9).

- **Membrane thinning/thickening affection model**

The thickness of the bilayer can be affected by the presence of the peptides or the membrane itself can be remodeled to form domains rich in anionic lipids surrounding the peptide (Grage et al. 2016) (Fig. 9).
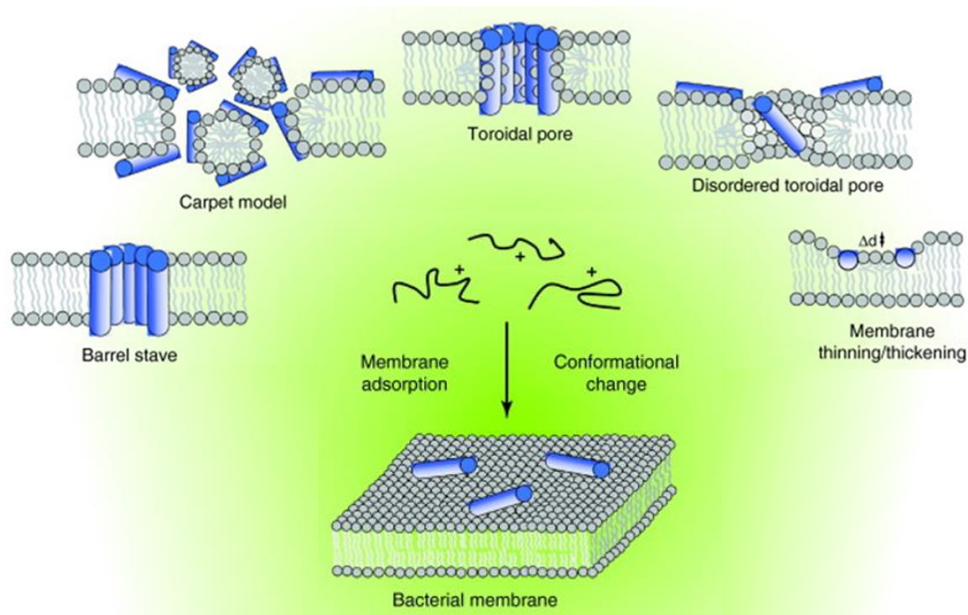
Fig. 9 Schematic representation of some mechanisms of action of membrane-active AMPs (modified by Nguyen et al. 2011).

Therefore, the main mechanism to kill bacteria, especially for peptides with an α-helical structure, is the permeabilization of the membrane without involving stereospecific interaction with chiral targets (such as receptors). These peptides are already active at very low concentrations, in the order of μM. Thanks to this general mechanism of action, based on the unspecific interaction of cationic AMPs with anionic phospholipids of microbial membranes, the emergence of microorganisms resistant to such molecules is very limited and significantly lower than that to the conventional antibiotics (Zasloff 2002; Kraus and Peschel 2006). In fact, the development of resistance to AMPs would lead to a drastic change in the lipid composition of an essential element of the cell, such as the cytoplasmic membrane, with a consequent serious damage to the microorganism survival.

22

However, recent studies demonstrate that there are non-membrane active antimicrobial peptides that can effectively cross the membrane barrier without disrupting it. These AMPs can exhibit their antimicrobial modes of action through the inhibition of intracellular processes, such as (i) synthesis of nucleic acids; (ii) synthesis of proteins, enzymatic activity or folding; (iii) synthesis of the cell wall or microbial septum formation (Yeung et al. 2011; Nguyen et al. 2011; Mojsoska and Jenssen 2015).

On the other hand, three mechanisms have been proposed to explain how AMPs activate mammalian cells (Lai and Gallo 2009) (Fig. 10):

- **Trans-activation model**

AMPs stimulate the release of a membrane-bound growth factor, which then binds to its high affinity receptor and activates it. It is the case of HB-EGF (heparin binding epidermal growth factor) and the EGF receptor (EGFR).

- **Alternate ligand model**

Some AMPs, such as defensins and cathelicidin, directly bind to a specific receptor, triggering the signaling pathway. This has been proposed for chemokine receptor 6 (CCR6) and formyl peptide receptor 1 (FPRL-1).

- **Membrane disruption model**

AMPs associate with and modify the membrane in a region containing the receptor, thus indirectly changing receptor function. In fact, the receptor may trigger the signaling cascade without a ligand or become insensitive to binding by its specific ligand. EGF receptors may be involved because of the disruption of ordered lipid domains, called lipid rafts, where these receptors

are located (Pike et al. 2005) and the consequent inhibition of ligands binding to EGFR and its activation.
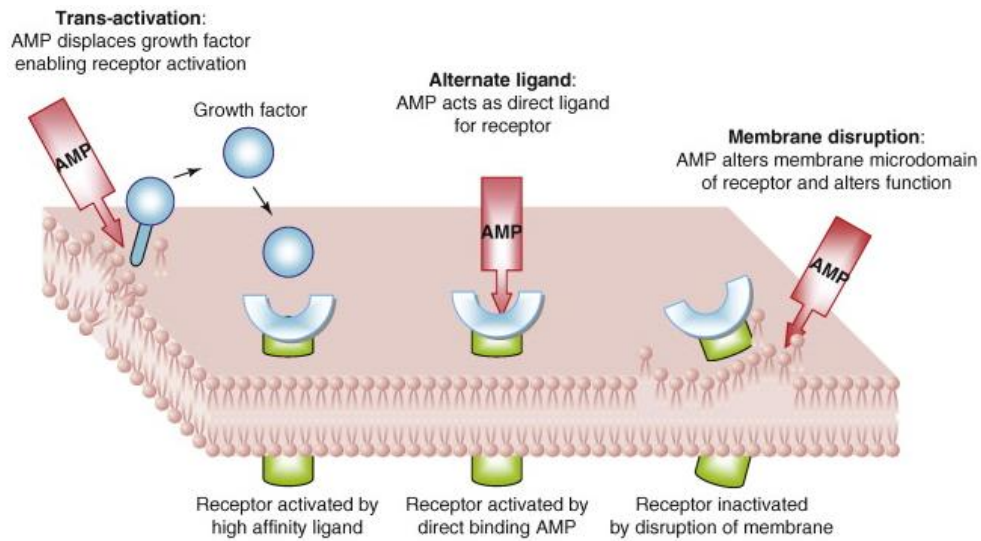
Fig. 10 Alternative models for host activation by antimicrobial peptides (from Lai and Gallo 2009).

1.5 Frog-skin antimicrobial peptides

The amphibia skin is among the richest sources of biologically active compounds, including biogenic amines, complex alkaloids and peptides, that play different roles, either in the regulation of physiological or defensive functions.

AMPs are stored in dermal serous glands, mainly located in the skin of the dorsal region of the animal, surrounded by myocytes and innervated by sympathetic fibers (Fig. 11). Adrenergic stimulation of myocytes, upon stress or physical injury, causes compression of the serous glands and discharge of their contents by a holocrine-like mechanism (Simmaco et al. 1998; Conlon et al. 2004).
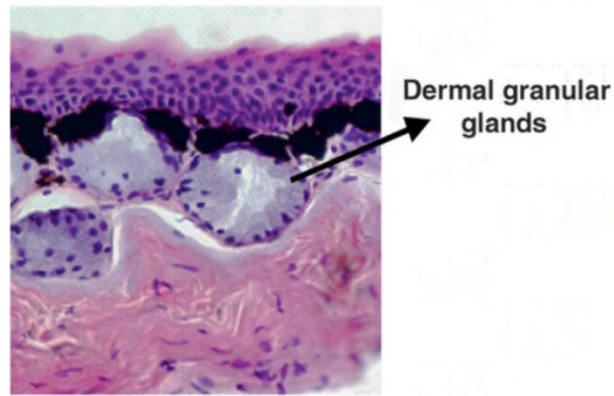
Fig. 11 Histological preparation of frog skin (from Mangoni 2006).

Each frog species synthesizes its own unique set of AMPs. On the basis of structural similarities, amphibian AMPs are grouped into different families, e.g. magainins, temporins, brevinines -1 and -2, ranalexins, ranacyclins, bombinins and esculentins-1 and -2 (Conlon 2004; Conlon et al. 2009; Mangoni et al. 2003; Morikawa et al. 1992) (Table 1). Since Zasloff isolated the magainins in the 1980s, many AMPs have been isolated and identified from different amphibian species belonging to the species *Xenopus laevis*, *Bombina variegata*, *Bombina orientalis*, *Phyllomedusa sauvagei* and different species of *Rana* (Ladram and Nicolas 2016).

Table 1 Primary structure of some frog-skin AMPs. C-terminal amidation is marked by -NH$_2$.

GENUS	PEPTIDE AND SEQUENCE
Xenopus	**Magainin-1** GIGKFLHSAGKFGKAFVGEIMKS
	Magainin-2 GIGKFLHSAKKFGKAFVGEIMNS
Bombina	**Bombinin** GIGALLSAAKVGLKGLAKGLAEHFAN-NH$_2$
	Bombinin H1 IIGPVLGMVGSALGGLLKKI-NH$_2$
Rana	**Temporin A** FLPLIGRVLSGIL-NH$_2$
	Brevinin-1 FLPVLAGIAAKVVPALFCKITKKC
	Brevinin-2 GLLDSLKGFAATAGKCVLQSLISTASCKLAKTC
	Ranalexin FLCCLIKIVPAMICAVTKKC
	Ranaciclin-T GALRGCWTKSYPPKPCK-NH$_2$
	Esculentin-1 GIFSKLGRKKIKNLLISGLKNVGKEVGMDVVRTGIDIAGCKIKGEC
	Esculentin-2a GILSLVKGVAKLAGKGLAKEGGKFGLELIACKIAKQC

26

1.6 Esculentins and Esc(1-21)

The esculentin-1 family was first isolated and purified from the skin secretion of the European frogs belonging to *Pelophylax lessonae/ridibundus* (previously known as *Rana esculenta*) (Conlon 2008) specimen (Fig. 12) by reverse phase high performance liquid chromatography (RP-HPLC) (Simmaco et al. 1993). All members of this family have a highly conserved amino acid sequence consisting of 46 residues and characterized by a C-terminal loop stabilized by a disulphide bridge forming a hepta peptide ring (Simmaco et al. 1994). They have a net charge of +5 at neutral pH and an amphipathic α-helical structure in membrane mimetic environments (Mangoni et al. 2015; Wang et al. 2016b).

Fig. 12 A specimen of *Pelophylax lessonae/ridibundus*.

Esculentins-1 have a broad spectrum of action against Gram-positive and Gram-negative bacteria, including *Pseudomonas aeruginosa*, and fungal species, such as *Candida albicans* (lethal concentrations ranging from 0.1 to 1.5 μM). They also show low toxicity on mammalian cells (Simmaco et al. 1993; Ponti et al. 1999; Mangoni et al. 2015).

Table 2 shows the amino acid sequences of some members of esculentins-1 family and their derivatives.

A fragment corresponding to the 19-46 portion of esculentins-1, named Esculentin-1a(19-46), was also isolated from skin secretions. It was devoid of antimicrobial activity, presumably due to its low net positive charge (+1 *versus* +5 of the whole molecule) at neutral pH (Simmaco et al. 1994).

Since no antimicrobial activity was detected for this fragment, the 1-18 portion of esculentins (which was not found in the HPLC fractionation of the secretion possibly because of its proteolytic degradation) was chemically synthesized and its antimicrobial activity was analyzed. The synthetic peptide, Esc(1-18), (Table 2) was amidated at the C-terminus to maintain a net charge of +5 at neutral pH and to increase its stability (Mangoni et al. 2003). It was found that the Esc(1-18) adopted an α-helical structure in lipid vesicles mimicking the anionic character of microbial membranes. Moreover, its antimicrobial activity resulted to be comparable to that of the full-length peptide (Mangoni et al. 2003) showing that this activity was in its N-terminal portion, and that the first 18 residues are required to maintain antimicrobial properties.

Since the minimum length for a peptide in α-helix conformation to span a phospholipid bilayer (~30 Å thick) is about 20 amino acids (Gamberi et al. 2007), a longer analog named esculentin-1a(1-21)NH$_2$, [Esc(1-21)], was further synthesized and characterized for its biological properties (Table 2).

Esc(1-21) has the same first 20 residues of the natural esculentin-1a followed by an amidated glycine (Islas-Rodrìguez et al. 2009). Differently from Esc(1-18), Esc(1-21) carries the substitution Leu-11-Ile and three additional C-terminal residues (Leu-Lys-Gly) which give it a higher net positive charge (+6) at neutral pH, an important feature for the electrostatic interaction with

28

the negatively charged membranes of microbial cells (Gellatly and Hancock 2013; Mangoni et al. 2015).

Esc(1-21) has a potent antimicrobial activity, mainly against Gram-negative bacteria, e.g. *P. aeruginosa* (Luca et al. 2013). In particular, Esc(1-21) showed the same efficacy against reference and clinical isolates of *P. aeruginosa* as indicated by the similar minimal peptide concentration which inhibits microbial growth (MIC) (4 μM) and the comparable bactericidal concentration causing 99.9% killing of these strains (0.5 μM or 1 μM) (Luca et al. 2013). Differently, Esc(1-21) showed a weaker activity against Gram-positive bacteria (Kolar et al. 2015) and a lower toxicity against human erythrocytes (Islas-Rodriguez et al. 2009; Luca et al. 2013).

Table 2 Primary structure of Esc-1a(1-21)NH_2 and Esc-1b(1-18)NH_2 and the corresponding full-length natural esculentin-1 peptides.

PEPTIDE DESIGNATION and SEQUENCE[a]	Net charge at neutral pH
Esculentin-1a GIFS**K**LAG**KKIK**NLLISGL**K**NVG**K**E VGM**D**VV**R**TGI**D**IAGC**K**I**K**G**E**C	**+5**
Esculentin-1a(19-46) L**K**NVG**K**E VGM**D**VV**R**TGI**D**IAGC**K**I**K**G**E**C	**+1**
Esculentin-1a(1-21)NH_2 GIFS**K**LAG**KKIK**NLLISGL**K**G-NH$_2$	**+6**
Esculentin-1b GIFS**K**LAG**KK**L**K**NLLISGL**K**NVG**K**E VGM**D**VVRTGI**D**IAGC**K**I**K**G**E**C	**+5**
Esculentin-1b(1-18)NH_2 GIFS**K**LAG**KK**L**K**NLLISG-NH$_2$	**+5**

[a] Basic and acidic amino acids are indicated by red and blue letters, respectively.

29

1.7 *Pseudomonas aeruginosa* **and cystic fibrosis**

P. aeruginosa is a ubiquitous and opportunistic Gram-negative bacterium that colonizes abiotic and biological surfaces, particularly moist environments. In fact, it thrives in soil and aquatic habitats, colonizes medical devices (e.g. catheters and implants) and the surfaces of plants, animals and humans (Klockgether and Tümmler 2017).

P. aeruginosa can cause a wide range of local or systemic infections in humans; in most cases, these are life-threatening infections, such as keratitis, otitis, pneumonia and skin (burn wounds) infections, primarily in immunocompromised and hospitalized patients (Gellatly and Hancock 2013; Wu et al. 2011).

This bacterium is intrinsically resistant to a wide range of antimicrobials, including β-lactams, aminoglycosides and fluoroquinolones, because of its low membrane permeability and multidrug efflux pumps (Smith et al. 2017). It is also equipped with a large repertoire of virulence factors and a complex regulatory network of intracellular and intercellular signals, that allow the bacteria to develop resistance to antimicrobial agents and to escape host defense. This is likely due to the selection of mutations in chromosomal genes or to the horizontal acquisition of resistant determinants (Morita et al. 2014; Ruiz-Garbajosa and Cantón 2017; Klockgether and Tümmler 2017; Rodrigo-Troyano and Sibila 2017).

P. aeruginosa can be found either as planktonic or sessile form (Fig. 13). The latter is called biofilm and corresponds to a bacterial community of cells which adheres to biological or inert surfaces embedded in a self-produced matrix of extracellular polymeric substances, including polysaccharides,

proteins, lipids and extracellular DNA. This confers bacteria a greater resistance to physical and chemical factors, including conventional antibiotics, and to immune cells, favoring colonization of nearby surfaces (Flemming et al. 2016).
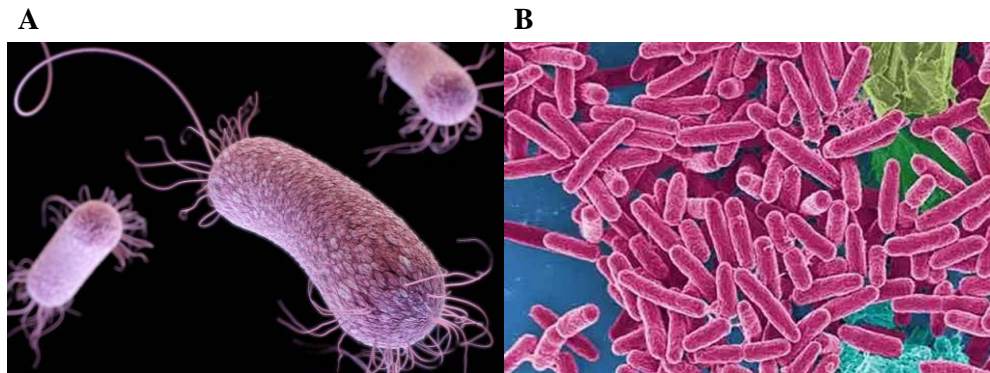
Fig. 13 Electron microscopy images of *P. aeruginosa* free-living cells (A) and biofilm (B).

One of the environments commonly colonized by *P. aeruginosa* is the respiratory tract of cystic fibrosis (CF) patients (Gaspar et al. 2013). CF is a genetic disorder that affects a wide range of populations (approximately 75,000 individuals worldwide) and involves several organs, including pancreas, liver, gastrointestinal tract, reproductive system, sweat glands and, particularly, the respiratory system. This disease is caused by mutations in the cystic fibrosis transmembrane conductance regulator (CFTR) gene on chromosome 7 that lead to malfunctioning chloride channels. A deletion of phenylalanine in the amino acid position 508 is the most common mutation, but more than 2000 mutations have been reported, although not all of these have functional consequences (Fajac and Wainwright 2017).

Specifically, the CFTR regulator acts as a channel that pumps chloride ions from the intracellular to the extracellular space through the apical membrane

31

of the epithelial cells. Chloride ion transport partially controls the movement of sodium ions and water into the cell and consequently influences the production of a thin and low viscous mucus layer in order to protect the lungs, sweeping bacteria trapped in mucus outside, and to ensure gas exchange (Kreda et al. 2012; Folkesson et al. 2012) (Fig. 14).

In CF sufferers, the dehydration of the mucus layer and its resulting thick and sticky consistency provides an environment for propagation of persistent bacterial biofilms, such as in the case of *P. aeruginosa* (Gaspar et al. 2013) (Fig. 14).

Chronic lung infections cause an influx of cellular infiltrates and inflammatory cells that stimulate pro-inflammatory cytokine release impairing lung function.
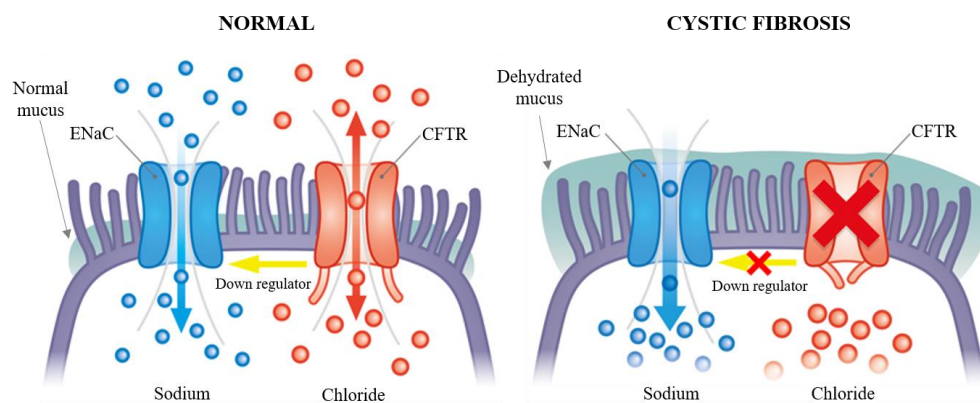
Fig. 14 Schematic representation of a functional (left panel) and non-functional CFTR (right panel). ENaC is the epithelial sodium channel.

1.8 Limitations of AMPs

Despite the great potential of AMPs to work as new effective anti-infective agents, they still have several limitations for the development as therapeutics (Kang et al. 2014):

- Toxicity against mammalian cells at therapeutic dosages

While the bacterial cell membrane contains negatively-charged lipids (20-25%), the human cell membrane possesses zwitterionic lipids and cholesterol (Dawson and Liu 2008). Usually, cationic AMPs use this difference for their selective antimicrobial activity by interacting with the negatively-charged bacterial membrane. However, several studies have shown that mammalian cells can also be the targets of these molecules. In fact, AMPs can directly bind to host cells and induce adverse effects (Zheng et al. 2010; de Sa et al. 2010). Furthermore, the administration of broad-spectrum AMPs can eliminate the host microflora in humans, causing other infections due to the absence of protective function of the microflora. For these reasons, all clinical trials up to date are limited to topical application for surface infections rather than parenteral and oral administration (Mylne et al. 2010; Kang et al. 2014).

- Physical instability under physiological conditions

Potentially, AMPs show susceptibility to proteases, serum, salt, pH, etc.

For example, the structural stability of AMPs can be affected by high ionic strength preventing their initial electrostatic interaction with the bacterial surface.

The linear structure of AMPs can be easily attacked by host proteases and peptidases (Ganz 1999; Tossi et al. 2000; Tam et al. 2002). In fact, peptide drugs are generally characterized by low oral bioavailability and poor

penetration into the intestinal mucosa, thus making the oral administration not possible. Furthermore, systemic administration of peptides by, e.g., intravenous injection, is limited by a short half-life because of rapid degradation by serum proteases (Chan et al. 2006) and rapid removal from the circulation by the liver and kidneys (Vlieghe et al. 2010).

Therefore, AMPs are usually used for the treatment of skin infections associated with burns, diabetic wounds or eyes infections (Mahlapuu et al. 2016; Kang et al. 2014).

- Production cost

Compared to small chemical drugs, the production costs of AMPs are extremely high. It is known that the production of 1 g of peptide costs $100-600 by solid phase peptide synthesis, the most commonly used method for chemical synthesis of therapeutic peptides (Amblard et al. 2006). Moreover, during manufacturing, there are numerous technical difficulties in the synthesis and purification processes (Hancock and Sahl 2006).

1.9 Strategies for AMPs development as new therapeutics and synthesis of Esc(1-21)-1c

To develop AMPs able to overcome the aforementioned drawbacks without causing a significant reduction in their antimicrobial efficacy, several strategies are adopted (Fjell et al. 2011).

To reduce toxicity of AMPs the control of hydrophobicity and charge or the improvement of target cell-selectivity of AMPs are highly important (Kang et al. 2014). Indeed, high hydrophobicity is related to increased hemolytic activity (Yeaman and Yount 2003; Chou et al. 2008).

To reduce the susceptibility to degradation by peptidases/proteases, several methods have been introduced in AMPs synthesis:

i) cyclization, by linking the N- and C-terminus, which is a well-known method to improve both microbicidal activity and serum stability, in comparison to the linear peptide form (Giuliani et al. 2007; Oyston et al. 2009).

ii) incorporation of D-amino acids and non-natural amino acids, since host proteases can recognize and hydrolyze natural L-amino acids.

One of the non-natural amino acid mainly used to increase the stability of α-helix conformation and presumably the spectrum of activity of AMPs, is the α-aminoisobutyric acid (Aib) (Bellanda et al. 2001; De Zotti et al. 2012). Moreover, the substitution of L-amino acids with the corresponding D-enantiomers is often used to reduce AMPs cytotoxicity without negative effects on the peptide's functionality (Giuliani and Rinaldi 2011).

iii) modification by different natural amino acids.
For example, changes in the proline content, because of low propensity of proline to form α-helical structures, may lead to alteration of the peptide conformation and a resulting reduction in the cytotoxicity (Zhang et al. 1999).

iv) acetylation and/or amidation of the N- and C-terminal ends.
The N-acetylation of peptides enhances stability against proteases (Nguyen et al. 2005; Papo and Shai 2004). The C-amidation is frequently used to improve peptide activity and to decrease hemolytic activity by reducing the negative charge of the carboxylic group in the peptide and by stabilizing the amphipathic helix formation (Nguyen et al. 2010).

v) design of antimicrobial peptide conjugates.

AMPs can be attached/incorporated to/into nano-micro systems (e.g. nanoparticles) to improve their biostability. This strategy does also allow the peptide to reach the infection site at high concentrations, thus minimizing potential side-effects and increasing its pharmacological effect reducing the number of administrations (Eckert 2011; d'Angelo et al. 2015a; d'Angelo et al. 2015b).

Particularly interesting in this context is the use of biocompatible and biodegradable materials, such as lipids (e.g., phospholipids, triglycerides, cholesterol, and monoolein) and polymers [e.g., cellulose, chitosan, hyaluronic acid, poly lactic-co-glycolic acid (PLGA), and poly lactic acid (PLA)] or inorganic particles (such as gold or silver) for new therapeutic formulations (Rai et al. 2016; Ramesh et al. 2016; Ali et al. 2016).

Regarding the cost of production, pharmaceutical companies have tried to develop AMPs of smaller size derived from more expensive and larger natural peptides (Aoki et al. 2012).

In our case, with the aim to protect Esc(1-21) from proteolytic degradation and to reduce its toxicity against mammalian cells, without affecting its antimicrobial activity, an analogue named Esc(1-21)-1c was designed by replacing two L-amino acids with the corresponding D-amino acid enantiomers (Tab. 3).

Table 3 Primary structure of Esc(1-18), Esc(1-21) and Esc(1-21)-1c. D-amino acids are underlined and in italics.

PEPTIDE DESIGNATION	SEQUENCE[a]	Net charge at neutral pH
Esc(1-18)	GIFS**K**LAG**KK**L**K**NLLISG-NH$_2$	**+5**
Esc(1-21)	GIFS**K**LAG**KK**I**K**NLLISGL**K**G-NH$_2$	**+6**
Esc(1-21)-1c	GIFS**K**LAG**KK**I**K**N*L*LI*S*GL**K**G-NH$_2$	**+6**

[a] Basic amino acids are indicated by red letters.

The design of the diastereomer Esc(1-21)-1c was realized on the bases of the following considerations:

- the reduction of α-helical content of a peptide correlates with its reduced ability in perturbing mammalian membranes causing cell lysis (Shai and Oren 1996; Strahilevitz et al. 1994);

- D-amino acids are known to be α-helix breakers (Grieco et al. 2013a).

Previous studies performed with the shorter analog of Esc(1-21), [Esc(1-18)], indicated that the C-terminal half of this latter adopted an α-helical conformation in a hydrophobic environment mimicking the electrically neutral membranes of mammalian cells (Manzo et al. 2014). Esc(1-18) differs from Esc(1-21) by a single amino acid in position 11 and lacks the 3 residues tail at its carboxyl end. Since this tail contains two achiral glycine residues at positions 18 and 21, it is very unlikely that this region of Esc(1-21) folds in a stable helical conformation. Therefore, replacement of two L-amino acids, i.e. L-Leu14 and L-Ser17, with the corresponding D-enantiomers, would break the first turn of the expected C-terminal α-helix of Esc(1-21) [please refer to the work attached at the end of the manuscript: "D-Amino acids incorporation in the frog skin-derived peptide esculentin-1a(1-

21)NH$_2$ is beneficial for its multiple functions." By Di Grazia A, Cappiello F, Cohen H, Casciaro B, Luca V, Pini A, Di YP, Shai Y, Mangoni ML].

Esc(1-21)-1c displayed potent bactericidal activity *in vitro* against the free-living form of *P. aeruginosa* strains (either reference or clinical isolates from CF patients), even if this activity resulted to be slightly weaker than that of the all-L peptide. Esc(1-21), at 1 µM, reduced ≥ 3 log$_{10}$ the number of viable bacterial cells within 30 min, compared to the untreated cells, while the diastereomer had the same efficacy at a concentration of 4 µM against all the examined bacteria.

2. Aims of the work

To counteract antibiotic resistance caused by the widespread use of conventional antibiotics against bacterial infections, such as those caused by the Gram-negative bacterium *P. aeruginosa* in the lungs of patients with cystic fibrosis, the discovery of new classes of antimicrobial agents with a new mechanism of action is highly required. AMPs hold promise for the development of alternative therapeutics.

Recently, a derivative of the frog-skin AMP esculentin-1a, that is Esc(1-21), was found to display a fast and potent killing activity against both the planktonic and biofilm forms of *P. aeruginosa*. However, the development of AMPs as new drugs has some limitations, including their high susceptibility to proteolytic degradation and cytotoxicity. Interestingly, one promising strategy to overcome these drawbacks is given by the incorporation of D-amino acids in the peptide sequence, due to their resistance to enzymatic digestion and ability to disrupt the alpha-helical content of a peptide, which is expected to decrease its cytotoxicity.

Therefore a diastereomer of Esc(1-21), named Esc(1-21)-1c, was designed and synthesized by replacing two L-amino acids in the C-terminal portion, i.e. L-Leu14 and L-Ser17, with the corresponding D-enantiomers.

The aim of this work was to investigate and compare the effect of the two D-amino acid substitutions on the peptide's:

(i)   cytotoxicity;
(ii) resistance to proteolytic enzymes;
(iii) biological features including antipseudomonal activity, wound healing and anti-inflammatory properties.

Along with these aims, experimental protocols were developed and performed to evaluate:

- the effect of both peptides on mammalian cell viability along with their ability to perturb model membranes;
- their structural properties in membrane-mimicking environments;
- their stability to elastase from *P. aeruginosa* and human neutrophils;
- their ability in killing CF strains of *P. aeruginosa* either in their biofilm phenotype or once internalized into bronchial epithelial cells;
- their ability to stimulate migration of bronchial epithelial cells and presumably to promote the repair of a damaged airway epithelium, which can be formed upon bacterial infections;
- their ability to inhibit the production and secretion of pro-inflammatory mediators from macrophages activated by *P. aeruginosa* LPS.

3. Materials and Methods

3.1 Materials

Synthetic Esc(1-21) and its diastereomer, Esc(1-21)-1c, as well as rhodamine-labeled peptides [rho-Esc(1-21) and rho-Esc(1-21)-1c], were purchased from Chematek Spa (Milan, Italy). Minimum essential medium (MEM), Dulbecco's modified Eagle's medium (DMEM), glutamine, heat-inactivated fetal bovine serum (FBS), Hank's buffer, non-essential amino acids (NEAA), sodium pyruvate and penicillin-streptomycin were from Euroclone (Milan, Italy); puromycin, gentamicin, 3(4,5-dimethylthiazol-2yl)2,5-diphenyltetrazolium bromide (MTT), Triton X-100, Tyrphostin AG1478 inhibitor, 4',6-diamidino-2-phenylindole (DAPI), rhodamine, Mowiol 4-88, Hoechst 33258, Phalloidin Fluorescein Isothiocyanate Labeled, carboxyfluorescein (CxF), LPS from *P. aeruginosa* serotype 10 (purified by phenol extraction), and elastase from human leukocytes were purchased from Sigma-Aldrich (St. Luis, MO). Elastase from *P. aeruginosa*, GM6001 metalloproteinases inhibitor and Bromodeoxyuridine (BrdU) Cell Proliferation Assay Kit was from Millipore Merck (Merck, Milan, Italy). Trypsin–EDTA and agarose were purchased from Invitrogen (Life-Technologies Europe, Monza, Italy). Mouse Tumor necrosis factor alpha (TNF-α) enzyme-linked immunosorbent assay kit was from eBioscience. The lipids 1-palmitoyl-2-oleoyl-sn-glycero-3-phosphoethanolamine (POPE), 1-palmitoyl-2-oleoyl-sn-glycero-3-phosphoglycerol (POPG), 1-palmitoyl-2-oleoyl-sn-glycero-3-phosphocholine (POPC) and cholesterol (Cho) were purchased from Avanti Polar Lipids (Alabaster, AL, USA). Sodium-dodecylsulfate (SDS) and dodecylphosphocholine (DPC) were obtained from

41

Cambridge Isotope Laboratory (Tewksbury, MA). All other chemicals were reagent grade.

3.2 Cell cultures

The following cell cultures were employed: immortalized human bronchial epithelial cells derived from a CF patient (CFBE41o-) transduced with a lentiviral system to stably express ΔF508CFTR (ΔF508-CFBE) or functional CFTR (wt-CFBE) (Bebok et al. 2005); adenocarcinoma human alveolar epithelial cells (A549) and murine RAW 264.7 macrophage cell line (from the American Type Culture Collection).

CFBE cells were cultured in MEM supplemented with 2 mM glutamine (MEMg), 10% FBS, antibiotics (0.1 mg/ml of penicillin and streptomycin) and puromycin (0.5 µg/ml or 2 µg/ml for wt-CFBE or ΔF508-CFBE, respectively) at 37 °C and 5% CO_2 in 75-cm^2 flasks.

A549 and RAW 264.7 cells were cultured in DMEM supplemented with 2 mM glutamine (DMEMg), 10% FBS and antibiotics (0.1 mg/ml of penicillin and streptomycin) at 37 °C and 5% CO_2 in 75-cm^2 and 25-cm^2 flasks, respectively. In the case of RAW cells NEAA and sodium pyruvate (1 mM) were also added in the culture medium.

3.3 Microorganisms

The strains of *P. aeruginosa* used for the antimicrobial assays against biofilms were: the standard non-mucoid ATCC 27853 (Li et al. 2001) and the following ones from collection of the CF clinic Medizinische Hochschule of Hannover, Germany: the mucoid AA11 and the non-mucoid TR1 and KK1 (Bragonzi et al. 2009).

P. aeruginosa KK1, an invasive clinical isolate from the early stage of chronic lung infection (Bragonzi et al. 2009; Lore et al. 2012), was also used for cell infection.

3.4 Cytotoxicity assay

The effect of Esc(1-21) and its diastereomer, Esc(1-21)-1c, on the viability of wt-CFBE, ΔF508-CFBE and RAW 264.7 cells was evaluated by the colorimetric method based on the intracellular reduction of the yellow tetrazolium salt (MTT) to a purple compound, called formazan, by mitochondrial dehydrogenases (Fig. 15A) (Grieco et al. 2013b). The intensity of this color transformation is directly proportional to the number of metabolically active cells (Fig. 15B).
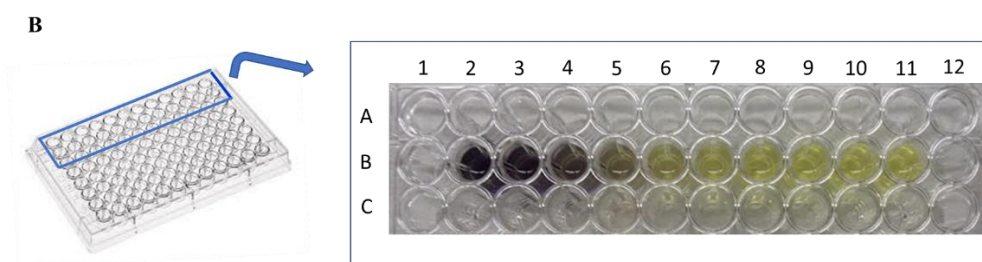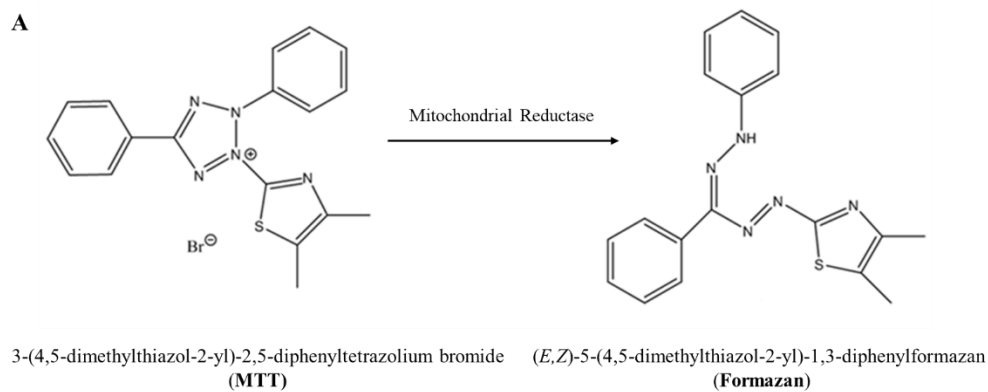
Fig. 15 Reduction of the yellow tetrazolium salt (MTT) to purple insoluble formazan, by metabolically-active cells (A). The intensity of the purple dye is proportional to the number of viable cells. The transparent yellow color in the B11 well corresponds to MTT solution without cells (B).

About 4×10^4 cells resuspended in the corresponding culture medium supplemented with glutamine and 2% FBS, without antibiotics, were plated in each well of a 96-well microtiter plate. After overnight incubation at 37 °C in a 5% CO_2 atmosphere, the medium was removed and replaced in each well with 100 µl of fresh serum-free MEMg, DMEMg or Hank's buffer (136 mM NaCl; 4.2 mM Na_2HPO_4; 4.4 mM KH_2PO_4; 5.4 mM KCl; 4.1 mM $NaHCO_3$, pH 7.2, supplemented with 20 mM D-glucose) with or without the peptide at different concentrations.

After 2 h or 24 h at 37 °C in a 5% CO_2 atmosphere, the medium was removed and replaced with 100 µl of Hank's buffer containing 0.5 mg/ml MTT. The plate was incubated at 37 °C and 5% CO_2 for 4 h, and the formazan crystals were dissolved by adding 100 µl of acidified isopropanol. Absorption of each well was measured using a microplate reader (Infinite M200; Tecan, Salzburg, Austria) at 570 nm [please refer to the work attached at the end of the manuscript: "The frog skin-derived antimicrobial peptide esculentin-1a(1-21)NH_2 promotes the migration of human HaCaT keratinocytes in an EGF receptor-dependent manner: a novel promoter of human skin wound healing?" By Di Grazia A, Cappiello F, Imanishi A, Mastrofrancesco A, Picardo M, Paus R, Mangoni ML]. The percentage of metabolically active cells compared to control samples (cells not treated with peptide) was calculated according to the formula:

(absorbance$_{sample}$ − absorbance$_{blank}$) / (absorbance$_{control}$ − absorbance$_{blank}$) × 100,

where the blank is given by samples without cells and not treated with the peptide.

3.5 Preparation of lipid vesicles and membrane perturbing assays

3.5.1 Liposomes preparation

Lipid films of POPC/Cho and POPE/POPG were prepared by dissolving lipids (2 mg of POPC/Cho mixture, 1:1, mol/mol or 2 mg of POPE/POPG, 7:3, mol/mol) in chloroform/methanol (2:1, v/v). The solvents were then evaporated under reduced argon atmosphere until a thin film was formed. The lipid film was then hydrated with 500 µl of 10 mM phosphate buffer containing 140 mM NaCl and 0.1 mM EDTA, pH 7.4 (buffer A). For CxF

leakage experiments, the lipid film was hydrated with a CxF solution (Fig. 16) at a self-quenching concentration, i.e. 30 mM in 10 mM phosphate buffer containing 80 mM NaCl and 0.1 mM EDTA, adjusted to pH 7.4 with NaOH. The liposome suspension was subjected to 10 freeze and thaw cycles and extruded for 31 times through two stacked polycarbonate membranes with 100 nm pores to obtain liposomes. The free CxF (when present) was removed by gel filtration, using a 40 cm Sephadex G-50 at room temperature, equilibrated with buffer A. The final lipid concentration was determined by the Stewart phospholipid assay [please refer to the article attached at the end of the manuscript: "Membrane Perturbing Activities and Structural Properties of the Frog-skin Derived Peptide Esculentin-1a(1-21)NH$_2$ and its Diastereomer Esc(1-21)-1c: Correlation With Their Antipseudomonal and Cytotoxic Activity." By Loffredo MR, Ghosh A, Harmouche N, Casciaro B, Luca V, Bortolotti A, Cappiello F, Stella L, Bhunia A, Bechinger B, Mangoni ML].
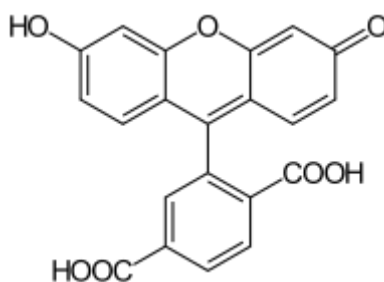
Fig. 16 Chemical structure of carboxyfluorescein.

46

3.5.2 Carboxyfluorescein leakage assay

Peptide-membrane interaction can be investigated by the use of liposomes as model membranes, due to their bilayer structure, which is in principle identical to the lipid organization of biological membranes (Mouritsen 2011).

CxF release from liposomes due to membrane permeation induced by the peptide was monitored at 37 °C by the fluorescence increase (excitation = 488 nm; emission = 520 nm). A concentration of lipid vesicles of 200 µM was used and CxF leakage after peptide addition at 20 µM was monitored for 30 min. Complete dye release was obtained using 0.1% Triton X-100, which causes total destruction of lipid vesicles (Marcellini et al. 2009; Makovitzki et al. 2006). The percentage of CxF leakage was calculated according to the following formula (Matsuzaki 1999): leakage (%) = $100(F_1 - F_0) / (F_t - F_0)$, where F_0 represents the fluorescence of intact vesicles, and F_1 and F_t denote the intensities of the fluorescence achieved by peptide and Triton X-100 treatment, respectively, at different time points, as indicated. A schematic representation of CxF-encapsulated liposomes is shown in (Fig. 17).
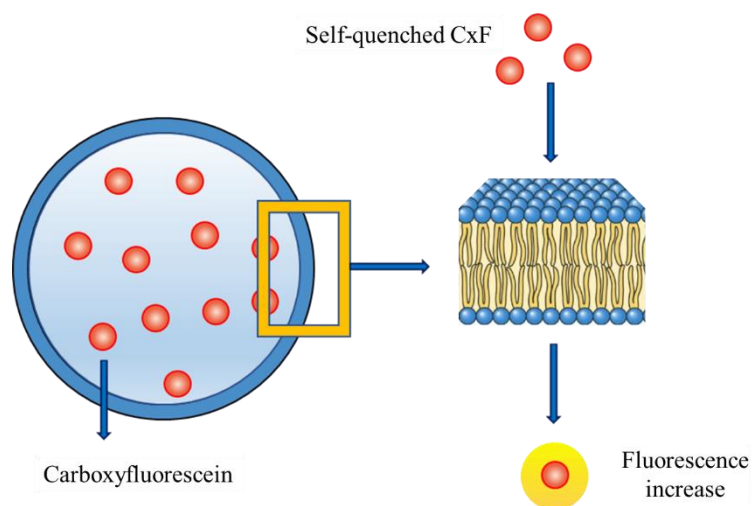
Fig. 17 Schematic representation of a CxF-encapsulated liposome.

3.6 Circular dichroism spectroscopy

In order to investigate the change in the secondary structure of Esc(1-21) and Esc(1-21)-1c in membrane mimicking environments, circular dichroism (CD) experiments were performed in DPC and SDS micelles using a Jasco J-815 spectrometer (Jasco International Co., Ltd. Tokyo, Japan) with a Peltier cell holder and temperature controller unit accessory. CD spectra were recorded for both the peptides in water (25 μM) and in the presence of DPC (10 mM) and SDS (40 mM) at 37 °C. Both working concentrations of DPC and SDS micelles were above their critical micelle concentration as previously reported in the literature (Manzo et al. 2013). The far-UV spectra were scanned over a range of 190-260 nm with 1 nm data interval and averaged over 4 scans. Blank sample spectra were subtracted from the raw data and the CD values were converted to per residue molar ellipticity ([θ]) (deg cm^2 dmol^{-1}).

48

3.7 Stability of peptides to proteolytic degradation

Peptides were dissolved in 10 mM Tris-HCl, pH 7.5, at a final concentration of 1 mg/ml; afterwards, 130 µl were incubated with 4 µg of human or bacterial elastase (final enzyme concentration equal to 1 µM). At the indicated time intervals, 30-µl aliquots were withdrawn, diluted with 770 µl of 0.1% trifluoroacetic acid (TFA)–water, and analyzed by Reversed-Phase High-Performance Liquid Chromatography (RP-HPLC) and mass spectrometry. Liquid chromatography was performed on a Phenomenex Jupiter C18 analytical column (300 Å, 5 µm, 250 by 4.6 mm) in a 30-min gradient, using 0.1% TFA in water as solvent A and methanol as solvent B. Mass spectrometry analysis was performed with a Bruker Daltonic ultraflex matrix-assisted laser desorption ionization tandem time-of-flight (MALDI-TOF/TOF) mass spectrometer on withdrawn samples as well as on HPLC-eluted peaks.

3.8 Antimicrobial assays

3.8.1 Antibiofilm activity

Biofilm formation was performed by adapting the procedure described in (Ceri et al. 2001; Falciani et al. 2012), using the Calgary Biofilm Device (Innovotech, Innovotech Inc. Edmonton, Canada). Briefly, 96-well plates, each well containing 150 µl of the bacterial inoculum [1×10^7 colony-forming units (CFU)/ml)] in Luria-Bertani (LB) medium were sealed with 96 peg-lids on which biofilm cells can build up. Afterwards, plates were placed in a humidified orbital incubator at 35 °C for 20 h under agitation at 125 rpm. Once biofilms were allowed to form, the pegs were rinsed twice with phosphate buffered saline (PBS) to remove planktonic cells. Each peg-lid

was then transferred to a "challenge 96-well microtiter plate", each well containing 200 μl of a twofold serial dilution of peptide in PBS. The "challenge plate" was incubated at 37 °C for 2 h. Peptide activity was evaluated by determining the amount of viable biofilm cells by measuring the reduction of MTT to its insoluble formazan. Briefly, after peptide treatment, the pegs-lid was washed with PBS and used to close another 96-well microtiter plate, each well containing 200 μl of Hank's buffer containing 1 mg/ml MTT. The plate was incubated at 37 °C for 4 h. Afterwards, 50 μl of 25% SDS were added to each well to dissolve formazan crystals. Bacterial viability was determined by absorbance measurements at 595 nm and calculated with respect to control cells (bacteria not treated with the peptide) (Mangoni et al. 2005). The percentage of viable cells was calculated according to the equation: (absorbance$_{sample}$ − absorbance$_{blank}$) / (absorbance$_{control}$ − absorbance$_{blank}$) x 100, where the blank is given by samples without cells and not treated with the peptide.

3.8.2 Cell infection and peptides' effect on intracellular bacteria

About 1×10^5 bronchial cells in MEMg supplemented with 10% FBS were seeded in 24-well plates and grown for 2 days at 37 °C and 5% CO_2. The clinical isolate KK1 was grown in LB broth at 37 °C with mild shaking (125 rpm) to mid-log phase (optical density of 0.8 at 590 nm) and subsequently harvested by centrifugation. The pellet was then resuspended in MEMg and properly syringed using a 21-gauge needle to avoid clump formation before infecting cells. A multiplicity of infection (MOI) of 100:1 (bacteria to cells) was used. Two hundred microliters of this bacterial suspension, containing about 1×10^7 CFU, was coincubated for 1 h with wt-CFBE/ΔF508-CFBE at 37 °C and 5% CO_2. After infection, the medium was removed and the cells

50

were washed three times with MEMg and then incubated for 1 h with a gentamicin solution (200 µg/ml in MEMg) to remove extracellular bacteria. Afterwards, the medium was aspirated and the infected cells were washed three times as described above. Two hundred microliters of Hanks' solution with or without the peptide at different concentrations was added to each well, and the plate was incubated for 1 h at 37 °C and 5% CO_2. After peptide treatment, cells were washed with PBS and lysed with 300 µl of 0.1% Triton X-100 in PBS for 15 min at 37 °C and 5% CO_2. Each sample was then sonicated in a water bath for 5 min to break up possible bacterial clumps, and appropriate aliquots were plated on agar plates for counting of CFU after 24 h at 37 °C.

3.8.3 Localization of rhodamine-labelled peptides by fluorescence microscopy

About 2×10^5 bronchial cells in MEMg supplemented with 10% FBS were seeded on 0.13- to 0.17-mm-thick coverslips which were put into 35-mm dish plates and incubated at 37 °C and 5% CO_2. After 24 h, samples were washed with 1 ml PBS and treated with 4 µM rhodamine-labeled peptide or rhodamine (for control samples) in MEMg. After 30 min and 24 h of incubation at 37 °C and 5% CO_2, cells were washed four times with PBS and fixed with 700 µl of 4% formaldehyde for 15 min at room temperature. Afterwards, they were washed twice with PBS and stained with DAPI (1 µg/ml) for 5 min at room temperature to visualize the nuclei. After three additional washes, the coverslips were mounted on clean glass slides using Mowiol mounting medium and observed under an Olympus FV1000 confocal microscope with a 60× objective lens (oil). Data analysis was done using Olympus Fluoview (version 4.1) and ImageJ. Results are reported as

the ratio between the fluorescence intensity of rhodamine-labeled peptides in the cytoplasm *versus* that in the nucleus.

3.9 *In vitro* cell migration assays

3.9.1 Pseudo-wound healing activity

The ability of single peptides to stimulate migration of CFBE cells was evaluated by a modified scratch assay, as reported previously [please refer to the work attached at the end of the manuscript: "D-Amino acids incorporation in the frog skin-derived peptide esculentin-1a(1-21)NH$_2$ is beneficial for its multiple functions." By Di Grazia A, Cappiello F, Cohen H, Casciaro B, Luca V, Pini A, Di YP, Shai Y, Mangoni ML]. Briefly, special cell culture inserts for live cell analysis (Ibidi, Munich, Germany) were placed into wells of a 12-well plate. Alternatively, 35-mm dishes can also be used (Fig. 18). About 35,000 cells suspended in MEMg supplemented with 10% FBS were seeded in each compartment of the culture insert and incubated at 37 °C and 5% CO$_2$ for approximately 24 h to allow cells to grow to confluence. Afterwards, inserts were removed to create a cell-free area (pseudo-wound) of approximately 500 µm; 1 ml MEMg with or without the peptide at different concentrations was added to each well. Plates were incubated as described above to allow cells to migrate, and samples were visualized at different time intervals under an inverted microscope (Olympus CKX41) at 4× magnification and photographed with a Color View II digital camera. The percentage of cell-covered area at each time was determined by the WIMASIS Image Analysis program. In another set of experiments, cell migration was evaluated in the presence of hydroxyurea alone or with peptides [Esc(1-21) or Esc(1-21)-1c] at the indicated concentration to

determine the involvement of proliferation. Furthermore, pseudo-wound closure assays were performed by pretreating cells for 30 min with 5 µM AG1478 or with 25 µM GM6001 to assess the implication of epidermal growth factor receptor (EGFR) or metalloproteinase activity in peptide-induced cell migration, respectively.
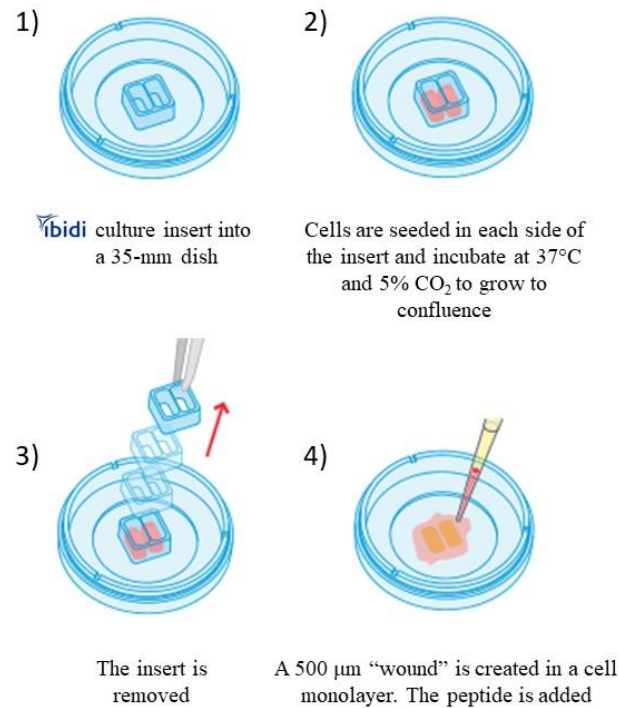
Fig. 18 Schematic representation for the usage of the Ibidi silicone culture inserts: placement of the insert into a 35-mm dish (1); cell seeding (2); removal of the insert (3); addition of treatments (4).

3.9.2 Effect of the peptides on cell morphology

A549 or CFBE cells (1.5×10^5) in 1 ml of DMEMg or MEMg, respectively, supplemented with 10% FBS, were seeded on 0.13- to 0.17-mm-thick coverslips put into 35-mm dish plates. The plates were incubated at 37 °C

and 5% CO_2. After overnight incubation, A549 cells were washed with PBS and pretreated or not with 0.2 μM AG1478 before adding 10 μM Esc(1-21) or 4 μM Esc(1-21)-1c in 1 ml of DMEMg supplemented with 2% FBS. Cells only pretreated with 0.2 μM AG1478 or without any treatment served as control.

CFBE cells were washed with PBS and treated with 10 μM Esc(1-21) or 1 μM Esc(1-21)-1c in 1 ml of MEMg.

After 24 h incubation at 37 °C and 5% CO_2, cells were washed with PBS. Then cells were fixed with 3.7% formaldehyde for 10 min at 4 °C or with 4% formaldehyde for 15 min at room temperature for A549 and CFBE cells, respectively. Afterwards, cells were washed with PBS, permeabilized with 0.1% Triton X-100 in PBS for 10-15 min at room temperature, washed again and stained with phalloidin-fluorescein isothiocyanate (40 μM in PBS) for 20-30 min at room temperature to visualize the cytoskeleton. The nuclei were stained by adding 50 μl of Hoechst 33258 (2 μg/ml) for 10 min or DAPI (1 μg/ml) for 5 min at room temperature for A549 and CFBE cells, respectively. The coverslips were mounted on slides using buffered glycerol or Mowiol mounting medium, observed under the fluorescent microscope KOZO OPTICS XJF800 at 20× magnification and photographed with a Color View II digital camera.

3.10 Cell proliferation studies

About 2×10^4 wt-CFBE cells in MEMg supplemented with 10% FBS were seeded in each well of a 96-well microtiter plate. After overnight incubation at 37 °C and 5% CO_2 atmosphere, the medium was replaced with 100 μl fresh MEMg supplemented with 10 μM Esc(1-21), 1 μM Esc(1-21)-1c, 250 μM hydroxyurea or peptide combined with hydroxyurea for 24 h. Two hours

54

after the start of the treatment, cells were pulsed with BrdU. The percentage of cell proliferation was analyzed by BrdU Cell Proliferation Assay Kit (Fig. 19) and normalized to that of cells growing in MEMg (100% cell proliferation; Ctrl).
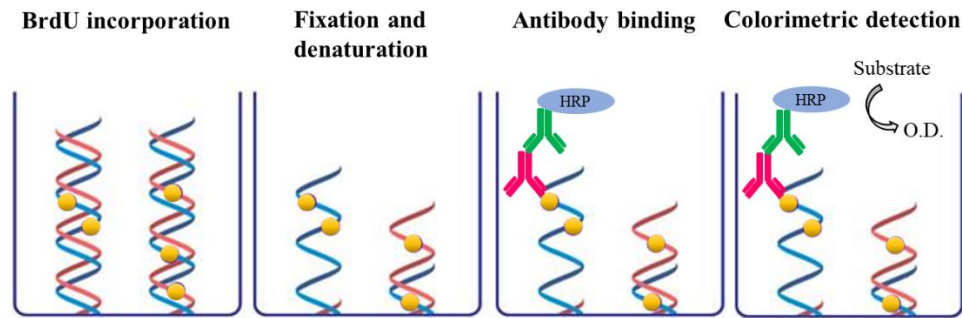

Fig. 19 Schematic representation of a BrdU Cell Proliferation ELISA to detect BrdU incorporated into cellular DNA during cell proliferation. When cells are incubated in media containing BrdU, the pyrimidine analog is incorporated in place of thymidine into the newly synthesized DNA of proliferating cells. Once the labeling media is removed, the cells are fixed and the DNA is denatured (denaturation of the DNA is necessary to improve the accessibility of the incorporated BrdU for detection). Afterwards, an anti-BrdU mouse monoclonal antibody is added followed by an Horseradish peroxidase (HRP) conjugated secondary antibody to detect the incorporated BrdU. The magnitude of the absorbance for the developed color is proportional to the quantity of BrdU incorporated into cells and can be directly correlated to cell proliferation.

3.11 Anchored-independent growth assay (Soft Agar Colony Formation Assay)

About 1×10^6 A549 cells in DMEMg supplemented with 10% FBS were seeded in 25-cm^2 flasks. After overnight incubation at 37 °C and 5% CO_2 atmosphere, medium was removed and replaced with fresh medium supplemented with 2% FBS and containing 10 µM Esc(1-21) or 4 µM Esc(1-21)-1c for 24 h. As previously described in (Ranieri et al. 2016), 60mm dishes were coated with 5 ml/dish of 0.6% agar prepared in DMEMg supplemented with 10% FBS (complete medium) and allowed to solidify for

55

at least 5 min at room temperature. After 24 h treatment with the peptide, cells were trypsinized, resuspended (1.5×10^4 cells) in 3 ml of complete medium supplemented with 0.4% agar and poured on top of the 0.6% agar layer coating the 60-mm dish plate. The plates were then incubated for 2 weeks at 37 °C and 5% CO_2 atmosphere. Immediately after plating, only single cells were visible in each dish. To prevent desiccation, 0.5 ml of complete medium was added to each dish plate, twice per week.

After two weeks, cells were stained with 0.001% crystal violet until they were clearly visible (Fig. 20). Quantitative analysis was performed counting visible colonies.
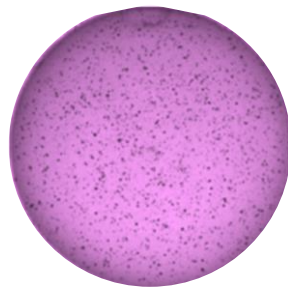
Fig. 20 Representative scanned digital image of A549 colonies stained with crystal violet in a 60-mm dish.

3.12 Anti-inflammatory assays

3.12.1 Lipopolysaccharide (LPS)-neutralizing activity

Macrophages were cultured overnight in 96-well plates (1×10^5 cells/well) in DMEMg supplemented with sodium pyruvate, NEAA and 10% FBS. The medium was then removed and replaced with fresh medium + 10% FBS containing 10 ng/ml LPS, derived from *P. aeruginosa* 10, in the presence of 1, 5, 10, 20 μM Esc(1-21) or Esc(1-21)-1c. Samples were incubated at 37 °C for 4 h.

56

To verify if the peptides competed with LPS for binding to the LPS receptor, macrophages were stimulated with each peptide at the concentrations indicated above in fresh medium + 10% FBS, for 2 h at 37 °C and 5% CO_2. Afterwards, the peptides were removed and the cells were stimulated with 10 ng/ml LPS for 5 h.

The medium was then collected and TNF-α concentration was evaluated using a mouse TNF-α enzyme-linked immunosorbent assay kit according to the manufacturer's protocol (eBioscience, Affymetrix, San Diego, CA, USA) (Fig. 21). Cells that were stimulated with LPS alone and untreated cells served as controls. All experiments were done in triplicates.
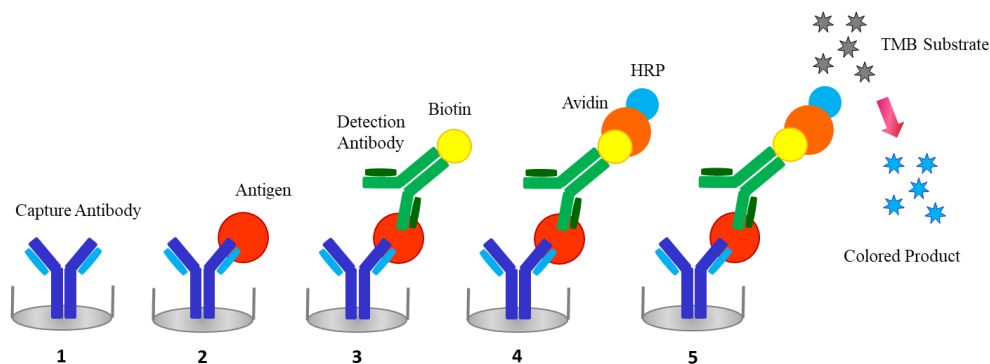
Fig. 21 Schematic representation of a sandwich enzyme-linked immunosorbent assay (ELISA). The plate is coated with a suitable capture antibody (1). Then the sample is added and the antigen present is bound to the capture antibody (2). A suitable biotin labeled detection antibody (BDAb), which binds to the antigen, is added (3). Avidin-Horseradish peroxidase HRP binds BDAb (4). Finally, 3,3′,5,5′-Tetramethylbenzidine (TMB) substrate is added and converted to a detectable form.

3.12.2 Effect of the peptides on the structural organization of LPS

Dynamic light scattering (DLS) is a well-known technique used to measure the Brownian motion (diffusion) and the size distribution of particles in solution. Here, the DLS machine (802 DLS manufactured by Viscotek) was

57

used to determine the size of LPS micelles in solution. To estimate the average size of the LPS particles, the measurements were done in wavelength of 830 nm, the detection was performed at 90°, temperature between 22 and 25 °C (the refractive index was measured, respectively) and analyzed by the Software of OMNISIZE (Viscotek). LPS measurement was performed before and after peptides addition. LPS:peptide molar ratio was 1:1 and the solvent was filtered water.

3.12.3 Western blotting analysis for cyclooxygenase-2 (COX-2) protein expression

Macrophages were cultured overnight in 90 mm plates (1.5×10^6 cells/well) in DMEMg supplemented with sodium pyruvate, NEAA and 10% FBS. The medium was then removed and cells were stimulated with LPS from *P. aeruginosa* (20 ng/ml), Esc(1-21), Esc(1-21)-1c or both LPS and peptides for 4 h. After treatment, the cells were washed and solubilized in lysis buffer [PBS 1X, 1% Tergitol-type NP-40, 0.5% sodium deoxycholate, 0.1% SDS, Protease Inhibitor Cocktail, 1 mM sodium orthovanadate (Na_3VO_4), 5 mM Dithiothreitol (DTT)] for 30 min on ice. The samples were centrifuged at $1000 \times g$ for 10 min and the supernatants were collected. Twenty µg of lysate protein from each sample were separated by SDS-PAGE on 10% gels and transferred to polyvinylidene fluoride (PVDF) membrane. After blocking overnight with buffer (5% non fat dry milk) the membranes were incubated with primary anti-COX-2 or anti-β-actin antibody for 1 h, washed in tris-buffered saline-Tween 20 (TBST buffer) and incubated with HRP-conjugated secondary antibody for 1 h. Blots were developed by enhanced chemiluminescent (ECL) system. Densitometry analyses of bands were done by ImageJ gel system.

58

3.13 Statistical analyses

Quantitative data, collected from independent experiments, were expressed as the means ± standard errors of the means (SEM) or standard deviation (SD). Statistical analysis was performed using one- or two-way analysis of variance (ANOVA) with PRISM software (GraphPad, San Diego, CA) or using Student's t-test. Differences were considered to be statistically significant for a P value of <0.05. The levels of statistical significance are indicated in the legends to the figures.

4. Results

4.1 Effect of Esc(1-21) and Esc(1-21)-1c on cell viability and mode of action on model membranes

To investigate whether the incorporation of the two D-amino acids in the peptide sequence of Esc(1-21) was harmful to mammalian cells, the effect of the all-L peptide and its diastereomer on the viability of mammalian cells as well as on the perturbation of model membranes were assessed.

4.1.1 Peptides' effect on the viability of mammalian cells

The effect of Esc(1-21) and its diastereomer Esc(1-21)-1c on the viability of human airway epithelial cells stably expressing either a functional or the most common CFTR mutation (ΔF508), as well as of murine macrophages (RAW 264.7 line), were evaluated by the MTT colorimetric assay in MEMg and DMEMg, respectively.

The results obtained on CFBE cells are shown in Fig. 22. The two peptides were not toxic to wt-CFBE and ΔF508-CFBE cell lines at a concentration range between 2 µM and 64 µM within 2 h. However, Esc(1-21) was toxic at 128 µM, causing ~25% and 70% reduction in the amount of metabolically active wt-CFBE and ΔF508-CFBE cells, respectively (Fig. 22A and B). Furthermore, at a longer-term treatment (24 h), the cytotoxicity of Esc(1-21) became more pronounced, inducing about 20-25% killing of epithelial cells at 32 µM and 64 µM (Fig. 22C and D). At 128 µM, ~60% and 90% reduction of metabolically active wt-CFBE and ΔF508-CFBE cells was found, respectively. Importantly, the diastereomer did not induce any reduction in the percentage of metabolically-active cells at any concentration (Fig. 22).

61

Fig. 22 Peptides' effect on the viability of bronchial epithelial cells. About 4×10^4 wt-CFBE (A and C) or ΔF508-CFBE (B and D) cells were plated in wells of a microtiter plate. After overnight incubation at 37 °C in a 5% CO_2 atmosphere, the medium was replaced with 100 µl fresh MEMg supplemented with the peptides at different concentrations. After 2 h or 24 h, cell viability was determined by MTT reduction to insoluble formazan. Cell viability is expressed as percentage with respect to the peptide untreated cells used as a control (Ctrl). All data are the mean from four independent experiments ± SEM. The levels of statistical significance between the two peptides are P values of <0.05 (*), <0.01 (**), and <0.0001 (****).

In the case of RAW 264.7 cell line, both peptides gave rise to ~20% reduction in the number of metabolically-active cells when tested at a concentration range between 2 µM and 8 µM within 2 h. The cell viability decreased in a dose-dependent manner up to 128 µM, where 20% or 60% of viable cells were detected after incubation with Esc(1-21) or Esc(1-21)-1c, respectively (Fig. 23A). However, after 24 h treatment (Fig. 23B), Esc(1-21) induced more than 50% reduction in the number of metabolically active cells

at 64 μM and the complete cell death at 128 μM. In contrast, Esc(1-21)-1c induced only ~20% reduction of metabolically-active cells.

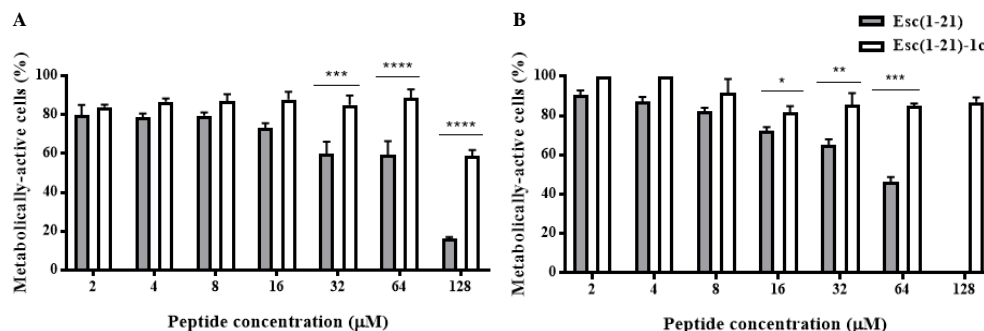**Fig. 23** Peptides' effect on the viability of RAW 264.7 macrophages. About 4×10^4 RAW 264.7 cells were plated in wells of a microtiter plate. After overnight incubation at 37 °C in a 5% CO_2 atmosphere, the medium was replaced with 100 μl fresh DMEMg supplemented with the peptides at different concentrations. After 2 h or 24 h, cell viability was determined by MTT reduction to insoluble formazan. Cell viability is expressed as percentage with respect to the peptide untreated cells used as a control (Ctrl). All data are the mean from four independent experiments ± SEM. The levels of statistical significance between the two peptides are *P* values of <0.05 (*), <0.01 (**), <0.001 (***), and <0.0001 (****).

4.1.2   Membrane perturbation of lipid vesicles (Liposomes)

To verify whether the lower cytotoxicity of the diastereomer in comparison to the all-L peptide reflected a weaker ability in destabilizing zwitterionic membranes, the leakage of a fluorescent marker from neutral lipid vesicles mimicking the composition of mammalian cell membranes was assessed and compared to what found for anionic vesicles mimicking the composition of bacterial membranes.

A fluorescent molecule, i.e. CxF, entrapped in the water volume inside the lipid vesicles at high concentration, can be used to test the membrane permeability. This condition induces self-association and quenching of the dye (Stella et al. 2004). After peptide addition, the consequent membrane

63

perturbation leads to probe release and dissociation with a resulting fluorescence increase.

Both peptides were tested at a concentration of 20 µM on zwitterionic liposomes made of POPC/cholesterol (1:1, mol:mol) to simulate the neutral membrane of mammalian cells. As indicated in Fig. 24A, the diastereomer induced a 5-fold lower leakage of entrapped CxF compared to Esc(1-21) in line with its lower cytotoxicity.

In comparison, when the two isomers were assayed on POPE/POPG liposomes (7:3 mol:mol, 200 µM), to mimic the lipid composition of the anionic membrane of Gram-negative bacteria, Esc(1-21) induced a 2-fold higher membrane-perturbing activity than that of the diastereomer within 30 min after addition to the lipid vesicles (Fig. 24B).

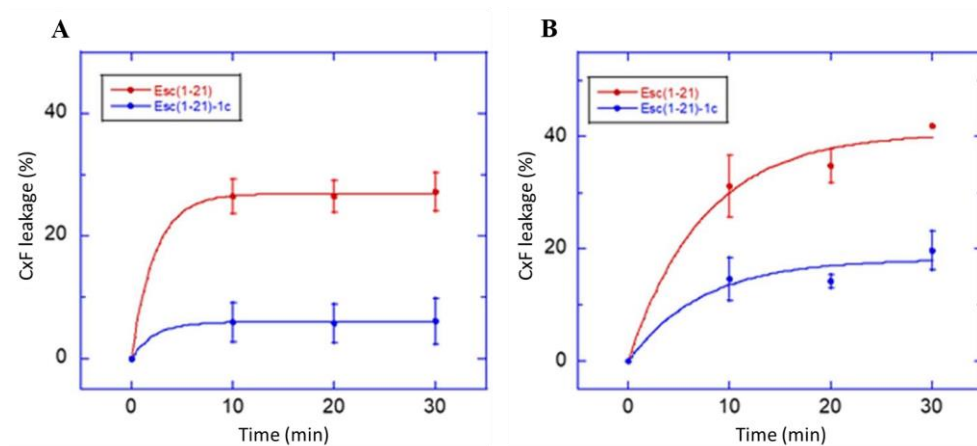**Fig. 24** CxF release from POPC/Cho liposomes (A) and POPE⁄POPG (B) (final lipid concentration 200 µM) during 30 min after addition of peptides (20 µM) at 37 °C. The percentage of leakage was calculated according to the formula: $100(F_t - F_0) ⁄ (F_1 - F_0)$ as explained in the Materials and Methods. Data points are means of three independent measurements ± SD.

64

4.2 Structural studies

Studies aimed at understanding the structural properties of the two peptides were performed by circular dichroism spectroscopy (CD) in the presence of DPC (solid line) and SDS micelles (broken line), mimicking the zwitterionic and the anionic composition of the outer leaflet of the cell membrane of mammalian cells and bacteria, respectively (Fig. 25A and B).

CD spectra were measured in collaboration with Prof. Bhunia (Department of Biophysics, Bose Institute, India).

In aqueous solution (black line), the two peptides assumed a random-coil conformation. Differently, in DPC and SDS, the spectral intensities typical of α-helices (two negative minima at 208 nm and 222 nm) were observed, but this was less pronounced for Esc(1-21)-1c (Fig. 25B), probably because of the presence of D-amino acids that break the α-helical structure.

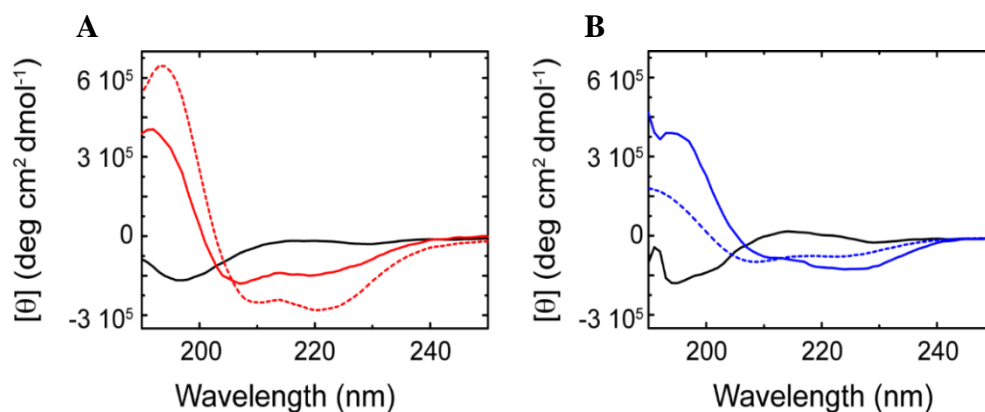

Fig. 25 Circular dichroism spectra of Esc(1-21) (A) and Esc(1-21)-1c (B), measured in the presence of aqueous solution (black line), SDS (broken colored line) and DPC (solid colored line) (25 µM peptide, 40 mM SDS or 10 mM DPC).

The conformational transition from random coil to α-helical structure in the presence of membrane-mimicking environments, as detected by CD spectra, prompted the exploration of the peptide structures at atomistic detail. DPC and/or SDS assemble as small size detergent micelles which provide appropriate systems for the structural analysis of AMPs in membrane mimetic environments by multidimensional nuclear magnetic resonance (NMR) spectroscopy. NMR studies were performed in the lab of Prof. Bhunia.

In DPC micelles, Esc(1-21) resulted to adopt mainly an α-helical conformation with a tilt at the N-terminal end (Fig. 26A). The central region of the α-helix is straight and amphipathic due to the presence of several polar residues across one face of the helix, while hydrophobic residues (i.e. I2, F3, L6, A7, I11, L14, L15, I16 and L19) are along the other face of the helix (Fig. 26B). In contrast, Esc(1-21)-1c exhibits a partial α-helical conformation only at the N-terminal region but the helix breaks after residue N13, likely due to the presence of D-L14 and D-S17. The C-terminal region (N13-G21) is unstructured and adopts a flexible conformation (Fig. 27A and B).

Unfortunately, it was not possible to determine the structure of both peptides in SDS micelles [please refer to the article attached at the end of the manuscript: "Membrane Perturbing Activities and Structural Properties of the Frog-skin Derived Peptide Esculentin-1a(1-21)NH$_2$ and its Diastereomer Esc(1-21)-1c: Correlation With Their Antipseudomonal and Cytotoxic Activity." By Loffredo MR, Ghosh A, Harmouche N, Casciaro B, Luca V, Bortolotti A, Cappiello F, Stella L, Bhunia A, Bechinger B, Mangoni ML].
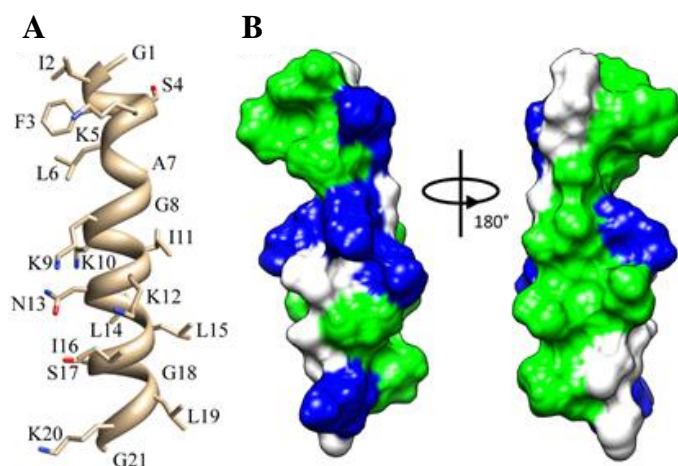
Fig. 26 Three dimensional solution structures of Esc(1-21) in DPC micelles. Cartoon representations of side chain orientation of a representative NMR structure of Esc(1-21) showing different residues (A). Electrostatic potential surface of Esc(1-21) showing the distribution of polar and non-polar residues (B). The hydrophobic and positively charged amino acid residues are indicated by green and blue, respectively, while all other residues are in white. These images were produced using the PyMOL and Chimera software (Pettersen et al. 2004).
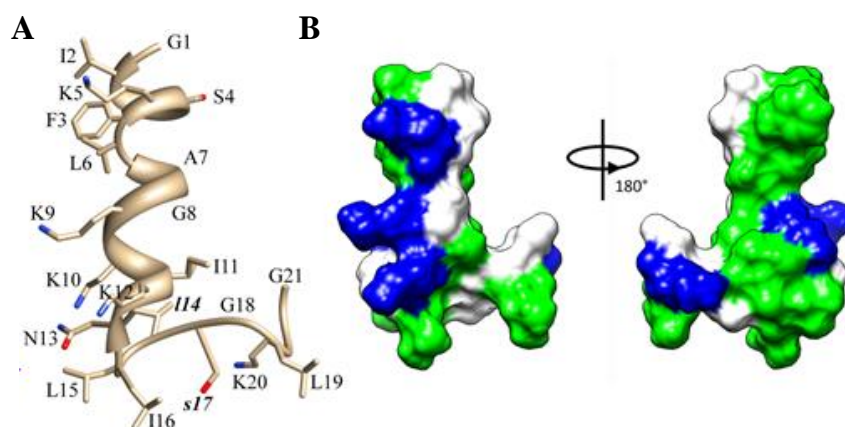
Fig. 27 Three dimensional solution structures of Esc(1-21)-1c in DPC micelles. Cartoon representations of side chain orientation of a representative NMR structure of Esc(1-21)-1c showing different residues (A). Electrostatic potential surface of Esc(1-21)-1c showing the distribution of polar and non-polar residues (B). The hydrophobic and positively charged amino acid residues are indicated by green and blue, respectively, while all other residues are in white. These images were produced using the PyMOL and Chimera software.

67

4.3 Peptide stability

It is worth to mention that: (i) one of the reasons accounting for the limited development of AMPs as new therapeutics (e.g. for treatment of *P. aeruginosa* lung infection) is related to their susceptibility to enzymatic degradation (Midura-Nowaczek and Markowska et al. 2014; Nguyen et al. 2010); and that (ii) the lung environment of CF patients is rich in proteases, i.e. elastase from host neutrophils and from *P. aeruginosa* (Liu et al. 1999; Lovewell et al. 2014; Mariencheck et al. 2003). Therefore, to investigate whether the replacement of two ʟ-amino acids with the corresponding ᴅ-enantiomers resulted in a higher resistance of the peptide to proteolytic digestion compared to the all-ʟ Esc(1-21), the stability of both isomers in the presence of elastases was studied in collaboration with Prof. Pini (Department of Medical Biotechnology, University of Siena).

4.3.1 Peptides' susceptibility to human elastase

When elastase from human leukocytes was used, Esc(1-21) was completely degraded within 5 h (Table 4). In contrast, the diastereomer was highly stable with 78% and 13% amount of non-degraded peptide after 5 h and 24 h incubation, respectively (Table 4). In comparison, when the human cathelicidin AMP LL-37 was used as a reference, 44% of the peptide was found after 5 h treatment, but nothing was detected after 24 h (Table 4). Mass spectrometry analysis of Esc(1-21) after 5 h treatment (Fig. 28C) confirmed the presence of two main peaks, corresponding to degradation products of 1,743 Da (fragment 1-16, the most abundant one) and 1,160 Da (fragment 1-11) obtained after cleavage of the peptide bonds between Ile16 and Ser17 and between Ile11 and Lys12, respectively (see table at the bottom of Fig. 28). Additional peaks corresponding to degradation products of 1,096 Da and

1,338 Da were detected after 24 h (Fig. 28E). Differently, in the case of Esc(1-21)-1c, one single peak at 2,185 Da corresponding to the calculated molecular mass of the unmodified peptide was detected within 5 h of enzymatic treatment (Fig. 28D). This is probably due to the presence of D-Ser at position 17 which prevents the enzyme from recognizing its main cleavage site. Only after 24 h, three additional peaks with 1,781 Da, 1,539 Da and 1,041 Da corresponding to different secondary products were visible (Fig. 28F). Fig. 29 shows the mass spectra profile and the corresponding degradation products of LL-37 after human elastase treatment.

Table 4 Peptide amount after 5 and 24 h of incubation with human and *P. aeruginosa* elastase at 37 °C.

Peptide designation	Peptide amount[a] (%)			
	Human elastase		*P. aeruginosa* elastase	
	5 h	24 h	5 h	24 h
Esc(1-21)	0	0	0	0
Esc(1-21)-1c	78	13	91	77
LL-37	44	0	0	0

[a] Peptide amounts were determined by the peak areas of the RP-HPLC relative to those of the control peptide (dissolved in buffer) at 0 min (set as 100%).

Fig. 28 Proteolytic activity of elastase from human neutrophils on both Esc(1-21) and Esc(1-21)-1c. Mass spectrometry profile of the two peptides immediately after enzyme addition (A, B) and after 5 h (C, D) or 24 h (E, F) incubation with the enzyme are reported. Molecular masses for intact peptides and proteolytic fragments produced by elastase treatment are indicated. Insets within each panel show HPLC profile of the sample. The retention time of the intact peptide is also indicated (18 min). The tables show the mass spectra peaks and the corresponding cleavage fragments. Proteolytic sites of the enzyme on the two peptides are indicated by the arrows. D-amino acids are in italics and underlined.
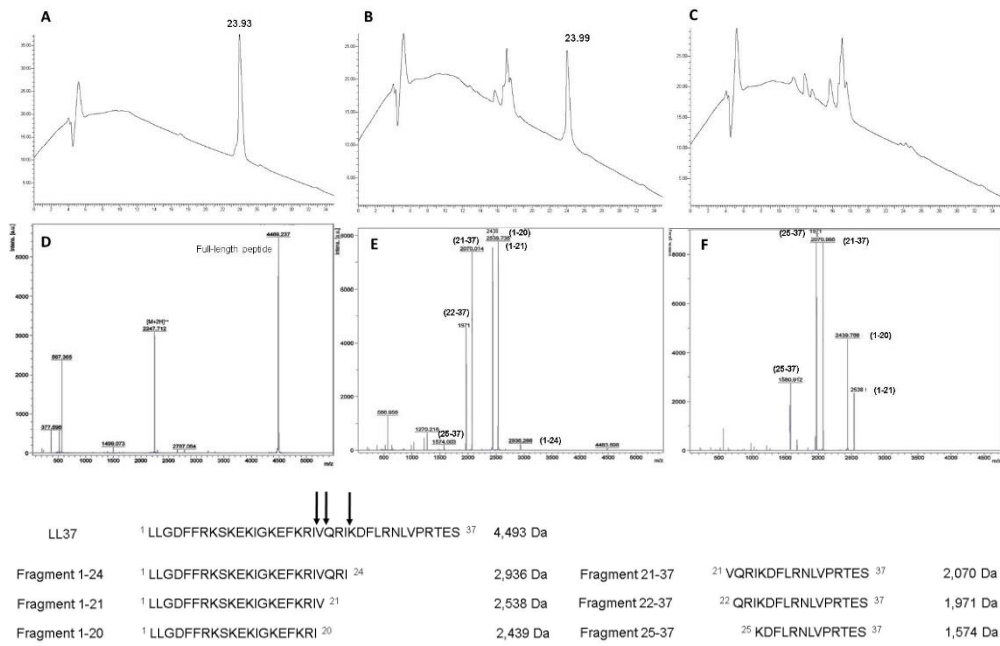
Fig. 29 Proteolytic activity of elastase from human neutrophils on LL-37. HPLC (A-C) and mass spectrometry profiles (D-F) of the peptide immediately after enzyme addition (A, D) and after 5 h (B, E) or 24 h (C, F) incubation with the enzyme are reported. Molecular masses for intact peptides and proteolytic fragments produced by elastase treatment are indicated. Retention time of intact peptide is also indicated (23,9 min). Proteolytic sites of the enzyme on LL-37 are indicated by the arrows.

4.3.2 Peptides' susceptibility to *P. aeruginosa* elastase

When *P. aeruginosa* elastase was used, both LL-37 and Esc(1-21) were completely degraded within 5 h (Table 4), while in the case of Esc(1-21)-1c about 91% and 77% of non-degraded peptide was detected after 5 h and 24 h, respectively (33% after 48 h, data not shown). Interestingly, when the corresponding mass spectra were analyzed, peaks with different molecular masses than those found after treatment with human elastase were distinguished, indicating different cleavage sites by the two elastases either in the two esculentin isoforms (Fig. 30) or in LL-37 (Fig. 31). Indeed, the first principal digestion product obtained after 5 h treatment of Esc(1-21) with this enzyme had a molecular mass of 1,403 Da and corresponded to the 1-13 fragment (Fig. 30C). This points out that the main cleavage site by *Pseudomonas* elastase in Esc(1-21) is between Asn13 and Leu14 (see table at the bottom of Fig. 30) while an additional secondary product corresponding to the fragment 1-10 was visible after 24 h (Fig. 30E). Note that the major peptide binding site of *Pseudomonas* elastase flanks the D-Leu14 in Esc(1-21)-1c, thus preventing its proteolytic cleavage compared to the all-L peptide (Fig. 30D, F).

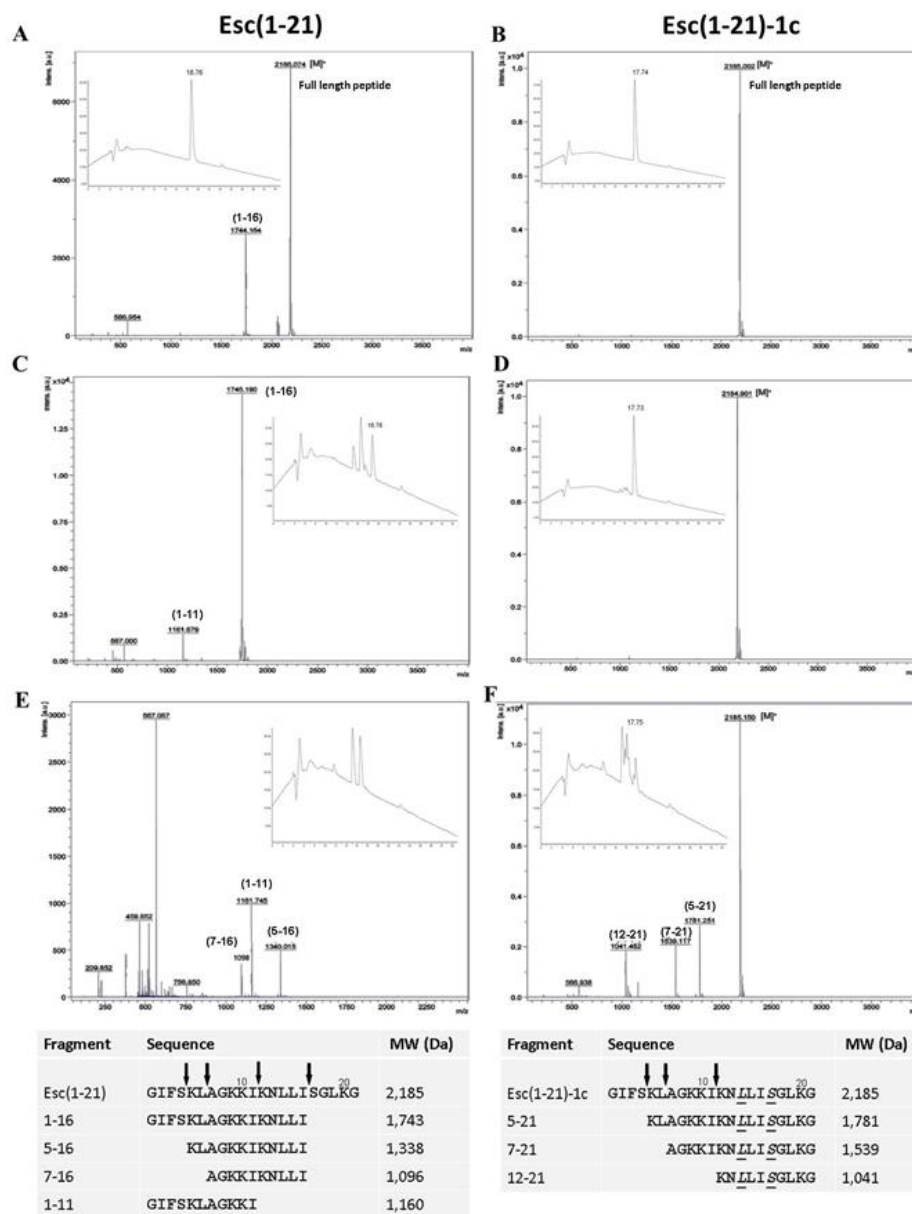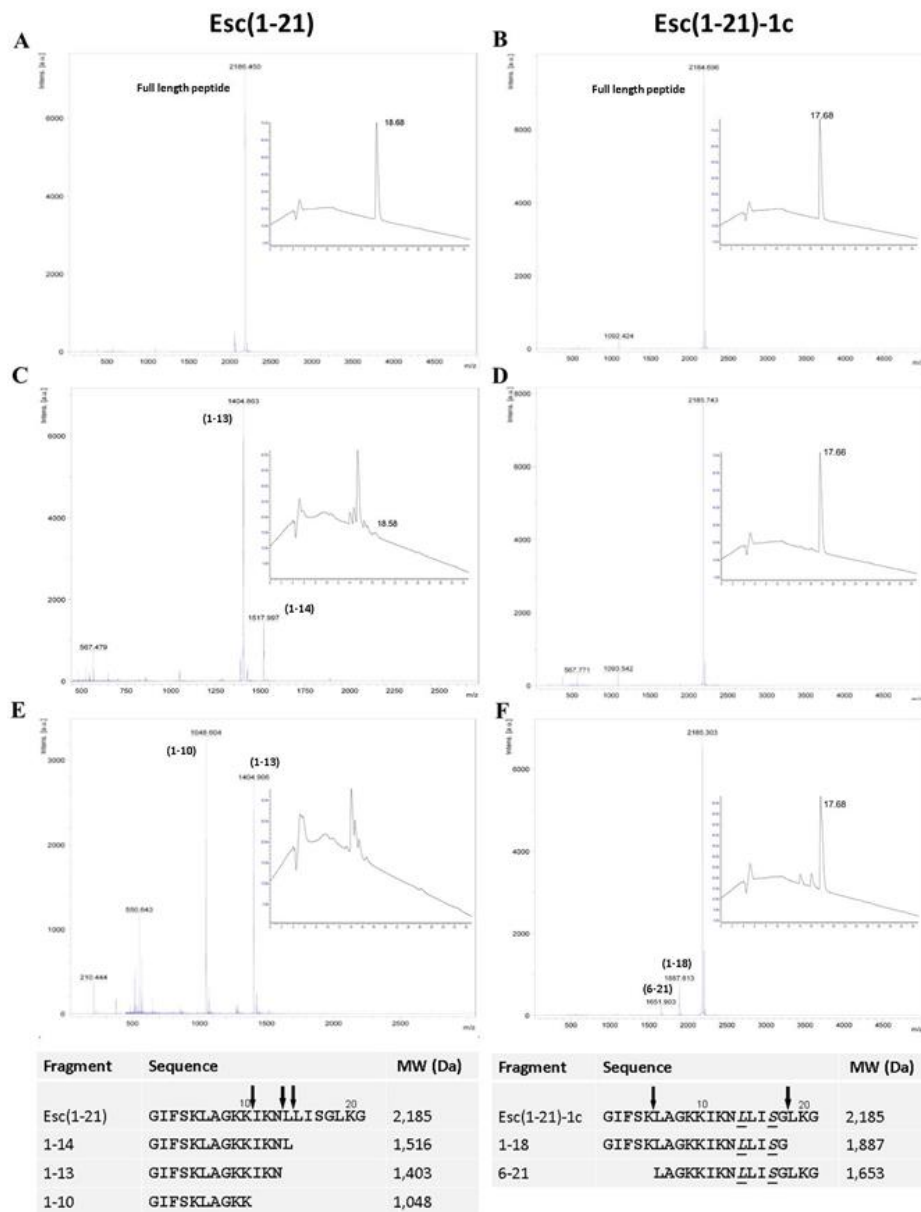**Fig. 30** Proteolytic activity of elastase from *P. aeruginosa* on both Esc(1-21) and Esc(1-21)-1c. Mass spectrometry profile of each peptide immediately after enzyme addition (A, B) and after 5 h (C, D) or 24 h (E, F) incubation with the enzyme are reported. Molecular masses for intact peptides and proteolytic fragments produced by elastase treatment are indicated. Insets within each panel show HPLC profile of the sample. The retention time of the intact peptide is also indicated (18 min). The tables show the mass spectra peaks and the corresponding cleavage fragments. Proteolytic sites of the enzyme on the two peptides are indicated by the arrows. D-amino acids are in italics and underlined.

73
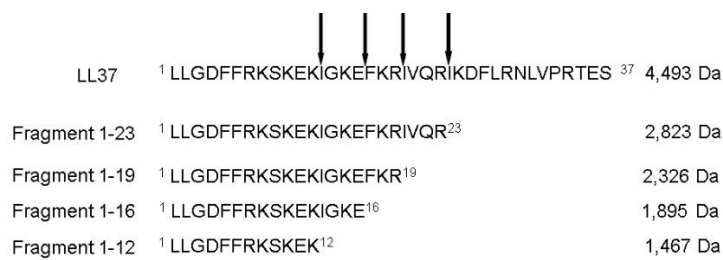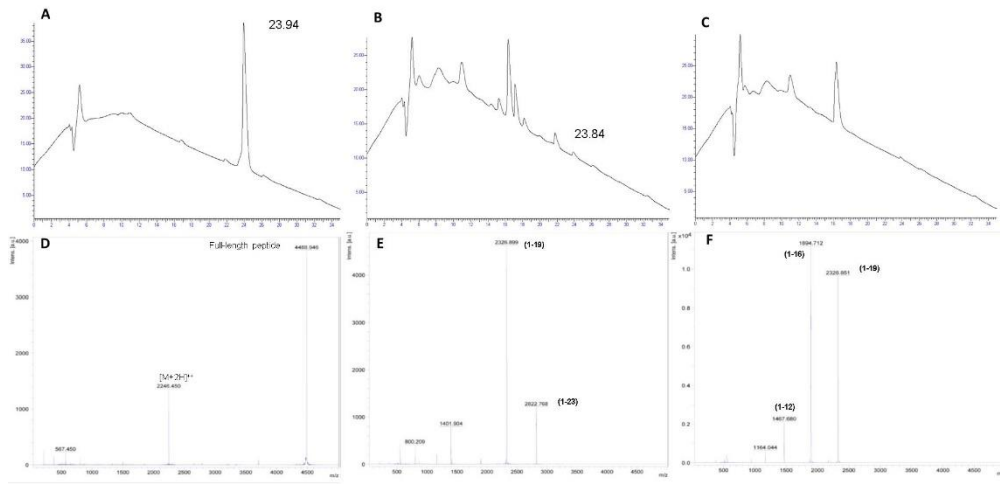
Fig. 31 Proteolytic activity of elastase from *P. aeruginosa* on LL-37. HPLC (A-C) and mass spectrometry profiles (D-F) of the peptide immediately after enzyme addition (A, D) and after 5 h (B, E) or 24 h (C, F) incubation with the enzyme are reported. Molecular masses for intact peptides and proteolytic fragments produced by elastase treatment are indicated. Retention time of intact peptide is also indicated (23,9 min). Proteolytic sites of the enzyme on LL-37 are indicated by the arrows.

4.4 Antimicrobial properties

To enlarge the knowledge on the effect of the two L- to D-amino acids substitution on the antimicrobial properties of the peptide, the killing activity of Esc(1-21) and its diastereomer either against the more dangerous phenotype of *P. aeruginosa* i.e. the biofilm form, or against intracellular *Pseudomonas* cells were analyzed and compared.

74

4.4.1 Activity of the peptides against *P. aeruginosa* biofilm

Esc(1-21) and its diastereomer were tested for their ability to kill the biofilm form of *P. aeruginosa* strains associated with the persistent chronic infection and colonization of lungs in CF patients. Interestingly, the diastereomer Esc(1-21)-1c displayed an equal or higher anti-biofilm activity than the Esc(1-21) (Table 5). More specifically, it gave rise to ~95% reduction in the amount of viable biofilm cells of the CF isolates AA11 and TR1 at 12.5 μM compared to 25 μM found for Esc(1-21), while a concentration of 12.5 μM was needed for both peptides against *P. aeruginosa* ATCC 27853 and KK1 (Table 5).

Table 5 Anti-biofilm activity of Esc(1-21) isomers.

Bacterial strains	Anti-biofilm activity[a] (μM)	
	Esc(1-21)	Esc(1-21)-1c
P. aeruginosa ATCC 27853	12.5	12.5
P. aeruginosa AA11	25	12.5
P. aeruginosa KK1	12.5	12.5
P. aeruginosa TR1	25	12.5

[a] Antibiofilm activity was defined as the lowest peptide concentration that is sufficient to cause 95% reduction in the amount of viable biofilm cells in 2 h. The results are the average of three independent experiments.

4.4.2 Killing activity against *P. aeruginosa* internalized in bronchial epithelial cells

It was reported that the clinical isolate of *P. aeruginosa*, KK1 strain, can invade bronchial cells *in vitro* (Lore et al. 2012). Therefore, the effect of the two peptides on wt-CFBE (Fig. 32A and B) and ΔF508-CFBE cells (Fig. 32C and D) after infection with KK1 was monitored. The number of intracellular

bacteria was expressed either as CFU per sample (Fig. 32A and C) or as percentage (Fig. 32B and D) with respect to the peptide untreated infected cells (control). According to the literature (Ko et al. 1997), *P. aeruginosa* usually targets particular CF epithelial cells rather than the whole population of cells. Note that the number of internalized bacteria (~3,500 CFU) in our control bronchial cells (Fig. 32A and C) well correlated to the previously described uptake of different *P. aeruginosa* strains by CF airway epithelial cells (Pier et al. 1996).

In our experiment, the two peptides were used in Hanks' buffer to better simulate a physiological environment without the presence of cell culture medium components. In wt-CFBE cells, at 5 µM the peptides caused about 15 to 20% killing of intracellular bacteria within 1 h (Fig. 32B). However, the killing effect was more evident in ΔF508-CFBE cells (Fig. 32D); in fact, at 5 µM Esc(1-21) and its diastereomer caused ~40% and 60% decrease in the number of intracellular bacteria, respectively, compared to untreated infected cells. Since the cytotoxicity of Esc(1-21)-1c in Hanks' buffer was significantly lower than that of the all-L isomer (Table 6), the diastereomer could be used at higher concentrations without damaging host epithelial cells. As reported in Fig. 32, 10 µM and 15 µM Esc(1-21)-1c led to about 70% and 90% reduction in the survival of intracellular bacteria in ΔF508-CFBE (Fig. 32D), whereas only ~50% bacterial killing was observed in wt-CFBE cells after exposure to 15 µM Esc(1-21)-1c (Fig. 32B). Note that the higher toxicity of Esc(1-21) to bronchial cells when tested in Hanks' buffer, compared to that in MEMg (Fig. 22), could be due to the absence of medium components that may affect its activity, resulting in lower cytotoxicity.

Fig. 32 Effect of Esc(1-21) and its diastereomer, Esc(1-21)-1c, on the intracellular killing of *P. aeruginosa* KK1 in wt-CFBE (A and B) and ΔF508-CFBE (C and D) cells. About 1×10^5 cells were seeded in 24-well plates and grown to confluence. Afterwards, they were infected with the bacterium for 1 h; nonadherent extracellular bacteria were removed upon antibiotic treatment, and infected cells were left untreated or were treated for 1 h with the peptide at different concentrations, as indicated. Control samples (Ctrl) are peptide-untreated infected cells. The number of intracellular bacteria is expressed either as CFU per sample (A and C) or as a percentage with respect to the control (B and D). All data are the mean from four independent experiments ± SEM. The levels of statistical significance between peptide-treated infected cells and control samples are *P* values of <0.05 (*), <0.001 (***) and <0.0001 (****).

77

Table 6 Peptides' effect on the viability of bronchial epithelial cells in Hank's buffer.

Peptide	Concentration (µM)	Metabolically-active cells (%)	
		wt-CFBE	ΔF508-CFBE
Esc(1-21)	10	62	88
	15	43	71
	30	10	15
Esc(1-21)-1c	10	97	99
	15	94	95
	30	88	92

About 4×10^4 wt-CFBE (A) or ΔF508-CFBE (B) cells were plated in wells of a microtiter plate. After overnight incubation at 37 °C in a 5% CO_2 atmosphere, the medium was removed and replaced with 100 µl Hank's supplemented with the peptides at different concentrations. After 2 h, cell viability was determined by the MTT reduction to insoluble formazan. Cell viability is expressed as percentage with respect to the control (cells not treated with the peptide). All data are the mean of a representative single experiment, performed in triplicates. The SD at each point did not exceed 2.5%.

4.4.3 Peptides' distribution within bronchial cells

The peptides' distribution in wt-CFBE and ΔF508-CFBE cells was then investigated by using rhodamine-labeled peptides and confocal microscopy. Fig. 33A and B show that rho-Esc(1-21) was mainly aligned to the perinuclear region of the cell already after 30 min from its addition, as well as after 24 h. Importantly, to exclude that rhodamine facilitated the uptake of the peptide, the rhodamine dye not conjugated to the peptide was employed. In this case, no fluorescence was observed inside bronchial cells (Fig. 33C and D). Differently, in the case of rho-Esc(1-21)-1c, the fluorescence intensity appeared equally distributed within the cytosol and nucleus (Fig. 33E and F). These results were confirmed by the quantitative analysis of fluorescence intensity of the two peptides between the cytoplasm and nucleus in both types of cells. This indicated a greater distribution of the fluorescent Esc(1-21) in the cytoplasm rather than in the nucleus, after 30 min and 24 h from its

addition, compared to rho-Esc(1-21)-1c, which was almost evenly distributed all over the cells (Fig. 34).
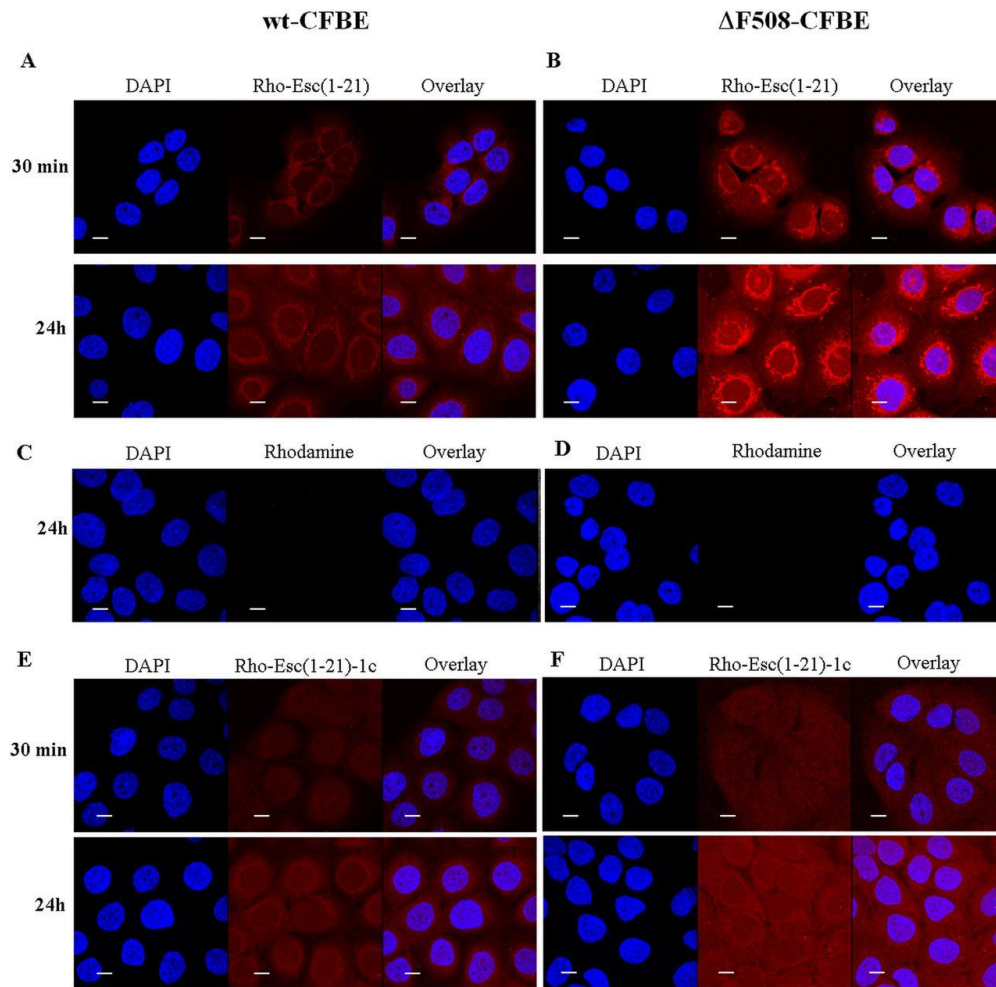
Fig. 33 Confocal laser-scanning microscopy images of wt-CFBE and ΔF508-CFBE cells treated with rho-Esc(1-21) (A and B), rhodamine alone (C and D), or rho-Esc(1-21)-1c (E and F) at different times. After treatment with the peptide (or rhodamine), cells were stained with DAPI for nucleus detection. DAPI fluorescence, rhodamine-labeled peptide (or rhodamine) signal, and the overlay of the two fluorescent probes are shown. All images are *z* sections taken from the mid-cell height. All bars represent 10 µm.

Fig. 34 Peptide distribution between cytoplasm and nucleus in wt-CFBE and ΔF508-CFBE cells. Each peptide was tested on a minimum of 35 cells. The ratio between the fluorescence intensity of rhodamine-labeled peptides in the cytoplasm *versus* the nucleus was calculated for each cell, and the mean ± SEM value was reported on the *y*-axis. If the ratio is equal to 1, this means that the peptide is evenly distributed all over the cell. When the ratio is higher than 1, the amount of fluorescent peptide is higher in the cytoplasm than the nucleus. The level of statistical significance between the calculated ratios of the two peptides at different time points is indicated as a *P* value of <0.001 (***).

4.5 Wound healing activity in bronchial epithelial cells

Since the healing of an infected tissue does not only require the elimination of microbial cells but also the recovery of tissue integrity, the peptides' effect on the migratory activity of bronchial epithelial cells was investigated by means of an *in vitro* pseudo-wound healing assay. Even though wound healing is a complex event which cannot be easily reproduced *in vitro*, studies on the peptides ability in promoting cell migration are indicative of their propensity to accelerate healing of a compromised epithelium. This is an important advantage for the development of a new therapeutic agent to be used not only as antibiotic but also as a multifunctional mediator of the host immune system.

80

4.5.1 Wound-healing activity in the presence of peptides

As shown in Fig. 35, both AMPs stimulated migration of wt-CFBE and ΔF508-CFBE cells by inducing ~100% coverage of the pseudo-wound field produced in the monolayer of bronchial cells by means of the Ibidi culture inserts (see Materials and Methods) within 20 h at an optimal concentration of 10 μM (Fig. 35A and B) or 1 μM (Fig. 35C and D) for Esc(1-21) or its diastereomer, respectively. As shown in Fig. 35 both peptides significantly stimulated migration of bronchial cells at a concentration range from 4 μM to 10 μM and from 1 μM to 10 μM for wt-CFBE and ΔF508-CFBE, respectively.

The results reported in Fig. 35 are supported by the representative micrographs showing wt-CFBE (Fig. 36A) and ΔF508-CFBE (Fig. 36B) pseudo-wound closure before (T0) and 20 h after treatment with each peptide at the optimal concentration (10 μM and 1μM for Esc(1-21) and Esc(1-21)-1c, respectively) in comparison to the untreated control cells.

To further validate that both peptides induced cell migration, fluorescence studies on wt-CFBE cells were performed by using phalloidin for cytoskeleton detection. Untreated control cells appeared rounded, linked together and organized in clusters (Fig. 37A), while typical morphological changes associated with a migratory phenotype, such as cytoplasmic protrusions developing into lamellipodia (Schiller et al. 2010; Mihai et al. 2012; Shaykhiev et al. 2005), were detected in wt-CFBE cells upon treatment with each peptide (at the optimal concentration to induce cell migration) (Fig. 37B and C).

Noteworthy, according to what found in the literature (Trinh et al. 2012), the migration speed of the mutant ΔF508-CFBE resulted to be slower than that of wt-cells. This finding can be related to the defective function of CFTR which

has been shown to play a crucial role in maintaining lung function and wound repair (Trinh et al. 2012) and to cause a reduced lamellipodium area from the leading edge of airway epithelial cells (Schiller et al. 2010).
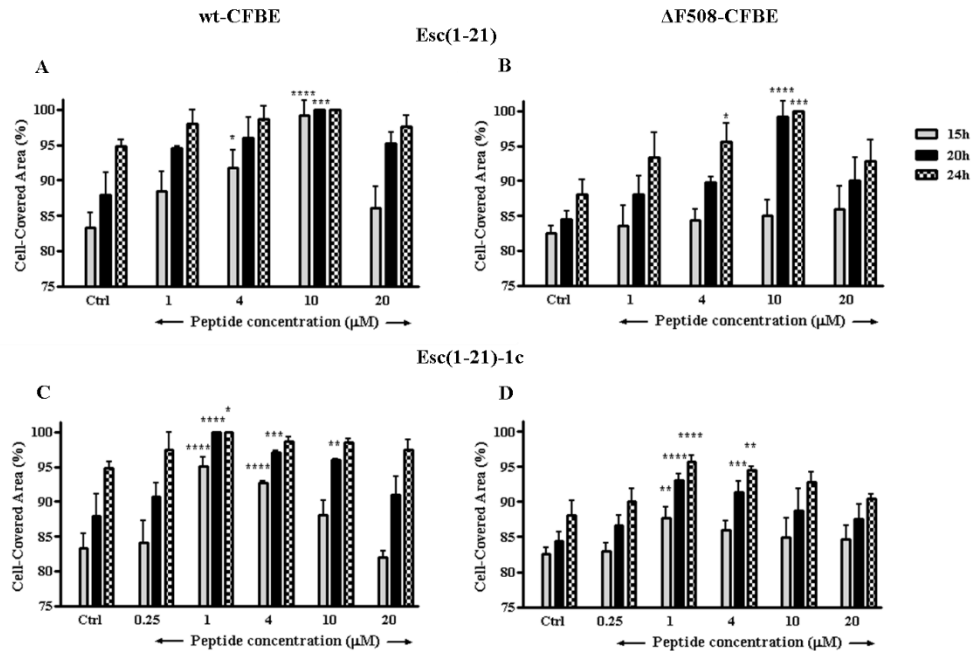
Fig. 35 Effect of Esc(1-21) and Esc(1-21)-1c on the closure of a pseudo-wound field produced in a monolayer of wt-CFBE (A, C) and ΔF508-CFBE (B, D). Cells were seeded in each side of an Ibidi culture insert and grown to confluence; afterwards, they were treated or not with the peptide. Cells were photographed at the time of insert removal and examined for cell migration after 15, 20 and 24 h from peptide addition. The percentage of cell-covered area at each time point is reported on the *y*-axis. Peptide untreated cells were used as control (Ctrl). The data are the mean of four independent experiments ± SEM. The levels of statistical significance between Ctrl and treated samples are *P* values of <0.05 (*), <0.01 (**), <0.001 (***), and <0.0001 (****).
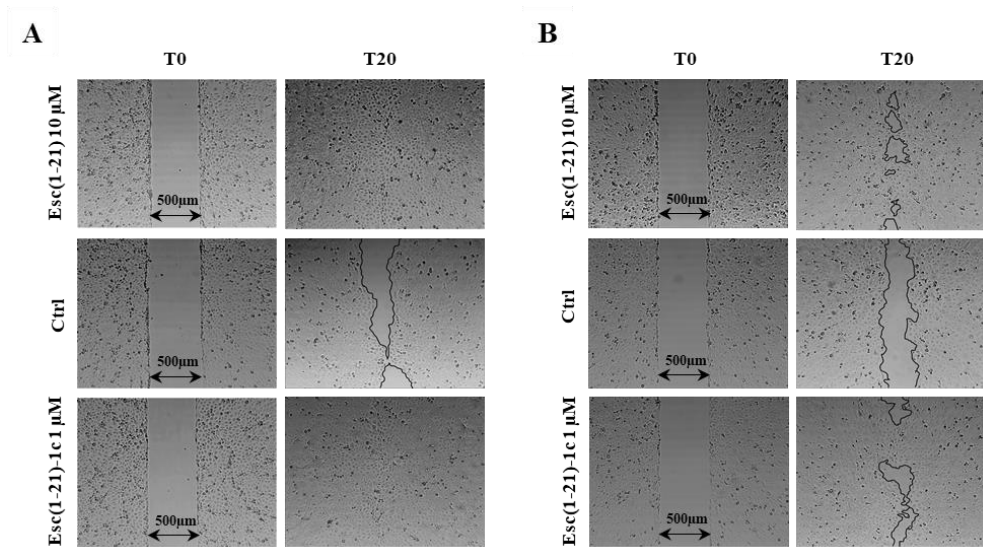
Fig. 36 Micrographs showing representative results of pseudo-wound closure of wt-CFBE (A) and ΔF508-CFBE cells (B) before (T0) and 20 h after treatment with each peptide at the optimal concentration, i.e. 10 µM and 1 µM for Esc(1-21) and Esc(1-21)-1c, respectively, in comparison to the untreated control samples (Ctrl).
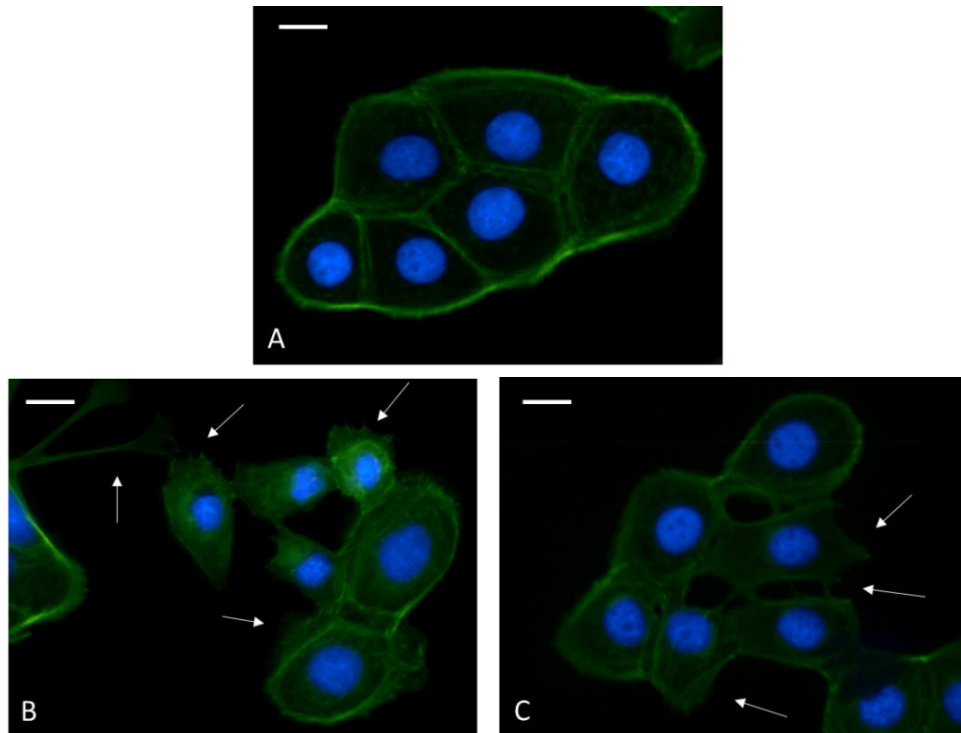
Fig. 37 Effects of Esc(1-21) and Esc(1-21)-1c on the morphology of wt-CFBE cells. After fixation in formaldehyde, cells were stained with DAPI (for nuclei detection) and phalloidin (for cytoskeletal detection). The untreated control cells (A) appeared organized in clusters; those treated with 10 μM Esc(1-21) (B) or 1 μM Esc(1-21)-1c (C) for 24 h showed lamellipodia protrusions indicated by white arrows. Bars are 10 μm long.

4.5.2 Wound-healing activity in the presence of hydroxyurea

To discriminate the contribution of cell migration and proliferation in the peptide-induced recovery of the integrity of wt-CFBE monolayers, the wound healing assay was performed by treating cells with the cell proliferation blocker hydroxyurea (Schiller et al. 2010). As shown in Fig. 38, proliferation of CFBE cells was not essential for the re-epithelialization process. Indeed, no statistically significant difference was found between the percentage of cell-covered area in samples treated with 250 µM hydroxyurea plus 10 µM Esc(1-21) or 1 µM Esc(1-21)-1c and those treated with the peptide alone, at

84

all time intervals. This suggested that the wound healing activity stimulated by both peptides was primarily dependent on the migration activity of CFBE cells.
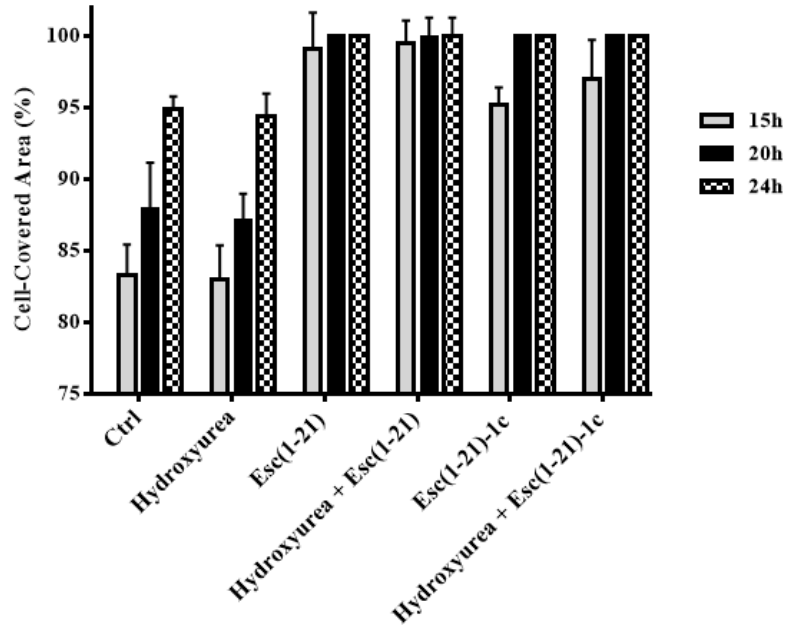
Fig 38 Effect of hydroxyurea on the closure of a pseudo-wound field produced in a monolayer of wt-CFBE cells. Cells were seeded in each side of an Ibidi culture insert and grown to confluence. Afterwards, the cells were treated with 250 μM hydroxyurea and 10 μM Esc(1-21) or 1 μM Esc(1-21)-1c. Some samples were treated with the peptides or hydroxyurea alone. Cells incubated with MEMg were used as control (Ctrl). Cells were photographed at the time of insert removal and examined for cell migration after 15, 20, and 24 h from peptide addition. The percentage of cell-covered area was calculated and reported on the *y-axis*. All data are the mean from four independent experiments ± SEM. No statistically significant difference was found between samples treated with hydroxyurea and peptide and those treated with the peptide alone, at all time intervals.

4.5.3 Role of cell proliferation in the wound healing activity

To confirm whether hydroxyurea and peptides treatment at the concentrations used for the wound healing assay affected or not the proliferation of wt-CFBE cells, measurement of incorporated BrdU into newly synthesized DNA

of proliferating cells, was carried out (see Materials and Methods). The results were expressed as percentage with respect to cells incubated with MEMg (Ctrl).

As expected, hydroxyurea inhibited cell proliferation either when used alone or in combination with each of the two peptides (Fig. 39) in comparison to the control. Otherwise, both peptides alone did not significantly affect cell proliferation compared to the control sample. Similar results were obtained for ΔF508-CFBE cells and therefore are not shown. These data highly contributed to support the notion that the wound healing activity promoted by Esc(1-21) and Esc(1-21)-1c was mainly due to the peptide-induced migration of bronchial epithelial cells rather than to their proliferation.
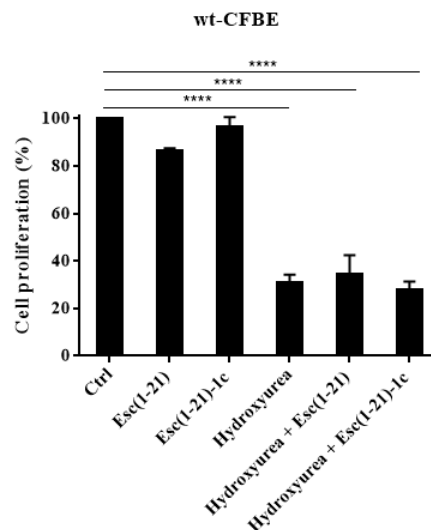
Fig. 39 Effect of hydroxyurea on cell proliferation. About 2×10^4 wt-CFBE cells were seeded in each well of a microtiter plate. After overnight incubation at 37 °C and 5% CO_2 atmosphere, the medium was replaced with 100 µl fresh MEMg supplemented with 10 µM Esc(1-21), 1 µM Esc(1-21)-1c, 250 µM hydroxyurea or the combination peptide and hydroxyurea, for 24 h. Two hours after the start of the treatment, cells were pulsed with BrdU. The percentage of cell proliferation was normalized to that of cells growing in MEMg (100% cell proliferation; Ctrl). All the results are the mean of three independent experiments ± SEM. The level of statistical significance between Ctrl and treated samples is P value of <0.0001 (****).

86

4.5.4 Mechanism of peptide-induced cell migration

The involvement of an EGFR-mediated signaling pathway had been found to control the Esc peptides-induced migration of immortalized human keratinocytes (HaCaT cell line) [please refer to the work attached at the end of the manuscript: "The frog skin-derived antimicrobial peptide esculentin-1a(1-21)NH$_2$ promotes the migration of human HaCaT keratinocytes in an EGF receptor-dependent manner: a novel promoter of human skin wound healing?" By Di Grazia A, Cappiello F, Imanishi A, Mastrofrancesco A, Picardo M, Paus R, Mangoni ML]. Since EGFR is also expressed in the airways of healthy or CF human subjects (Kim et al. 2013) and plays a crucial role in the repair of damaged airway epithelium (Burgel and Nadel 2004), studies aimed at elucidating whether migration of CFBE cells induced by the peptides was a process mediated by activation of EGFR, were carried out. To this purpose, cells were pretreated with 5 µM of the tyrosine inhibitor of EGFR, AG1478 (Gan et al. 2007), before adding each of the two peptides at their optimal concentrations in stimulating bronchial cell migration [10 µM and 1 µM for Esc(1-21) and Esc(1-21)-1c, respectively]. As shown in Fig. 40, the peptide-promoted migration of bronchial cells was significantly impaired by inhibiting EGFR-mediated signaling. This is indicated by the significantly lower percentages of cell-covered area in AG1478-pretreated samples at all time intervals (15 h, 20 h and 24 h) compared to those obtained in bronchial cells which were not pretreated with AG1478 before peptide addition. Overall, these findings clearly highlighted that the peptides-induced re-epithelialization of bronchial epithelium implies EGFR activation.

Furthermore, to assess whether activation of EGFR required metalloproteinases, which are known to cleave membrane-anchored EGFR ligands and to be involved in EGFR trans-activation (Tjabringa et al. 2003),

the effect of a broad-spectrum MMP inhibitor, GM6001 (Stoll et al. 2012; He et al. 2008), was analyzed on the peptide-induced cell migration.

Analogously to what found for AG1478, pretreatment of bronchial cells with 25 µM GM6001 counteracted the peptide-induced closure of the pseudo-wound field produced in the cell monolayer (Fig. 40). This supports the contribution of metalloproteinase activity in the peptide-induced stimulation of bronchial cells migration.

Similar results were obtained with the mutant ΔF508-CFBE cells and therefore are not shown.
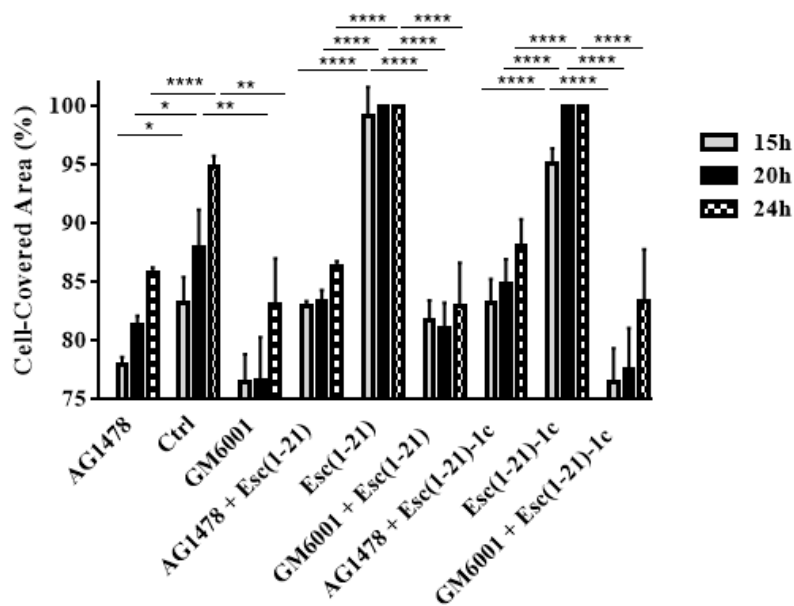
Fig. 40 Effect of AG1478 and GM6001 inhibitors on the peptide-mediated migration of wt-CFBE cells. Before removing the Ibidi culture insert, cells were preincubated with 5 µM AG1478 or 25 µM GM6001 for 30 min and subsequently treated with 10 µM Esc(1-21) or 1 µM Esc(1-21)-1c. Some samples were treated with the peptide or inhibitors alone at the same concentration and cells incubated with MEMg were used as a control (Ctrl). Samples were photographed at different time intervals as indicated and the percentage of cell-covered area was calculated and reported on the *y-axis*. The data are the mean from four independent experiments ± SEM. The levels of statistical significance between samples pretreated with AG1478 or GM6001 and Ctrl or between samples pretreated with AG1478 or GM6001 before incubation with the peptide and those treated with the peptide alone at the corresponding time intervals are *P* values of <0.05 (*), <0.01 (**) and <0.0001 (****).

4.6 Effect of the peptides on the migration of adenocarcinoma human alveolar epithelial cells (A549)

Similar to what found for CFBE, the two peptides were able to stimulate migration of A549 cells, promoting the closure of a gap area produced in a monolayer of these cells at optimal concentrations of 10 µM and 4 µM for Esc(1-21) and (1-21)-1c, respectively. Also in this case the cell migration activity induced by both peptides resulted to be dependent on EGFR-signaling pathway [please refer to the work attached at the end of the manuscript: "D-Amino acids incorporation in the frog skin-derived peptide esculentin-1a(1-21)NH$_2$ is beneficial for its multiple functions." By Di Grazia A, Cappiello F, Cohen H, Casciaro B, Luca V, Pini A, Di YP, Shai Y, Mangoni ML].

4.6.1 Morphological studies

Also in this case, fluorescence microscopy was used to further assess whether the peptide-induced cell migration was accompanied by morphological changes. As explained in Materials and Methods section, A549 cells were stained with Hoechst and phalloidin for nuclei and cytoskeleton detection, respectively. Fig. 41 shows that A549 control cells (panel A) and those treated with AG1478 (panel A') appeared organized into clusters with a regular morphological shape, characteristic of epithelial cells with poor motility (Lauand et al. 2013). Differently, cells treated either with Esc(1-21) or Esc(1-21)-1c appeared elongated, with an altered organization of actin filaments and cytoplasmic protrusions, polarized and separated one from each other (Fig. 41 panels B and B', respectively), which is consistent with an enhanced cell motility. However, these morphological changes were not identified in A549 cells treated with peptides after exposure to AG1478 (Fig.

89

41 panels C, C'), supporting the participation of EGFR in the esculentin-elicited migration of alveolar epithelial cells.
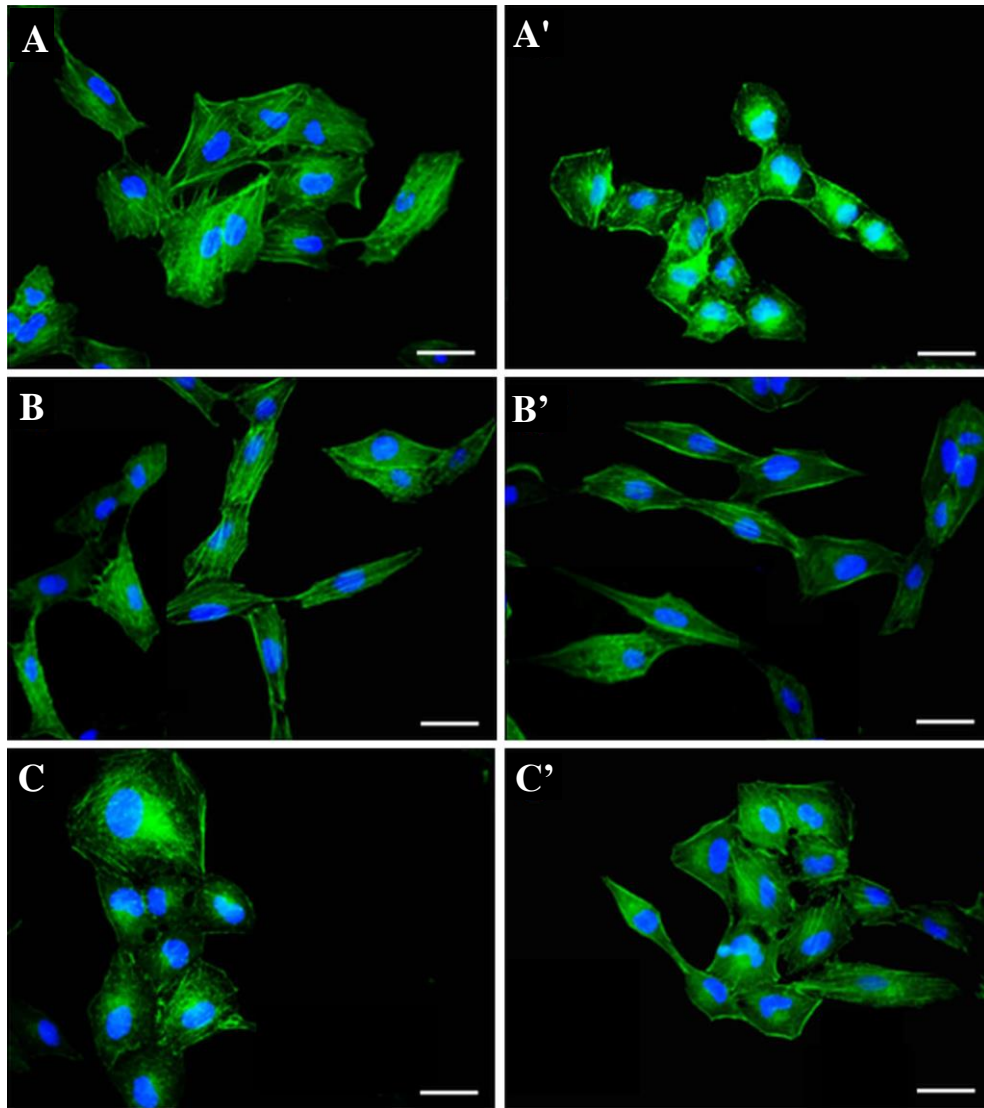
Fig. 41 Effects of Esc(1-21) and Esc(1-21)-1c on the morphology of A549 cells. After fixation in formaldehyde, cells were stained with Hoechst (for nuclei detection) and phalloidin (for cytoskeletal detection). The untreated control cells (panel A) as well as those treated with 0.2 μM AG1478 for 15 min (panel A') appeared organized in clusters. The Esc(1-21) and Esc(1-21)-1c-treated cells (panels B and B' respectively) appeared elongated with cytoplasmic protrusions. These alterations were not identified in A549 cells pretreated with AG1478 and subsequently exposed to Esc(1-21) and Esc(1-21)-1c (panels C and C', respectively). Bars are 20 μm long.

4.6.2 Cell anchorage-independent growth

To verify if peptides treatment of A549 cells promoted an anchoring-independent cell growth, a soft agar assay for colony formation was carried out.

A549 cells were treated for 24 h with 10 µM Esc(1-21) or 4 µM Esc(1-21)-1c in DMEMg supplemented with 2% FBS to reproduce the conditions used in the wound healing assays. Indeed, these two peptide concentrations were found to be optimal to stimulate A549 cell migration [please refer to the work attached at the end of the manuscript: "D-Amino acids incorporation in the frog skin-derived peptide esculentin-1a(1-21)NH$_2$ is beneficial for its multiple functions." By Di Grazia A, Cappiello F, Cohen H, Casciaro B, Luca V, Pini A, Di YP, Shai Y, Mangoni ML]. As shown in Fig. 42, treatment of cells with each peptide did not induce any increase in the number of single colonies in soft-agar. The results were expressed as percentage of colonies formation with respect to the peptide-untreated control sample (100% colonies).

These findings indicated that the peptide-induced migration of A549 would not translate into cells invasiveness and/or metastasis.
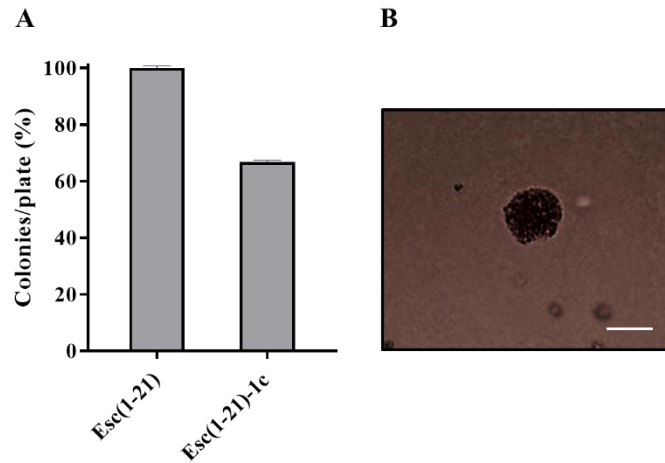
Fig. 42 A549 cells, previously treated with 10 µM Esc(1-21) or 4 µM Esc(1-21)-1c in DMEMg supplemented with 2% FBS, were grown at a density of 15,000 cells/plate in soft agar medium. After 14 days, formed colonies were stained with 0.001% crystal violet and counted. Untreated A549 cells were used as control (100% colonies/plate). The data are the mean from three independent experiments ± SEM (A). Image of an A549 colony captured with a 4× objective using an inverted microscope (Olympus CKX41) and photographed with a Color View II digital camera. Bar is 80 µm long (B).

4.7 Anti-inflammatory activity

The LPS aggregates are recognized as pathogen-associated molecular patterns by specific receptors which are expressed on innate immune cells (e.g. monocytes and macrophages), promoting their activation. This is characterized by increased phagocytic activity and secretion of pro-inflammatory cytokines such as tumor necrosis factor-alpha (TNF-α) (Woltmann et al. 1998; Cohen 2002; Lee and Yang 2013).

Despite activation of the immune system is beneficial, its overstimulation characterized by increased production of various pro-inflammatory agents is recognized as a key factor for lung deterioration (Nathan and Ding 2010). In addition, high levels of TNF-α can lead to septic shock syndrome (Rittirsch et al. 2008).

Interestingly, beside displaying antimicrobial activity, several AMPs have been found to detoxify LPS and/or to reduce the expression of cyclooxygenase-2 (COX-2) which is an important enzyme controlling the production of several pro-inflammatory mediators (Rosenfeld et al. 2008; Fabisiak et al. 2016; Brunetti et al. 2016). Therefore, the discovery of alternative antimicrobials with the potential to both kill bacteria and to display an anti-inflammatory activity is extremely helpful.

4.7.1 Neutralization of the toxic effect of *P. aeruginosa* lipopolysaccharide

To further investigate additional host-defense properties, Esc(1-21) and its diastereomer were tested for their ability to inhibit the secretion of TNF-α from murine macrophages after activation with LPS (10 ng/ml) from *P. aeruginosa,* as already observed for some human AMPs (Hancock et al. 2012; Pulido et al. 2012). The results demonstrated a dose-dependent effect in the inhibition of TNF-α release; 80 and 90% inhibition at 10 and 20 μM Esc(1-21), respectively, compared to that of LPS alone (Fig. 43). In comparison, a weaker activity was detected with the diastereomer Esc(1-21)-1c; 20 and 30% inhibition at 10 and 20 μM, respectively (Fig. 43).
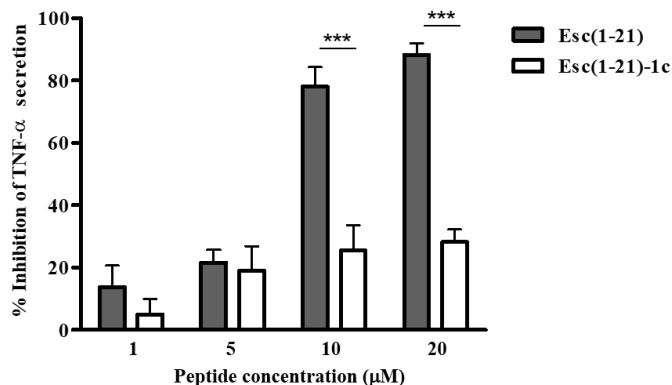
Fig. 43 The effect of peptides on the secretion of TNF-α from murine macrophages. RAW 264.7 macrophages stimulated with LPS (10 ng/ml) derived from *P. aeruginosa* 10 in the presence of 1, 5, 10 and 20 μM Esc(1-21) or Esc(1-21)-1c for 4 h at 37 °C and 5% CO_2. The percentage of inhibition of TNF-α release was normalized to that of macrophages stimulated with LPS without peptides (0% inhibition). All the results are the mean of three independent experiments ± SEM. The level of statistical significance between samples treated with Esc(1-21) and Esc(1-21)-1c is *P* value of <0.001 (***).

To get insight into the molecular mechanism underlying the LPS-detoxification activity of the two peptides and whether these latter competed with LPS for binding to the LPS receptor, macrophages were first treated with the peptides and then exposed to LPS. As shown in Table 7 an invariant secretion of TNF-α was observed compared to what found for the control sample (cells stimulated with LPS, 100% TNF-α secretion).

Table 7 Effect of each peptide on the secretion of TNF-α from murine macrophages RAW 264.7 macrophages after 2 h treatment at 37 °C.

Peptide concentration (μM)	TNF-α secretion (%)	
	Esc(1-21)	Esc(1-21)-1c
1	96	92
5	97	99
10	92	98
20	105	97

Esc(1-21) or Esc(1-21)-1c at 1, 5, 10 and 20 μM were used. After 2 h incubation peptides were removed and the cells were stimulated with LPS (10 ng/ml) derived from *P. aeruginosa* 10 for 5 h. The percentage of TNF-α secretion was normalized to that of macrophages stimulated with LPS without peptide (100% secretion). All the results are the mean of a representative single experiment, performed in triplicates. The SD at each point did not exceed 2.5%.

These results suggested that the detoxification of LPS was presumably due to a physical interaction of the peptides with LPS. One possible mechanism of action in which AMPs neutralize LPS consists in the breakage of LPS aggregates into smaller-size particles (Rosenfeld et al. 2006a, b; Bhunia et al. 2011). This would prevent LPS from binding to LPS binding protein (LBP) and therefore the activation of the host immune cells.

4.7.2 Effect of the peptides on the structural organization of lipopolysaccharide

Light scattering experiments were used to understand whether the peptides could alter the micelle morphology of LPS. Fig. 44 shows that LPS from *Pseudomonas* was poly-dispersed in solution with major size-populations having hydrodynamic radius centered at 355 nm. When LPS was incubated with Esc(1-21) a shift of the average size of LPS to a lower value centered at 67.7 nm was observed, compared to the diastereomer Esc(1-21)-1c which induced a larger LPS mean diameter centered at 116, indicating weaker

potency to dissociate LPS aggregates. These experiments were performed in collaboration with the group of Prof. Shai (Department of Biological Chemistry, The Weizmann Institute of Science, Israel).
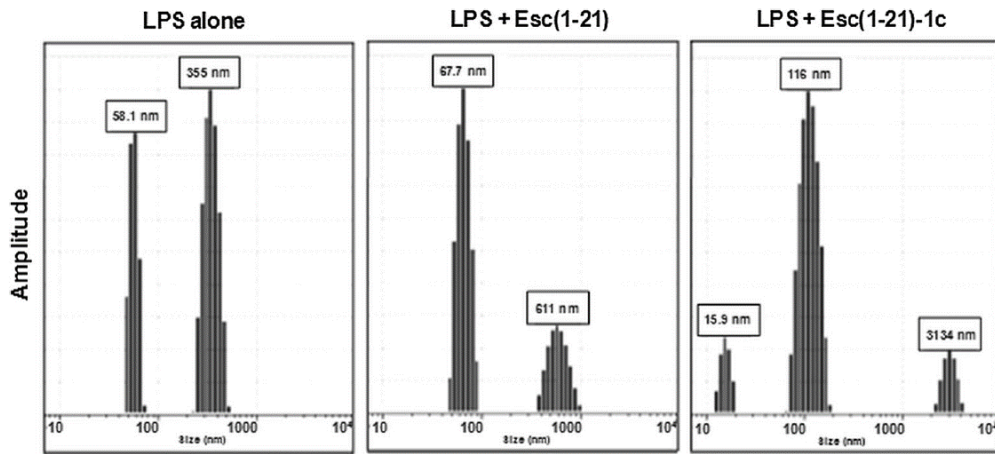
Fig. 44 The effect of peptides on the structural organization of LPS micelles. Light scattering of LPS from *P. aeruginosa* 10 in water before and after incubation with Esc(1-21) or Esc(1-21)-1c at equimolar concentration.

4.7.3 Effect of the peptides on the expression level of cyclooxigenase-2 in macrophages activated by *P. aeruginosa* lipopolysaccharide

During an inflammatory process, large amounts of pro-inflammatory mediators are generated by the cyclooxygenase-2 (COX-2), which is induced in immune cells, such as macrophages, in response to infection, injury or other stresses (Kim et al. 2007; Kumar and Abraham 2017; Lee et al. 2017). Therefore, the production of COX-2 was evaluated in macrophages stimulated by LPS from *Pseudomonas aeruginosa* (20 ng/ml), with or without Esc(1-21) or Esc(1-21)-1c at different concentrations. The results obtained by western blot analysis are reported in Fig. 45. They show that LPS induced an increase of COX-2 expression, whereas Esc(1-21) (Fig. 45A and B) and its diastereomer (Fig. 45C and D) led to a significant reduction in the expression level of COX-2, in a dose-dependent manner. However, the inhibitory effect was less pronounced for the diastereomer Esc(1-21)-1c as indicated by the higher peptide concentrations needed to achieve the same results as those found for Esc(1-21). These data are in line with those observed for the inhibition of TNF-α secretion.
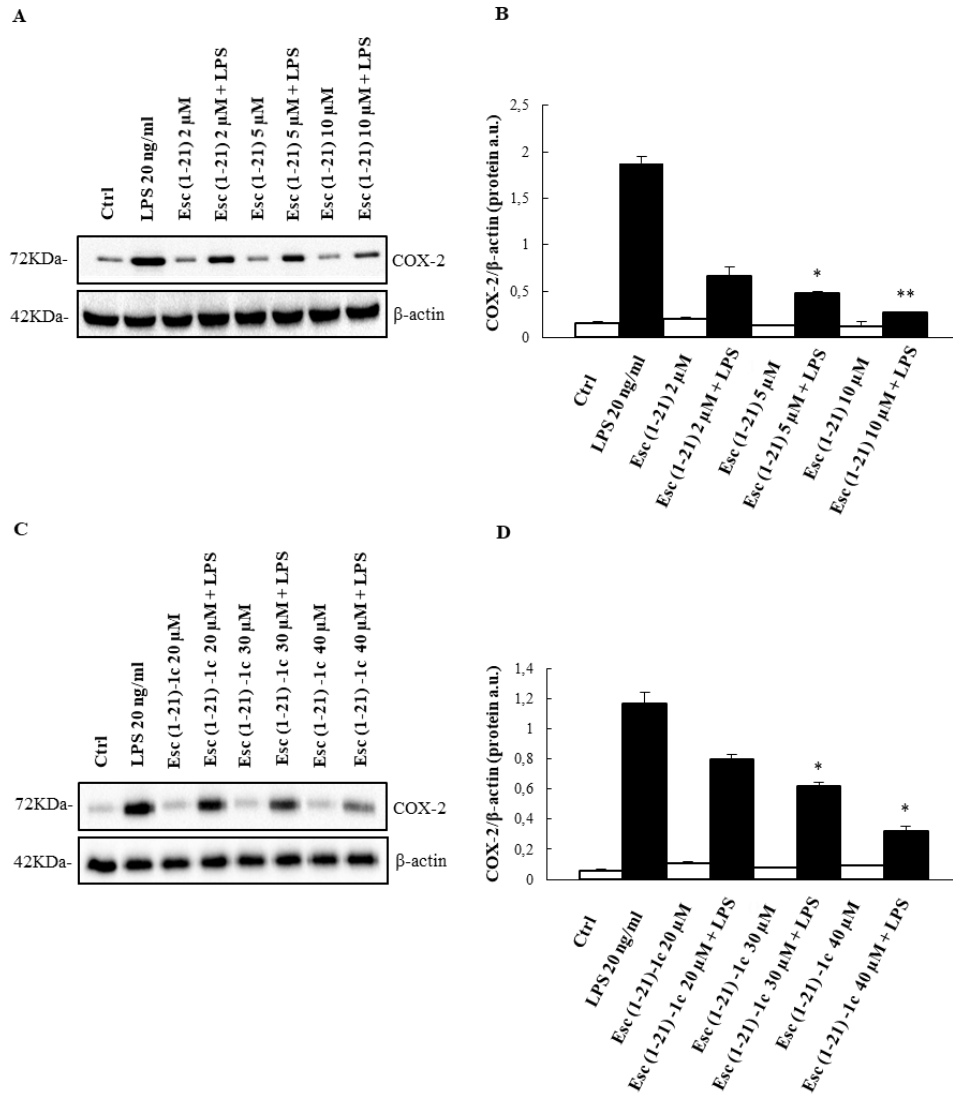
Fig. 45 Effect of Esc(1-21) (A and B) or Esc(1-21)-1c (C and D) on LPS-induced expression of COX-2 in murine RAW 264.7 cells. Cells were stimulated with: LPS from *Pseudomonas aeruginosa* (20 ng/ml), peptides or LPS and peptides as indicated for 4 h. Relative COX-2 levels were analyzed by western blot, normalized to β-actin and quantified by densitometry by using ImageJ software. Data are presented as the mean ± SD of three independent experiments. The levels of statistical significance between samples treated with LPS and LPS+peptide are *P* values of <0.05 (*) and <0.01 (**).

98

5. Discussion

Multidrug-resistant (MDR) bacterial infections represent a serious worldwide health hazard causing almost 50,000 deaths per year in Europe and in the US. Since this number is expected to grow up to tenfold by 2050 (Grundmann et al. 2011; O'Neill 2016), the discovery of novel antimicrobial agents is an urgent need. In this regard AMPs represent a promising alternative to the commonly used drugs.

Among microorganisms that develop resistance to the available antibiotics there is the opportunistic Gram-negative bacterium *P. aeruginosa*. It is able to colonize multiple tissues and to cause persistent chronic or lethal infections, such as those associated with the respiratory tract of CF patients. In fact, *P. aeruginosa* can create sessile communities, defined biofilms, which are extremely difficult to eradicate (Mangoni et al. 2015; Larrosa et al. 2012; Millar et al. 2009).

With the aim to develop new anti-infective agents with a different mechanism of action, the biological properties of two AMPs, Esc(1-21) and Esc(1-21)-1c, were studied and compared.

Esc(1-21) is a derivative of the frog skin AMP esculentin-1a. It has a broad spectrum of activity, especially against Gram-negative bacteria including both the planktonic and the sessile form of *P. aeruginosa* (Luca et al. 2013).

Esc(1-21)-1c is a diastereomer of Esc(1-21) which was designed by replacing two L-amino acids with the corresponding D-enantiomers. These modifications had the purpose to overcome those unfavorable aspects for the therapeutic development of AMPs, that are the cytotoxicity and the susceptibility to proteolytic degradation (Hancock and Sahl 2006; Aoki and Ueda 2013).

99

Cell viability assays initially performed on eukaryotic cells showed that the diastereomer is significantly less toxic than Esc(1-21) towards both bronchial epithelial cells and murine macrophages.

Structural studies, performed by CD analysis, showed that both peptides adopt an α-helix conformation in zwitterionic and anionic environments, e.g. DPC and SDS micelles, that mimic the neutral membrane of mammalian cells and the anionic bacterial membrane, respectively. However, compared to Esc(1-21), the presence of two D-enantiomers in the C-terminal region of the all-L peptide, significantly reduces its α-helical content, especially in zwitterionic lipids. These results are in line with the lower cytotoxicity of Esc(1-21)-1c compared to Esc(1-21); indeed, numerous studies based on several native AMPs have underlined the importance of an amphipathic α-helical structure for mammalian cell lysis (Pouny et al. 1992; Gazit et al. 1994; Strahilevitz et al. 1994). Moreover, the lower cytotoxicity of the diastereomer reflects in a weaker ability to destabilize zwitterionic membranes as demonstrated by the results of CxF leakage assay from neutral liposomes. This is also in agreement with previous studies (Carotenuto et al. 2008; Mangoni et al. 2011) showing a deeper insertion of peptides with a higher helical content into the hydrophobic core of mammalian cell membranes.

The data obtained by CD spectra analysis are also supported by solution NMR studies in DPC micelles: an α-helical structure is preserved along the entire amino acid sequence of Esc(1-21), while a highly flexible C-terminal arm is present in Esc(1-21)-1c. This is due to the presence of D-amino acids at 14th and 17th position, which break the integrity of the α-helix made of L-amino acids, as also observed for other naturally occurring AMPs, e.g.

magainin, cytolysin and melittin (Shai and Oren 1996; Saravanan et al. 2010; Wieprecht et al. 1999).

The lung environment of CF patients is rich in proteases, i.e., elastase from host neutrophils and also from *P. aeruginosa*.

Neutrophils elastase degrades almost all extracellular matrix and key plasma proteins, upregulates pro-inflammatory cytokine expression and is required for maximal intracellular killing of Gram-negative bacteria by neutrophils (Kelly et al. 2008). *P. aeruginosa* elastase is one of the extracellular and cell-associated virulence factors that contributes to tissue damage in *Pseudomonas* infections; it degrades elastin, collagen, several cytokines as well as several complement components (Mariencheck et al. 2003).

Interestingly, the incorporation of two D-amino acids at specific positions in Esc(1-21) makes the peptide significantly more resistant to degradation by both human and bacterial elastases. Moreover, the diastereomer is also more resistant than the human cathelicidin LL-37, an antimicrobial peptide which is found in granules of polymorphonuclear leukocytes and keratinocytes and involved in mammalian innate immune defense against invasive bacterial infections (Zanetti 2004).

This result can explain the better effectiveness of the diastereomer, compared to the all-L peptide, against the biofilm form of *P. aeruginosa*. Indeed, proteases are mainly produced by bacteria in their biofilm form. Thanks to its higher biostability, the diastereomer would have a prolonged residence time with a resulting higher antibacterial activity in comparison to Esc(1-21), which would be rapidly degraded. In addition, it is worthwhile noting that D-amino acids have been reported to promote the disassembly of the extracellular matrix of biofilm cells (Romero et al. 2011; Segev-Zarko et al. 2015).

101

The diastereomer was also found to be more efficient than the all-L peptide in killing *Pseudomonas* internalized in bronchial cells either with a functional or a mutated CFTR. Furthermore, this activity is comparable to that of ciprofloxacin (Chadwick and Mellersh 1987), one of the few conventional antibiotics (fluoroquinolones) able to penetrate the plasma membrane (Bonventre et al. 1967; Brayton et al. 2002) and that is currently used against *P. aeruginosa* despite its toxicity (Ilgin et al. 2015).

As revealed by confocal microscopy analysis, rho-Esc(1-21) has a prevalent perinuclear distribution in bronchial cells, while rho-Esc(1-21)-1c appears equally distributed within the cytosol and nucleus.

Therefore, it is likely that the clearance of intracellular *Pseudomonas* is mainly due to the interaction of the internalized peptides with the intracellular bacterial cells. The weaker efficacy of the all-L peptide Esc(1-21) in killing intracellular bacteria compared to its diastereomer may be due either to its stereospecific binding to intracellular components or to its higher susceptibility to virulence factors, i.e. proteases released from the intracellular bacteria. However, it has to be underlined that rhodamine-labelled peptides were used for confocal microscopy studies and that the fluorescence intensity cannot indicate if the peptide is intact, partially degraded or present in an inactive form. It cannot be excluded that additional mechanisms of host cell protection against microbial pathogens are also involved in the clearance of intracellular microorganisms.

All these data contributed to justify the higher *in vivo* antipseudomonal activity of the diastereomer Esc(1-21)-1c compared to that of the all-L peptide and LL-37 in a murine model of acute lung infection upon intratracheal instillation (Chen et al. 2017).

Another relevant aspect to take into consideration for the development of new anti-infective agents is their ability to promote re-epithelialization of a compromised epithelium. Indeed, healing of an infected tissue does not only require elimination of microbial pathogens but also recovery of the tissue integrity along with its barrier function preventing pathogens penetration. It is known that a persistent lung infection by *Pseudomonas* (especially in CF patients) results in the development of lesions (Goldberg and Pier 2000). Therefore, the capacity of drugs to accelerate wound repair of the bronchial epithelium is extremely advantageous to restore lung functionality. This is very important mainly in CF patients where wound healing processes are significantly slow.

Wound healing in animals is an essential process for the repair and restoration of tissues function after injury or infections. This quite complex event occurs in distinct yet overlapping phases that include inflammation, cell migration, cell proliferation, epithelialization, angiogenesis and tissue remodeling (Mangoni et al. 2016). Therefore, wound healing is very difficult to simulate *in vitro* because of the absence of different cell types, the interaction between them and the production of cellular debris that greatly affect the tissue repair process. However, the use of special silicone inserts (Ibidi) allows to create a pseudo-wound in the monolayer of epithelial cells with a well-defined width. This provides an optimal experimental condition for a quantitative and reproducible evaluation of cell migration. In addition, in contrast to the traditional "scratch" method, based on the creation of a pseudo-wound by using plastic tips, such inserts do not alter the plastic surface on which the cells adhere, thus avoiding a possible variation of the cell migration results.

As described for A549 cells [please refer to the work attached at the end of the manuscript: "D-Amino acids incorporation in the frog skin-derived peptide esculentin-1a(1-21)NH$_2$ is beneficial for its multiple functions." By Di Grazia A, Cappiello F, Cohen H, Casciaro B, Luca V, Pini A, Di YP, Shai Y, Mangoni ML], the diastereomer is more effective in inducing re-epithelialization of the wounded area, with a mechanism that implies an EGFR mediated signaling pathway.

EGF receptors are located in ordered lipid domains called lipid rafts (Pike et al. 2005) whose alteration may inhibit ligands binding to EGFR and its activation. The lower wound healing efficacy of the more helical Esc(1-21) compared to its diastereomer may be a consequence of its stronger ability in perturbing zwitterionic phospholipid membranes. Nevertheless, the different wound-healing activity between the two peptides may also be related to their different binding affinity to target receptors, such as membrane-bound metalloproteases (Kim et al. 2013; Peschon et al. 1998). Note that our *in vitro* assays have indicated trans-activation of EGFR mediated by metalloproteinases in the peptide-induced migration of epithelial bronchial cells. This was previously demonstrated also for HaCaT cells [please refer to the work attached at the end of the manuscript: "The frog skin-derived antimicrobial peptide esculentin-1a(1-21)NH$_2$ promotes the migration of human HaCaT keratinocytes in an EGF receptor-dependent manner: a novel promoter of human skin wound healing?" By Di Grazia A, Cappiello F, Imanishi A, Mastrofrancesco A, Picardo M, Paus R, Mangoni ML]. Furthermore, the bronchial cells migration may be controlled by alternative processes that imply, for example, CFTR (especially in mutant cells) (Hussain et al. 2014).

Importantly, in line with what lately observed for HaCaT cells and A549 cells [please refer to the work attached at the end of the manuscript: "D-Amino acids incorporation in the frog skin-derived peptide esculentin-1a(1-21)NH$_2$ is beneficial for its multiple functions." By Di Grazia A, Cappiello F, Cohen H, Casciaro B, Luca V, Pini A, Di YP, Shai Y, Mangoni ML], the wound closure driven by both esculentin peptides does not appear to be affected by cell proliferation, but rather depends on the cell migration activity. Indeed, bronchial cells exposed to the cell-proliferation inhibitor hydroxyurea in combination with each peptide have the same migration behavior as that obtained when the peptides are used alone.

These data are further corroborated by the typical morphological changes of migrating cells (Schiller et al. 2010; Mihai et al. 2012; Shaykhiev et al. 2005), observed in both A549 and CFBE cells. Remarkably, we can rule out that the peptide-induced cell migration promotes an invasive behavior of the cells and/or their malignant transformation. Indeed, no anchoring-independent cell growth is detected in A549 cells upon their exposure to the peptides.

It is well known that antibiotic treatment of microbial infections is frequently associated with the release of bacterial cell wall components, such as LPS, in the case of Gram-negative bacteria, or lipoteichoic acid (LTA), in the case of Gram-positive bacteria. These molecules stimulate the innate immune cells (mainly mononuclear cells and macrophages), inducing the secretion of pro-inflammatory cytokines (e.g., tumor necrosis factor alpha, TNF-α). High levels of TNF-α can lead to deterioration of lung tissue or, to sepsis in most serious cases (Miller et al. 2005; Hancock and Sahl 2006).

Esc(1-21)-1c is able to inhibit the release of TNF-α from macrophages activated by *P. aeruginosa* LPS, albeit to a lesser extent compared to the all-L

105

peptide. This weaker anti-inflammatory activity of the diastereomer compared to Esc(1-21) might be an advantage when the host's innate immune response to bacterial infection is at the beginning stage.

As previously reported in the literature, in aqueous solution, LPS molecules aggregate into micelles, that represent the biologically active form of the endotoxin (Takayama et al. 1994; Rosenfeld and Shai 2006). LPS micelles interact with the LPS-binding protein (LBP) and then, the LPS–LBP complex binds to CD14, the primary receptor of LPS, mainly expressed in macrophages (Schumann et al. 1990). The LPS-CD14 complex interacts with the transmembrane protein Toll-like receptor-4 (TLR4) and activates the intracellular signaling cascade resulting in the production and secretion of pro-inflammatory cytokines (Rosenfeld et al. 2006b).

One of the mechanism by which AMPs can neutralize the toxic effect of LPS is their ability to disrupt the lipopolysaccharide micelles into smaller sized particles (Rosenfeld et al. 2006a, b; Bhunia et al. 2011). This would prevent LPS from binding to the LPB, and then to CD14 and to the TLR4 by blocking, consequently, the activation of intracellular signaling pathway for cytokine synthesis (Rosenfeld et al. 2006a, b; Mangoni and Shai 2011). Light scattering analysis highlighted the formation of smaller-sized LPS micelles upon addition of the esculentin peptides, with a stronger effect in the presence of Esc(1-21). Note that peptides with a well-defined and stabilized structure in both LPS and cytoplasmic membrane and the capability to disassemble the structural organization of LPS micelles are known to have a potent LPS detoxification activity (Rosenfeld et al. 2008). Therefore, the higher α-helical content of Esc(1-21) in LPS and its stronger efficacy in disrupting LPS aggregates are consistent with its stronger anti-endotoxin activity compared to its diastereomer. It can be excluded that the peptides

106

compete with LPS for their binding to the LPS receptor on the membrane of immune cells. Indeed, when macrophages are stimulated with the peptides prior to addition of LPS, no effect on the LPS-neutralization activity is observed.

Moreover, these peptides can contribute to down-regulate the acute inflammatory response induced during infection or injury, by also acting on COX-2 synthesis, an enzyme responsible for the production of inflammatory mediators in response to LPS stimulation (Brunetti et al. 2016). COX-2 production was proved to be inhibited by Esc(1-21) and Esc(1-21)-1c when macrophages are treated with the peptides and LPS from *P. aeruginosa*. As already observed for TNF-α secretion, the diastereomer has a weaker inhibitory effect compared to Esc(1-21).

Considering these properties, there is an increasing interest in AMPs, which show not only a bactericidal activity against pathogenic microorganisms, but also the ability to detoxify LPS and to stimulate re-epithelialization, unlike conventional antibiotics.

6. Conclusions and future perspectives

In conclusion, our studies have shown multiple functions for both the frog skin-derived AMP, Esc(1-21), and its designed diastereomer, Esc(1-21)-1c.

Only two L-to-D-amino acids substitutions in the C-terminal end of Esc(1-21) are sufficient to:

i) significantly reduce its cytotoxic effect towards mammalian cells (e.g., bronchial epithelial cells and macrophages) in agreement with a lower α-helical structure, as determined by circular dichroism spectroscopy and NMR studies;

ii) increase its effectiveness against the biofilm form of *P. aeruginosa* (either reference or clinical isolates from CF patients), while maintaining a high activity against the free-living form of this pathogen;

iii) more effectively kill *Pseudomonas* cells once internalized into CF bronchial cells;

iv) improve the ability of the peptide to promote migration of bronchial epithelial cells and presumably its capacity to restore the integrity of the injured lung tissue;

v) enhance the peptide's biostability to human and *P. aeruginosa* elastases.

These multiple beneficial properties, along with the ability to detoxify LPS and to inhibit COX-2 synthesis, albeit less than the wild-type peptide, make the diastereomer a better candidate for the generation of new antimicrobial drugs that not only eliminate microbial pathogens, but also have the potentiality to recover the tissue's integrity.

Further experiments will be carried out to investigate other possible pathways involved in the peptide-induced wound healing process, that is an attractive feature not detected for conventional antibiotics. In parallel, *in vivo* efficacy studies in murine models of chronic *Pseudomonas* lung infections will be performed.

7. References

- Afacan NJ, Yeung AT, Pena OM, Hancock RE (2012) "Therapeutic potential of host defense peptides in antibiotic-resistant infections." *Curr Pharm Des* 18(6):807-819.

- Ageitos JM, Sánchez-Pérez A, Calo-Mata P, Villa TG (2016) "Antimicrobial peptides (AMPs): ancient compounds that represent novel weapons in the fight against bacteria." *Biochem Pharmacol* 133:117-138.

- Alba A, López-Abarrategui C, Otero-González AJ (2012) "Host defense peptides: an alternative as antiinfective and immunomodulatory therapeutics." *Biopolymers* 98(4):251-67.

- Ali A, Zafar H, Zia M, UI Haq I, Phull AR, Ali JS, Hussain A (2016) "Synthesis, characterization, applications, and challenges of iron oxide nanoparticles." *Nanotechnol Sci Appl* 9:49-67.

- Amblard M, Fehrentz JA, Martinez J, Subra G (2006) "Methods and protocols of modern solid phase Peptide synthesis." *Mol Biotechnol* 33:239-254.

- Aoki W and Ueda M (2013) "Characterization of Antimicrobial Peptides toward the Development of Novel Antibiotics." *Pharmaceuticals* 6(8):1055-1081.

- Aoki W, Kuroda K, Ueda M (2012) "Next generation of antimicrobial peptides as molecular targeted medicines." *J Biosci Bioeng* 114(4):365-70.

- Bals R (2000) "Epithelial antimicrobial peptides in host defense against infection." *Respir Res* 1(3):141-50.

- Bebok Z, Collawn JF, Wakefield J, Parker W, Li Y, Varga K, Sorscher EJ, Clancy JP (2005) "Failure of cAMP agonists to activate rescued deltaF508 CFTR in CFBE41o-airway epithelial monolayers." *J Physiol* 569:601-615.

- Bechinger B and Gorr SU (2017) "Antimicrobial Peptides: mechanisms of action and resistance." *J Dent Res* 96:254-260.

- Bellanda M, Peggion E, Bürgi R, van Gunsteren W, Mammi S (2001) "Conformational study of an Aib-rich peptide in DMSO by NMR." *J Pept Res* 57(2):97-106.

- Bhunia A, Saravanan R, Mohanram H, Mangoni ML, Bhattacharjya S (2011) "NMR structures and interactions of temporin-1Tl and temporin-1Tb with lipopolysaccharide micelles: mechanistic insights into outer membrane permeabilization and synergistic activity." *J Biol Chem* 286:24394-24406.

- Boman HG (1991) "Antibacterial peptides: key components needed in immunity." *Cell* 65:205-207.

- Boman HG (1995) "Peptide Antibiotics and Their Role in Innate Immunity." *Annu Rev Immunol* 13:61-92.

- Bonventre PF, Hayes R, Imhoff J (1967) "Autoradiographic evidence for the impermeability of mouse peritoneal macrophages to tritiated streptomycin." *J Bacteriol* 93:445-450.

- Bragonzi A, Paroni M, Nonis A, Cramer N, Montanari S, Rejman J, Di Serio C, Doring G, Tummler B (2009) "*Pseudomonas aeruginosa* microevolution during cystic fibrosis lung infection establishes clones with adapted virulence." *Am J Respir Crit Care Med* 180:138-145.

- Brayton JJ, Yang Q, Nakkula RJ, Walters JD (2002) "An *in vitro* model of ciprofloxacin and minocycline transport by oral epithelial cells." *J Periodontol* 73:1267-1272.

- Brogden KA (2005) "Antimicrobial peptides: pore formers or metabolic inhibitors in bacteria?" *Nat Rev Microbiol* 3:238-250.

- Brunetti J, Roscia G, Lampronti I, Gambari R, Quercini L, Falciani C, Bracci L, Pini A (2016) "Immunomodulatory and anti-inflammatory activity *in vitro* and *in vivo* of a novel antimicrobial candidate." *J Biol Chem* 291(49):25742-25748.

- Burgel PR and Nadel JA (2004) "Roles of epidermal growth factor receptor activation in epithelial cell repair and mucin production in airway epithelium." *Thorax* 59:992-996.

- Carotenuto A, Malfi S, Saviello MR, Campiglia P, Gomez-Monterrey I, Mangoni ML, Gaddi LM, Novellino E, Grieco P (2008) "A different molecular mechanism underlying antimicrobial and hemolytic actions of temporins A and L." *J Med Chem* 51:2354-2362.

112

- Ceri H, Olson M, Morck D, Storey D, Read R, Buret A, Olson B (2001) "The MBEC assay system: multiple equivalent biofilms for antibiotic and biocide susceptibility testing." *Methods Enzymol* 337:377-385.

- Chadwick PR and Mellersh AR (1987) "The use of a tissue culture model to assess the penetration of antibiotics into epithelial cells." *J Antimicrob Chemother* 19:211-220.

- Chan DI, Prenner EJ, Vogel HJ (2006) "Tryptophan- and arginine-rich antimicrobial peptides: structures and mechanisms of action." *Biochim Biophys Acta* 1758(9):1184-202.

- Chen C, Mangoni ML, Di YP (2017) "*In vivo* therapeutic efficacy of frog skin-derived peptides against *Pseudomonas aeruginosa*-induced pulmonary infection." *Sci Rep.* 7: 8548.

- Chen LF, Chopra T, Kaye KS (2011) "Pathogens Resistant to Antibacterial Agents." *Med Clin North Am* 95(4):647-76.

- Chou HT, Kuo TY, Chiang JC, Pei MJ, Yang WT, Yu HC, Lin SB, Chen WJ (2008) "Design and synthesis of cationic antimicrobial peptides with improved activity and selectivity against Vibrio spp." *Int J Antimicrob Agents* 32(2):130-8.

- Cohen J (2002) "The immunopathogenesis of sepsis." *Nature* 420: 885-91.

- Conlon JM (2008) "Reflections on a systematic nomenclature for antimicrobial peptides from the skins of frogs of the family Ranidae." *Peptides* 29:1815-1819.

- Conlon JM, Kolodziejek J, Nowotny N (2004) "Antimicrobial peptides from ranid frogs: taxonomic and phylogenetic markers and a potential source of new therapeutic agents." *Biochim Biophys Acta* 1696(1):1-14.

- Conlon JM, Meetani MA, Coquet L, Jouenne T, Leprince J, Vaudry H, Kolodziejek J, Nowotny N, King JD (2009) "Antimicrobial peptides from the skin secretions of the New World frogs Lithobates capito and Lithobates warszewitschii (Ranidae)." *Peptides* 30:1775-81.

- D'Este F, Tomasinsig L, Skerlavaj B, Zanetti M (2012) "Modulation of cytokine gene expression by cathelicidin BMAP-28 in LPS-stimulated and -unstimulated macrophages." *Immunobiology* 217(10):962-71.

- d'Angelo I, Conte C, Miro A, Quaglia F, Ungaro F (2015a) "Pulmonary drug delivery: a role for polymeric nanoparticles?" *Curr Top Med Chem* 15(4):386-400.

- d'Angelo I, Quaglia F, Ungaro F (2015b) "PLGA carriers for inhalation: where do we stand, where are we headed?" *Ther Deliv* 6(10):1139-1144.

- Davidson DJ, Currie AJ, Reid GS, Bowdish DM, MacDonald KL, Ma RC, Hancock RE, Speert DP (2004) "The cationic antimicrobial peptide LL-37 modulates dendritic cell differentiation and dendritic cell-induced T cell polarization." *J Immunol* 172(2):1146-1156.

- Davies J and Davies D (2010) "Origins and Evolution of Antibiotic Resistance." *Microbiol Mol Biol Rev* 74(3):417-33.

- Dawson RM and Liu CQ (2008) "Properties and applications of antimicrobial peptides in biodefense against biological warfare threat agents." *Crit Rev Microbiol* 34(2):89-107.

- de Sa PB, Havens WM, Ghabrial SA (2010) "Characterization of a novel broad-spectrum antifungal protein from virus-infected Helminthosporium (Cochliobolus) victoriae." *Phytopathology* 100(9):880-9.

- De Zotti M, Biondi B, Park Y, Hahm KS, Crisma M, Toniolo C, Formaggio F (2012) "Antimicrobial lipopeptaibol trichogen GA IV: role of the three Aib residues on conformation and bioactivity." *Amino Acids* 43(4):1761-1777.

- Eckert R (2011) "Road to clinical efficacy: challenges and novel strategies for antimicrobial peptide development." *Fut Microbiol* 6:635-651.

- Ehrenstein G and Lecar H (1977) "Electrically gated ionic channels in lipid bilayers." *Q Rev Biophys* 10:1-34.

- Fabisiak A, Murawska N, Fichna J (2016) "LL-37: Cathelicidin-related antimicrobial peptide with pleiotropic activity." *Pharmacol Rep* 68 802-808.

- Fajac I and Wainwright CE (2017) "New treatments targeting the basic defects in cystic fibrosis." *Presse Med* 46(6 Pt 2):e165-e175.

- Falciani C, Lozzi L, Pollini S, Luca V, Carnicelli V, Brunetti J, Lelli B, Bindi S, Scali S, Di Giulio A, Rossolini GM, Mangoni ML, Bracci L, Pini

A (2012) "Isomerization of an antimicrobial Peptide broadens antimicrobial spectrum to gram-positive bacterial pathogens." *PLoS One* 7:e46259.

- Fjell CD, Hiss JA, Hancock RE, Schneider G (2011) "Designing antimicrobial peptide form follows function." *Nat Rev Drug Discov* 11:37-51.

- Flemming HC, Wingender J, Szewzyk U, Steinberg P, Rice SA, Kjelleberg S (2016) "Biofilms: an emergent form of bacterial life." *Nat Rev Microbiol* 14(9):563-575.

- Folkesson A, Jelsbak L, Yang L, Johansen HK, Ciofu O, Hoiby N, Molin S (2012) "Adaptation of *Pseudomonas aeruginosa* to the cystic fibrosis airway: An evolutionary perspective." *Nat Rev Microbiol* 10:841-851.

- Gamberi T, Cavalieri D, Magherini F, Mangoni ML, De Filippo C, Borro M, Gentile G, Simmaco M, Modesti A (2007) "An integrated analysis of the effects of Esculentin 1–21 on *Saccharomyces cerevisiae*." *Biochim Biophys Acta* 1774(6):688-700.

- Gan HK, Walker F, Burgess AW, Rigopoulos A, Scott AM, Johns TG (2007) "The epidermal growth factor receptor (EGFR) tyrosine kinase inhibitor AG1478 increases the formation of inactive untethered EGFR dimers. Implications for combination therapy with monoclonal antibody 806." *J Biol Chem* 282:2840-2850.

- Ganz T (1999) "Defensins and host defense." *Science* 286(5439):420-1.

- Ganz T (2003) "Defensins: antimicrobial peptides of innate immunity." *Nat Rev Immunol* 3(9):710-20.

- Gaspar MC, Couet W, Olivier JC, Pais AA, Sousa JJ (2013) "*Pseudomonas aeruginosa* infection in cystic fibrosis lung disease and new perspectives of treatment: a review." *Eur J Clin Microbiol Infect Dis* 32(10):1231-52.

- Gazit E, Lee WJ, Brey PT, Shai Y (1994) "Mode of action of the antibacterial cecropin B2: a spectrofluorometric study." *Biochemistry* 33:10681-10692.

- Gellatly SL and Hancock RE (2013) "*Pseudomonas aeruginosa*: new insights into pathogenesis and host defenses." *Pathog Dis* 67(3):159-173.

- Giuliani A and Rinaldi AC (2011) "Beyond natural antimicrobial peptides: multimeric peptides and other peptidomimetic approaches." *Cell Mol Life Sci* 68(13):2255-2266.

- Giuliani A, Pirri G, Nicoletto SF (2007) "Antimicrobial peptides: an overview of a promising class of therapeutics." *Cent Eur J Biol* 2(1):1-33.

- Goldberg JB and Pier GB (2000) "The role of the CFTR in susceptibility to *Pseudomonas aeruginosa* infections in cystic fibrosis." *Trends Microbiol* 8(11):514-520.

- Grage SL, Afonin S, Kara S, Buth G, Ulrich AS (2016) "Membrane Thinning and Thickening Induced by Membrane-Active Amphipathic Peptides." *Front Cell Dev Biol* 4:65.

- Grieco P, Carotenuto A, Auriemma L, Limatola A, Di Maro S, Merlino F, Mangoni ML, Luca V, Di Grazia A, Gatti S, Campiglia P, Gomez-Monterrey I, Novellino E, Catania A (2013b) "Novel alpha-MSH peptide analogues with broad spectrum antimicrobial activity." *PLoS One* 8:e61614.

- Grieco P, Carotenuto A, Auriemma L, Saviello MR, Campiglia P, Gomez Monterrey IM, Marcellini L, Luca V, Barra D, Novellino E, Mangoni ML. (2013a). "The effect of d-amino acid substitution on the selectivity of temporin L towards target cells: identification of a potent anti-Candida peptide." *Biochim Biophys Acta* 1828(2):652-660.

- Grundmann H, Klugman KP, Walsh T, Ramon-Pardo P, Sigauque B, Khan W, Laxminarayan R, Heddini A, Stelling J (2011) "A framework for global surveillance of antibiotic resistance." *Drug Resist Updat* 14(2):79-87.

- Guilhelmelli F, Vilela N, Albuquerque P, Derengowski Lda S, Silva-Pereira I, Kyaw CM (2013) "Antibiotic development challenges: the various mechanisms of action of antimicrobial peptides and of bacterial resistance." *Front Microbiol* 9(4):353.

- Hancock RE (1997) "Peptide antibiotics." *Lancet* 349(9049):418-22.

- Hancock RE and Diamond G (2000) "The role of cationic antimicrobial peptides in innate host defences." *Trends Microbial* 8:402-410.

- Hancock RE and Sahl HG (2006) "Antimicrobial and host-defense peptides as new anti-infective therapeutic strategies." *Nat Biotechnol* 24(12):1551-1557.

- Hancock RE, Nijnik A, Philpott DJ (2012) "Modulating immunity as a therapy for bacterial infections." *Nat Rev Microbiol* 10:243-254.

- He YY, Council SE, Feng L, Chignell CF (2008) "UVA-induced cell cycle progression is mediated by a disintegrin and metalloprotease/epidermal growth factor receptor/AKT/Cyclin D1 pathways in keratinocytes." *Cancer Res* 68:3752-3758.

- Huang Y, Huang J, Chen Y (2010) "Alpha-helical cationic antimicrobial peptides: relationships of structure and function." *Protein Cell* 1(2):143-152.

- Hussain R, Umer HM, Björkqvist M and Roomans GM (2014) "ENaC, iNOS, mucins expression and wound healing in cystic fibrosis airway epithelial and submucosal cells." *Cell Biol Int Rep* 21:25-38.

- Ilgin S, Can OD, Atli O, Ucel UI, Sener E, Guven I (2015) "Ciprofloxacininduced neurotoxicity: evaluation of possible underlying mechanisms." *Toxicol Mech Methods* 25:374-381.

- Islas-Rodriguez AE, Marcellini L, Orioni B, Barra D, Stella L, Mangoni ML (2009) "Esculentin 1-21: a linear antimicrobial peptide from frog skin with inhibitory effect on bovine mastitis-causing bacteria." *J Pept Sci* 15(9):607-614.

- Jenssen H, Hamill P, Hancock RE (2006) "Peptide antimicrobial agents." *Clin Microbiol Rev* 19:491-511.

- Kang SJ, Park SJ, Mishig-Ochir T, Lee BJ (2014) "Antimicrobial peptides: therapeutic potentials." *Expert Rev Anti Infect Ther* 12(12):1477-86.

- Kelly E, Greene CM, McElvaney NG (2008) "Targeting neutrophil elastase in cystic fibrosis." *Expert Opin Ther Targets* 12(2):145-157.

- Kim JB, Han AR, Park EY, Kim JY, Cho W, Lee J, Seo EK, Lee KT (2007) "Inhibition of LPS-Induced iNOS, COX-2 and Cytokines Expression by Poncirin through the NF-kB Inactivation in RAW 264.7 Macrophage." *Cells Biol Pharm Bull* 30(12):2345-2351.

- Kim S, Beyer BA, Lewis C, Nadel JA (2013) "Normal CFTR inhibits epidermal growth factor receptor-dependent pro-inflammatory chemokine production in human airway epithelial cells." *PLoS One* 8:e72981.

- Klockgether J and Tümmler B (2017) "Recent advances in understanding *Pseudomonas aeruginosa* as a pathogen." Version 1. F1000Res. 2017 6: 1261.

- Ko YH, Delannoy M, Pedersen PL (1997) "Cystic fibrosis, lung infections, and a human tracheal antimicrobial peptide (hTAP)." *FEBS Lett* 405:200-208.

- Kolar SS, Luca V, Baidouri H, Mannino G, McDermott AM, Mangoni ML (2015) "Esculentin-1a(1-21)NH2: a frog skin derived peptide for microbial keratitis." *Cell Mol Life Sci* 72(3): 617-627.

- Kraus D and Peschel A (2006) "Molecular mechanisms of bacterial resistance to antimicrobial peptides." *Curr Top Microbiol Immunol* 306:231-250.

- Kreda SM, Davis CW, Rose MC (2012) "CFTR, mucins, and mucus obstruction in cystic fibrosis." *Cold Spring Harb Perspect Med* 2:a009589.

- Kumar RP and Abraham A (2017) "Inhibition of LPS induced pro-inflammatory responses in RAW 264.7 macrophage cells by PVP coated naringenin nanoparticle via down regulation of NF-κB/P38MAPK mediated stress signaling." *Pharmacol Rep* 69(5):908-915.

- Ladram A and Nicolas P (2016) "Antimicrobial peptides from frog skin: biodiversity and therapeutic promises." *Front Biosci (Landmark Ed)* 21: 1341-1371.

- Lai Y and Gallo RL (2009) "AMPed up immunity: how antimicrobial peptides have multiple roles in immune defense." *Trends Immunol* 30(3): 131-141.

- Larrosa M, Truchado P, Espin JC, Tomas-Barberan FA, Allende A, Garcia-Conesa MT (2012) "Evaluation of *Pseudomonas aeruginosa* (PAO1) adhesion to human alveolar epithelial cells A549 using SYTO 9 dye." *Mol Cell Probes* 26:121-126.

- Lauand C, Rezende-Teixeira P, Cortez BA, Niero EL, Machado-Santelli GM (2013) "Independent of ErbB1 gene copy number, EGF stimulates

migration but is not associated with cell proliferation in non-small cell lung cancer." *Cancer Cell Int* 13(1):38.

- Lee I-Ta and Yang CM (2013) "Inflammatory signalings involved in airway and pulmonary diseases mediators of inflammation." *Mediators of Inflammation*, vol. 2013, Article ID 791231, 12 pages.

- Lee SB, Lee WS, Shin JS, Jang DS, Lee KT (2017) "Xanthotoxin suppresses LPS-induced expression of iNOS, COX-2, TNF-α, and IL-6 via AP-1, NF-κB, and JAK-STAT inactivation in RAW 264.7 macrophages." *Int Immunopharmacol* 49:21-29.

- Li J, Koh JJ, Liu S, Lakshminarayanan R, Verma CS, Beuerman RW (2017) "Membrane Active Antimicrobial Peptides: Translating Mechanistic Insights to Design." *Front Neurosci* 11:73.

- Li J, Turnidge J, Milne R, Nation RL, Coulthard K (2001) "*In vitro* pharmacodynamic properties of colistin and colistin methanesulfonate against *Pseudomonas aeruginosa* isolates from patients with cystic fibrosis." *Antimicrob Agents Chemother* 45:781-785.

- Liu H, Lazarus SC, Caughey GH, Fahy JV (1999) "Neutrophil elastase and elastase-rich cystic fibrosis sputum degranulate human eosinophils *in vitro*." *Am J Physiol* 276:L28–L34.

- Livermore DM (2011) "Discovery research: the scientific challenge of finding new antibiotics." *J Antimicrob Chemother* 66(9):1941-1944.

- Lohner K (2009) "New strategies for novel antibiotics: peptides targeting bacterial cell membranes." *Gen Physiol Biophys* 28:105-116.

- Lore NI, Cigana C, De Fino I, Riva C, Juhas M, Schwager S, Eberl L, Bragonzi A (2012) "Cystic fibrosis-niche adaptation of *Pseudomonas aeruginosa* reduces virulence in multiple infection hosts." *PLoS One* 7:e35648.

- Lovewell RR, Patankar YR, Berwin B (2014) "Mechanisms of phagocytosis and host clearance of *Pseudomonas aeruginosa*." *Am J Physiol Lung Cell Mol Physiol* 306: L591–L603.

- Luca V, Stringaro A, Colone M, Pini A, Mangoni ML (2013) "Esculentin(1-21), an amphibian skin membrane-active peptide with potent activity on both planktonic and biofilm cells of the bacterial pathogen *Pseudomonas aeruginosa*." *Cell Mol Life Sci* 70(15):2773-86.

- Ludtke SJ, He K, Heller WT, Harroun TA, Yang L, Huang HW (1996) "Membrane pores induced by magainin." *Biochemistry* 35:13723-13728.

- Ma B, Niu C, Zhou Y, Xue X, Meng J, Luo X, Hou Z (2016) "The disulfide bond of the peptide Thanatin is dispensible for its antimicrobial activity *In Vivo* and *In Vitro*." *Antimicrob Agents Chemother* 60(7):4283-4289.

- Mahlapuu M, Håkansson J, Ringstad L, Björn C (2016) "Antimicrobial Peptides: An Emerging Category of Therapeutic Agents." *Front Cell Infect Microbiol* 6:194.

- Makovitzki A, Avrahami D, Shai Y (2006) "Ultrashort antibacterial and antifungal lipopeptides." *Proc Natl Acad Sci U S A* 103:15997-16002.

- Mangoni ML (2006) "Temporins, anti-infective peptides with expanding properties." *Cell Mol Life Sci* 63:1060-1069.

- Mangoni ML (2011) "Host-defense peptides: from biology to therapeutic strategies." *Cell Mol Life Sci* 68:2157-9.

- Mangoni ML and Shai Y (2011) "Short native antimicrobial peptides and engineered ultrashort lipopeptides: similarities and differences in cell specificities and modes of action." *Cell Mol Life Sci* 68:2267-2280.

- Mangoni ML, Carotenuto A, Auriemma L, Saviello MR, Campiglia P, Gomez-Monterrey I, Malfi S, Marcellini L, Barra D, Novellino E, Grieco P (2011) "Structure-activity relationship, conformational and biological studies of temporin L analogues." *J Med Chem* 54:1298-1307.

- Mangoni ML, Fiocco D, Mignogna G, Barra D, Simmaco M (2003) "Functional characterisation of the 1-18 fragment of esculentin-1b, an antimicrobial peptide from *Rana esculenta*." *Peptides* 24(11):1771-1777.

- Mangoni ML, Luca V, McDermott AM (2015) "Fighting microbial infections: A lesson from amphibian skin-derived esculentin-1 peptides." *Peptides* 71:286–295.

- Mangoni ML, McDermott AM, Zasloff M (2016) "Antimicrobial Peptides and Wound Healing: Biological and Therapeutic Considerations." *Exp Dermatol* 25(3):167-173.

- Mangoni ML, Papo N, Saugar JM, Barra D, Shai Y, Simmaco M, Rivas L (2006) "Effect of natural L- to D-amino acid conversion on the

organization, membrane binding, and biological function of the antimicrobial peptides bombinins H." *Biochemistry* 45(13):4266-4276.

- Mangoni ML, Saugar JM, Dellisanti M, Barra D, Simmaco M, Rivas L (2005) "Temporins, small antimicrobial peptides with leishmanicidal activity." *J Biol Chem* 280:984-990.

- Manzo G, Carboni M, Rinaldi AC, Casu M, Scorciapino MA (2013) "Characterization of sodium dodecylsulphate and dodecylphosphocholine mixed micelles through NMR and dynamic light scattering." *Magn Reson Chem* 51:176-183.

- Manzo G, Casu M, Rinaldi AC, Montaldo NP, Luganini A, Gribaudo G, Scorciapino MA (2014) "Folded structure and insertion depth of the frog-skin antimicrobial Peptide esculentin-1b(1-18) in the presence of differently charged membrane-mimicking micelles." *J Nat Prod* 77:2410-2417.

- Marcellini L, Borro M, Gentile G, Rinaldi AC, Stella L, Aimola P, Barra D, Mangoni ML (2009) "Esculentin-1b(1-18)-a membrane-active antimicrobial peptide that synergizes with antibiotics and modifies the expression level of a limited number of proteins in *Escherichia coli*." *FEBS J* 276:5647-5664.

- Mariencheck WI, Alcorn JF, Palmer SM, Wright JR (2003) "*Pseudomonas aeruginosa* elastase degrades surfactant proteins A and D." *Am J Respir Cell Mol Biol* 28:528-537.

- Matsuzaki K (1999) "Why and how are peptide-lipid interactions utilized for self-defense? Magainins and tachyplesins as archetypes." *Biochim Biophys Acta* 1462:1-10.

- Matsuzaki K, Murase O, Fujii N, Miyajima K (1996) "An antimicrobial peptide, magainin 2, induced rapid flip-flop of phospholipids coupled with pore formation and peptide translocation." *Biochemistry* 35:11361-11368.

- Midura-Nowaczek K and Markowska A (2014) "Antimicrobial peptides and their analogs: searching for new potential therapeutics." *Perspect Medicin Chem* 6:73-80.

- Mihai C, Bao S, Lai JP, Ghadiali SN, Knoell DL (2012) "PTEN inhibition improves wound healing in lung epithelia through changes in

cellular mechanics that enhance migration." *Am J Physiol Lung Cell Mol Physiol* 302:L287-L299.

- Millar FA, Simmonds NJ, Hodson ME (2009) "Trends in pathogens colonising the respiratory tract of adult patients with cystic fibrosis, 1985-2005." *J Cyst Fibros* 8:386-391.

- Miller SI, Ernst RK, Bader MW (2005) "LPS, TLR4 and infectious disease diversity." *Nat Rev Microbiol* 3:36-46.

- Mojsoska B and Jenssen H (2015) "Peptides and Peptidomimetics for Antimicrobial Drug Design." *Pharmaceuticals* 8(3):366-415.

- Mookherjee N and Hancock RE (2007) "Cationic host defence peptides: innate immune regulatory peptides as a novel approach for treating infections." *Cell Mol Life Sci* 64(7-8):922-933.

- Morikawa N, Hagiwara K, Nakajima T (1992) "Brevinin-1 and -2, unique antimicrobial peptides from the skin of the frog, *Rana brevipoda porsa*." *Biochem Biophys Res Commun* 189:184-90.

- Morita Y, Tomida J, Kawamura Y (2014) "Resistance and Response to Anti-Pseudomonas Agents and Biocides." *Pseudomonas* 173-187.

- Mouritsen OG (2011) "Model answers to lipid membrane questions." *Cold Spring Harb Perspect Biol* 3(9):a004622.

- Mukerji S, O'Dea M, Barton M, Kirkwood R, Lee T, Abraham S (2017) "Development and transmission of antimicrobial resistance among Gram-negative bacteria in animals and their public health impact." *Essays Biochem* 61(1)23-35.

- Mylne JS, Wang CK, van der Weerden NL (2010) "Cyclotides are a component of the innate defense of Oldenlandia affinis." *Biopolymers* 94(5):635-46.

- Nathan C and Ding A (2010) "Nonresolving Inflammation." *Cell* 140:871-882.

- Nguyen LT, Chau JK, Perry NA, de Boer L, Zaat SA, Vogel HJ (2010) "Serum stabilities of short tryptophan- and arginine-rich antimicrobial peptide analogs." *PLoS One* 5(9). pii: e12684.

- Nguyen LT, Haney EF, Vogel HJ (2011) "The expanding scope of antimicrobial peptide structures and their modes of action." *Trends Biotechnol* 29(9):464-72.

- Nguyen LT, Schibli DJ, Vogel HJ (2005) "Structural studies and model membrane interactions of two peptides derived from bovine lactoferricin." *J Pept Sci* 11(7):379-89.

- Nicolas P and El Amri C (2009) "The dermaseptin superfamily: a genebased combinatorial library of antimicrobial peptides." *Biochim Biophys Acta* 1788(8):1537-1550.

- Nordqvist C (2017) "Antibiotics: All You Need To Know." Medical News Today. Retrieved from https://www.medicalnewstoday.com/articles/ 10278.php.

- O'Neill J (2014) "Review on Antimicrobial Resistance. Antimicrobial Resistance: Tackling a crisis for the health and wealth of nations." Available from https://amr-review.org/sites/default/files/AMR%20Review%20Paper%20-%20Tackling%20a%20crisis%20for%20the%20health%20and%20wealth%20of%20nations_1.pdf

- O'Neill J (2016) "Review on Antimicrobial Resistance. Tackling drug-resistant infections globally: final report and recommendations." Available from https://amr review.org/sites/default/files/160525_Final%20paper_with%20cover.pdf

- Oyston PC, Fox MA, Richards SJ, Clark GC (2009) "Novel peptide therapeutics for treatment of infections." *J Med Microbiol* 58(Pt 8):977-87.

- Papo N and Shai Y (2004) "Effect of drastic sequence alteration and D-amino acid incorporation on the membrane binding behavior of lytic peptides." *Biochemistry* 43(21):6393-403.

- Peschon JJ, Slack JL, Reddy P, Stocking KL, Sunnarborg SW, Lee DC, Russell WE, Castner BJ, Johnson RS, Fitzner JN, Boyce RW, Nelson N, Kozlosky CJ, Wolfson MF, Rauch CT, Cerretti DP, Paxton RJ, March CJ, Black RA (1998) "An essential role for ectodomain shedding in mammalian development." *Science* 282:1281-1284.

- Pettersen EF, Goddard TD, Huang CC, Couch GS, Greenblatt DM, Meng EC, Ferrin TE (2004) "UCSF Chimera--a visualization system for exploratory research and analysis." *J Comput Chem* 25(13):1605-12.

- Pier GB, Grout M, Zaidi TS, Olsen JC, Johnson LG, Yankaskas JR, Goldberg JB (1996) "Role of mutant CFTR in hypersusceptibility of cystic fibrosis patients to lung infections." *Science* 271:64-67.

- Pike LJ, Han X, Gross RW (2005) "Epidermal growth factor receptors are localized to lipid rafts that contain a balance of inner and outer leaflet lipids: a shotgun lipidomics study." *J Biol Chem* 280:26796-26804.

- Ponti D, Mignogna G, Mangoni ML, De Biase D, Simmaco M, Barra D (1999) "Expression and activity of cyclic and linear analogues of esculentin-1, an anti-microbial peptide from amphibian skin." *Eur J Biochem* 263(3):921-7.

- Pouny Y, Rapaport D, Mor A, Nicolas P, Shai Y (1992) "Interaction of antimicrobial dermaseptin and its fluorescently labeled analogues with phospholipid membranes." *Biochemistry* 31:12416-12423.

- Powers JP and Hancock RE (2003) "The relationship between peptide structure and antibacterial activity." *Peptides* 24:1681-1691.

- Pulido D, Nogues MV, Boix E, Torrent M (2012) "Lipopolysaccharide neutralization by antimicrobial peptides: a gambit in the innate host defense strategy." *J Innate Immun* 4:327-336.

- Rai A, Pinto S, Velho TR, Ferreira AF, Moita C, Trivedi U, Evangelista M, Comune M, Rumbaugh KP, Simões PN, Moita L, Ferreira L (2016) "One-step synthesis of high-density peptideconjugated gold nanoparticles with antimicrobial efficacy in a systemic infection model." *Biomaterials* 85:99-110.

- Ramesh S, Grijalva M, Debut A, de la Torre BG, Albericio F, Cumbal LH (2016) "Peptides conjugated to silver nanoparticles in biomedicine - a "value-added" phenomenon." *Biomater Sci* 4(12):1713-1725.

- Ranieri D, Rosato B, Nanni M, Magenta A, Belleudi F, Torrisi MR (2016) "Expression of the FGFR2 mesenchymal splicing variant in epithelial cells drives epithelial-mesenchymal transition." *Oncotarget* 7(5):5440-60.

- Rinaldi AC (2002) "Antimicrobial peptides from amphibian skin: an expanding scenario." *Curr Opin Chem Biol* 6(6):799-804.
124

- Rittirsch D, Flierl MA and Ward PA (2008) "Harmful molecular mechanisms in sepsis." *Nat Rev Immunol* 8(10):776-787.

- Rodrigo-Troyano A and Sibila O (2017) "The respiratory threat posed by multidrug resistant Gram-negative bacteria." *Respirology* 22:1288–1299.

- Romero D, Vlamakis H, Losick R, Kolter R (2011) "An accessory protein required for anchoring and assembly of amyloid fibres in *B. subtilis* biofilms." *Mol Microbiol* 80:1155-1168L.

- Rosenfeld Y and Shai Y (2006) "Lipopolysaccharide (Endotoxin)-host defense antibacterial peptides interactions: role in bacterial resistance and prevention of sepsis." *Biochim Biophys Acta* 1758:1513-1522.

- Rosenfeld Y, Barra D, Simmaco M, Shai Y, Mangoni ML (2006a) "A synergism between temporins toward gram-negative bacteria overcomes resistance imposed by the lipopolysaccharide protective layer." *J Biol Chem* 281:28565-28574.

- Rosenfeld Y, Papo N, Shai Y (2006b) "Endotoxin (lipopolysaccharide) neutralization by innate immunity host-defense peptides. Peptide properties and plausible modes of action." *J Biol Chem* 281:1636-1643.

- Rosenfeld Y, Sahl HG, Shai Y (2008) "Parameters involved in antimicrobial and endotoxin detoxification activities of antimicrobial peptides." *Biochemistry* 47:6468-6478.

- Ruiz-Garbajosa P and Cantón R (2017) "Epidemiology of antibiotic resistance in *Pseudomonas aeruginosa*. Implications for empiric and definitive therapy." *Rev Esp Quimioter* 30(Suppl. 1):8-12.

- Saravanan R, Bhunia A, Bhattacharjya S (2010) "Micelle-bound structures and dynamics of the hinge deleted analog of melittin and its diastereomer: implications in cell selective lysis by D-amino acid containing antimicrobial peptides." *Biochim Biophys Acta* 1798:128-139.

- Schiller KR, Maniak PJ, O'Grady SM (2010) "Cystic fibrosis transmembrane conductance regulator is involved in airway epithelial wound repair." *Am J Physiol Cell Physiol* 299:C912–C921.

- Schmieder R and Edwards R (2012) "Insights into antibiotic resistance through metagenomic approaches." *Future Microbiol* 7(1):73-89.

- Schumann RR, Leong SR, Flaggs GW, Gray PW, Wright SD, Mathison JC, Tobias PS, Ulevitch RJ (1990) "Structure and function of lipopolysaccharide binding protein." *Science* 249:1429-1431.

125

- Segev-Zarko L, Saar-Dover R, Brumfeld V, Mangoni ML, Shai Y (2015) "Mechanisms of biofilm inhibition and degradation by antimicrobial peptides." *Biochem J* 468:259-270.

- Sengupta D, Leontiadou H, Mark AE, Marrink SJ (2008) "Toroidal pores formed by antimicrobial peptides show significant disorder." *Biochim Biophys Acta* 1778(10):2308-2317.

- Shai Y (1999) "Mechanism of the binding, insertion and destabilization of phospholipid bilayer membranes by K-helical antimicrobial and cell non-selective membrane-lytic peptides." *Biochim Biophys Acta* 1462(1-2):55-70.

- Shai Y (2002) "Mode of action of membrane active antimicrobial peptides." *Biopolymers* 66(4):236-48.

- Shai Y and Oren Z (1996) "Diastereoisomers of cytolysins, a novel class of potent antibacterial peptides." *J Biol Chem* 271(13):7305-7308.

- Shaykhiev R, Beisswenger C, Kandler K, Senske J, Puchner A, Damm T, Behr J, Bals R (2005) "Human endogenous antibiotic LL-37 stimulates airway epithelial cell proliferation and wound closure." *Am J Physiol Lung Cell Mol Physiol* 289: L842-L848.

- Simmaco M, Mignogna G, Barra D (1998) "Antimicrobial peptides from amphibian skin: what do they tell us?" *Biopolymers* 47(6):435-50.

- Simmaco M, Mignogna G, Barra D, Bossa F (1993) "Novel antimicrobial peptides from skin secretion of the European frog *Rana esculenta*." *FEBS Lett* 324(2):159-161.

- Simmaco M, Mignogna G, Barra D, Bossa F (1994) "Antimicrobial peptides from skin secretions of *Rana esculenta*. Molecular cloning of cDNAs encoding esculentin and brevinins and isolation of new active peptides." *J Biol Chem* 269:11956-61.

- Smith WD, Bardin E, Cameron L, Edmondson CL, Farrant KV, Martin I, Murphy RA, Soren O, Turnbull AR, Wierre-Gore N, Alton EW, Bundy JG, Bush A, Connett GJ, Faust SN, Filloux A, Freemont PS, Jones AL, Takats Z, Webb JS, Williams HD, Davies JC (2017) "Current and future therapies for *Pseudomonas aeruginosa* infection in patients with cystic fibrosis." *FEMS Microbiol Lett* 364(14).

- Stella L, Mazzuca C, Venanzi M, Palleschi A, Didonè M, Formaggio F, Toniolo C, Pispisa B (2004) "Aggregation and water-membrane partition as major determinants of the activity of the antibiotic peptide trichogin GA IV." *Biophys J* 86(2):936-945.

- Stoll SW, Rittie L, Johnson JL, Elder JT (2012) "Heparin-binding EGF-like growth factor promotes epithelial-mesenchymal transition in human keratinocytes." *J Invest Dermatol* 132:2148-2157.

- Strahilevitz J, Mor A, Nicolas P, Shai Y (1994) "Spectrum of antimicrobial activity and assembly of dermaseptin-b and its precursor form in phospholipid membranes." *Biochemistry* 33(36):10951-10960.

- Takahashi D, Shukla SK, Prakash O, Zhang G (2010) "Structural determinants of host defense peptides for antimicrobial activity and target cell selectivity." *Biochimie* 92:1236-1241.

- Takayama K, Mitchell DH, Din ZZ, Mukerjee P, Li C, Coleman DL (1994) "Monomeric Re lipopolysaccharide from *Escherichia coli* is more active than the aggregated form in the Limulus amebocyte lysate assay and in inducing Egr-1 mRNA in murine peritoneal macrophages." *J Biol Chem* 269:2241-2244.

- Tam JP, Lu YA, Yang JL (2002) "Correlations of cationic charges with salt sensitivity and microbial specificity of cystine-stabilized beta-strand antimicrobial peptides." *J Biol Chem* 277(52):50450-6.

- Taylor K, Barran PE, Dorin JR (2008) "Structure–Activity Relationships in β-Defensin Peptides." *Biopolymers* 90(1):1-7.

- Thaiss CA, Levy M, Itav S, Elinav E (2016) "Integration of Innate Immune Signaling." *Trends Immunol* 37(2):84-101.

- Tjabringa GS, Aarbiou J, Ninaber DK, Drijfhout JW, Sorensen OE, Borregaard N, Rabe KF, Hiemstra PS (2003) "The antimicrobial peptide LL-37 activates innate immunity at the airway epithelial surface by transactivation of the epidermal growth factor receptor." *J Immunol* 171: 6690-6696.

- Tossi A, Sandri L, Giangaspero A (2000) "Amphipathic, alpha-helical antimicrobial peptides." *Biopolymers* 55(1):4-30.

- Trinh NT, Bardou O, Prive A, Maille E, Adam D, Lingee S, Ferraro P, Desrosiers MY, Coraux C, Brochiero E (2012) "Improvement of

defective cystic fibrosis airway epithelial wound repair after CFTR rescue." *Eur Respir J* 40:1390-1400.

- Vlieghe P, Lisowski V, Martinez,J, Khrestchatisky M (2010) "Synthetic therapeutic peptides: science and market." *Drug Disc Today* 15:40-56.

- Wang G (2012) "Post-translational Modifications of Natural Antimicrobial Peptides and Strategies for Peptide Engineering." *Curr Biotechnol* 1(1): 72-79.

- Wang G, Li X, Wang Z (2016a) "APD3: the antimicrobial peptide database as a tool for research and education." *Nucleic Acids Res* 44(D1):D1087-D1093.

- Wang Y, Zhang Y, Lee WH, Yang X, Zhang Y (2016b) "Novel peptides from skins of amphibians showed broad-spectrum antimicrobial activities." *Chem Biol Drug Des* 87(3):419-424.

- Wieprecht T, Apostolov O, Beyermann M, Seelig J (1999) "Thermodynamics of the alpha-helix-coil transition of amphipathic peptides in a membrane environment: implications for the peptide-membrane binding equilibrium." *J Mol Biol* 294:785-794.

- Woltmann A, Hamann L, Ulmer AJ, Gerdes J, Bruch HP, Rietschel ET (1998) "Molecular mechanisms of sepsis." *Langenbecks Arch Surg* 383:2-10.

- WHO [World Health Organization] (2014) "Antimicrobial resistance: global report on surveillance. Geneva: World Health Organization." ISBN: 978 92 4 156474 8.

- WHO [World Health Organization] (2017) "ANTIBACTERIAL AGENTS IN CLINICAL DEVELOPMENT An analysis of the antibacterial clinical development pipeline, including tuberculosis." WHO/EMP/IAU/2017.11

- Wu DC, Chan WW, Metelitsa AI, Fiorillo L, Lin AN (2011) "*Pseudomonas* skin infection: clinical features, epidemiology, and management." *Am J Clin Dermatol* 12:157-169.

- Wu WK, Wong CC, Li ZJ, Zhang L, Ren SX, Cho CH (2010) "Cathelicidins in inflammation and tissue repair: Potential therapeutic applications for gastrointestinal disorders." *Acta Pharmacol Sin* 31(9): 1118-1122.

- Yeaman MR and Yount NY (2003) "Mechanisms of Antimicrobial Peptide Action and Resistance." *Pharmacol Rev* 55:27-55.

- Yeung AT, Gellatly SL, Hancock RE (2011) "Multifunctional cationic host defence peptides and their clinical applications." *Cell Mol Life Sci* 68:2161-2176.

- Zanetti M (2004) "Cathelicidins, multifunctional peptides of the innate immunity." *J Leukoc Biol* 75(1):39-48.

- Zanetti M, Gennaro R, Skerlavaj B, Tomasinsig L, Circo R (2002) "Cathelicidin Peptides as Candidates for a Novel Class of Antimicrobials." *Curr Pharm Des* 8(9):779-93.

- Zasloff M (2002) "Antimicrobial peptides of multicellular organisms." *Nature* 415:389-395.

- Zhang L, Benz R, Hancock RE (1999) "Influence of proline residues on the antibacterial and synergistic activities of alpha-helical peptides." *Biochemistry* 38(25):8102-8111.

- Zheng R, Yao B, Yu H, Wang H, Bian J, Feng F (2010) "Novel family of antimicrobial peptides from the skin of Rana shuchinae." *Peptides* 31(9):1674-7.

8. Acknowledgments

I would like to express my sincere thanks to my tutor Prof. Maria Luisa Mangoni for her support, encouragement and her valuable advices during my PhD and the writing of this thesis.

I thank my lab group, both past and present members, with whom I had the pleasure to work and to share difficult and funny moments.

I would like to thank all the collaborators involved in this thesis work:

Prof. Anirban Bhunia (Bose Institute, Kolkata, India) for the spectroscopic analysis of Esc(1-21) and Esc(1-21)-1c;

Prof. Alessandro Pini (Department of Medical Biotechnology, University of Siena, Italy) for the peptides' stability experiments;

Prof. Yechiel Shai (Department of Biological Chemistry, The Weizmann Institute of Science, Israel) for the light scattering experiments;

Dr. Loretta Ferrera and Dr. Luis JV Galietta (U.O.C. Genetica Medica, Istituto Giannina Gaslini, Genova, Italy) for providing human bronchial epithelial cells (wt-CFBE and ΔF508-CFBE);

Dr. Veronica Carnicelli (Università degli Studi dell'Aquila, Italy) for the support during western blot analyses;

Prof. Lorenzo Stella (University of Tor Vergata, Rome, Italy) for the supervision during the liposomes preparation;

Dr. Alessandra Bragonzi (San Raffaele Institute, Milan, Italy) for providing the *P. aeruginosa* clinical isolates.

Last but not the least, I would like to thank my family and all my friends for supporting and believing in me during this hard but exciting period.

Appendix: reprint of the papers

CrossMark

Membrane perturbing activities and structural properties of the frog-skin derived peptide Esculentin-1a(1-21)NH$_2$ and its Diastereomer Esc(1-21)-1c: Correlation with their antipseudomonal and cytotoxic activity

Maria Rosa Loffredo[a,1], Anirban Ghosh[b,1], Nicole Harmouche[c], Bruno Casciaro[a], Vincenzo Luca[a], Annalisa Bortolotti[d], Floriana Cappiello[a], Lorenzo Stella[d], Anirban Bhunia[b], Burkhard Bechinger[c], Maria Luisa Mangoni[a,*]

[a] Laboratory affiliated to Pasteur Italia-Fondazione Cenci Bolognetti, Department of Biochemical Sciences, Sapienza University of Rome, Rome, via degli Apuli, 9, 00185, Italy
[b] Department of Biophysics, Bose Institute, P-1/12, CIT Road, Scheme VII (M), Kolkata 700054, India
[c] University of Strasbourg/CNRS, Chemistry Institute, UMR, 7177, 4, rue Blaise Pascal, 67070 Strasbourg, France
[d] University of Rome Tor Vergata, Department of Chemical Sciences and Technologies, 00133, Rome, Italy

ARTICLE INFO

ABSTRACT

Antimicrobial peptides (AMPs) represent new alternatives to cope with the increasing number of multi-drug resistant microbial infections. Recently, a derivative of the frog-skin AMP esculentin-1a, Esc(1-21), was found to rapidly kill both the planktonic and biofilm forms of the Gram-negative bacterium *Pseudomonas aeruginosa* with a membrane-perturbing activity as a plausible mode of action. Lately, its diastereomer Esc(1-21)-1c containing two D-amino acids i.e. DLeu14 and DSer17 revealed to be less cytotoxic, more stable to proteolytic degradation and more efficient in eradicating *Pseudomonas* biofilm. When tested *in vitro* against the free-living form of this pathogen, it displayed potent bactericidal activity, but this was weaker than that of the all-L peptide. To investigate the reason accounting for this difference, mechanistic studies were performed on *Pseudomonas* spheroplasts and anionic or zwitterionic membranes, mimicking the composition of microbial and mammalian membranes, respectively. Furthermore, structural studies by means of optical and nuclear magnetic resonance spectroscopies were carried out. Our results suggest that the different extent in the bactericidal activity between the two isomers is principally due to differences in their interaction with the bacterial cell wall components. Indeed, the lower ability in binding and perturbing anionic phospholipid bilayers for Esc(1-21)-1c contributes only in a small part to this difference, while the final effect of membrane thinning once the peptide is inserted into the membrane is identical to that provoked by Esc(1-21). In addition, the presence of two D-amino acids is sufficient to reduce the α-helical content of the peptide, in parallel with its lower cytotoxicity.

1. Introduction

Most living organisms produce gene-encoded antimicrobial peptides (AMPs) as readily available weapons against a wide variety of microbial pathogens [1–3]. The majority of these AMPs are cationic molecules at neutral pH and they adopt an amphipathic α-helical structure in membrane environments [4]. These two remarkable features are fundamental for their broad microbicidal activity, which generally relies on the perturbation of the target cell membrane, thus limiting the induction of resistance [1,5]. Their ability to recognize and distinguish bacterial membranes from those of mammalian cells is based on an

initial electrostatic interaction between the positively charged residues of the peptide and the negatively charged membrane phospholipids [6,7]. The latter are much more abundant at the outside of microbial cells when compared to the external leaflet of mammalian cell membranes, which are mostly made of zwitterionic phosphatidylcholine and sphingomyelin [5]. However, in the case of Gram-negative bacteria, before reaching the cytoplasmic membrane (i.e. inner membrane), bacteria need to cross the lipopolysaccharide (LPS)-outer layer in a self-promoted uptake mechanism [8]. Subsequently, the phospholipid bilayer of the inner membrane is destabilized via pore formation or micellization, leading to cell death [9–11]. After membrane passage, inner

---

targets may also exist for some of the peptides [12,13]. In contrast, conventional antibiotics generally inhibit intracellular biological function(s) upon interaction with a single stereospecific target that can be mutated [14,15], making it easier for the microbes to become resistant to this class of drugs [16,17]. Due to the alarming worldwide emergence of multi-drug resistant (MDR) pathogenic microorganisms [18] and the concomitant decrease in the pharmaceutical industry research pipeline for novel antibiotics, the search for new antimicrobial strategies has become strictly necessary [19–21]. AMPs hold promise for the development of new anti-infective compounds [22–25]. Interestingly, a few years ago we discovered that a short-sized AMP, esculentin-1a(1-21)NH$_2$, Esc(1-21), derived from a natural AMP of amphibian origin was endowed with: (i) a wide and potent spectrum of activity especially against Gram-negative bacteria [26–28] and (ii) rapid killing kinetics on planktonic and biofilm cells of *Pseudomonas aeruginosa*. It also showed a membrane-perturbing activity as a plausible mode of action [29]. In addition, it was found to have additional non-antimicrobial properties. Among those, the ability (i) to detoxify *P. aeruginosa* LPS [30] and (ii) to induce re-epithelialization of a pseudo-"wound"; a property which is not shown by any traditional antibiotic [30,31].

Furthermore, we recently demonstrated that a diastereomer of Esc (1-21), named Esc(1-21)-1c, containing two D-amino acids i.e. ^{D}Leu14 and ^{D}Ser17 had significant lower cytotoxicity and higher biostability than its all-L isomer [30]. In addition, it was more efficient in promoting clearance of *P. aeruginosa* internalized in bronchial cells as well as in stimulating wound-healing in an *in vitro* bronchial epithelial cells model [32]. However, when tested *in vitro* against the free living form of *P. aeruginosa* strains, even if it displayed a potent killing activity this was weaker than the parent Esc(1-21) [32].

With the aim to understand whether this discrepancy reflected a different ability of the peptides in damaging the cytoplasmic membrane of bacterial cells or a different interaction with the bacterial cell surface, mechanistic studies have been performed on intact bacterial cells, with bacteria devoid of their cell wall (i.e. spheroplasts) as well as micelles mimicking the head group composition and/or surface charge of membranes. In parallel, to verify whether the lower cytotoxicity of the diastereomer in comparison to the all-L peptide reflected a weaker ability in destabilizing zwitterionic membranes, the leakage of a fluorescent marker from neutral lipid vesicles was assessed in comparison to anionic vesicles. Furthermore, by using optical and nuclear magnetic resonance spectroscopies, the secondary structure of the peptides in membrane-mimicking environments has been investigated. Our studies revealed that the weaker *in vitro* antimicrobial activity of the two D-amino acid containing Esc(1-21)-1c in comparison with the all-L Esc(1-21) is mainly associated to a different interaction of the peptide with microbial cell wall components and only partially due to a weaker ability in binding and perturbing anionic membranes. Furthermore, the presence of two D-amino acids was found to be sufficient to reduce the α-helical content of the peptide, in line with its lower cytotoxicity.

2. Materials and methods

2.1. Materials

Synthetic Esc(1-21) and its diastereomer Esc(1-21)-1c (Scheme 1) were purchased from Chematek Spa (Milan, Italy). Each peptide was assembled by stepwise solid-phase synthesis using a standard F-moc
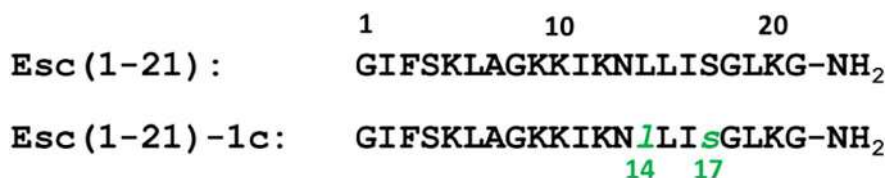
strategy and purified via reverse-phase high-performance liquid chromatography (RP-HPLC) to a purity of 98%, while the molecular mass was verified by mass spectrometry. The following lipids: 1-palmitoyl-2-oleoyl-*sn*-glycero-3-phosphoethanolamine (POPE); 1-palmitoyl-2-oleoyl-*sn*-glycero-3-phosphoglycerol (POPG); 1-palmitoyl-2-oleoyl-*sn*-glycero-3-phosphocholine (POPC), POPE-^{2}H$_{31}$ and cholesterol (Cho) were purchased from Avanti Polar Lipids (Alabaster, AL, USA). Sodium-dodecylsulfate (SDS), dodecylphosphocholine (DPC) were obtained from Cambridge Isotope Laboratories (Tewksbury, MA); carboxy-fluorescein (CF), water (HPLC grade), deuterium depleted water (≤ 1 ppm), 3-(4,5-dimethylthiazol-2-yl)-2,5-diphenyltetrazolium bromide (MTT) were from Sigma (St. Quentin Fallavier, France). Sytox Green was from Molecular Probes (Invitrogen, Carlsbad, CA, USA).

2.2. Microorganisms

The following bacterial strains were used for the antimicrobial assays: the standard *P. aeruginosa* PAO1 [29] and the clinical isolate *P. aeruginosa* AA43 from the strains collection of the cystic fibrosis clinic Medizinische Hochschule of Hannover, Germany [33].

2.3. Spheroplasts preparation

Spheroplasts of *P. aeruginosa* PAO1 were prepared by adapting the procedure described in [34]. Briefly, bacteria from a log-phase culture were collected by centrifugation at $3000 \times g$ and washed in 0.01 M phosphate buffer, pH 7.0 (PB). The cells were then harvested by centrifugation and resuspended in half-volume of 0.5 M sucrose solution in PB to induce plasmolysis. Lysozyme was added to the cell suspension at a final concentration of 50 μg/ml. After incubation at 37 °C for 90 min with moderate shaking, the sample was diluted 1:1 with PB and ethylenediaminetetraacetic acid (EDTA) was added to a final concentration of 10 mM. The cell suspension was incubated again at 37 °C for additional 60 min. Thereafter, transition of the rod-shaped bacteria into spheres was determined by light microscopy. When ~80% of the cells were spheroplasted (as visualized by phase-contrast microscopy), the reaction was stopped by pelleting the cells at $500 \times g$ for 15 min. The spheroplasts were then washed in 0.25 mM sucrose in PB (SPB2), centrifuged at $500 \times g$ for 15 min, and resuspended in SPB2.

2.4. Antimicrobial activity

Aliquots of 100 μl of SPB2 containing spheroplasts derived from 1×10^7 intact bacteria were treated with Esc(1-21) and its diastereomer for 30 min at 37 °C. Afterwards, spheroplasts viability was assayed by the reduction of MTT to insoluble formazan. Briefly, 100 μl of 1 mg/ml MTT were added to the bacterial suspension, transferred into a 96-wells microplate, which was incubated for 90 min at 37 °C. The reduced formazan was then solubilized by the addition of an equal volume of 10% (w/v) SDS, measured in a microplate reader (Infine M 200, Tecan) at 590 nm. All assays were performed in triplicate, and the experiments were repeated three times.

2.5. Sytox green assay on intact bacterial cells

The ability of the peptide to alter the membrane permeability of whole *Pseudomonas* cells was assessed by the Sytox Green (~660 Da) assay. Approximately 1×10^6 cells in 100 μl of phosphate buffered

Scheme 1. Amino acid sequence of Esc(1-21) and Esc(1-21)-1c. The D-amino acids at position 14 and 17 are shown in green and in italics.

Esc(1-21):　　GIFSKLAGKKIKNLLISGLKG–NH$_2$

Esc(1-21)-1c:　GIFSKLAGKKIKN*l*LI*s*GLKG–NH$_2$
　　　　　　　　　　　　　　　　14　17

saline (PBS) were mixed with 1 μM Sytox Green for 5 min in the dark. After adding peptides at different concentrations, the increase of fluorescence, due to the binding of the dye to intracellular DNA, was measured at 37 °C in the microplate reader (Infinite M200). The excitation and emission wavelengths were 485 and 535 nm, respectively. Cells not exposed to the peptides were used as control, whereas the maximal membrane perturbation was obtained after treating bacteria with the highest peptide concentration used (32 μM) followed by the addition of 1 mM EDTA + 0. 5% Triton X-100 (final concentration) to completely destabilize the LPS-outer membrane and to solubilize the cytoplasmic membrane [35]. Samples were run in triplicate and the experiments were performed three times.

2.6. Preparation of large unilamellar vesicles (LUVs)

Lipid films of POPE/POPG and POPC/Cho were prepared by dissolving lipids (2 mg of POPE/POPG mixture, 7:3, mol/mol or 2 mg of POPC/Cho, 1:1, mol/mol) in chloroform/methanol (2:1, v/v). The solvents were then evaporated under reduced argon atmosphere until a thin film was formed. Complete evaporation was ensured by applying a rotary vacuum pump for at least 2 h. The lipid film was then hydrated with a 10 mM phosphate buffer containing 140 mM NaCl and 0.1 mM EDTA, pH 7.4 (buffer A), or with a CF solution at a self-quenching concentration, i.e. 30 mM (for CF leakage experiments) in 10 mM phosphate buffer containing 80 mM NaCl and 0.1 mM EDTA, brought to pH 7.4 with NaOH. The liposome suspension was subjected to 10 freeze and thaw cycles and extruded for 31 times through two stacked polycarbonate membranes with 100 nm pores to obtain LUVs. The free CF (when present) was removed by gel filtration, using a 40 cm Sephadex G-50 at room temperature, equilibrated with buffer A. NaF was used in place of NaCl for CD experiments, to avoid the high absorption by Cl- ions in the far UV [36]. The final lipid concentration was determined by the Stewart phospholipid assay [37].

2.7. CF leakage assay

CF release from LUVs due to membrane permeation induced by the peptide was monitored at 37 °C by the fluorescence increase (excitation = 488 nm; emission = 520 nm). A concentration of lipid vesicles of 200 μM was used and CF leakage after peptide addition at 20 μM was monitored for 30 min. Complete dye release was obtained using 0.1% Triton X-100, which causes total destruction of lipid vesicles [38,39]. The percentage of CF leakage was calculated according to the following formula [40]: leakage (%) = 100(F1 − F0) / (Ft − F0), where F0 represents the fluorescence of intact vesicles, and F1 and Ft denote the intensities of the fluorescence achieved by peptide and Triton X-100 treatment, respectively, at different time points, as indicated. The experiments were performed in duplicate and repeated three times.

2.8. Circular dichroism spectroscopy

In order to investigate the change in secondary structure of Esc(1-21) and Esc(1-21)-1c in SDS and DPC micelles, circular dichroism (CD) experiments were performed using a Jasco J-815 spectrometer (Jasco International Co., Ltd. Tokyo, Japan) with a Peltier cell holder and temperature controller unit accessory. CD spectra were recorded for both the peptides in water (25 μM) and in the presence of different concentrations of SDS (peptide 25 μM, detergent 40 mM), DPC (peptide 25 μM, detergent 10 mM) at 37 °C, or in liposomes of POPE/POPG 7:3 (mol/mol) (peptide 5 or 20 μM, lipids up to 1 mM), at 25 °C. Both working concentrations of SDS and DPC micelles were above previously published critical micellar concentrations (CMC) [41]. The far-UV spectra were scanned over a range of 190–260 nm with 1 nm data interval and averaging over 4 scans. Blank sample spectra were subtracted from the raw data and the CD values were converted to per

residue molar ellipticity ([θ]) (deg cm^2 dmol^{-1}).

2.9. Solution-state NMR experiments

All solution-state NMR experiments were executed on a Bruker Avance III 700 MHz spectrometer furnished with a CryoProbe at 310 K and/or 335 K. Topspin 3.1 (Bruker Biospin, Rheinstetten, Germany) and SPARKY 3.113 (UCSF) was used for processing and analysis of NMR data [42]. Two-dimensional total correlation (TOCSY) and nuclear Overhauser effect (NOESY) spectra of Esc(1-21) and Esc(1-21)-1c alone (1 mM) and in the presence of perdeuterated d_{25}-SDS (200 mM) and d_{38}-DPC (125 mM) were performed in aqueous solution comprising 10% D$_2$O (pH ~ 4.5). All spectra were acquired at 1024 and 512 complex data points along t_2 and t_1 dimensions, respectively, where the States-TPPI-mode was used for quadrature detection in the t_1 dimension [43]. The spectral width was 12 ppm, the offset was adjusted at the water resonance (4.703 ppm) and the relaxation delay was of 2.0 s. TOCSY spectra were acquired using the standard pulse sequence of the pulse sequence library of the Bruker spectrometer, having excitation sculpting for water suppression and spin-lock mixing times of 80 ms (using MLEV-17 mixing scheme), whereas NOESY experiments with 80, 100, 150 and 250 ms mixing time were performed. Sequence-specific resonance assignment was accomplished based on 2D TOCSY and NOESY spectra of peptides in DPC micelles by means of standard assignment procedures [44]. All ^{1}H chemical shifts were referenced using DSS (2,2-Dimethyl-2-silapentane-5-sulfonate sodium salt) as an internal standard.

2.10. NMR derived structure calculation

The three-dimensional solution NMR structures of Esc(1-21) and Esc (1-21)-1c in DPC micelles were determined using the CYANA 2.1 software [45]. From NOESY spectra of Esc(1-21) and Esc(1-21)-1c in SDS and DPC micelles, NOE cross peak intensities were converted to upper bound distance limits of 3.0, 4.0, and 5.5 Å, corresponding to strong, medium, and weak intensities, respectively. The lower limits for all distance restraints were kept at 2.0 Å. In addition, the dihedral angle constraints were estimated from PREDITOR by means of C$_\alpha$H chemical shifts and were used for structure calculations with ± 20° variation, from the derived dihedral angle values [46]. Several rounds of structure calculation were performed for iterative refinement using the standard protocol of CYANA 2.1, as described previously [47,48]. Finally, the best 20 structures with lowest target function values were selected, depending upon low RMSD and minimum violation of distance and dihedral angle constraint. The stereochemical nature of the final structures was analyzed using PROCHECK-NMR validation suite [49]. To estimate the convergence of NMR-derived ensemble of structures, NH order parameters (S^2) [50] for both the peptides were calculated.

2.11. Preparation of peptide-loaded liposomes for solid-state NMR spectroscopy

Multilamellar vesicles (MLVs) were prepared by co-solubilization of lipids [POPE:POPE-^{2}H$_{31}$:POPG (2:1:1)] and peptides at the appropriate lipid-to-peptide molar ratio in chloroform/methanol 2:1 (v/v) to ensure homogenous mixing of the components, followed by solvent evaporation under a stream of nitrogen gas, removal of solvent traces by lyophilisation from a water suspension and then rehydration at h = 0.9 [h = mass of water over the total mass of the system (phospholipids and water)]. To improve sample homogeneity the liposomes were repeatedly vortexed for 40 s, frozen in liquid nitrogen for 30 s and heated in a water bath at 40 °C for 10 min. After 1 to 3 freeze-thaw-vortex cycles, Esc(1-21) and Esc(1-21)-1c embedded in liposomes were obtained.

2.12. Solid-state NMR spectroscopy

[2]H quadrupole echo experiments [51,52] were acquired with a spectral width of 100 kHz, a recycle delay of 1 s, 25 μs echo delay, 30 ms acquisition time, π/2 pulses of 3.4 μs, and between 50 k and 80 k scans. All samples were investigated at temperatures at least 15 K above the phase transition of the individual lipids of the mixture.

Oriented ^{2}H spectra were obtained from the powder pattern by de-Pakeing [53] thus the splitting can be measured more easily. The de-Paking procedure was performed according to the fast Fourier transform-based deconvolution algorithm [54] and first spectral moments were calculated using the NMR-Depaker software (available from the Launchpad Web site: https://launchpad.net/nmr-friend).

Individual C−[2]H bond order parameters ($S_{CD}i$) were calculated from quadrupolar splittings as described previously [52,55],

$$S_{CD} = 4^{\Delta v_Q}/3^{A_Q} \qquad (1)$$

where A_Q is 167 KHz.

2.13. Average acyl chain length measurement

Calculation of acyl chain length is performed according to Douliez et al. [56–60] and can be performed by considering the average projection of each C−C bond along the bilayer normal. This is achieved by connecting the S_{CD} order parameter to the C−C bonds order parameters (S_{CC}), and to sum all the average lengths of the aliphatic chain C−C bonds, projected on the normal to the bilayer. The average length of an aliphatic chain with an even number of carbons is obtained by the following expression:

$$\langle Lchain \rangle = \frac{1 + \sqrt{1 + 8S_{mol}}}{4}\left[\langle l_{C_n\text{-}D} \rangle + 1.,25 \cdot \sum_{k=2}^{n}\left(\frac{1}{2} + \frac{S_k^{CC}}{S_{mol}}\right)\right] \qquad (2)$$

where $\langle l_{C_n}\text{-}D \rangle$ represents the contribution of the terminal methyl C_n−[2]H bond, and S_{mol} is the molecular order parameter (taking into account wobbling motions).

By taking n = 14 for DMPC and DMPE and n = 16 for POPC and POPE; $S_{mol} = 1$, $\langle l_{C_n}\text{-}D \rangle$ is estimated equal to 1.09 Å cos (35,35°) = 0.89 Å, and the angle between the C_n−[2]H bond and C_{nl}−C_n being 111° the equation reduces to:

$$\langle Lchain \rangle = \left[0.89 + 1.,25 \cdot \sum_{k=2}^{n}\left(\frac{1}{2} + S_k^{CC}\right)\right] \qquad (3)$$

The order parameter S_{CC} can be obtained after considering a fast axial rotation of the methyl group around the C_{nl}−C_n bond; hence, S_{CC} is obtained from measured S_{CD} using the recurring equation $S_n^{CC} + S_{n+1}^{CC} = -2S_n^{CD}$. The order parameter for the nth term can be obtained from:

$$S_n^{CD} = \frac{3\cos^2(111°)\text{-}1}{2}S_n^{CC} \qquad (4)$$

The area per lipid A is determined according to de Planque et al., and Nagle [61,62]:

$$A = 2[27.6 \text{ Å}^2/(1.27(0.5 + Sp))] \qquad (5)$$

where Sp is the average order parameter of the plateau region (carbons 2–6).

2.14. Statistical analysis

Quantitative data were expressed as the mean ± standard deviation (SD). Statistical analysis was performed using Student's *t*-test with the PRISM software (GraphPad, San Diego, CA). Differences were considered to be statistically significant for $p < 0.05$ and are indicated in the legend to figures.

3. Results

3.1. Cytoplasmic membrane perturbation

The diastereomer Esc(1-21)-1c was previously found to display a potent killing activity against the planktonic form of reference and cystic fibrosis strains of *P. aeruginosa* [30]. However, this activity was less pronounced than that of the parent Esc(1-21), as proved by the corresponding minimal bactericidal concentration (MBC) causing 99.9% reduction in the number of viable cells within 30 min, in PBS. This was 4 μM versus 1 μM of Esc(1-21) when tested against a bacterial cell density of 1×10^6 CFU/ml [30].

To assess whether this difference reflected a different perturbation of the cytoplasmic membrane of this pathogen by the two peptides, a Sytox Green assay was carried out on two different bacterial strains: the reference *P. aeruginosa* PAO1 and the clinical isolate *P. aeruginosa* AA43. Sytox Green is a membrane-impermeable probe whose fluorescence intensity rapidly enhances upon binding to nucleic acids of bacterial cells with damaged cytoplasmic membrane; and its fluorescent signal is positively correlated to the level of membrane injury. Note that a significantly higher number of bacterial cells (i.e. 1×10^7 CFU/ml) than that generally used for *in vitro* antimicrobial assays is needed, in order to get a detectable signal [29]. As reported in Fig. 1 for *P. aeruginosa* AA43, both peptides were able to destabilize the bacterial membrane, but with a higher potency and faster kinetics for Esc(1-21) (see also the dose-response relationship after 5 min from peptide addition in the Supplementary Fig. S1). While almost total membrane perturbation was achieved by Esc(1-21) within 5 min (at the concentrations of 16 μM and 32 μM, Fig. 1 and Fig. S1) or 15 min (in the concentration range from 2 μM to 8 μM, Fig. 1), a significantly weaker and slower effect was recorded for Esc(1-21)-1c (Figs. 1 and S1). With reference to the latter, ~40% of membrane damage was caused at the highest peptide concentration of 32 μM within 5 min (Fig. S1). The degree of membrane injury gradually diminished in a dose-dependent manner and became negligible at 1 μM. Differently, ~40% of membrane perturbation was registered at 1 μM of Esc(1-21) at the same time point of 5 min (Fig. S1). Similar results were also found for the reference PAO1 [29] and ATCC 27853 strains (data not shown). These data indicate a significant discrepancy between the two peptides in perturbing the cytoplasmic membrane of intact bacterial cells (i.e. much more than the 4 times ratio observed for the MBC values).

3.2. Activity on spheroplasts of P. aeruginosa

To investigate whether the bacterial cell wall was a barrier that differently interferes with the activity of the two peptides, their effect on *Pseudomonas* cells lacking of cell wall (i.e. spheroplasts) was studied. The reference strain of *P. aeruginosa* PAO1 was employed for this purpose and the peptides' effect on the viability of its spheroplasts (1×10^8 cells/ml) was evaluated by the MTT assay, 30 min after peptide addition at different concentrations, with respect to untreated control cells. As shown in Fig. 2, the percentage of metabolically-active spheroplasts after incubation with the all-ʟ peptide at 2 μM was about 70%, while it dropped down to ~2% at 10 μM, in a dose-dependent manner. In comparison, the activity of the diastereomer on spheroplasts was lower, but the difference was much smaller than what was observed on intact cells: Esc(1-21)-1c was only ~1.5-fold less effective, with an LD_{50} of 4.4 ± 0.5 μM versus 2.9 ± 0.5 μM of Esc(1-21).

3.3. Peptides' effect on LUVs of different composition

To expand our knowledge on the membrane perturbing activities of Esc(1-21) and Esc(1-21)-1c, the leakage of CF entrapped in the water volume inside liposomes made of both anionic and zwitterionic phospholipid bilayers was evaluated. A CF concentration of 30 mM was used to induce self-association and the consequent quenching of the dye
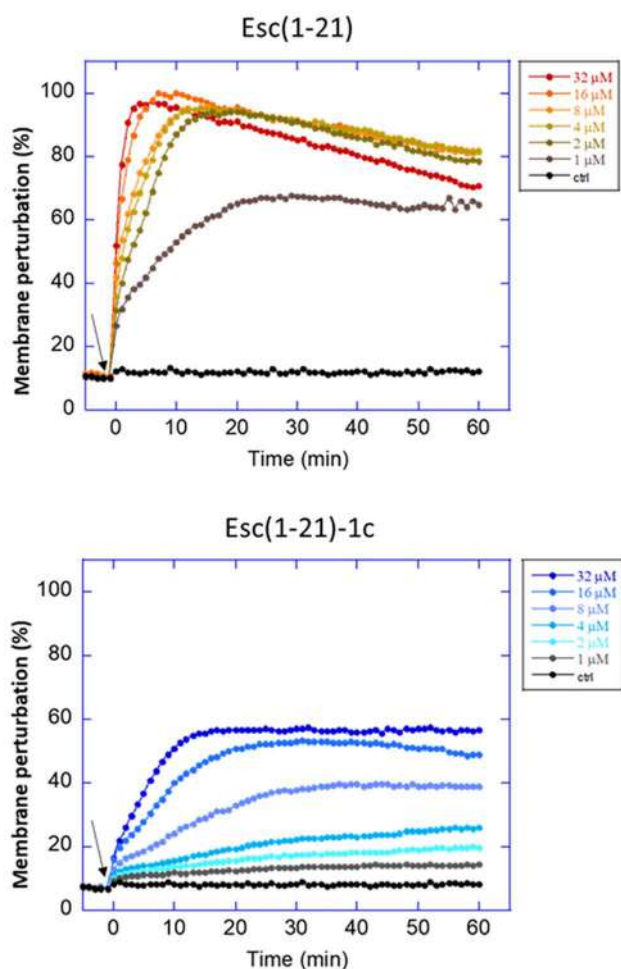
Esc(1-21)

Esc(1-21)-1c

Fig. 1. Kinetics of cytoplasmic membrane permeabilization of the planktonic form of *P. aeruginosa* AA43. Cells (1×10^7 CFU/ml) were incubated with 1 μM Sytox Green in PBS. Once basal fluorescence reached a constant value, the peptide was added (*arrow*, $t = 0$) at different concentrations and changes in fluorescence ($\lambda_{exc} = 485$ nm, $\lambda_{ems} = 535$ nm) were monitored for 60 min and plotted as the percentage of membrane perturbation relative to that obtained after treating bacteria with the highest peptide concentration (32 μM) and the addition of 1 mM EDTA + 0.5% Triton-×100. Data points represent the mean of triplicate samples from a single experiment, representative of three different experiments. Cells not exposed to the peptide were used as control (Ctrl).

[63]. After peptide administration, the membrane destabilization leads to probe release and dissociation with a resulting fluorescence increase. Both peptides were tested at a concentration of 20 μM on POPE/POPG liposomes (7:3 mol:mol, 200 μM), which mimic the lipid composition of the anionic membrane of Gram-negative bacteria. After addition to the lipid vesicles, Esc(1-21) gave rise to a 2-fold higher membrane-perturbing activity than the diastereomer, within 30 min (Fig. 3 panel A) and this was consistent with the results on spheroplasts.

When the two isomers were used on zwitterionic liposomes made of POPC/cholesterol (1:1, mol:mol) to simulate the neutral membrane of mammalian cells, a 5-fold lower leakage of entrapped CF was found for the diastereomer in comparison with its all-L counterpart (Fig. 3 panel B) in line with the lower cytotoxicity of Esc(1-21)-1c on mammalian cells [30,32].

3.4. Structural studies by CD and NMR spectroscopy

In parallel, studies aimed at understanding the structural properties of the two peptides were performed by CD and multidimensional solution-state NMR spectroscopy, in the presence of micellar and liposomal membrane mimetics.
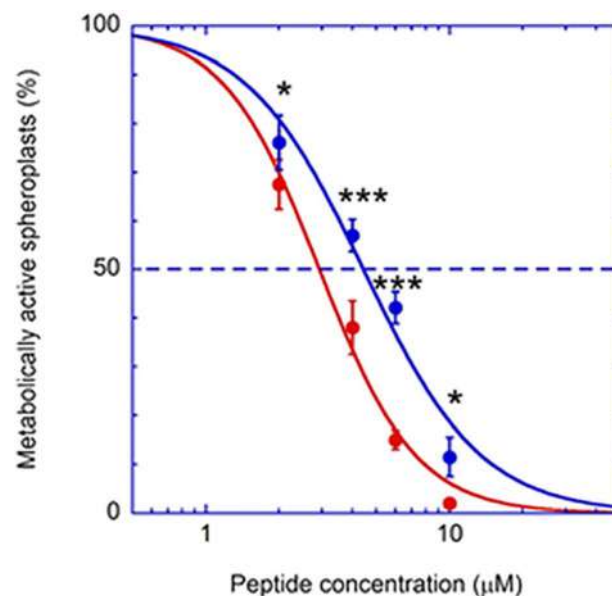
Fig. 2. Effect of different concentrations of Esc(1-21), red line, and its diastereomer, blue line, on the viability of spheroplasts of *P. aeruginosa* PAO1, 30 min after treatment at 37 °C. Cell viability was determined by the MTT reduction to insoluble formazan (see Materials and Methods) and is expressed as percentage with respect to the control (cells not treated with the peptide). Data represent the mean ± SD of three independent experiments performed in triplicate. The level of statistical significance between samples treated with Esc(1-21) and Esc(1-21)-1c are indicated as follows *p < 0.05, ***p < 0.001.

3.4.1. CD

The secondary structure of Esc(1-21) and Esc(1-21)-1c in membranes, and their affinity for lipid bilayers, was initially characterized by CD spectroscopy, in the presence of increasing concentrations of POPE/POPG liposomes (Fig. 4). Their spectra presented a single negative minimum around 200 nm, a characteristic spectral signature for random coil conformations. By contrast, after addition of increasing concentrations of vesicles, the appearance of two negative minima at 208 nm and 222 nm was indicative of α-helical conformations of both peptide isomers, although to a lesser extent in the case of Esc(1-21)-1c (Fig. 4, panels A and B). The change in CD intensity at a fixed wavelength upon binding is directly proportional to the amount of complex formed.

$$[\theta]([L]) = [\theta]_{free} + ([\theta]_{bound} - [\theta]_{free}) \cdot f_{bound} \qquad (6)$$

Here, $[\theta]([L])$, $[\theta]_{free}$ and $[\theta]_{bound}$ are the values of molar ellipticity (in our case at 222 nm) observed at a given lipid concentration $[L]$, in the absence of liposomes, and in the completely bound state, respectively, and f_{bound} is the fraction of membrane-bound peptide [64].

In an ideal water-membrane partition equilibrium, f_{bound} depends on lipid concentration according to the following equation, where K_p is an apparent partition constant [63].

$$f_{bound} = \left(\frac{[L]/K_p}{1 + [L]/K_p} \right) \qquad (7)$$

Combining these two equations, the expected lipid dependence of the molar ellipticity is given by

$$[\theta]([L]) = [\theta]_{free} + ([\theta]_{bound} - [\theta]_{free}) \cdot \left(\frac{[L]/K_p}{1 + [L]/K_p} \right) \qquad (8)$$

In our case, unfortunately, significant binding (and increase in helicity) took place only at lipid concentrations in the 100 μM range (Fig. 4 panels C and D), so that in the experimentally useful range of lipid concentrations (limited to 1 mM by the necessity to avoid
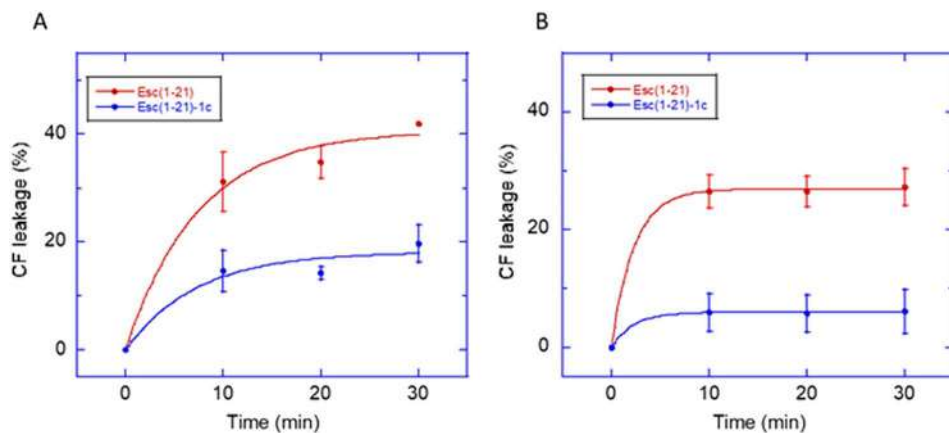
Fig. 3. CF release from POPE/POPG (panel A) and POPC/chol (panel B) LUVs (final lipid concentration 200 μM) within 30 min after addition of peptides (20 μM) at 37 °C. The percentage of leakage was calculated according to the formula: $100(F1 - F0)/(Ft - F0)$ as explained in the Materials and Methods. Data points are means ± SD of three independent measurements performed in duplicate. The difference between the two peptides was significant ($p < 0.05$).
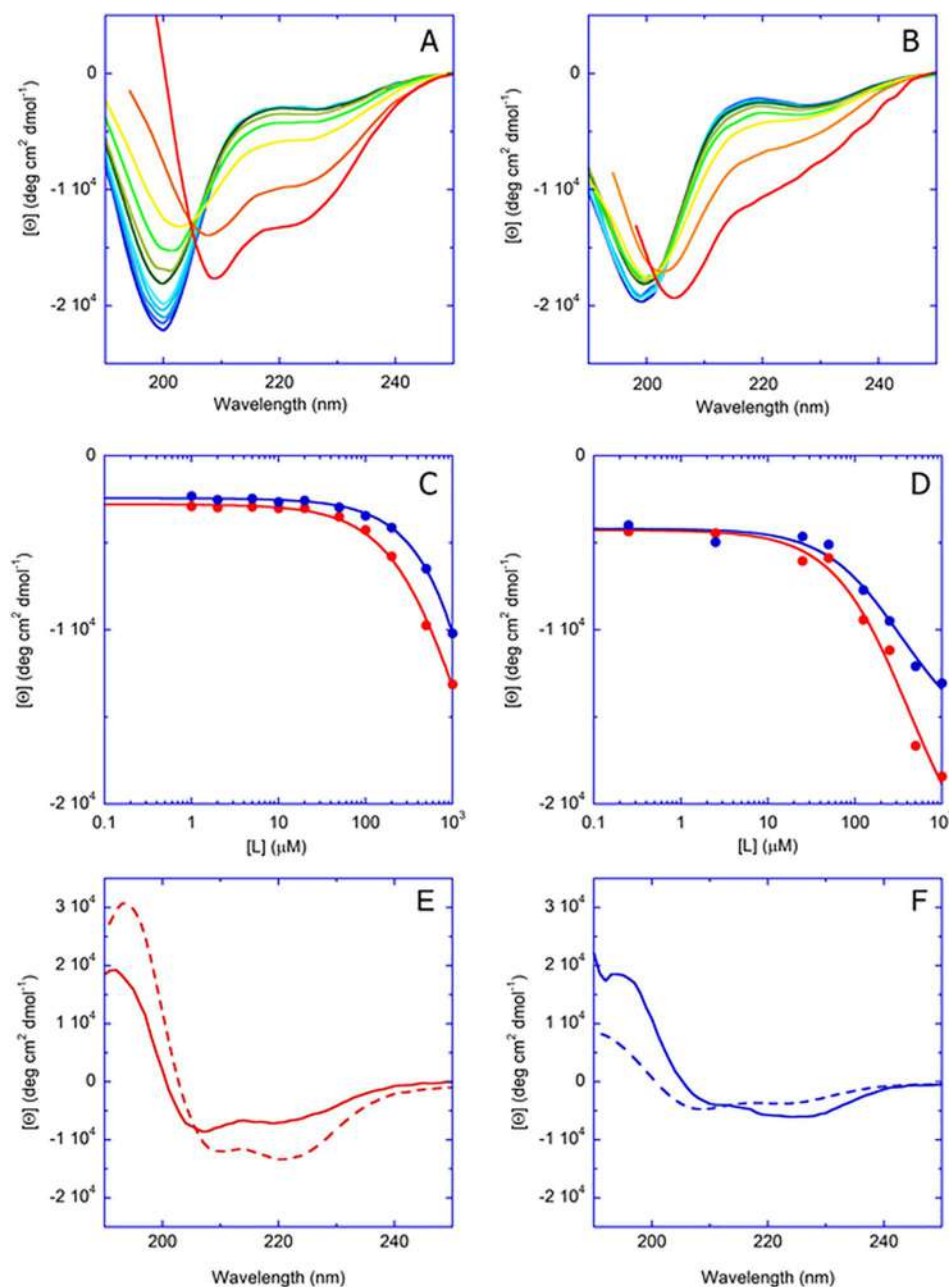

Fig. 4. Top row: Circular dichroism spectra of Esc(1-21) (panel A) and Esc(1-21)-1c (panel B), measured in the presence of increasing lipid concentrations (POPE/POPG 7/3, mol/mol). Peptide concentration: 20 μM, lipid concentrations: 1 μM, 2 μM, 5 μM, 10 μM, 20 μM, 50 μM, 100 μM, 200 μM, 500 μM and 1 mM. The CD spectra are colored from blue to red, in order of increasing concentrations and following the order of colors in the visible spectrum. Middle row: Mean residue ellipticity ([θ]) at 222 nm as function of lipid concentrations, [peptide] = 20 μM (panel C) and [peptide] = 5 μM (panel D), Esc(1-21) in red and Esc(1-21)-1c in blue. Bottom row: Circular dichroism spectra of Esc(1-21) (panel E) and Esc(1-21)-1c (panel F), measured in the presence of SDS (broken line) and DPC (solid line) (25 μM peptide, 40 mM SDS or 10 mM DPC).

scattering artefacts [65]) a plateau was not observed. For this reason, data fitting with the above equation was affected by a large uncertainty on the values of $[\theta]_{bound}$, and thus of K_p. However, the data are sufficient to indicate that the latter constant is of the same order of magnitude for the two peptides (~1 mM), although its value is possibly higher for Esc(1-21)-1c (blue lines).

In order to characterize the conformation of the two peptides when associated to a membrane-mimicking environment, CD spectra were measured in the presence of SDS (broken line) and DPC micelles (solid line), mimicking the anionic and zwitterionic composition of the outer leaflet of the cell membrane of bacteria and mammalian cells, respectively (Fig. 4, panels E, F). In this case, the smaller size of the amphiphilic aggregates reduced light scattering effects, compared to studies in the presence of vesicles. Therefore, surfactant concentrations much higher than the K_p values estimated for POPE/POPG liposomes could be employed, thus favouring peptide association to the micelles. In all cases, the spectral intensities typical of alpha helices were observed, although this was less pronounced in the case of Esc(1-21)-1c (Fig. 4 panel F), probably as a consequence of the presence of D-amino acids. The spectra in SDS exhibited a 222 nm intensity that is more negative than the 208 nm peaks. This finding is often considered indicative of the formation of helical aggregates [66].

3.4.2. NMR studies of Esc(1-21) and Esc(1-21)-1c in SDS and DPC micelles

The conformational transition from random coil to α-helical in the presence of membrane-mimicking environments, as detected by CD spectra, motivated us to explore the peptide structures at atomistic detail by high-resolution solution state NMR spectroscopy. DPC and/or SDS assemble as small size detergent micelles which, in contrast to large liposomes, provide appropriate systems for the structural analysis of AMPs in membrane mimetic environments by multidimensional NMR spectroscopy, due to fast tumbling of the peptide-micellar complex in solution [67,68].

Fig. 5 shows the amide proton region of the one-dimensional ^{1}H NMR spectra of Esc(1-21) and Esc(1-21)-1c in water and in the presence of SDS and DPC micelles. In water, both peptides displayed little dispersion and broad signals in the amide proton region of the spectra whereas in the presence of zwitterionic DPC micelles the spectra were not only well dispersed but also well resolved. The difference in one-dimensional proton spectral pattern demonstrated that micelles induced conformational transformation of both peptides with well-defined secondary structure. Moreover, in the presence of DPC micelles the spectra were better dispersed when compared to their association with SDS micelles, which can be accounted as differential conformational stabilization in the different micellar environment.
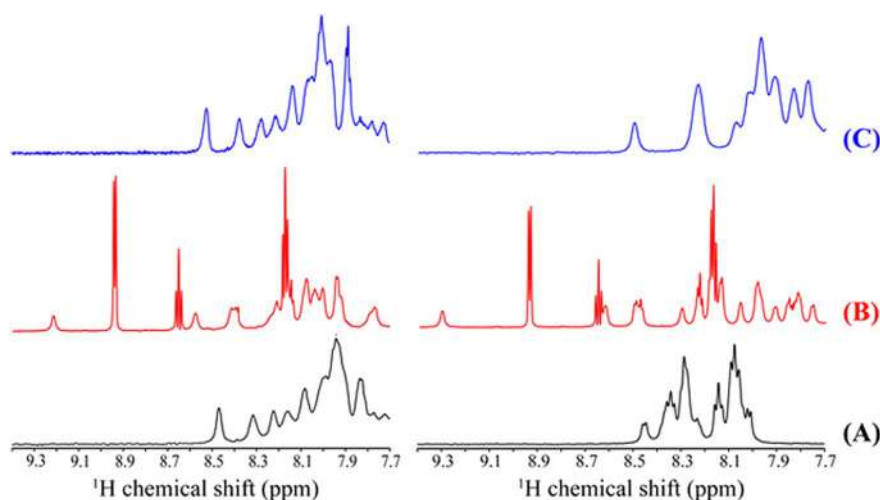
Unfortunately, due to poor spectral resolution, in SDS micelles for both peptides extensive peak overlap in the fingerprint region of two-dimensional ^{1}H−^{1}H NOESY and TOCSY precludes further analysis of the 2D spectra.

With the help of two-dimensional ^{1}H−^{1}H TOCSY and NOESY spectra, sequential resonance assignment of Esc(1-21) and Esc(1-21)-1c in DPC was performed. It is noteworthy that the NOESY spectra in DPC micelles contained the adequate number of sequential and medium-range NOE cross peaks in comparison to the spectra in aqueous solution (Fig. S2 in SI). Therefore, the lack of diagnostic NOEs for both peptides in aqueous solution confirmed the CD spectral analysis where random coil conformations were observed. Differently, in zwitterionic DPC micelles the peptides adopted a more ordered conformation, as reported below. Intense sequential CαH/HN (i to i + 1) NOEs were observed for all residues of both peptides (Fig. 6A and B). In addition, several medium range CαH/HN (i to i + 2/i + 3/i + 4) NOEs were observed for Esc(1-21) throughout the peptide (Fig. S2 A and Fig. 6A). Furthermore, the presence of medium range NH/NH (i to i + 2) NOE contacts reinforced the α-helical conformation of Esc(1-21). Overall the distribution of medium range CαH/HN (i to i + 3/i + 4) as well as NH/NH (i to i + 2) backbone NOEs throughout the sequence established an α-helical conformation in DPC micelles for Esc(1-21), in good accordance with the CD spectral analysis.

On the other hand, Esc(1-21)-1c in DPC micelles contained less diagnostic CαH/HN (i to i + 2/i + 3/i + 4) NOEs in comparison to Esc(1-21) (Fig. S2 B). Most of the medium range NOEs (i to i + 2/i + 3/i + 4) were observed in the N-terminal G1-N13 region (Fig. 6B). This was also in agreement with the trend in backbone NH/NH (i to i + 2) NOE patterns which showed that most NOEs are in the N terminal region such as I2/F4, F3/K5, S4/L6, K5/A7 while the C-terminal stretch, having D-amino acid mutations at 14th and 17th position contained very few NOEs such as K12/L14, N13/L15 and I16/G18.

The discrepancy in NOE distribution for both peptides indicated that the N-terminal portion was mostly well-organized in the parent peptide while the C-terminal region of Esc(1-21)-1c was relatively unstructured and flexible in zwitterionic DPC micellar environments. This was supported by the trend in the ΔH$^{\alpha}$ values for each residue of Esc(1-21) and Esc(1-21)-1c where the chemical shift deviation of the alpha proton resonances from the reported values of random coil resonances provided information about the secondary structure of the peptide [69]. Here, a helical segment is characteristic of negative chemical shift deviation of ΔH$^{\alpha}$ for consecutive 4 residues while a positive chemical shift deviation is a signature of the beta sheet structure. In our systems in DPC micelles, all the CαH resonances throughout the sequence of Esc(1-21) and Esc(1-21)-1c experienced a downfield trend for the CαH chemical shifts (Fig. S3). This chemical shift deviation is a signature of the
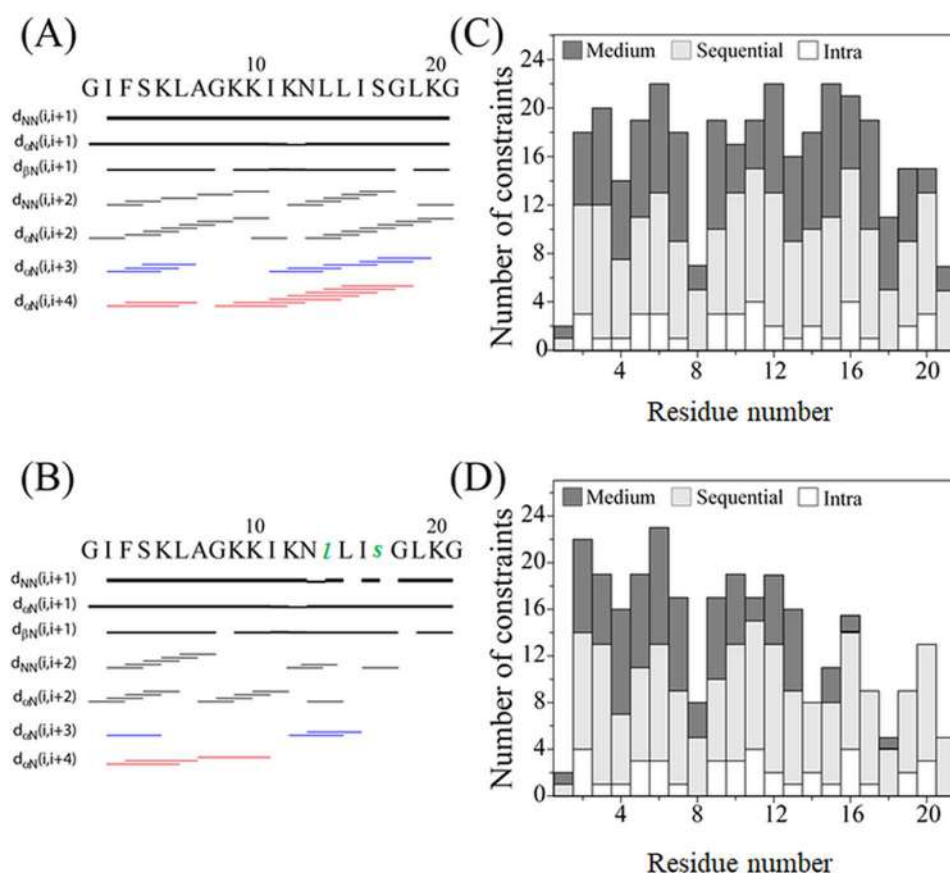

Fig. 5. Amide proton region of ^{1}H NMR spectra of 1 mM Esc(1-21) (left column) and of 1 mM Esc(1-21)-1c (right column) in the absence of detergent (A), and in the presence of (B) 200 mM perdeuterated DPC or (C) 125 mM perdeuterated SDS. The NMR experiments were performed using a Bruker Avance III 700 MHz spectrometer at pH ~4.5 and at 37 ˚C.

Fig. 6. Summary of NOE contacts of Esc(1-21) and Esc(1-21)-1c peptides in the DPC micelles. Left panel: Bar diagram demonstrating different (sequential, medium range, and long range) NOE contacts of Esc (1–21) (A) and Esc(1–21)-lc (B) in deuterated DPC micelles. The intensity of the NOESY peaks are designated by the thickness of the bars which are assigned as strong, medium, and weak during structure calculation. CαH/NH (i to i + 3) NOEs are marked by blue bars and CαH/NH (i to i + 4) NOEs are marked by red bars. Right panel: A histogram displaying the number and type (intra, sequential, medium) of NOEs of Esc(1-21) (C) and Esc(1-21)-lc (D) as a function of residue number in complex with DPC micelles. The NOESY experiments (mixing time 150 ms) were performed using Bruker Avance III 700 MHz spectrometer with 1 mM peptide in aqueous solution (pH ~ 4.5) at 37 ℃.

predominance of α-helical conformations in DPC micelles. Moreover, it was noted that the overall average chemical shift deviation was little higher in case of Esc(1-21) in comparison to Esc(1-21)-1c. The difference in average chemical shift deviation in the L14-G21 region was almost double for Esc(1-21) in comparison to Esc(1-21)-1c in line with the previous observation from NOESY spectra of both peptides.

3.5. Structure calculations for Esc(1-21) and Esc(1-21)-1c in DPC micelles

The NOESY derived distance constraints in conjunction with angular constrains, obtained from PREDITOR, were used to elucidate the three-dimensional conformations of Esc(1-21) and Esc(1-21)-1c peptides in DPC micellar solution. For structure calculations of Esc(1-21), a total of 190 distance restraints including 38 intra-residue, 85 sequential and 67 medium range constraints were used while in the case of Esc(1-21)-1c 39 intra-residue, 82 sequential and 44 medium range constraints (as a total of 165 NOEs) were available (Table 1). It is also evident that the number of medium range NOE constraints (i to i + 2/i + 3/i + 4) was much less for Esc(1-21)-1c compared to Esc(1-21), which is also reflected in the RMSD from the ensemble of the 20 lowest energy structures, as reported below. The Esc(1-21) conformations converged to a helical structure extending from I2 to G21 with an average root mean square deviation (RMSD) for the backbone atoms (N, Cα, and C′) and the heavy atoms of 0.31 ± 0.13 and 0.67 ± 0.14 Å, respectively. On the other hand, the ensemble of conformations of Esc(1-21)-1c was not precise and diverged especially at the C-terminal residues N13-G18 as designated by RMSD values of 0.96 ± 0.20 and 1.28 ± 0.21 Å for backbone and heavy atoms, respectively. From the Ramachandran plot, it was seen that the backbone dihedral angles (Φ, Ψ) accumulate in the most favoured regions for most of the residues of both Esc(1-21) and Esc(1-21)-lc, respectively.

In DPC micelles, Esc(1-21) adopted mainly α-helical conformations with a tilt at the N-terminal end (Fig. 7 A and B), whereas the central

Table 1

Summarizes the information for the 20 final NMR structures of Esc(1-21) and Esc(1-21)-1c in DPC micelles.

Distance restrains	Esc(1-21)	Esc(1-21)-lc
Intra-residue (i–j = 0)	38	39
Sequential (|i–j| = 1)	85	82
Medium-range (2 ≤ |i–j| ≤ 4)	67	44
Long-range (|i–j| ≥ 5)	0	0
Total	190	165
Angular restraints	40	40
Φ (phi)	20	20
Ψ (psi)	20	20
Distance restraints from violations (≥ 0.3 Å)	0	1
Deviation from mean structure (Å)	0.31 ± 0.13	0.96 ± 0.20
Average back bone to mean structure (G1-N13)	0.08 ± 0.02	
Average heavy atom to mean structure	0.67 ± 0.14	1.28 ± 0.21
Ramachandran plot analysis for ensemble		
% Residues in the most favourable and additionally allowed regions	(98.4 + 1.6) = 100	(90.0 + 6.6) = 96.6
% Residues in the generously allowed Region	0	3.4
% Residues in the disallowed region	0	0

region of the α-helix was straight and amphipathic due to the presence of several polar residues such as K5, K9, K10, N13 and K20, across one face of the helix. In contrast, the other face of the helix consists of the hydrophobic residues I2, F3, L6, A7, I11, L14, L15, I16 and L19. In the N-terminal region of Esc(1-21), I2, F3 and L6 were in close vicinity; thereby facilitating CH₃-π interaction among β-branched side chains and the phenyl ring of the respective residues. Collectively, the amphipathicity of Esc(1-21) was conserved in its structure so that the cumulative hydrophobic and hydrophilic interactions governed the peptide stabilization in DPC micelles. The amphipathic character was also obvious from a representation emphasizing the separation of hydrophobic and hydrophilic residues on opposite sides of the helix.
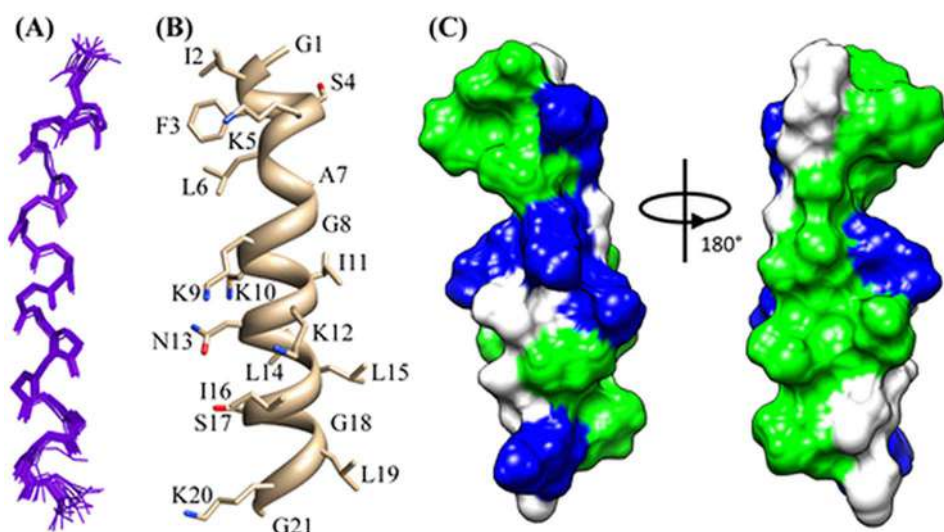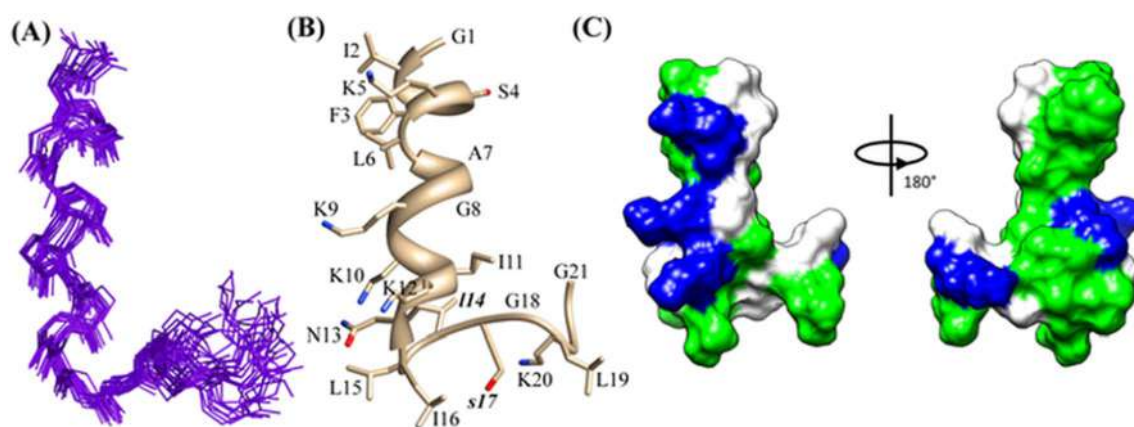
Fig. 7. Three dimensional solution structures of Esc(1-21) in DPC micelles (PDB ID 5XDJ). Superposition of backbone atoms (N, Cα, C′) of the 20 lowest energy conformations of Esc(1–21) (A). Cartoon representation of side chain orientation of a representative NMR structure of Esc(1–21) showing different residues (B). Electrostatic potential surface of Esc(1–21) showing the distribution of polar and non-polar residues (C). The hydrophobic and positively charged amino acid residues are indicated by green and blue, respectively, while all other residues are in white. These images were produced using the PyMOL software.

Fig. 8. Three dimensional solution structures of Esc(1-21)-1c in DPC micelles. Superposition of backbone atoms (N, Cα, C′) of the 20 lowest energy conformations of Esc(1-21)-1c (A). Cartoon representation of side chain orientation of a representative NMR structure of Esc(1-21)-lc showing different residues (B). Electrostatic potential surface of Esc(1–21)-1c showing the distribution of polar and non-polar residues (C). The hydrophobic and positively charged amino acid residues are indicated by green and blue, respectively, while all other residues are in white. These images were produced using the PyMOL and Chimera software.

(Fig. 7C).

In contrast, Esc(1-21)-1c in DPC micelles exhibits a partial α-helical conformation only at the N-terminal region between residues I2-N13, with an average backbone RMSD of 0.08 ± 0.02 (Fig. 8). However, the helix breaks after residue N13, likely due to the presence of two D-amino acids ^{D}L14 and ^{D}S17 [70]. It is also worth mentioning that the polar residues K5, K9 and K12 of Esc(1-21)-1c are located on one face of the N-terminal helical region, while the non-polar residues I2, F3, L6, A7 and I11 are on the opposite face of the helix, thereby maintaining an amphipathic character. Therefore, in comparison to Esc(1-21), Esc(1-21)-lc adopts a partial helical conformation only at the N-terminal region (G1-K12) while the C-terminal region (N13-G21) is unstructured and adopts a flexible conformation, which is well supported by the trend in N−H order parameter (S^2) for both peptides (Fig. S3). An order parameter of ~0.8 designates a well-defined backbone conformation, while smaller values indicate disorder. Both peptides exhibited similar trends in the order parameters of the (G1-K12) region, which are almost overlapping. The high order parameters indicate formation of well-defined backbone conformations for both Esc(1-21) and Esc(1-21)-1c. However, due to the incorporation of D-amino acids in the C-terminal part of Esc(1-21)-1c, the order parameter fluctuates in the (N13-G21) segment which supports the existence of poorly defined backbone conformations (Fig. S4). Collectively, close inspection suggests that the main difference between both structures are in the C-terminal region

L14-G21 (Fig. 9).

3.6. Membrane disorder induced by both Esc(1-21) and Esc(1-21)-1c

To gain insight into how membrane insertion of these amphiphilic peptides changes the fatty acyl chain packing of phospholipid bilayers, solid-state ^{2}H NMR spectra of membranes encompassing 75 mol% of POPE and 25 mol% of PG lipid were recorded. To assess how the lipid chain mobility and the conformational distribution of the methylene segments is influenced by Esc(1-21) or its diastereomer, the quadrupolar splittings of the ^{2}H NMR spectra were recorded and converted into fatty acyl chain order parameter profiles. The corresponding order parameter profiles of POPE-d_{31} are shown in Fig. 10 and display the characteristic signature of bilayer packing, with a plateau of $|S_{CD}|$ values extending towards the 6th carbon position. The plateau regions exhibit a value of ca. 0.23 for the pure lipid system and of ca. 0.21 for membrane embedded with Esc(1-21) or Esc(1-21)-1c. In both cases, the chain order of the POPE palmitoyl was found to be significantly reduced when compared to the pure lipid sample (Fig. 10). As outlined in the methods section, the ^{2}H NMR order parameters can be converted into the thickness of the acyl chain region of the bilayer ($< L_{chain} >$) and into the area per lipid (A) assuming that these values reflect the distribution of the acyl chain conformation. Therefore, one obtains $< L_{chain} > = 13.4 ± 0.1$ Å for the pure system and 13.1 ± 0.1 Å upon addition of 2 mol% Esc(1-21) or Esc(1-21)-1c. Although the difference
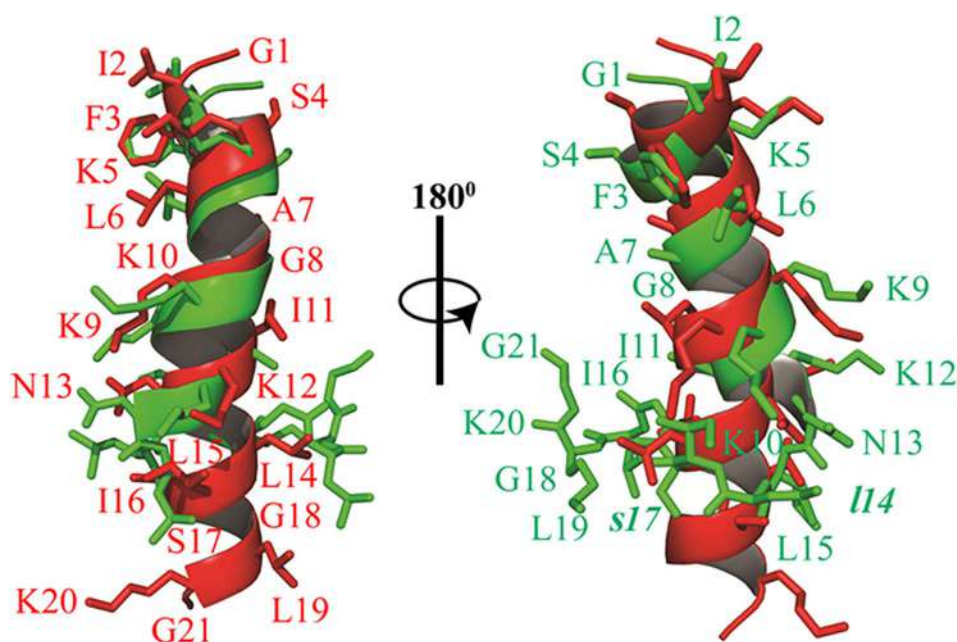
Fig. 9. Overlaid structures of Esc(1-21) (red) and Esc (1-21)-1c (green) in DPC micelles. The N-terminal helical segment (I2-N13) is superimposed nicely with a backbone RMS deviation of 0.482.

in average thickness may appear small, the membrane disordering effects in the direct vicinity of the peptides are probably more pronounced and the decreases in order parameters are significant.

4. Discussion

Recently, the short-sized AMP Esc(1-21) and especially its diastereomer Esc(1-21)-1c have been identified as encouraging candidates for the development of new anti-infective agents, because of their unique properties [30,32]. The diastereomer showed a relevant bactericidal activity against the planktonic form of the bacterial pathogen *P. aeruginosa*, albeit ∼4-fold lower than that of Esc(1-21). Here, to investigate the reasons accounting for this difference, the bacterial membrane perturbation was initially assessed by the Sytox Green assay on intact bacterial cells. Similarly to the bactericidal activity, but with a more pronounced difference between the two peptides, a stronger and faster membrane permeabilization was recorded for Esc(1-21). Therefore, it can be stated that the weaker *in vitro* antibacterial activity of Esc(1-21)-1c on the planktonic phenotype of the Gram-negative bacterium *P. aeruginosa*, as compared to Esc(1-21) is mainly associated to a weaker ability in perturbing the bacterial membrane of this pathogen with consequent cell death. In general, such a difference can have three origins [71–73]: a) a different peptide ability in crossing the LPS outer

layer and reaching the target bacterial membrane; b) a different affinity for the anionic bacterial membrane; c) differential effects once the peptides are bound to phospholipid bilayers.

Interestingly, when the effect of the two peptides was tested on cells devoid of cell wall i.e. spheroplasts of *Pseudomonas* instead of whole bacterial cells, only a slightly more (1.5-fold) pronounced microbicidal activity was obtained for the wild-type Esc(1-21) with respect to the diastereomer. Similarly, when the two isomers were analyzed on anionic model membranes, the all-L Esc(1-21) was found to induce ∼2-fold higher leakage of vesicle contents in comparison to Esc(1-21)-1c. Indeed, CD studies indicated that the affinities of the two peptides for these membranes were only slightly different, while solid-state NMR studies revealed a similar effect of the two peptides on the membrane order parameters. Based on these observations, we can exclude that differences in the antibacterial activity between the two esculentin-derived peptides are mainly due to significant differences in their membrane affinity (hypothesis b) or to a different ability to affect the phospholipid bilayer of the cytoplasmic membrane once inserted into it (hypothesis c). By exclusion, we are led to conclude that the bactericidal activity of the diastereomer against planktonic *P. aeruginosa* cells, compared to the parent peptide, is significantly impaired by a different interaction with the cell wall components, including the LPS outer membrane, which is lacking in spheroplasts. This is in agreement with
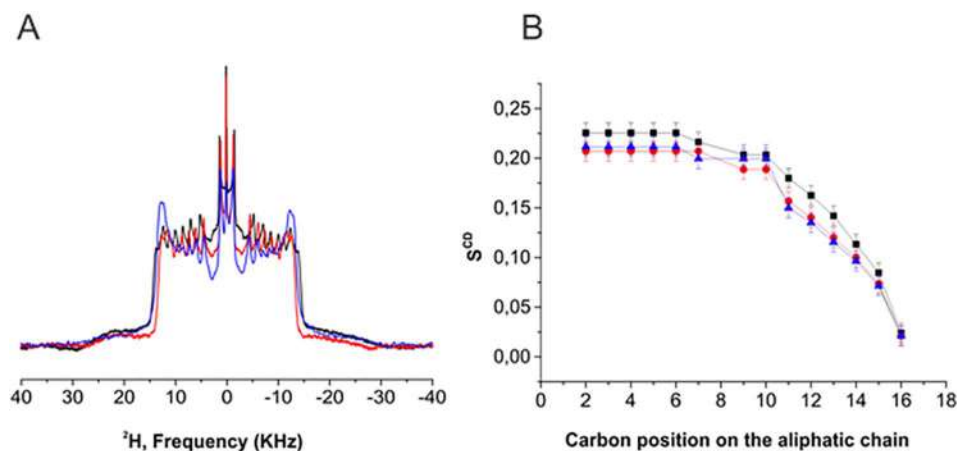

Fig. 10. ^{2}H solid state NMR spectra (A) and the corresponding S_{CD} order parameters profiles (B) of POPE:POPE^{2}H$_{31}$:POPG (2:1:1) at T = 310 K, in the absence (black line) and presence of 2 mol% Esc(1-21) (red line) and 2 mol% Esc(1-21)-lc (blue line), respectively, with an estimated uncertainty of ± 1%.

previous studies revealing that the relative binding affinity of Esc(1-21)-1c to *P. aeruginosa* LPS is ~8-fold lower in magnitude than Esc(1-21) binding to LPS and that a minor perturbation of LPS structure is caused by the diastereomer when compared to Esc(1-21) [48].

In this work we have also seen how replacement of two amino acids with the corresponding D-enantiomers in the C-terminal region of Esc(1-21) is sufficient to obtain a peptide, Esc(1-21)-1c, with a reduced α-helical content along with a lower tendency in perturbing zwitterionic model membranes. This is in line with its reduced effect on mammalian cells compared to the all-L peptide, as indicated by the corresponding concentrations causing 50% cell death (> 256 μM in comparison to a LD$_{50}$ ranging from 64 μM to 150 μM for the all-L peptide) [30]).

According to the literature, the ease of adopting stable amphipathic three-dimensional folds, which for many peptides is achieved by α-helix formation is an essential factor for AMPs to cause cytotoxicity [74,75]. As demonstrated by solution NMR studies in DPC micelles which simulate the neutral membrane of mammalian cells, an α-helical structure is preserved along the entire amino acid sequence of Esc(1-21), while a highly flexible C-terminal arm is present in Esc(1-21)-1c. This is attributed to the presence of D-amino acids at 14th and 17th position, which break the stereo chemical integrity of the sequence made of L-amino acids. This corroborates well previous structural studies of naturally occurring AMPs e.g. magainin, cytolysin and melittin [76–78].

Interestingly, a remarkable structural difference was observed between the two peptides either in aggregates of LPS, the major component of the outer-membrane of Gram-negative bacteria or in DPC micelles mimicking the lipid composition of the mammalian cell membrane (Fig. S5). The main difference is at the C-terminal region (N13-G18) of Esc(1-21)-1c (Fig. S5 B and Table 1), whose higher flexibility (RMSD = 0.96 ± 0.20 Å) (Table 1) may interfere with the peptide ability to destabilize bacterial and mammalian cell membranes in comparison to the parent Esc(1-21) [32].

Importantly, even though the two amino acid substitutions cause a somewhat weaker activity of the peptide against free-living cells of *P. aeruginosa* [30], a higher potency was shown by Esc(1-21)-1c against the more resistant form of *P. aeruginosa*, that is its biofilm community [30].

Note that the lower antimicrobial activity against the planktonic state of Pseudomonas is not in contradiction with its stronger effectiveness in killing the more dangerous biofilm phenotype [79]. Compared to the all-L peptide, Esc(1-21)-1c is more resistant to proteases which are mainly produced by cells within biofilms and much less by free living bacteria [80]. This may prolong the residence time of the diastereomer and therefore its exposure to the bacterial cells, resulting in a prolonged antimicrobial efficacy in comparison with the all-L peptide, which would be rapidly degraded. In addition, it has been lately demonstrated that D-amino acids can promote the disassembly of the extracellular matrix of biofilm cells [81,82].

Finally, it is worthwhile recalling that the diastereomer showed a reduced cytotoxicity and anti-inflammatory activity [30] than the all-L peptide. This would represent an advantage for the host immune response to bacterial infection at the initial stage.

5. Conclusions

In this work we demonstrated how the cell wall of the free living form of *P. aeruginosa* plays a major role in determining differences in the antibacterial activity between the two esculentin isomers. Most likely, a weaker binding of the diastereomer Esc(1-21)-1c to LPS and presumably slower translocation into the target bacterial membrane account for its weaker activity in comparison to the all-L peptide. The slightly lower ability in binding and perturbing anionic phospholipid bilayers for Esc(1-21)-1c contributes only in a small part to this difference, while the final effect on membrane thinning once the peptide is inserted into the membrane is identical to that provoked by Esc(1-21).

Moreover, we showed how two L- toD- amino acid substitutions in Esc(1-21) led to a lower tendency in perturbing zwitterionic model membranes in line with the lower cytotoxicity of the diastereomer.

In summary, even if Esc(1-21)-1c has a weaker bactericidal activity than the all-L peptide against the planktonic form of Pseudomonas, this still occurs at a low micromolar range [30] and it comes with a significant higher peptide biostability, higher wound-healing activity, less pronounced cytotoxicity and anti-inflammatory property [30]. Overall, these findings represent a valuable compromise for the development of a safer antibacterial agent with an extended in vivo activity. This is supported by our recent *in vivo* efficacy studies on the two selected peptide isoforms [83]. Finally, besides providing information on the structural organization of the two esculentin-derived AMPs, our data may assist in the design of new anti-infective agents with optimized biological properties.

Transparency document

The http://dx.doi.org/10.1016/j.bbamem.2017.09.009 associated with this article can be found, in the online version.

Acknowledgments

Appendix A. Supplementary data

Supplementary data to this article can be found online at http://dx.doi.org/10.1016/j.bbamem.2017.09.009.

References

[1] Y. Shai, Mode of action of membrane active antimicrobial peptides, Biopolymers 66 (2002) 236–248.

[2] N. Mookherjee, R.E. Hancock, Cationic host defence peptides: innate immune regulatory peptides as a novel approach for treating infections, Cell. Mol. Life Sci. 64 (2007) 922–933.

[3] H.G. Boman, Peptide antibiotics and their role in innate immunity, Annu. Rev. Immunol. 13 (1995) 61–92.

[4] H. Jenssen, P. Hamill, R.E. Hancock, Peptide antimicrobial agents, Clin. Microbiol. Rev. 19 (2006) 491–511.

[5] R.M. Epand, H.J. Vogel, Diversity of antimicrobial peptides and their mechanisms of action, Biochim. Biophys. Acta 1462 (1999) 11–28.

[6] R.F. Epand, M.A. Schmitt, S.H. Gellman, R.M. Epand, Role of membrane lipids in the mechanism of bacterial species selective toxicity by two alpha/beta-antimicrobial peptides, Biochim. Biophys. Acta 1758 (2006) 1343–1350.

[7] R.M. Epand, R.F. Epand, Bacterial membrane lipids in the action of antimicrobial

agents, J. Pept. Sci. 17 (2011) 298–305.

[8] K.L. Piers, R.E. Hancock, The interaction of a recombinant cecropin/melittin hybrid peptide with the outer membrane of *Pseudomonas aeruginosa*, Mol. Microbiol. 12 (1994) 951–958.

[9] M. Zasloff, Antimicrobial peptides of multicellular organisms, Nature 415 (2002) 389–395.

[10] E.F. Haney, S. Nathoo, H.J. Vogel, E.J. Prenner, Induction of non-lamellar lipid phases by antimicrobial peptides: a potential link to mode of action, Chem. Phys. Lipids 163 (2010) 82–93.

[11] K. Lohner, S.E. Blondelle, Molecular mechanisms of membrane perturbation by antimicrobial peptides and the use of biophysical studies in the design of novel peptide antibiotics, Comb. Chem. High Throughput Screen. 8 (2005) 241–256.

[12] K.A. Brogden, Antimicrobial peptides: pore formers or metabolic inhibitors in bacteria? Nat. Rev. Microbiol. 3 (2005) 238–250.

[13] A. Ghosh, R.K. Kar, J. Jana, A. Saha, B. Jana, J. Krishnamoorthy, D. Kumar, S. Ghosh, S. Chatterjee, A. Bhunia, Indolicidin targets duplex DNA: structural and mechanistic insight through a combination of spectroscopy and microscopy, ChemMedChem 9 (2014) 2052–2058.

[14] H. Bai, Y. Zhou, Z. Hou, X. Xue, J. Meng, X. Luo, Targeting bacterial RNA polymerase: promises for future antisense antibiotics development, Infect. Disord. Drug Targets 11 (2011) 175–187.

[15] J.K. Savjani, A.K. Gajjar, K.T. Savjani, Mechanisms of resistance: useful tool to design antibacterial agents for drug - resistant bacteria, Mini-Rev. Med. Chem. 9 (2009) 194–205.

[16] Y. Carmeli, N. Troillet, G.M. Eliopoulos, M.H. Samore, Emergence of antibiotic-resistant *Pseudomonas aeruginosa*: comparison of risks associated with different antipseudomonal agents, Antimicrob. Agents Chemother. 43 (1999) 1379–1382.

[17] K. Lohner, Membrane-active antimicrobial peptides as template structures for novel antibiotic agents, Curr. Top. Med. Chem. 17 (2017) 508–519.

[18] A.P. Magiorakos, A. Srinivasan, R.B. Carey, Y. Carmeli, M.E. Falagas, C.G. Giske, S. Harbarth, J.F. Hindler, G. Kahlmeter, B. Olsson-Liljequist, D.L. Paterson, L.B. Rice, J. Stelling, M.J. Struelens, A. Vatopoulos, J.T. Weber, D.L. Monnet, Multidrug-resistant, extensively drug-resistant and pandrug-resistant bacteria: an international expert proposal for interim standard definitions for acquired resistance, Clin. Microbiol. Infect. 18 (2012) 268–281.

[19] M.L. Mangoni, Host-defense peptides: from biology to therapeutic strategies, Cell. Mol. Life Sci. 68 (2011) 2157–2159.

[20] C.R. Lee, I.H. Cho, B.C. Jeong, S.H. Lee, Strategies to minimize antibiotic resistance, Int. J. Environ. Res. Public Health 10 (2013) 4274–4305.

[21] A. Nigam, D. Gupta, A. Sharma, Treatment of infectious disease: beyond antibiotics, Microbiol. Res. 169 (2014) 643–651.

[22] D.K. Mercer, D.A. O'Neil, Peptides as the next generation of anti-infectives, Future Med. Chem. 5 (2013) 315–337.

[23] K. Fosgerau, T. Hoffmann, Peptide therapeutics: current status and future directions, Drug Discov. Today 20 (2015) 122–128.

[24] A.A. Kaspar, J.M. Reichert, Future directions for peptide therapeutics development, Drug Discov. Today 18 (2013) 807–817.

[25] P. Kosikowska, A. Lesner, Antimicrobial peptides (AMPs) as drug candidates: a patent review (2003–2015), Expert. Opin. Ther. Pat. 26 (2016) 689–702.

[26] A.E. Islas-Rodriguez, L. Marcellini, B. Orioni, D. Barra, L. Stella, M.L. Mangoni, Esculentin 1-21: a linear antimicrobial peptide from frog skin with inhibitory effect on bovine mastitis-causing bacteria, J. Pept. Sci. 15 (2009) 607–614.

[27] T. Gamberi, D. Cavalieri, F. Magherini, M.L. Mangoni, C. De Filippo, M. Borro, G. Gentile, M. Simmaco, A. Modesti, An integrated analysis of the effects of Esculentin 1-21 on *Saccharomyces cerevisiae*, Biochim. Biophys. Acta 1774 (2007) 688–700.

[28] M.L. Mangoni, V. Luca, A.M. McDermott, Fighting microbial infections: a lesson from amphibian skin-derived esculentin-1 peptides, Peptides 71 (2015) 286–295.

[29] V. Luca, A. Stringaro, M. Colone, A. Pini, M.L. Mangoni, Esculentin(1 − 21), an amphibian skin membrane-active peptide with potent activity on both planktonic and biofilm cells of the bacterial pathogen *Pseudomonas aeruginosa*, Cell. Mol. Life Sci. 70 (2013) 2773–2786.

[30] A. Di Grazia, F. Cappiello, H. Cohen, B. Casciaro, V. Luca, A. Pini, Y.P. Di, Y. Shai, M.L. Mangoni, D-amino acids incorporation in the frog skin-derived peptide esculentin-1a(1-21)NH is beneficial for its multiple functions, Amino Acids 47 (2015) 2505–2519.

[31] A. Di Grazia, F. Cappiello, A. Imanishi, A. Mastrofrancesco, M. Picardo, R. Paus, M.L. Mangoni, The frog skin-derived antimicrobial peptide esculentin-1a(1-21)NH2 promotes the migration of human HaCaT keratinocytes in an EGF receptor-dependent manner: a novel promoter of human skin wound healing? PLoS One 10 (2015) e0128663.

[32] F. Cappiello, A. Di Grazia, L.A. Segev-Zarko, S. Scali, L. Ferrera, L. Galietta, A. Pini, Y. Shai, Y.P. Di, M.L. Mangoni, Esculentin-1a-derived peptides promote clearance of *Pseudomonas aeruginosa* internalized in bronchial cells of cystic fibrosis patients and lung cell migration: biochemical properties and a plausible mode of action, Antimicrob. Agents Chemother. 60 (2016) 7252–7262.

[33] A. Bragonzi, M. Paroni, A. Nonis, N. Cramer, S. Montanari, J. Rejman, C. Di Serio, G. Doring, B. Tummler, *Pseudomonas aeruginosa* microevolution during cystic fibrosis lung infection establishes clones with adapted virulence, Am. J. Respir. Crit. Care Med. 180 (2009) 138–145.

[34] C.J. Sullivan, J.L. Morrell, D.P. Allison, M.J. Doktycz, Mounting of *Escherichia coli* spheroplasts for AFM imaging, Ultramicroscopy 105 (2005) 96–102.

[35] D. Uccelletti, E. Zanni, L. Marcellini, C. Palleschi, D. Barra, M.L. Mangoni, Antipseudomonas activity of frog skin antimicrobial peptides in a *Caenorhabditis elegans* infection model: a plausible mode of action *in vitro* and *in vivo*, Antimicrob. Agents Chemother. 54 (2010) 3853–3860.

[36] S.M. Kelly, T.J. Jess, N.C. Price, How to study proteins by circular dichroism, Biochim. Biophys. Acta 1751 (2005) 119–139.

[37] J.C. Stewart, Colorimetric determination of phospholipids with ammonium ferrothiocyanate, Anal. Biochem. 104 (1980) 10–14.

[38] L. Marcellini, M. Borro, G. Gentile, A.C. Rinaldi, L. Stella, P. Aimola, D. Barra, M.L. Mangoni, Esculentin-1b(1-18)—a membrane-active antimicrobial peptide that synergizes with antibiotics and modifies the expression level of a limited number of proteins in *Escherichia coli*, FEBS J. 276 (2009) 5647–5664.

[39] A. Makovitzki, D. Avrahami, Y. Shai, Ultrashort antibacterial and antifungal lipopeptides, Proc. Natl. Acad. Sci. U. S. A. 103 (2006) 15997–16002.

[40] K. Matsuzaki, Why and how are peptide-lipid interactions utilized for self-defense? Magainins and tachyplesins as archetypes, Biochim. Biophys. Acta 1462 (1999) 1–10.

[41] G. Manzo, M. Carboni, A.C. Rinaldi, M. Casu, M.A. Scorciapino, Characterization of sodium dodecylsulphate and dodecylphosphocholine mixed micelles through NMR and dynamic light scattering, Magn. Reson. Chem. 51 (2013) 176–183.

[42] T. Goddard, D.G. Kneller, SPARKY 3, 14 University of California, San Francisco, 2004, p. 15.

[43] M. Piotto, V. Saudek, V. Sklenar, Gradient-tailored excitation for single-quantum NMR spectroscopy of aqueous solutions, J. Biomol. NMR 2 (1992) 661–665.

[44] K. Wuthrich, NMR of Proteins And Nucleic Acids, Wiley, 1986.

[45] P. Guntert, C. Mumenthaler, K. Wuthrich, Torsion angle dynamics for NMR structure calculation with the new program DYANA, J. Mol. Biol. 273 (1997) 283–298.

[46] M.V. Berjanskii, S. Neal, D.S. Wishart, PREDITOR: a web server for predicting protein torsion angle restraints, Nucleic Acids Res. 34 (2006) W63–69.

[47] A. Datta, A. Ghosh, C. Airoldi, P. Sperandeo, K.H. Mroue, J. Jimenez-Barbero, P. Kundu, A. Ramamoorthy, A. Bhunia, Antimicrobial peptides: insights into membrane permeabilization, lipopolysaccharide fragmentation and application in plant disease control, Sci Rep 5 (2015) 11951.

[48] A. Ghosh, S. Bera, Y. Shai, M.L. Mangoni, A. Bhunia, NMR structure and binding of esculentin-1a (1-21)NH2 and its diastereomer to lipopolysaccharide: correlation with biological functions, Biochim. Biophys. Acta 1858 (2016) 800–812.

[49] R.A. Laskowski, J.A. Rullmann, M.W. MacArthur, R. Kaptein, J.M. Thornton, AQUA and PROCHECK-NMR: programs for checking the quality of protein structures solved by NMR, J. Biomol. NMR 8 (1996) 477–486.

[50] F. Zhang, R. Bruschweiler, Contact model for the prediction of NMR N-H order parameters in globular proteins, J. Am. Chem. Soc. 124 (2002) 12654–12655.

[51] J.H. Davis, K.R. Jeffrey, M. Bloom, M.I. Valic, Quadrupolar echo deuteron magnetic resonance spectroscopy in ordered hydrocarbon chains, Chem. Phys. Lett. 42 (1976) 390–394.

[52] J.H. Davis, The description of membrane lipid conformation, order and dynamics by 2H-NMR, Biochim. Biophys. Acta 737 (1983) 117–171.

[53] M. Bloom, J.H. Davis, A.L. Mackay Mackay, Direct determination of the oriented sample NMR spectrum from the powder spectrum for the systems with local axial symmetry, Chem. Phys. Lett. 80 (1981) 198–202.

[54] M.A. McCabe, S.R. Wassall, Rapid deconvolution of NMR powder spectra by weighted fast Fourier transformation, Solid State Nucl. Magn. Reson. 10 (1997) 53–61.

[55] J. Seelig, Deuterium magnetic resonance: theory and application to lipid membranes, Q. Rev. Biophys. 10 (1977) 353–418.

[56] J.P. Douliez, A. Leonard, E.J. Dufourc, Restatement of order parameters in biomembranes: calculation of C−C bond order parameters from C-D quadrupolar splittings, Biophys. J. 68 (1995) 1727–1739.

[57] L.A. Douliez Jean-Paul, Erick J. Dufourc, Conformational order of DMPC sn-1 versus sn-2 chains and membrane thickness: an approach to molecular protrusion by solid state 2H–NMR and neutron diffraction, J. Chim. Phys. 100 (1996) 18450–18457.

[58] H. Schindler, J. Seelig, Deuterium order parameters in relation to thermodynamic properties of a phospholiped bilayer. A statistical mechanical interpretation, Biochemistry 14 (1975) 2283–2287.

[59] S.L. Grage, S. Afonin, S. Kara, G. Buth, A.S. Ulrich, Membrane thinning and thickening induced by membrane-active amphipathic peptides, Front. Cell. Dev. Biol. 4 (2016) 65.

[60] A. Grelard, P. Guichard, P. Bonnafous, S. Marco, O. Lambert, C. Manin, F. Ronzon, E.J. Dufourc, Hepatitis B subvirus particles display both a fluid bilayer membrane and a strong resistance to freeze drying: a study by solid-state NMR, light scattering, and cryo-electron microscopy/tomography, FASEB J. 27 (2013) 4316–4326.

[61] M.R. de Planque, D.V. Greathouse, R.E. Koeppe 2nd, H. Schafer, D. Marsh, J.A. Killian, Influence of lipid/peptide hydrophobic mismatch on the thickness of diacylphosphatidylcholine bilayers. A 2H NMR and ESR study using designed transmembrane alpha-helical peptides and gramicidin A, Biochemistry 37 (1998) 9333–9345.

[62] J.F. Nagle, Area/lipid of bilayers from NMR, Biophys. J. 64 (1993) 1476–1481.

[63] L. Stella, C. Mazzuca, M. Venanzi, A. Palleschi, M. Didone, F. Formaggio, C. Toniolo, B. Pispisa, Aggregation and water-membrane partition as major determinants of the activity of the antibiotic peptide trichogin GA IV, Biophys. J. 86 (2004) 936–945.

[64] G. Bocchinfuso, S. Bobone, C. Mazzuca, A. Palleschi, L. Stella, Fluorescence spectroscopy and molecular dynamics simulations in studies on the mechanism of membrane destabilization by antimicrobial peptides, Cell. Mol. Life Sci. 68 (2011) 2281–2301.

[65] A.S. Ladokhin, M. Fernandez-Vidal, S.H. White, CD spectroscopy of peptides and proteins bound to large unilamellar vesicles, J. Membr. Biol. 236 (2010) 247–253.

[66] S.Y. Lau, A.K. Taneja, R.S. Hodges, Synthesis of a model protein of defined secondary and quaternary structure. Effect of chain length on the stabilization and formation of two-stranded alpha-helical coiled-coils, J. Biol. Chem. 259 (1984) 13253–13261.

[67] L. Maler, Solution NMR studies of peptide-lipid interactions in model membranes,

Mol. Membr. Biol. 29 (2012) 155–176.

[68] R. Wimmer, L.E. Uggerhoj, Determination of structure and micellar interactions of small antimicrobial peptides by solution-state NMR, Methods Mol. Biol. 1548 (2017) 73–88.

[69] D.S. Wishart, C.G. Bigam, J. Yao, F. Abildgaard, H.J. Dyson, E. Oldfield, J.L. Markley, B.D. Sykes, 1H, 13C and 15N chemical shift referencing in biomolecular NMR, J. Biomol. NMR 6 (1995) 135–140.

[70] P.Y. Chou, G.D. Fasman, Empirical predictions of protein conformation, Annu. Rev. Biochem. 47 (1978) 251–276.

[71] M.L. Mangoni, R.F. Epand, Y. Rosenfeld, A. Peleg, D. Barra, R.M. Epand, Y. Shai, Lipopolysaccharide, a key molecule involved in the synergism between temporins in inhibiting bacterial growth and in endotoxin neutralization, J. Biol. Chem. 283 (2008) 22907–22917.

[72] D. Roversi, V. Luca, S. Aureli, Y. Park, M.L. Mangoni, L. Stella, How many antimicrobial peptide molecules kill a bacterium? The case of PMAP-23, ACS Chem. Biol. 9 (2014) 2003–2007.

[73] F. Savini, V. Luca, A. Bocedi, R. Massoud, Y. Park, M.L. Mangoni, L. Stella, Cell-density dependence of host-defense peptide activity and selectivity in the presence of host cells, ACS Chem. Biol. 12 (2017) 52–56.

[74] E. Gazit, W.J. Lee, P.T. Brey, Y. Shai, Mode of action of the antibacterial cecropin B2: a spectrofluorometric study, Biochemistry 33 (1994) 10681–10692.

[75] Y. Pouny, D. Rapaport, A. Mor, P. Nicolas, Y. Shai, Interaction of antimicrobial dermaseptin and its fluorescently labeled analogues with phospholipid membranes, Biochemistry 31 (1992) 12416–12423.

[76] Y. Shai, Z. Oren, Diastereoisomers of cytolysins, a novel class of potent antibacterial peptides, J. Biol. Chem. 271 (1996) 7305–7308.

[77] R. Saravanan, A. Bhunia, S. Bhattacharjya, Micelle-bound structures and dynamics of the hinge deleted analog of melittin and its diastereomer: implications in cell selective lysis by D-amino acid containing antimicrobial peptides, Biochim. Biophys. Acta 1798 (2010) 128–139.

[78] T. Wieprecht, O. Apostolov, M. Beyermann, J. Seelig, Thermodynamics of the alpha-helix-coil transition of amphipathic peptides in a membrane environment: implications for the peptide-membrane binding equilibrium, J. Mol. Biol. 294 (1999) 785–794.

[79] E. Drenkard, F.M. Ausubel, Pseudomonas biofilm formation and antibiotic resistance are linked to phenotypic variation, Nature 416 (2002) 740–743.

[80] G. Singh, B. Wu, M.S. Baek, A. Camargo, A. Nguyen, N.A. Slusher, R. Srinivasan, J.P. Wiener-Kronish, S.V. Lynch, Secretion of *Pseudomonas aeruginosa* type III cytotoxins is dependent on pseudomonas quinolone signal concentration, Microb. Pathog. 49 (2010) 196–203.

[81] D. Romero, H. Vlamakis, R. Losick, R. Kolter, An accessory protein required for anchoring and assembly of amyloid fibres in *B. subtilis* biofilms, Mol. Microbiol. 80 (2011) 1155–1168.

[82] L. Segev-Zarko, R. Saar-Dover, V. Brumfeld, M.L. Mangoni, Y. Shai, Mechanisms of biofilm inhibition and degradation by antimicrobial peptides, Biochem. J. 468 (2015) 259–270.

[83] C. Chen, M.L. Mangoni, Y.P. Di, *In vivo* therapeutic efficacy of frog skin-derived peptides against *Pseudomonas aeruginosa*-induced pulmonary infection, Sci Rep 7 (2017) 8548.

CrossMark
click for updates

Esculentin-1a-Derived Peptides Promote Clearance of *Pseudomonas aeruginosa* Internalized in Bronchial Cells of Cystic Fibrosis Patients and Lung Cell Migration: Biochemical Properties and a Plausible Mode of Action

Floriana Cappiello,[a] Antonio Di Grazia,[a] Li-av Segev-Zarko,[b] Silvia Scali,[c] Loretta Ferrera,[d] Luis Galietta,[d] Alessandro Pini,[c] Yechiel Shai,[b] Y. Peter Di,[e] Maria Luisa Mangoni[a]

Department of Biochemical Sciences, Sapienza University of Rome, Rome, Italy[a]; Department of Biological Chemistry, The Weizmann Institute of Science, Rehovot, Israel[b]; Department of Medical Biotechnology, University of Siena, Siena, Italy[c]; U.O.C. Genetica Medica, Giannina Gaslini Institute, Genoa, Italy[d]; Department of Environmental and Occupational Health, University of Pittsburgh, Pittsburgh, Pennsylvania, USA[e]

Pseudomonas aeruginosa **is the major microorganism colonizing the respiratory epithelium in cystic fibrosis (CF) sufferers. The widespread use of available antibiotics has drastically reduced their efficacy, and antimicrobial peptides (AMPs) are a promising alternative. Among them, the frog skin-derived AMPs, i.e., Esc(1-21) and its diastereomer, Esc(1-21)-1c, have recently shown potent activity against free-living and sessile forms of** *P. aeruginosa.* **Importantly, this pathogen also escapes antibiotics treatment by invading airway epithelial cells. Here, we demonstrate that both AMPs kill** *Pseudomonas* **once internalized into bronchial cells which express either the functional or the ΔF508 mutant of the CF transmembrane conductance regulator. A higher efficacy is displayed by Esc(1-21)-1c (90% killing at 15 μM in 1 h). We also show the peptides' ability to stimulate migration of these cells and restore the induction of cell migration that is inhibited by** *Pseudomonas* **lipopolysaccharide when used at concentrations mimicking lung infection. This property of AMPs was not investigated before. Our findings suggest new therapeutics that not only eliminate bacteria but also can promote reepithelialization of the injured infected tissue. Confocal microscopy indicated that both peptides are intracellularly localized with a different distribution. Biochemical analyses highlighted that Esc(1-21)-1c is significantly more resistant than the all-ʟ peptide to bacterial and human elastase, which is abundant in CF lungs. Besides proposing a plausible mechanism underlying the properties of the two AMPs, we discuss the data with regard to differences between them and suggest Esc(1-21)-1c as a candidate for the development of a new multifunctional drug against** *Pseudomonas* **respiratory infections.**

*P*seudomonas aeruginosa is an opportunistic Gram-negative bacterium characterized by an intrinsic high resistance to commonly used antimicrobials (1, 2) and by its ability to form sessile communities, named biofilms (3–5). In this scenario, *P. aeruginosa* infections can easily take over and affect multiple organ systems, such as the respiratory tract, particularly in cystic fibrosis (CF) patients (6–8). The most common mutation associated with the CF phenotype is phenylalanine deletion at position 508 (ΔF508) in the CF transmembrane conductance regulator (CFTR) gene (9), encoding an ABC transporter that functions as a chloride channel in the membrane of epithelial cells (10). As a result of this mutation, the secretion of chloride ions outside the cell is inhibited, resulting in the generation of a dehydrated and sticky mucus layer coating the airway epithelia (11, 12). This helps the accumulation of trapped microbes, including *P. aeruginosa*, with deterioration of lung tissue and impairment of respiratory functions (13–15).

Importantly, *P. aeruginosa* colonization of host tissues is triggered by an initial attachment of the bacterium to epithelial cells (7, 16) via a variety of surface appendages (e.g., flagella and pili) (17–19). This is then followed by cell internalization, presumably mediated by binding of the bacterial lipopolysaccharide (LPS; i.e., the major component of the outer membrane in Gram-negative bacteria) to the CFTR (20–24). Other mechanisms include, e.g., interaction with asialoganglioside 1 (25). Invasion of host cells is a common process used by different microbial pathogens to facili-

tate escape from immune factors and/or to assist systemic diffusion and infection (26, 27). Intracellular persistence of bacteria that spread into the respiratory tract of CF patients may be one of the reasons responsible for the chronic nature of *P. aeruginosa* lung infections (17). It protects the bacteria from the host defense mechanisms and from the killing action of conventional antibiotics that hardly enter epithelial cells (28). Hence, the discovery of new antibiotics with new modes of action is highly demanding, and naturally occurring antimicrobial peptides (AMPs) represent potential alternatives (29, 30). AMPs are produced by all

living organisms as the first barrier against invading microorganisms (31), and the majority of them are characterized by having a net positive charge at neutral pH and the tendency to form an amphipathic structure in a hydrophobic environment (32, 33).

Recently, we studied a derivative of the frog skin AMP esculentin-1a, esculentin-1a(1-21)NH₂ [Esc(1-21) GIFSKLAGKKIKNLL ISGLKG-NH₂] (34, 35), corresponding to the first 20 residues of esculentin-1a, as well as its diastereomer, Esc(1-21)-1c, containing two D-amino acids at positions 14 and 17 (i.e., D-Leu and D-Ser, respectively). The data revealed that the two peptides have strong bactericidal activity against both the planktonic and biofilm forms of *P. aeruginosa*, with the diastereomer being more active than the wild-type peptide on the sessile form of this pathogen (36). Furthermore, the diastereomer is more stable in human serum (36). However, there are no studies on the effect of these peptides on infected lung epithelial cells, and only limited information is available for other AMPs.

Importantly, the ability of a peptide to restore the integrity of damaged infected tissue, for example, by accelerating migration of epithelial cells in addition to potent antimicrobial activity, would make it a more promising candidate for the development of a new anti-infective agent. Another advantage is the ability to resist degradation by proteases. Here, we report on the effect of the two esculentin-derived AMPs on the viability of bronchial epithelial cells expressing a functional CFTR or a mutant form of CFTR (ΔF508-CFTR). Furthermore, we investigated the peptides' ability (i) to kill a clinical isolate of *P. aeruginosa*, once internalized in the two bronchial cell lines, and (ii) to stimulate migration of bronchial cells in the presence of concentrations of LPS that better simulate an infection condition by means of a pseudo-wound-healing assay. To the best of our knowledge, this is the first demonstration of cell migration induced by AMPs in the presence of LPS. In addition, we studied the peptides' distribution within bronchial cells and their stability to elastase from *P. aeruginosa* and human neutrophils. The data are discussed with regard to the different biochemical properties of the two peptides, and a plausible mechanism for their antimicrobial and wound-healing properties is proposed.

MATERIALS AND METHODS

Materials. Minimal essential medium (MEM), heat-inactivated fetal bovine serum (FBS), and penicillin-streptomycin were from Euroclone (Milan, Italy); puromycin, gentamicin, 3(4,5-dimethylthiazol-2yl)2,5-diphenyltetrazolium bromide (MTT), Triton X-100, AG1478, 4′,6-diamidino-2-phenylindole (DAPI), rhodamine, Mowiol 4-88, LPS from *P. aeruginosa* serotype 10 (purified by phenol extraction), and elastase from human leukocytes were purchased from Sigma-Aldrich (St. Luis, MO). Elastase from *P. aeruginosa* was from Millipore Merck (Merck, Milan, Italy). All other chemicals were reagent grade.

Peptides synthesis. Synthetic Esc(1-21) and its diastereomer, Esc(1-21)-1c, as well as rhodamine-labeled peptides [rho-Esc(1-21) and rho-Esc(1-21)-1c], were purchased from Chematek Spa (Milan, Italy). Briefly, each peptide was assembled by stepwise solid-phase synthesis using a standard F-moc strategy and purified via reverse-phase high-performance liquid chromatography (RP-HPLC) to a purity of 98%, while the molecular mass was verified by mass spectrometry.

Cells and bacteria. The following cell cultures were employed: immortalized human bronchial epithelial cells derived from a CF patient (CFBE41o-) transduced with a lentiviral system to stably express ΔF508-CFTR (ΔF508-CFBE) or functional CFTR (wt-CFBE) (37). Cells were cultured in MEM supplemented with 2 mM glutamine (MEMg) plus 10%

FBS, antibiotics (0.1 mg/ml of penicillin and streptomycin), and puromycin (0.5 μg/ml or 2 μg/ml for wt-CFBE or ΔF508-CFBE, respectively) at 37°C and 5% CO_2 in 75-cm² flasks. The bacterial strain used was an invasive clinical isolate from the early stage of chronic lung infection, *P. aeruginosa* KK1, from the collection of the CF clinic Medizinische Hochschule of Hannover, Germany (38, 39).

Peptides' effect on the viability of airway epithelial cells. The effect of both peptides on the viability of wt-CFBE or ΔF508-CFBE cells was evaluated by the MTT colorimetric method (40). MTT is a tetrazolium salt which is reduced to a colored formazan product by mitochondrial reductases in metabolically active cells. Briefly, about 4×10^4 cells suspended in MEMg supplemented with 2% FBS were seeded in wells of a 96-well microtiter plate. After overnight incubation at 37°C in a 5% CO_2 atmosphere, the medium was removed and 100 μl of fresh serum-free MEMg or Hanks' buffer (136 mM NaCl, 4.2 mM Na_2HPO_4, 4.4 mM KH_2PO_4, 5.4 mM KCl, 4.1 mM $NaHCO_3$, pH 7.2, supplemented with 20 mM D-glucose), with or without the peptide at different concentrations, was added to each well. After 2 h or 24 h, as indicated, at 37°C in a 5% CO_2 atmosphere, the medium was replaced with 100 μl of Hanks' buffer containing 0.5 mg/ml MTT. The plate was incubated at 37°C and 5% CO_2 for 4 h, and the formazan crystals were dissolved by adding 100 μl of acidified isopropanol according to reference 41. Absorption of each well was measured using a microplate reader (Infinite M200; Tecan, Salzburg, Austria) at 570 nm. The percentage of metabolically active cells compared to control samples (cells not treated with peptide) was calculated according to the formula (absorbance$_{sample}$ − absorbance$_{blank}$)/(absorbance$_{control}$ − absorbance$_{blank}$) × 100, where the blank is given by samples without cells and not treated with the peptide.

Cell infection and peptide's effect on intracellular bacteria. About 100,000 bronchial cells in MEMg supplemented with 10% FBS were seeded in 24-well plates and grown for 2 days at 37°C and 5% CO_2. The clinical isolate KK1 was grown in Luria-Bertani broth at 37°C with mild shaking (125 rpm) to mid-log phase (optical density of 0.8 at 590 nm) and subsequently harvested by centrifugation. The pellet was then resuspended in MEMg and properly syringed using a 21-gauge needle to avoid clump formation before infecting cells. A multiplicity of infection (MOI) of 100:1 (bacteria to cells) was used. Two hundred microliters of this bacterial suspension, containing about 1×10^7 CFU, was coincubated for 1 h with wt-CFBE/ΔF508-CFBE at 37°C and 5% CO_2. After infection, the medium was removed and the cells were washed three times with MEMg and then incubated for 1 h with a gentamicin solution (200 μg/ml in MEMg) to remove extracellular bacteria. Afterwards, the medium was aspirated and the infected cells were washed three times as described above. Two hundred microliters of Hanks' solution with or without the peptide at different concentrations was added to each well, and the plate was incubated for 1 h at 37°C and 5% CO_2. After peptide treatment, cells were washed with phosphate-buffered saline (PBS) and lysed with 300 μl of 0.1% Triton X-100 in PBS for 15 min at 37°C and 5% CO_2. Each sample was then sonicated in a water bath for 5 min to break up possible bacterial clumps, and appropriate aliquots were plated on agar plates for counting of CFU after 24 h at 37°C.

***In vitro* cell migration assay.** The ability of single peptides or *P. aeruginosa* LPS to stimulate migration of CF cells was evaluated by a modified scratch assay, as reported previously (36). Briefly, special cell culture inserts for live cell analysis (Ibidi, Munich, Germany) were placed into wells of a 12-well plate. About 35,000 cells suspended in MEMg supplemented with 10% FBS were seeded in each compartment of the culture insert and incubated at 37°C and 5% CO_2 for approximately 24 h to allow cells to grow to confluence. Afterwards, inserts were removed to create a cell-free area (pseudo-wound) of approximately 500 μm; 1 ml MEMg with or without the peptide or LPS at different concentrations was added to each well. Plates were incubated as described above to allow cells to migrate, and samples were visualized at different time intervals under an inverted microscope (Olympus CKX41) at ×4 magnification and photographed with a Color View II digital camera. The percentage of cell-cov-
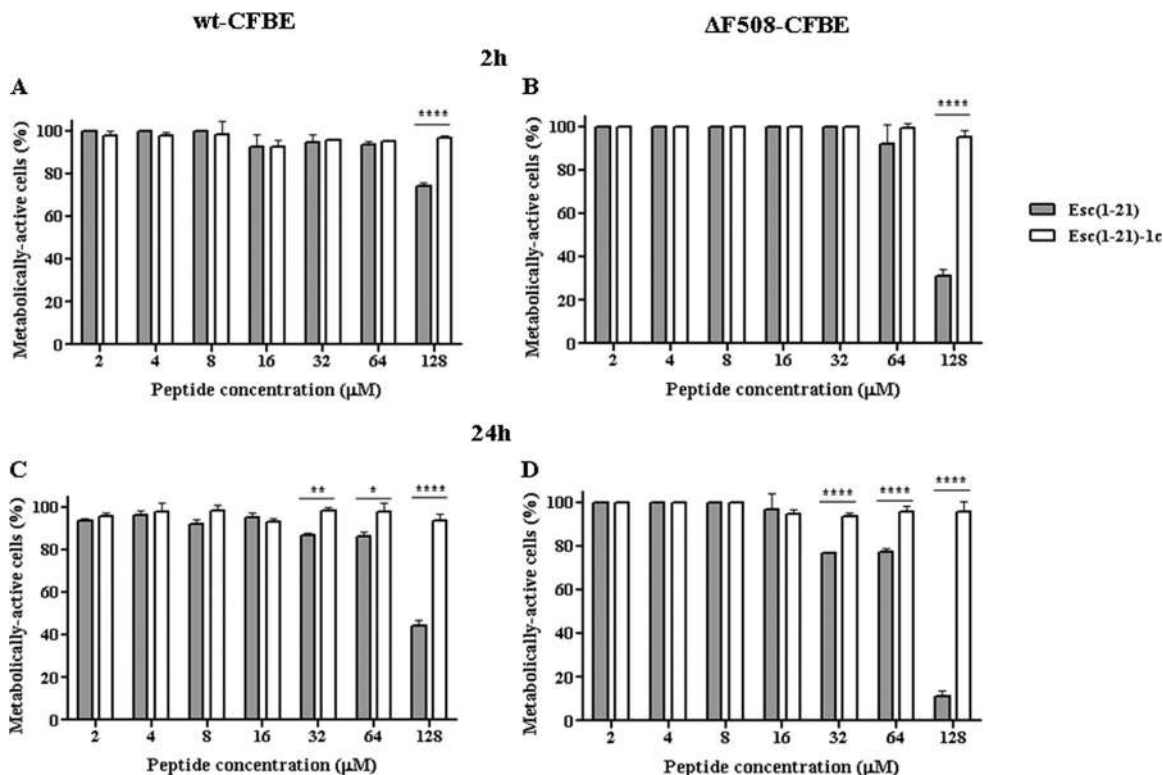
FIG 1 Peptides' effect on the viability of bronchial epithelial cells. About 4×10^4 wt-CFBE (A and C) or ΔF508-CFBE (B and D) cells were plated in wells of a microtiter plate. After overnight incubation at 37°C in a 5% CO_2 atmosphere, the medium was replaced with 100 μl fresh MEMg supplemented with the peptides at different concentrations. After 2 h or 24 h, cell viability was determined by MTT reduction to insoluble formazan. Cell viability is expressed as a percentage with respect to the control (cells not treated with the peptide). All data are the means from four independent experiments ± SEM. The levels of statistical significance between the two peptides are P values of <0.05 (*), <0.01 (**), and $P < 0.0001$ (****).

ered area at each time was determined by the WIMASIS Image Analysis program.

In another set of experiments, cell migration was evaluated in the presence of both LPS and Esc(1-21) or Esc(1-21)-1c at the indicated concentration. Furthermore, the implication of epidermal growth factor receptor (EGFR) in peptide-induced cell migration was analyzed by pretreating cells for 30 min with 5 μM tyrosine phosphorylation inhibitor tyrphostin (AG1478) (42).

Fluorescence studies. About 2×10^5 bronchial cells in MEMg supplemented with 10% FBS were seeded on 0.13- to 0.17-mm-thick coverslips (properly put into 35-mm dish plates) and incubated at 37°C and 5% CO_2. After 24 h, samples were washed with 1 ml PBS and treated with 4 μM rhodamine-labeled peptide or rhodamine (for control samples) in MEMg. After 30 min and 24 h of incubation at 37°C and 5% CO_2, cells were washed four times with PBS and fixed with 700 μl of 4% formaldehyde for 15 min at room temperature. Afterwards, they were washed twice with PBS and stained with DAPI (1 μg/ml) for 5 min at room temperature to visualize the nuclei. After three additional washes, the coverslips were mounted on clean glass slides using Mowiol mounting medium and observed under an Olympus FV1000 confocal microscope with a 60× objective lens (oil). Data analysis was done using Olympus Fluoview (version 4.1) and Image J. Results are reported as the ratio between the fluorescence intensity of rhodamine-labeled peptides in the cytoplasm versus that in the nucleus.

Peptides' stability to proteases. Peptides were dissolved in 10 mM Tris-HCl, pH 7.5, at a final concentration of 1 mg/ml; afterwards, 130 μl was incubated with 4 μg of human or bacterial elastase (final enzyme concentration equal to 1 μM). At the indicated time intervals, 30-μl aliquots were withdrawn, diluted with 770 μl of 0.1% trifluoroacetic acid

(TFA)–water, and analyzed by RP-HPLC and mass spectrometry. Liquid chromatography was performed on a Phenomenex Jupiter C_{18} analytical column (300 Å, 5 μm, 250 by 4.6 mm) in a 30-min gradient, using 0.1% TFA in water as solvent A and methanol as solvent B. Mass spectrometry analysis was performed with a Bruker Daltonic ultraflex matrix-assisted laser desorption ionization tandem time-of-flight (MALDI-TOF/TOF) mass spectrometer on withdrawn samples as well as on HPLC-eluted peaks.

Statistical analyses. Quantitative data, collected from independent experiments, were expressed as the means ± standard errors of the means (SEM). Statistical analysis was performed using two-way analysis of variance (ANOVA) with PRISM software (GraphPad, San Diego, CA). Differences were considered to be statistically significant for a P value of <0.05. The levels of statistical significance are indicated in the legends to the figures.

RESULTS

Peptides' effect on the viability of lung epithelial cells. In a previous study (36), it was reported that both Esc(1-21) and its diastereomer, Esc(1-21)-1c, are not toxic to A549 epithelial cells up to 64 μM, and that the diastereomer is substantially less toxic when used at higher concentrations (36). Although A549 cells possess morphological and biochemical properties of alveolar epithelial cells (type II pneumocytes) (17), they do not express CFTR (43, 44). Therefore, we studied the effect of both esculentin peptides on the viability of airway epithelial cells stably expressing the most common CFTR mutation (ΔF508)
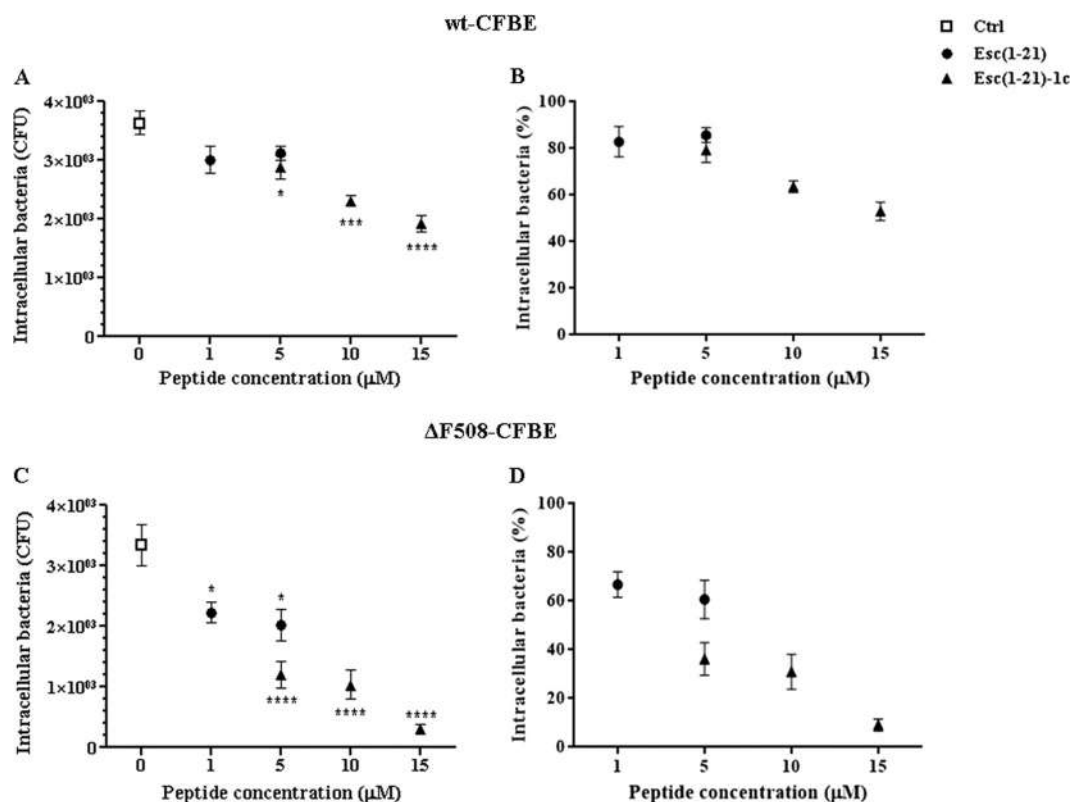
FIG 2 Effect of Esc(1-21) and its diastereomer, Esc(1-21)-1c, on the intracellular killing of *P. aeruginosa* KK1 in wt-CFBE (A and B) and ΔF508-CFBE (C and D) cells. About 1×10^5 cells were seeded in 24-well plates and grown to confluence. Afterwards, they were infected with the bacterium for 1 h; nonadherent extracellular bacteria were removed upon antibiotic treatment, and infected cells were left untreated or were treated for 1 h with the peptide at different concentrations, as indicated. Control samples (Ctrl) are peptide-untreated infected cells. The number of intracellular bacteria is expressed either as CFU per sample (A and C) or as a percentage with respect to the control (B and D). All data are the means from four independent experiments ± SEM. The levels of statistical significance between peptide-treated infected cells and control samples are *P* values of <0.05 (*), <0.001 (***), and <0.0001 (****).

and the corresponding wild-type cell line expressing a functional CFTR.

As indicated by the results of the viability assay performed in the cell culture medium, MEMg (Fig. 1), the two peptides were not toxic to either type of epithelial cells at a concentration range between 2 μM and 64 μM within 2 h. However, the wild-type peptide turned out to be toxic at 128 μM, causing approximately 25% and 70% reduction in the percentage of metabolically active wt-CFBE and ΔF508-CFBE cells, respectively (Fig. 1A and B). Furthermore, after a long-term treatment (24 h), the cytotoxicity of Esc(1-21) became more pronounced, inducing about 20 to 25% reduction of metabolically active epithelial cells at 32 μM and 64 μM (Fig. 1C and D). A higher cytotoxicity was recorded at 128 μM, with ~60% and 90% killing of wt-CFBE and ΔF508-CFBE cells, respectively. Importantly, the diastereomer did not induce any reduction in the percentage of metabolically active cells (Fig. 1).

Peptides' activity on bronchial cells infected by the CF clinical isolate KK1. We monitored the effect of the two peptides on wt-CFBE (Fig. 2A and B) and ΔF508-CFBE cells (Fig. 2C and D) after infection with a clinical isolate of *P. aeruginosa* (KK1 strain). This strain was already shown to invade bronchial cells *in vitro* (38). According to the published literature (25), *P. aeruginosa* tends to target particular CF epithelial cells rather than making a concerted attack on the whole population of cells. Figure 2 shows the number of intracellular bacteria that were calculated either as CFU per sample (Fig. 2A and C) or as percentage (Fig. 2B and D) with respect to the peptide-untreated infected cells (control). Note that the number of internalized bacteria (~3,500 CFU) in our control bronchial cells (Fig. 2A and C) was well correlated with the previously found uptake of different *P. aeruginosa* strains by CF airway epithelial cells (21).

The data shown in Fig. 2B reveal that the two peptides, at 5 μM, caused about 15 to 20% killing of intracellular bacteria 1 h after treatment. This is when they were used on wt-CFBE cells in Hanks' buffer. This condition was used to better simulate a physiological environment without the presence of cell culture medium components. However, the killing effect was more evident in ΔF508-CFBE cells (Fig. 2D), where 5 μM Esc(1-21) and its diastereomer caused an ~40% and 60% decrease in the number of intracellular bacteria, respectively, compared to untreated infected cells. Due to the negligible cytotoxicity of the diastereomer Esc(1-21)-1c compared to the all-L isomer in Hanks' buffer (see Fig. S1 in the supplemental material), it was possible to use Esc(1-21)-1c at higher concentrations without damaging host epithelial cells. Interestingly, 10 μM and 15 μM Esc(1-21)-1c gave rise to about 70% and 90% reduction in the survival of intracellular bacteria in ΔF508-CFBE (Fig. 2D), whereas only ~50% bacte-
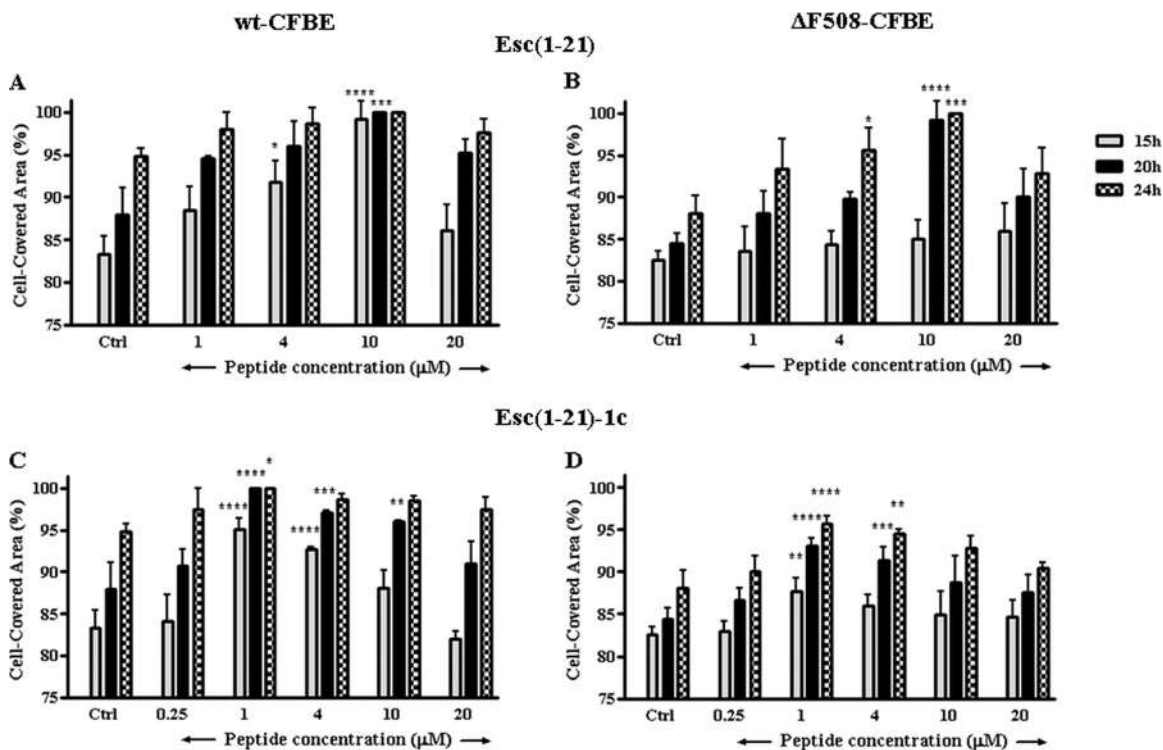
FIG 3 Effect of Esc(1-21) and Esc(1-21)-1c on the closure of a pseudo-wound field produced in a monolayer of wt-CFBE (A and C) and ΔF508-CFBE (B and D). Cells were seeded in each side of an Ibidi culture insert and grown to confluence; afterwards, they were left untreated or were treated with the peptide. Cells were photographed at the time of insert removal and examined for cell migration after 15, 20, and 24 h from peptide addition. The percentage of cell-covered area at each time point is reported on the *y* axis. Peptide-untreated cells were used as a control (Ctrl). The data are the means from four independent experiments ± SEM. The levels of statistical significance between Ctrl and treated samples are *P* values of <0.05 (*), <0.01 (**), <0.001 (***), and <0.0001 (****).

rial killing in wt-CFBE cells was obtained after exposure to 15 μM Esc(1-21)-1c (Fig. 2B). Note that the toxicity of Esc(1-21) to bronchial cells when tested in Hanks' buffer, compared to that in MEMg (Fig. 1), could be due to the absence of medium components that may affect its activity, resulting in lower cytotoxicity (Fig. 1).

Wound-healing assay in the presence of peptides, LPS, or their combination. Since airway epithelium and CFTR have been shown to play a crucial role in maintaining lung function and wound repair (45), we investigated the effect of the two peptides on the migratory activity of the bronchial cells in the cell culture medium MEMg. Both AMPs were able to stimulate migration of wt-CFBE and ΔF508-CFBE cells, as indicated by their ability to induce ~100% coverage of the pseudo-wound field produced in the cell monolayer (by means of special cell culture inserts) within 20 h at optimal concentrations of 10 μM for Esc(1-21) (Fig. 3A and B) and 1 μM for its diastereomer (Fig. 3C and D). A slower cell migration speed was observed for the mutant ΔF508-CFBE, in agreement with a previous study (45) that showed how the defective function of CFTR caused a reduced lamellipodium area from the leading edge of airway epithelial cells (46).

It is well known that following bacterial death or division, LPS (the major component of the outer membrane of Gram-negative bacteria) is released from the bacterial cell wall (6, 47). Recently, as described in reference 48, it was demonstrated that the presence of nontoxic levels of *P. aeruginosa* LPS accelerates wound repair in

airway epithelial cells. We therefore analyzed the effect of different concentrations of *P. aeruginosa* LPS on the migratory activity of both wt-CFBE and ΔF508-CFBE. As illustrated in Fig. 4A and B, within 20 h LPS promoted the closure of a 500-μm-wide gap created in a monolayer of wt-CFBE or ΔF508-CFBE cells at an optimal dose of 1,000 ng/ml or in the range of 1,000 to 10,000 ng/ml, respectively. Alternately, when LPS was used at higher concentrations (i.e., ≥15,000 ng/ml) that can be found in the sputum of CF patients with chronic *P. aeruginosa* lung infection (49), the coverage of the wounded area was significantly slackened (Fig. 4A and B). To verify whether this LPS concentration was lethal to the cells, a viability assay was carried out. However, no cell damage was observed up to 20 μg/ml LPS, as indicated by the percentage of metabolically active cells, which was comparable to that of control samples (data not shown). This correlates with the negligible toxicity already found for LPS on both normal human bronchial epithelial cells (48) and A549 cells (50).

Interestingly, the induction of cell migration was clearly restored (Fig. 4C to F) when the LPS dosage that blocks the closure of the wounded field was used in combination with the optimal wound-healing concentration of Esc(1-21)-1c (1 μM). A similar effect was noted when the inhibitory concentration of LPS was mixed with a concentration of Esc(1-21) lower than its optimal dosage in promoting migration of wt-CFBE and ΔF508-CFBE cells (4 μM and 1 μM, respectively) (Fig. 4C to F).
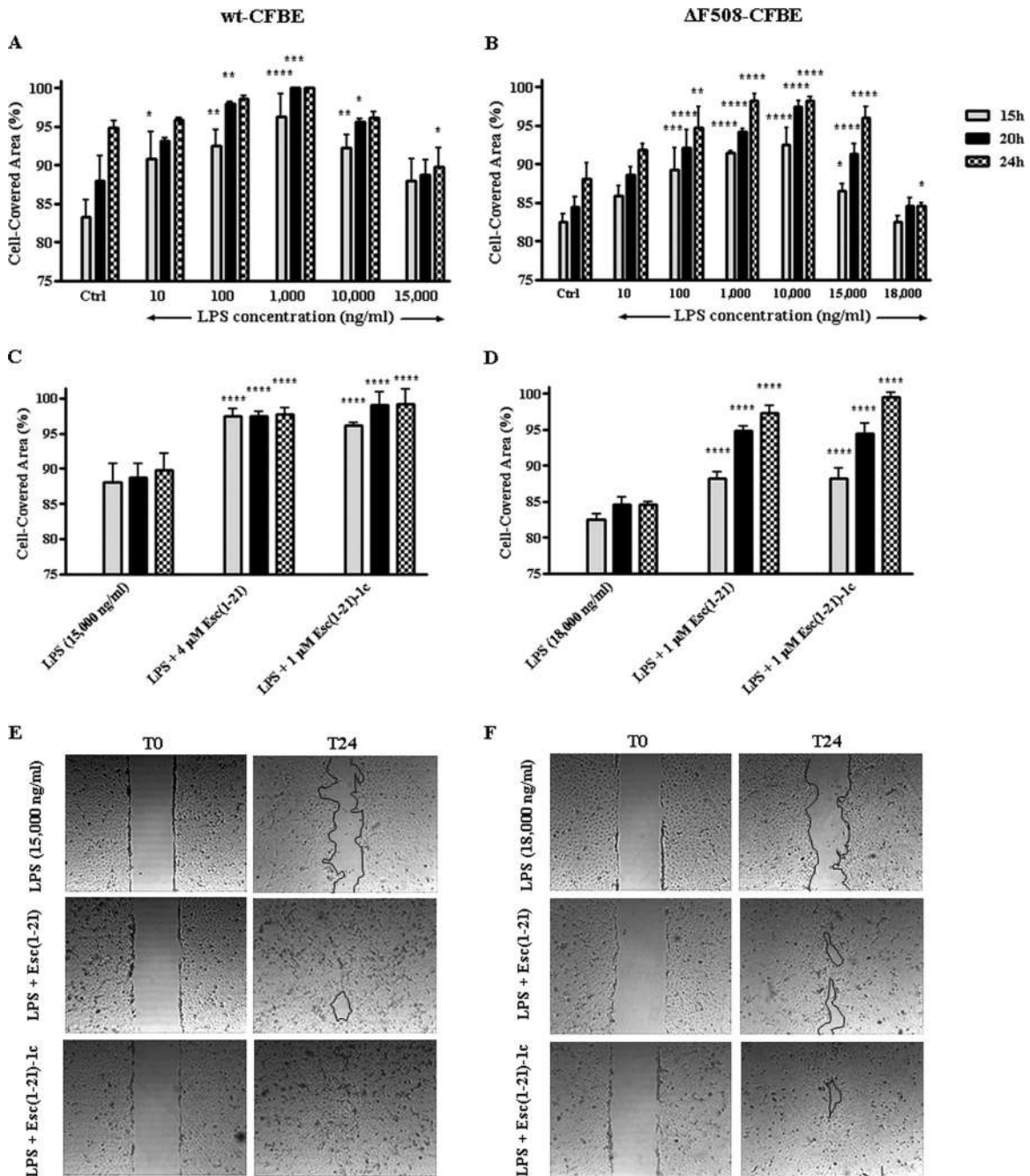
FIG 4 Effect of *P. aeruginosa* LPS alone (A and B) or in combination with Esc(1-21)/Esc(1-21)-1c (C to F) on the closure of a pseudo-wound field produced in a monolayer of wt-CFBE (A, C, and E) and ΔF508-CFBE (B, D, and F). Cells were seeded in each side of an Ibidi culture insert and grown to confluence; afterwards, they were left untreated or were treated with LPS or LPS plus peptide. Cells were photographed at the time of insert removal and examined for cell migration after 15, 20, and 24 h from addition of LPS or LPS plus peptide. The percentage of cell-covered area at each time point is reported on the *y* axis. The control (Ctrl) used was cells not treated with LPS or peptide. All data are the means from four independent experiments ± SEM. The levels of statistical significance of samples versus Ctrl (A and B) or LPS-treated (C and D) cells are *P* values of <0.05 (*), <0.01 (**), <0.001 (***), and <0.0001 (****). Micrographs showing representative results of wt-CFBE (E) or ΔF508-CFBE (F) before (T0) and 24 h after (T24) treatment with the combination of LPS and peptide (at the indicated concentrations in panels C or D) compared to samples treated with LPS are reported. The black line marks the cell-free area in samples after 24 h.

Mechanism of peptide-induced cell migration. The airways of healthy or CF human subjects express EGFR (42), which is involved in the repair of damaged airway epithelium (51). Hence, we examined whether the peptide-promoted cell mi-gration was a process mediated by the EGFR signaling pathway. For that purpose, we pretreated wt-CFBE cells with 5 μM AG1478, a selective inhibitor of EGFR tyrosine kinase (52), before adding each of the two peptides at their optimal concen-
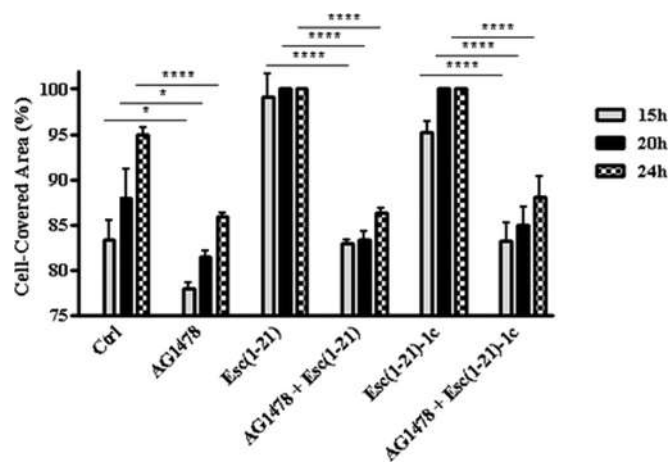
FIG 5 Effect of AG1478 inhibitor on the peptide-mediated migration of wt-CFBE cells. Before removing the Ibidi culture insert, cells were preincubated with 5 μM AG1478 for 30 min and subsequently treated with 10 μM Esc(1-21) or 1 μM Esc(1-21)-1c. Some samples were treated with the peptide alone at the same concentration or with 5 μM AG1478. Cells incubated with MEMg served as a control (Ctrl). Samples were photographed at different time intervals as indicated, and the percentage of cell-covered area was calculated and reported on the y axis. The data are the means from four independent experiments ± SEM. The levels of statistical significance between Ctrl and AG1478-treated samples or between samples pretreated with AG1478 before incubation with the peptide and those treated with the peptide alone at the corresponding time intervals are P values of <0.05 (*) and <0.0001 (****).

trations in stimulating cell migration [10 μM and 1 μM for Esc(1-21) and Esc(1-21)-1c, respectively]. A clear inhibition of pseudo-wound closure was observed, as was shown by the significantly lower percentages of cell-covered area at all time intervals (15 h, 20 h, and 24 h), with respect to the results found when the bronchial cells were not preincubated with the inhibitor (Fig. 5). These results highlight the involvement of EGFR in the peptide-induced migration of bronchial cells. Similar results were obtained with the mutant ΔF508-CFBE (data not shown).

Peptide distribution within bronchial cells. In order to know the peptides' distribution in wt-CFBE and ΔF508-CFBE cells, we used confocal microscopy and rhodamine-labeled peptides. As reported in Fig. 6A and B, rho-Esc(1-21) was mainly aligned to the perinuclear region of the cell already after 30 min from its addition, as well as after 24 h. To address the possibility that rhodamine facilitated the uptake of the peptide, we also used the rhodamine dye not conjugated to the peptide. However, rhodamine was not observed in the bronchial cells, as revealed by the lack of fluorescence inside them (Fig. 6C and D). In comparison, in the case of rho-Esc(1-21)-1c, the fluorescence intensity appeared to be evenly distributed within the cytosol and nucleus (Fig. 6E and F). These findings were corroborated by the quantitative analysis of fluorescence intensity of the two peptides between the cytoplasm and nucleus in both types of cells (Fig. 7).

Peptides' susceptibility to human and *P. aeruginosa* elastase. One of the main drawbacks in using AMPs for treatment of *P. aeruginosa* lung infection is their susceptibility to enzymatic degradation (53, 54). In particular, the lung environment of CF patients is rich in proteases, i.e., elastase from host neutrophils and

also from *P. aeruginosa* (55–57). Therefore, the stability of the two peptides in the presence of both enzymes was studied. When elastase from human leukocytes was used, Esc(1-21) was completely degraded within 5 h (Table 1; see also Fig. S2 in the supplemental material). In contrast, the diastereomer was highly stable, with 78% and 13% of nondegraded peptide after 5 h and 24 h of incubation, respectively (Table 1). Mass spectrometry analysis confirmed the presence of one main peak at 2,185 Da corresponding to the calculated molecular mass of Esc(1-21)-1c (see Fig. S2). In comparison, when the human cathelicidin AMP LL-37 was used as a reference, 44% of the peptide remained after 5 h of treatment but nothing was found after 24 h (Table 1). When *P. aeruginosa* elastase was used, both LL-37 and Esc(1-21) were completely degraded within 5 h (Table 1), while in the case of Esc(1-21)-1c about 91% and 77% of nondegraded peptide was detected after 5 h and 24 h, respectively (33% after 48 h, data not shown).

Interestingly, mass spectrometry analysis of the samples revealed the presence of peaks with different molecular masses than those found after treatment with human elastase (see Fig. S3 in the supplemental material), indicating different cleavage sites by the two elastases either in the two esculentin isoforms (see Fig. S2 and S3) or in LL-37 (see Fig. S4 and S5). Importantly, the main cleavage sites by human and bacterial elastase in Esc(1-21) were between Ile16 and Ser17 or between Asn13 and Leu14, respectively. Note that these two peptide bonds flank each of the two D-amino acids present in Esc(1-21)-1c (i.e., D-Leu14 and D-Ser17), thus preventing their proteolytic cleavage by both enzymes compared to the all-L peptide.

DISCUSSION

The airway epithelial surface represents an important place where the host breaks off signals from inhaled microbial pathogens and activates defense mechanisms to combat infections, especially in chronic diseases. However, administration of exogenous molecules endowed with anti-infective and/or immunomodulatory properties are highly needed to speed up the recovery process (58). Nevertheless, the challenge of treatment of respiratory infections has been compounded by the increasing resistance of pathogens to the commonly used drugs. Thus, new candidates are urgently needed, among which AMPs represent a promising alternative. With respect to this, Esc(1-21) and primarily its diastereomer Esc(1-21)-1c have several advantages that support their development as new antipseudomonal agents (6). However, no studies were reported on the ability of these two peptides to clear intracellular *Pseudomonas*, and only very limited information is documented for other AMPs with reference to this matter. Furthermore, the ability of AMPs to stimulate migration of lung epithelial cells in the context of a bacterial infection (e.g., in the presence of pathogen-associated molecular patterns, such as LPS) should be investigated in an attempt to develop a new drug that also has the ability to restore the normal architecture of the injured lung tissue. To the best of our knowledge, this has not yet been investigated for AMPs.

Here, we demonstrated the killing of intracellular *Pseudomonas* in bronchial cells with functional or mutated CFTR upon 1 h of exposure to the esculentin peptides. A significantly higher efficacy is displayed by the diastereomer Esc(1-21)-1c.

Note that conventional antibiotics (e.g., penicillins, cephalosporins, and aminoglycosides) are not ideal choices for treat-
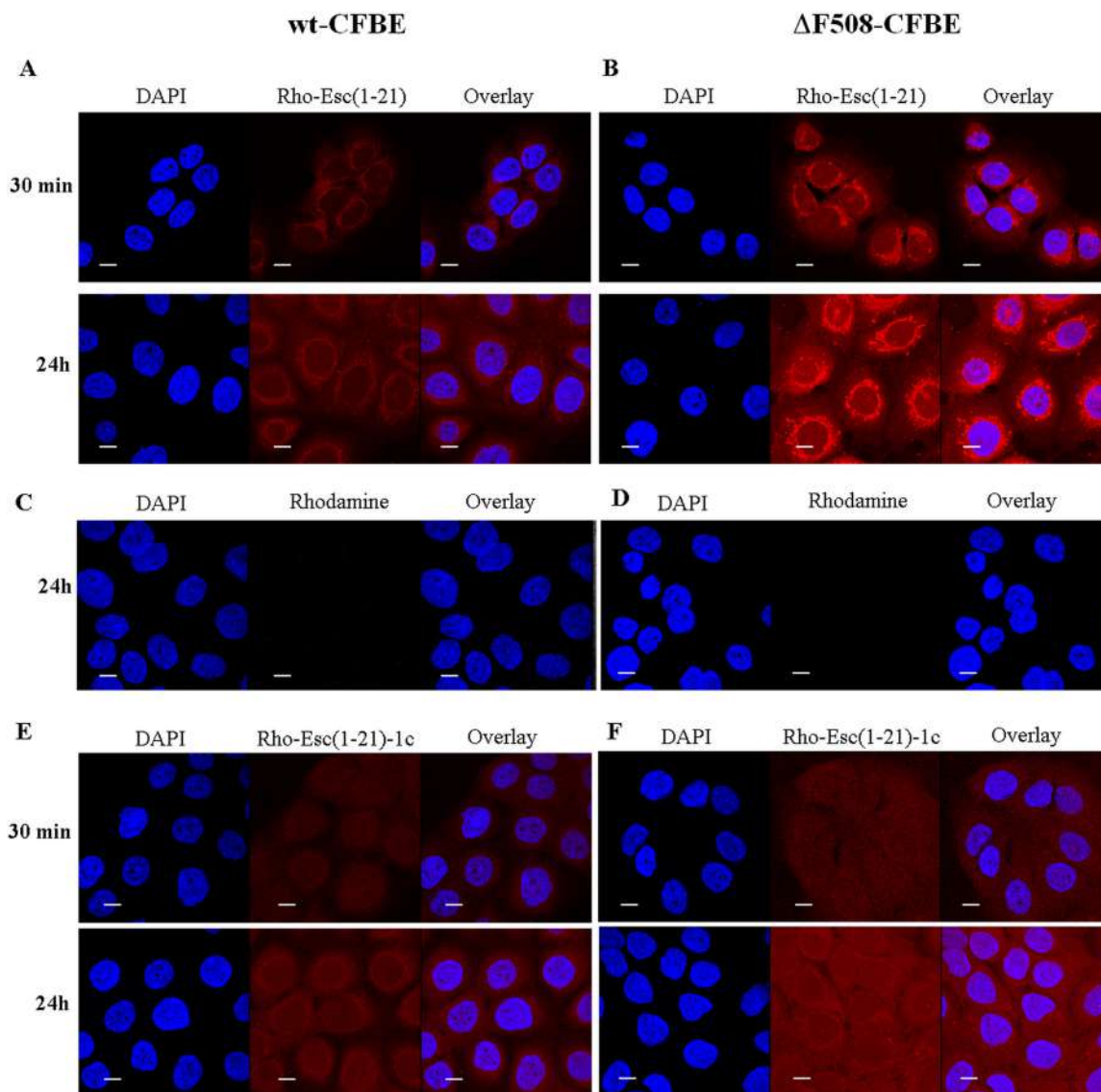
FIG 6 Confocal laser-scanning microscopy images of wt-CFBE and ΔF508-CFBE cells treated with rho-Esc(1-21) (A and B), rhodamine alone (C and D), or rho-Esc(1-21)-1c (E and F) at different times. After treatment with the peptide (or rhodamine), cells were stained with DAPI for nucleus detection. DAPI fluorescence, rhodamine-labeled peptide (or rhodamine) signal, and the overlay of the two fluorescent probes are shown. All images are *z* sections taken from the mid-cell height. All bars represent 10 μm.

ing invasive infections due to their inability to penetrate the plasma membrane (59, 60). An exception is fluoroquinolones, e.g., ciprofloxacin (61), which is currently used due to its strong activity against Gram-negative bacteria in spite of its toxicity (62) and the increasing number of bacteria that are resistant to it (63). Remarkably, the diastereomer had activity comparable to that of ciprofloxacin, which was found to cause ~64%, 77%, and 98% killing of intracellular bacteria when tested under our conditions on infected ΔF508-CFBE at 1 μM, 5 μM, and 15 μM, respectively (data not shown).

By means of rhodamine-labeled peptides and confocal microscopy analysis, we visualized an intracellular localization of the two molecules in which Esc(1-21) has a prevalent perinuclear distribution. No vesicular pattern of fluorescence was observed, excluding an endocytotic mechanism of peptide up-

take, which was shown in the case of Syn B peptides (64) and LL-37 in A549 cells after 30 min of incubation (65). A plausible explanation is that both esculentin isomers enter the cell by a self-translocation process through peptide-induced membrane lipid destabilization without affecting cell viability (66). Indeed, when tested at noncytotoxic concentrations, the peptides were able to perturb the membranes of both wt-CFBE and ΔF508-CFBE cells, as indicated by the increased fluorescence intensity of the small-sized membrane-impermeable dye Sytox green, upon peptides' addition to the cells (data not shown). This reflects the intracellular influx of Sytox green, presumably due to a mild membrane destabilization caused by the peptides during their translocation across the cytoplasmic/nuclear membrane into the cytosol/nucleus, respectively. Overall, we can assume that the clearance of intracellular *Pseudomonas* is

FIG 7 Peptide distribution between cytoplasm and nucleus in wt-CFBE and ΔF508-CFBE cells. Each peptide was tested on a minimum of 35 cells. The ratio between the fluorescence intensity of rhodamine-labeled peptides in the cytoplasm versus the nucleus was calculated for each cell, and the mean ± SEM value was reported on the y axis. If the ratio is equal to 1, this means that the peptide is evenly distributed all over the cell. When the ratio is higher than 1, the amount of fluorescent peptide is higher in the cytoplasm than the nucleus. The level of statistical significance between the calculated ratios of the two peptides at different time points is indicated as a P value of <0.001 (***).

due mainly to the interaction of the internalized peptides with the bacterial cells. A possible reason for the weaker efficacy of the all-L peptide Esc(1-21) in killing intracellular bacteria compared to its diastereomer is related to a stereochemical binding of Esc(1-21), but not Esc(1-21)-1c, to intracellular components, making it less available. In addition, Esc(1-21) is expected to be more susceptible to virulence factors, i.e., proteases released from intracellular *P. aeruginosa*. It is worth mentioning that the fluorescence intensity cannot tell us if the peptide is intact or partially degraded or whether it is present in an inactive form. Furthermore, the intranuclear location of the peptides suggest additional mechanisms to boost their antimicrobial potency, e.g., by directly/indirectly upregulating the expression of genes involved in host cell protection from microbial pathogens.

Another important finding in this study is the pseudo-wound-healing activity of the two peptides in both wt-CFBE and ΔF508-CFBE cells. As reported for A549 cells (36), the diastereomer is more effective in inducing reepithelialization of the wounded area, with a mechanism that implies an EGFR-mediated signaling pathway. We think that the lower wound-healing efficacy of the more helical Esc(1-21) compared to its diastereomer is a consequence of a stronger alteration of the phospholipid membrane region where EGF receptors are located. This would impair the binding of ligands to EGFR with a resulting weaker EGFR activation (36). However, the discrepancy between the two peptides in the wound-healing activity may also be related to a difference in the binding affinity of the two AMPs to the target receptor (presumably EGFR or membrane-bound metalloproteases [42, 66]). Furthermore, we cannot rule out the participation of alternative processes in controlling migration of bronchial cells. One of them could imply CFTR (especially in mutant cells) via a yet-to-be-discovered mechanism.

Here, we also demonstrated for the first time that bronchial cell migration stimulated by both esculentin isomers is maintained in the presence of high concentrations of LPS, presum-

ably found in CF sputum (49), and different plausible mechanisms underlying such events are discussed below. LPS has been found to regulate wound repair in airway epithelial cells through a signaling pathway triggered by its binding to Toll-like receptor 4 (TLR-4) (expressed on the airway epithelial cells) and implicating activation of EGFR (48, 67). Note that LPS binds TLR-4 in its monomeric form (68). However, in aqueous environments, micellar assemblies of LPS are formed above its critical micellar concentrations (≥14,000 ng/ml) (68, 69). This may hamper the binding of LPS to TLR-4, thus explaining the inhibitory pseudo-wound-healing effect of LPS when used at high concentrations (i.e., ≥15,000 ng/ml) (Fig. 4A and B). Note also that there is a reestablishment of the migratory activity of bronchial cells when LPS (at its inhibitory concentration) is combined with Esc(1-21)-1c (at the optimal wound-healing dosage of 1 μM) (Fig. 4C and D). This is presumably due to the diastereomer-induced reepithelialization process regardless of the presence of LPS. In contrast, a different mechanism would likely account for the increased pseudo-wound-healing activity of Esc(1-21) when combined with high concentrations of LPS (Fig. 4C and D) compared to the results found when the peptide is used alone at the same concentrations (Fig. 3A and B). As previously reported, Esc(1-21) is more efficient than its diastereomer in disrupting LPS micelles (36). Such LPS disaggregation might be sufficient to reset the availability of LPS monomers for an optimal binding to TLR-4 and retrieval/improvement of wound-healing activity.

Importantly, we also proved that the incorporation of two D-amino acids at specific positions in Esc(1-21) makes the peptide significantly more resistant to degradation by both human and bacterial elastases.

In conclusion, we have shown that (i) a derivative of a frog skin-derived AMP, and particularly its designed diastereomer, rapidly kills *Pseudomonas* cells once internalized in CF bronchial cells; (ii) the peptides accelerate bronchial cell migration under conditions that better simulate lung infection in CF (e.g., in the presence of LPS); and (iii) the diastereomer has an overall higher efficacy than the all-L parent isoform. These findings are very important for the generation of new antimicrobial drugs that not only eliminate microbial pathogens but also would recover the tissue's integrity.

In this specific case, the aforementioned properties of Esc(1-21)-1c, together with its higher biostability to elastases and undetectable cytotoxicity compared to wild-type Esc(1-21), support further studies toward the development and usage of the former peptide for local treatment of *P. aeruginosa*-induced lung infections.

TABLE 1 Peptide amount after 5 and 24 h of incubation with human and *P. aeruginosa* elastase at 37°C

	Peptide remaining[a] (%) by elastase type			
	Human		*P. aeruginosa*	
Peptide designation	5 h	24 h	5 h	24 h
Esc(1-21)	0	0	0	0
Esc(1-21)-1c	78	13	91	77
LL-37	44	0	0	0

[a] Peptide amounts were determined by the peak areas of the RP-HPLC relative to those of the control peptide (dissolved in buffer) at 0 min (set as 100%).

REFERENCES

1. **Hancock RE, Speert DP.** 2000. Antibiotic resistance in *Pseudomonas aeruginosa:* mechanisms and impact on treatment. Drug Resist Updat **3:**247–255. http://dx.doi.org/10.1054/drup.2000.0152.

2. **Mah TF, Pitts B, Pellock B, Walker GC, Stewart PS, O'Toole GA.** 2003. A genetic basis for *Pseudomonas aeruginosa* biofilm antibiotic resistance. Nature **426:**306–310. http://dx.doi.org/10.1038/nature02122.

3. **Drenkard E, Ausubel FM.** 2002. *Pseudomonas* biofilm formation and antibiotic resistance are linked to phenotypic variation. Nature **416:**740–743. http://dx.doi.org/10.1038/416740a.

4. **Costerton JW, Stewart PS, Greenberg EP.** 1999. Bacterial biofilms: a common cause of persistent infections. Science **284:**1318–1322. http://dx.doi.org/10.1126/science.284.5418.1318.

5. **Stewart PS, Costerton JW.** 2001. Antibiotic resistance of bacteria in biofilms. Lancet **358:**135–138. http://dx.doi.org/10.1016/S0140-6736(01)05321-1.

6. **Mangoni ML, Luca V, McDermott AM.** 2015. Fighting microbial infections: a lesson from amphibian skin-derived esculentin-1 peptides. Peptides **71:**286–295. http://dx.doi.org/10.1016/j.peptides.2015.04.018.

7. **Larrosa M, Truchado P, Espin JC, Tomas-Barberan FA, Allende A, Garcia-Conesa MT.** 2012. Evaluation of *Pseudomonas aeruginosa* (PAO1) adhesion to human alveolar epithelial cells A549 using SYTO 9 dye. Mol Cell Probes **26:**121–126. http://dx.doi.org/10.1016/j.mcp.2012.03.001.

8. **Millar FA, Simmonds NJ, Hodson ME.** 2009. Trends in pathogens colonising the respiratory tract of adult patients with cystic fibrosis, 1985-2005. J Cyst Fibros **8:**386–391. http://dx.doi.org/10.1016/j.jcf.2009.08.003.

9. **Kerem B, Rommens JM, Buchanan JA, Markiewicz D, Cox TK, Chakravarti A, Buchwald M, Tsui LC.** 1989. Identification of the cystic fibrosis gene: genetic analysis. Science **245:**1073–1080. http://dx.doi.org/10.1126/science.2570460.

10. **Welsh M, Tsui L, Boat T, Beaudet A.** 1995. Cystic fibrosis, p 3799–3863. *In* Scriver CR, Beaudet AL, Sly WS, Valle D (ed), The metabolic bases of inherited disease, 7th ed. McGraw-Hill, New York, NY.

11. **Evans CM, Koo JS.** 2009. Airway mucus: the good, the bad, the sticky. Pharmacol Ther **121:**332–348. http://dx.doi.org/10.1016/j.pharmthera.2008.11.001.

12. **Chace KV, Flux M, Sachdev GP.** 1985. Comparison of physicochemical properties of purified mucus glycoproteins isolated from respiratory secretions of cystic fibrosis and asthmatic patients. Biochemistry **24:**7334–7341. http://dx.doi.org/10.1021/bi00346a047.

13. **Moreau-Marquis S, Stanton BA, O'Toole GA.** 2008. *Pseudomonas aeruginosa* biofilm formation in the cystic fibrosis airway. Pulm Pharmacol Ther **21:**595–599. http://dx.doi.org/10.1016/j.pupt.2007.12.001.

14. **Bals R, Weiner DJ, Wilson JM.** 1999. The innate immune system in cystic fibrosis lung disease. J Clin Investig **103:**303–307. http://dx.doi.org/10.1172/JCI6277.

15. **Chiappini E, Taccetti G, de Martino M.** 2014. Bacterial lung infections in cystic fibrosis patients: an update. Pediatr Infect Dis J **33:**653–654. http://dx.doi.org/10.1097/INF.0000000000000347.

16. **Hirakata Y, Izumikawa K, Yamaguchi T, Igimi S, Furuya N, Maesaki S, Tomono K, Yamada Y, Kohno S, Yamaguchi K, Kamihira S.** 1998. Adherence to and penetration of human intestinal Caco-2 epithelial cell monolayers by *Pseudomonas aeruginosa*. Infect Immun **66:**1748–1751.

17. **Chi E, Mehl T, Nunn D, Lory S.** 1991. Interaction of *Pseudomonas aeruginosa* with A549 pneumocyte cells. Infect Immun **59:**822–828.

18. **Lyczak JB, Cannon CL, Pier GB.** 2000. Establishment of *Pseudomonas aeruginosa* infection: lessons from a versatile opportunist. Microbes Infect **2:**1051–1060. http://dx.doi.org/10.1016/S1286-4579(00)01259-4.

19. **Hart CA, Winstanley C.** 2002. Persistent and aggressive bacteria in the lungs of cystic fibrosis children. Br Med Bull **61:**81–96. http://dx.doi.org/10.1093/bmb/61.1.81.

20. **Pier GB, Grout M, Zaidi TS.** 1997. Cystic fibrosis transmembrane conductance regulator is an epithelial cell receptor for clearance of *Pseudomonas aeruginosa* from the lung. Proc Natl Acad Sci U S A **94:**12088–12093. http://dx.doi.org/10.1073/pnas.94.22.12088.

21. **Pier GB, Grout M, Zaidi TS, Olsen JC, Johnson LG, Yankaskas JR, Goldberg JB.** 1996. Role of mutant CFTR in hypersusceptibility of cystic fibrosis patients to lung infections. Science **271:**64–67. http://dx.doi.org/10.1126/science.271.5245.64.

22. **Esen M, Grassme H, Riethmuller J, Riehle A, Fassbender K, Gulbins E.** 2001. Invasion of human epithelial cells by *Pseudomonas aeruginosa* involves src-like tyrosine kinases p60Src and p59Fyn. Infect Immun **69:**281–287. http://dx.doi.org/10.1128/IAI.69.1.281-287.2001.

23. **Darling KE, Evans TJ.** 2003. Effects of nitric oxide on *Pseudomonas aeruginosa* infection of epithelial cells from a human respiratory cell line derived from a patient with cystic fibrosis. Infect Immun **71:**2341–2349. http://dx.doi.org/10.1128/IAI.71.5.2341-2349.2003.

24. **Darling KE, Dewar A, Evans TJ.** 2004. Role of the cystic fibrosis transmembrane conductance regulator in internalization of *Pseudomonas aeruginosa* by polarized respiratory epithelial cells. Cell Microbiol **6:**521–533. http://dx.doi.org/10.1111/j.1462-5822.2004.00380.x.

25. **Ko YH, Delannoy M, Pedersen PL.** 1997. Cystic fibrosis, lung infections, and a human tracheal antimicrobial peptide (hTAP). FEBS Lett **405:**200–208. http://dx.doi.org/10.1016/S0014-5793(97)00189-0.

26. **Ben Haj Khalifa A, Moissenet D, Vu Thien H, Khedher M.** 2011. Virulence factors in *Pseudomonas aeruginosa*: mechanisms and modes of regulation. Ann Biol Clin **69:**393–403.

27. **Sana TG, Baumann C, Merdes A, Soscia C, Rattei T, Hachani A, Jones C, Bennett KL, Filloux A, Superti-Furga G, Voulhoux R, Bleves S.** 2015. Internalization of *Pseudomonas aeruginosa* strain PAO1 into epithelial cells is promoted by interaction of a T6SS effector with the microtubule network. mBio **6:**e00712. http://dx.doi.org/10.1128/mBio.00712-15.

28. **Brinch KS, Frimodt-Moller N, Hoiby N, Kristensen HH.** 2009. Influence of antidrug antibodies on plectasin efficacy and pharmacokinetics. Antimicrob Agents Chemother **53:**4794–4800. http://dx.doi.org/10.1128/AAC.00440-09.

29. **Haney EF, Hancock RB.** 2013. Peptide design for antimicrobial and immunomodulatory applications. Biopolymers **100:**572–583. http://dx.doi.org/10.1002/bip.22250.

30. **Cruz J, Ortiz C, Guzman F, Fernandez-Lafuente R, Torres R.** 2014. Antimicrobial peptides: promising compounds against pathogenic microorganisms. Curr Med Chem **21:**2299–2321. http://dx.doi.org/10.2174/0929867321666140217110155.

31. **Mansour SC, Pena OM, Hancock RE.** 2014. Host defense peptides: front-line immunomodulators. Trends Immunol **35:**443–450. http://dx.doi.org/10.1016/j.it.2014.07.004.

32. **Epand RM, Vogel HJ.** 1999. Diversity of antimicrobial peptides and their mechanisms of action. Biochim Biophys Acta **1462:**11–28. http://dx.doi.org/10.1016/S0005-2736(99)00198-4.

33. **Shai Y.** 2002. Mode of action of membrane active antimicrobial peptides. Biopolymers **66:**236–248. http://dx.doi.org/10.1002/bip.10260.

34. **Islas-Rodriguez AE, Marcellini L, Orioni B, Barra D, Stella L, Mangoni ML.** 2009. Esculentin 1-21: a linear antimicrobial peptide from frog skin with inhibitory effect on bovine mastitis-causing bacteria. J Pept Sci **15:**607–614. http://dx.doi.org/10.1002/psc.1148.

35. **Luca V, Stringaro A, Colone M, Pini A, Mangoni ML.** 2013. Esculentin(1-21), an amphibian skin membrane-active peptide with potent activity on both planktonic and biofilm cells of the bacterial pathogen *Pseudomonas aeruginosa*. Cell Mol Life Sci **70:**2773–2786. http://dx.doi.org/10.1007/s00018-013-1291-7.

36. **Di Grazia A, Cappiello F, Cohen H, Casciaro B, Luca V, Pini A, Di YP, Shai Y, Mangoni ML.** 2015. D-Amino acids incorporation in the frog skin-derived peptide esculentin-1a(1-21)NH is beneficial for its multiple functions. Amino Acids **47:**2505–2519. http://dx.doi.org/10.1007/s00726-015-2041-y.

37. **Bebok Z, Collawn JF, Wakefield J, Parker W, Li Y, Varga K, Sorscher EJ, Clancy JP.** 2005. Failure of cAMP agonists to activate rescued deltaF508

CFTR in CFBE41o-airway epithelial monolayers. J Physiol **569**:601–615. http://dx.doi.org/10.1113/jphysiol.2005.096669.

38. **Lore NI, Cigana C, De Fino I, Riva C, Juhas M, Schwager S, Eberl L, Bragonzi A.** 2012. Cystic fibrosis-niche adaptation of *Pseudomonas aeruginosa* reduces virulence in multiple infection hosts. PLoS One **7**:e35648. http://dx.doi.org/10.1371/journal.pone.0035648.

39. **Bragonzi A, Paroni M, Nonis A, Cramer N, Montanari S, Rejman J, Di Serio C, Doring G, Tummler B.** 2009. *Pseudomonas aeruginosa* micro-evolution during cystic fibrosis lung infection establishes clones with adapted virulence. Am J Respir Crit Care Med **180**:138–145. http://dx.doi.org/10.1164/rccm.200812-1943OC.

40. **Grieco P, Carotenuto A, Auriemma L, Limatola A, Di Maro S, Merlino F, Mangoni ML, Luca V, Di Grazia A, Gatti S, Campiglia P, Gomez-Monterrey I, Novellino E, Catania A.** 2013. Novel alpha-MSH peptide analogues with broad spectrum antimicrobial activity. PLoS One **8**:e61614. http://dx.doi.org/10.1371/journal.pone.0061614.

41. **Di Grazia A, Cappiello F, Imanishi A, Mastrofrancesco A, Picardo M, Paus R, Mangoni ML.** 2015. The frog skin-derived antimicrobial peptide esculentin-1a(1-21)NH2 promotes the migration of human HaCaT keratinocytes in an EGF receptor-dependent manner: a novel promoter of human skin wound healing? PLoS One **10**:e0128663. http://dx.doi.org/10.1371/journal.pone.0128663.

42. **Kim S, Beyer BA, Lewis C, Nadel JA.** 2013. Normal CFTR inhibits epidermal growth factor receptor-dependent pro-inflammatory chemokine production in human airway epithelial cells. PLoS One **8**:e72981. http://dx.doi.org/10.1371/journal.pone.0072981.

43. **Renier M, Tamanini A, Nicolis E, Rolfini R, Imler JL, Pavirani A, Cabrini G.** 1995. Use of a membrane potential-sensitive probe to assess biological expression of the cystic fibrosis transmembrane conductance regulator. Hum Gene Ther **6**:1275–1283. http://dx.doi.org/10.1089/hum.1995.6.10-1275.

44. **Hamai H, Keyserman F, Quittell LM, Worgall TS.** 2009. Defective CFTR increases synthesis and mass of sphingolipids that modulate membrane composition and lipid signaling. J Lipid Res **50**:1101–1108. http://dx.doi.org/10.1194/jlr.M800427-JLR200.

45. **Trinh NT, Bardou O, Prive A, Maille E, Adam D, Lingee S, Ferraro P, Desrosiers MY, Coraux C, Brochiero E.** 2012. Improvement of defective cystic fibrosis airway epithelial wound repair after CFTR rescue. Eur Respir J **40**:1390–1400. http://dx.doi.org/10.1183/09031936.00221711.

46. **Schiller KR, Maniak PJ, O'Grady SM.** 2010. Cystic fibrosis transmembrane conductance regulator is involved in airway epithelial wound repair. Am J Physiol Cell Physiol **299**:C912–C921. http://dx.doi.org/10.1152/ajpcell.00215.2010.

47. **Rietschel ET, Kirikae T, Schade FU, Mamat U, Schmidt G, Loppnow H, Ulmer AJ, Zahringer U, Seydel U, Di Padova F, Schreier M, Brade H.** 1994. Bacterial endotoxin: molecular relationships of structure to activity and function. FASEB J **8**:217–225.

48. **Koff JL, Shao MX, Kim S, Ueki IF, Nadel JA.** 2006. *Pseudomonas* lipopolysaccharide accelerates wound repair via activation of a novel epithelial cell signaling cascade. J Immunol **177**:8693–8700. http://dx.doi.org/10.4049/jimmunol.177.12.8693.

49. **Bucki R, Byfield FJ, Janmey PA.** 2007. Release of the antimicrobial peptide LL-37 from DNA/F-actin bundles in cystic fibrosis sputum. Eur Respir J **29**:624–632. http://dx.doi.org/10.1183/09031936.00080806.

50. **Byfield FJ, Kowalski M, Cruz K, Leszczynska K, Namiot A, Savage PB, Bucki R, Janmey PA.** 2011. Cathelicidin LL-37 increases lung epithelial cell stiffness, decreases transepithelial permeability, and prevents epithelial invasion by *Pseudomonas aeruginosa*. J Immunol **187**:6402–6409. http://dx.doi.org/10.4049/jimmunol.1102185.

51. **Burgel PR, Nadel JA.** 2004. Roles of epidermal growth factor receptor activation in epithelial cell repair and mucin production in airway epithelium. Thorax **59**:992–996. http://dx.doi.org/10.1136/thx.2003.018879.

52. **Gan HK, Walker F, Burgess AW, Rigopoulos A, Scott AM, Johns TG.** 2007. The epidermal growth factor receptor (EGFR) tyrosine kinase inhibitor AG1478 increases the formation of inactive untethered EGFR dimers. Implications for combination therapy with monoclonal antibody 806. J Biol Chem **282**:2840–2850.

53. **Midura-Nowaczek K, Markowska A.** 2014. Antimicrobial peptides and their analogs: searching for new potential therapeutics. Perspect Medicin Chem **6**:73–80.

54. **Nguyen LT, Chau JK, Perry NA, de Boer L, Zaat SA, Vogel HJ.** 2010. Serum stabilities of short tryptophan- and arginine-rich antimicrobial peptide analogs. PLoS One **5**:e12684. http://dx.doi.org/10.1371/journal.pone.0012684.

55. **Liu H, Lazarus SC, Caughey GH, Fahy JV.** 1999. Neutrophil elastase and elastase-rich cystic fibrosis sputum degranulate human eosinophils *in vitro*. Am J Physiol **276**:L28–L34.

56. **Lovewell RR, Patankar YR, Berwin B.** 2014. Mechanisms of phagocytosis and host clearance of *Pseudomonas aeruginosa*. Am J Physiol Lung Cell Mol Physiol **306**:L591–L603. http://dx.doi.org/10.1152/ajplung.00335.2013.

57. **Mariencheck WI, Alcorn JF, Palmer SM, Wright JR.** 2003. *Pseudomonas aeruginosa* elastase degrades surfactant proteins A and D. Am J Respir Cell Mol Biol **28**:528–537. http://dx.doi.org/10.1165/rcmb.2002-0141OC.

58. **Morris CJ, Beck K, Fox MA, Ulaeto D, Clark GC, Gumbleton M.** 2012. Pegylation of antimicrobial peptides maintains the active peptide conformation, model membrane interactions, and antimicrobial activity while improving lung tissue biocompatibility following airway delivery. Antimicrob Agents Chemother **56**:3298–3308. http://dx.doi.org/10.1128/AAC.06335-11.

59. **Brayton JJ, Yang Q, Nakkula RJ, Walters JD.** 2002. An *in vitro* model of ciprofloxacin and minocycline transport by oral epithelial cells. J Periodontol **73**:1267–1272. http://dx.doi.org/10.1902/jop.2002.73.11.1267.

60. **Bonventre PF, Hayes R, Imhoff J.** 1967. Autoradiographic evidence for the impermeability of mouse peritoneal macrophages to tritiated streptomycin. J Bacteriol **93**:445–450.

61. **Chadwick PR, Mellersh AR.** 1987. The use of a tissue culture model to assess the penetration of antibiotics into epithelial cells. J Antimicrob Chemother **19**:211–220. http://dx.doi.org/10.1093/jac/19.2.211.

62. **Ilgin S, Can OD, Atli O, Ucel UI, Sener E, Guven I.** 2015. Ciprofloxacin-induced neurotoxicity: evaluation of possible underlying mechanisms. Toxicol Mech Methods **25**:374–381. http://dx.doi.org/10.3109/15376516.2015.1026008.

63. **Yayan J, Ghebremedhin B, Rasche K.** 2015. No outbreak of vancomycin and linezolid resistance in Staphylococcal pneumonia over a 10-year period. PLoS One **10**:e0138895. http://dx.doi.org/10.1371/journal.pone.0138895.

64. **Drin G, Cottin S, Blanc E, Rees AR, Temsamani J.** 2003. Studies on the internalization mechanism of cationic cell-penetrating peptides. J Biol Chem **278**:31192–31201. http://dx.doi.org/10.1074/jbc.M303938200.

65. **Lau YE, Rozek A, Scott MG, Goosney DL, Davidson DJ, Hancock RE.** 2005. Interaction and cellular localization of the human host defense peptide LL-37 with lung epithelial cells. Infect Immun **73**:583–591. http://dx.doi.org/10.1128/IAI.73.1.583-591.2005.

66. **Peschon JJ, Slack JL, Reddy P, Stocking KL, Sunnarborg SW, Lee DC, Russell WE, Castner BJ, Johnson RS, Fitzner JN, Boyce RW, Nelson N, Kozlosky CJ, Wolfson MF, Rauch CT, Cerretti DP, Paxton RJ, March CJ, Black RA.** 1998. An essential role for ectodomain shedding in mammalian development. Science **282**:1281–1284. http://dx.doi.org/10.1126/science.282.5392.1281.

67. **Shao MX, Ueki IF, Nadel JA.** 2003. Tumor necrosis factor alpha-converting enzyme mediates MUC5AC mucin expression in cultured human airway epithelial cells. Proc Natl Acad Sci U S A **100**:11618–11623. http://dx.doi.org/10.1073/pnas.1534804100.

68. **Park BS, Lee JO.** 2013. Recognition of lipopolysaccharide pattern by TLR4 complexes. Exp Mol Med **45**:e66. http://dx.doi.org/10.1038/emm.2013.97.

69. **Santos NC, Silva AC, Castanho MA, Martins-Silva J, Saldanha C.** 2003. Evaluation of lipopolysaccharide aggregation by light scattering spectroscopy. Chembiochem **4**:96–100. http://dx.doi.org/10.1002/cbic.200390020.

CrossMark

ORIGINAL ARTICLE

D-Amino acids incorporation in the frog skin-derived peptide esculentin-1a(1-21)NH$_2$ is beneficial for its multiple functions

Antonio Di Grazia[1] · Floriana Cappiello[1] · Hadar Cohen[2] · Bruno Casciaro[1] · Vincenzo Luca[1] · Alessandro Pini[3] · Y. Peter Di[4] · Yechiel Shai[2] · Maria Luisa Mangoni[1]

Abstract Naturally occurring antimicrobial peptides (AMPs) represent promising future antibiotics. We have previously isolated esculentin-1a(1-21)NH$_2$, a short peptide derived from the frog skin AMP esculentin-1a, with a potent anti-*Pseudomonal* activity. Here, we investigated additional functions of the peptide and properties responsible for these activities. For that purpose, we synthesized the peptide, as well as its structurally altered analog containing two D-amino acids. The peptides were then biophysically and biologically investigated for their cytotoxicity and immunomodulating activities. The data revealed that compared to the wild-type, the diastereomer: (1) is significantly less toxic towards mammalian cells, in agreement with its lower α-helical structure, as determined by circular dichroism spectroscopy; (2) is more effective against the biofilm form of *Pseudomonas aeruginosa* (responsible for lung infections in cystic fibrosis sufferers), while maintaining a high activity against the free-living form of this important pathogen; (3) is more stable in serum; (4) has a higher activity in promoting migration of lung epithelial cells, and presumably in healing damaged lung tissue, and (5) disaggregates and detoxifies the bacterial lipopolysaccharide (LPS), albeit less than the wild-type. Light scattering studies revealed a correlation between anti-LPS activity and the ability to disaggregate the LPS. Besides shedding light on the multifunction properties of esculentin-1a(1-21)NH$_2$, the D-amino acid containing isomer may serve as an attractive template for the development of new anti-*Pseudomonal* compounds with additional beneficial properties. Furthermore, together with other studies, incorporation of D-amino acids may serve as a general approach to optimize the future design of new AMPs.

Abbreviations

AMP	Antimicrobial peptide
CD	Circular dichroism
CFU	Colony-forming units
DMEMg	Dulbecco's modified Eagle's medium supplemented with glutamine
FBS	Heat-inactivated fetal bovine serum
LB	Luria–Bertani broth
LPC	Lysophosphatidylcholine
LPS	Lipopolysaccharide
MTT	3(4,5-Dimethylthiazol-2yl)2,5-diphenyltetrazolium bromide
PBS	Phosphate buffered saline

Handling Editor: M. S. Palma.

This manuscript is dedicated to Professor Emeritus Donatella Barra who passed away on September 28th, 2014.

✉ Maria Luisa Mangoni
marialuisa.mangoni@uniroma1.it

1 Istituto Pasteur-Fondazione Cenci Bolognetti, Department of Biochemical Sciences, Sapienza University of Rome, Via degli Apuli 9, 00185 Rome, Italy

2 Department of Biological Chemistry, The Weizmann Institute of Science, 76100 Rehovot, Israel

3 Department of Medical Biotechnology, University of Siena, 53100 Siena, Italy

4 Department of Environmental and Occupational Health, University of Pittsburgh, Pittsburgh, PA 15260, USA

Introduction

During the past three decades, the widespread use of conventional antibiotics has led to a drastic reduction in their

therapeutic efficacy with over 70 % of hospital bacterial infections being resistant to them (Chen et al. 2009; Grundmann et al. 2011; Kaye 2012). This has resulted in more difficult and costly treatments, longer hospitalization, higher risk of complications and increase in death. Furthermore, the number of new antibiotics approved by the FDA has steadily declined every year since 1980 and most therapeutics in clinical development are derivatives of existing medicines (Lohner and Staudegger 2001). Hence, the discovery of new classes of antimicrobial agents with a new mode of action is a major challenge. Cationic antimicrobial peptides (AMPs) are ancient elements of the innate immune defense of all living organisms (Boman 1995; Mangoni 2011; Yeung et al. 2011; Bevins 2013; Kai-Larsen et al. 2014; Mansour et al. 2014) with common properties, e.g., a net positive charge at neutral pH and an amphipathic character in a hydrophobic environment (Epand and Vogel 1999; Shai 2002). They hold promise for the generation of new drugs (Hancock and Sahl 2006; Dempsey et al. 2010; Alba et al. 2012; Guralp et al. 2013; Haney and Hancock 2013) and are considered as future compounds against both acute and chronic microbial infections (Brown and Hancock 2006; Cruz et al. 2014). Of particular interest are those caused by the multidrug-resistant biofilm-forming gram-negative bacterium *Pseudomonas aeruginosa* in the lungs of cystic fibrosis (CF) sufferers (Drenkard and Ausubel 2002; Bjarnsholt et al. 2009; Millar et al. 2009; Macia et al. 2014). In these patients, the lack of Cl⁻ secretion promotes airways drying and mucus plugging, predisposing the lungs to microbial colonization, deterioration of lung tissue and impairment of respiratory functions (Moreau-Marquis et al. 2008). Since the mechanism of killing by the majority of AMPs includes an irreversible membrane injury, it makes it difficult for the bacteria to develop resistance against them (Shai 2002; Mangoni 2006; Mangoni et al. 2007), although some AMPs have been reported to induce limited resistance (Peschel et al. 1999). Noteworthy, antibiotic treatment of gram-negative bacteria is accompanied with the release of bacterial cell wall components, such as the lipopolysaccharide (LPS), also named endotoxin. LPS activates immune cells (Rietschel et al. 1994), leading to the secretion of pro-inflammatory cytokines e.g., tumor necrosis factor-alpha (TNF-α) whose high levels can damage lung functionality and cause septic shock syndrome, in the most serious cases (Poltorak et al. 1998; Cohen 2002). Regarding this, several AMPs have already shown additional properties, including the capability to neutralize the toxic effect of LPS (Hancock et al. 2012; Pulido et al. 2012). This makes them important modulators of both adaptive and innate immunity, and distinguishes them from traditional antibiotics (Hancock and Sahl 2006; Fjell et al. 2012; Hancock et al. 2012; Semple and Dorin 2012).

Recent studies demonstrated that esculentin-1a(1-21) NH₂ [Esc(1-21)] derived from the N-terminal region of the 46 residues frog skin AMP esculentin-1a (Gamberi et al. 2007; Islas-Rodriguez et al. 2009) is endowed with antimicrobial activity at high ionic concentrations, which is a crucial aspect due to the high-salt environment existing at the apical side of CF epithelial cells. In addition, in vivo experiments revealed that Esc(1-21) prolongs survival of murine models of *P. aeruginosa*-induced sepsis or lung infection, upon intravenous or intra-tracheal administration, respectively (Luca et al. 2013). Despite this and other studies showing an in vivo antimicrobial activity of AMPs (Giacometti et al. 2006; Pini et al. 2010; Uccelletti et al. 2010; Xiong et al. 2011; Luca et al. 2014; Jung Kim et al. 2014; Kolar et al. 2015), inherent limitations for the development of these molecules as new anti-infective therapeutics include: (1) cytotoxicity outside their natural environment, which can strongly dampen the in vivo antimicrobial efficacy of AMPs, and (2) problems with stability, bioavailability and delivery systems. With reference to the latter, studies on the effect of the incorporation of D-amino acids into AMPs were mainly focused on the antimicrobial activity of the peptides, their reduced cytotoxicity and their increased stability to circulating enzymes (Hamamoto et al. 2002; Papo et al. 2002). However, before AMPs can be clinically used, evaluation of other beneficial properties (e.g., anti-inflammatory, wound healing) should be also investigated. Here, we report on the synthesis and properties of a diastereomer of Esc(1-21), named Esc-1a(1-21)-1cNH₂ [Esc(1-21)-1c], containing two D-amino acids, and compared its multiple functions with those of the wild-type Esc(1-21). The results are discussed in line with the advanced properties of the diastereomer as a potential nontoxic wound healing promoter in addition to its antimicrobial activity.

Materials and methods

Materials

Trypsin–EDTA was purchased from Invitrogen (Life-Technologies Europe, Monza, Italy); 3(4,5-dimethylthiazol-2yl)2,5-diphenyltetrazolium bromide (MTT), Triton X-100, AG1478, mitomycin C, Hoechst 33258, LPS from *P. aeruginosa* serotype 10, lysophosphatidylcholine (LPC, (1-0-palmitoyl-sn-glycero-3-phosphocholine) were all from Sigma–Aldrich (St. Luis, MO). Dulbecco's modified Eagle's medium (DMEM); non-essential amino acids (NEAA); sodium pyruvate (100 mM); heat-inactivated fetal bovine serum (FBS); glutamine; penicillin/streptomycin were from Euroclone (Milan, Italy). All other chemicals were reagent grade.

Peptides synthesis

Synthetic Esc(1-21) and the diastereomer Esc(1-21)-1c were purchased from Selleck Chemicals (Houston, TX, USA). Briefly, the peptides were assembled by step-wise solid-phase synthesis by a standard F-moc strategy and purified by RP-HPLC on a semipreparative C18-bonded silica column (Kromasyl, 5 μm, 100 Å, 25 cm × 4.6 mm) using a gradient of acetonitrile in 0.1 % aqueous trifluoroacetic acid at a flow rate of 1.0 ml/min, according to what reported in (Luca et al. 2013). Analytical RP-HPLC indicated a purity >98 %. The molecular mass was verified by using MALDI-TOF Voyager DE (Applied Biosystems) as previously described (Islas-Rodriguez et al. 2009).

Peptide stability

A total of 125 μl of a 0.92 mM solution of peptide was incubated at 37 °C with 20 and 60 μl human serum. Samples were collected from healthy volunteers after 5 and 24 h of incubation, precipitated with 200 μl methanol, and centrifuged for 2 min at $10,000 \times g$. The crude solution was then analyzed by HPLC and mass spectrometry. HPLC was performed with a Vydac C18 column, and the crude solution was diluted 5 times with 0.1 % trifluoroacetic acid before injection, and monitored at 280 nm.

Microorganisms

The strains of *P. aeruginosa* used for the antimicrobial assays were: the standard non mucoid ATCC 27853 (Li et al. 2001), and the following ones from collection of the CF clinic Medizinische Hochschule of Hannover, Germany: the mucoid AA11 and the non-mucoid TR1 and KK1 (Bragonzi et al. 2009).

Cell culture

The murine Raw 264.7 macrophage cell line and the human type II alveolar epithelial cell line A549 (from the American Type Culture Collection, Manassas, Va) were employed (Akram et al. 2013). Cells were cultured in DMEM supplemented with 10 % FBS, glutamine (2 mM), and antibiotics (0.1 mg/ml of penicillin and streptomycin) at 37 °C and 5 % CO_2 in 25-cm² flasks. In the case of macrophages, NEAA and sodium pyruvate were also added to the culture medium.

Antimicrobial activity

Bacteria were grown in Luria-Bertani (LB) broth at 37 °C till a mid-log phase which was aseptically monitored by absorbance at 590 nm ($A_{590nm} = 0.8$) with an UV-1700 Pharma Spec spectrophotometer (Shimadzu, Tokyo, Japan). Afterwards, bacterial cells were centrifuged at $1400 \times g$ for 10 min and resuspended in phosphate buffered saline (PBS).

About 1×10^5 colony-forming units (CFU) in 100 μl PBS were incubated at 37 °C with Esc(1-21) or Esc(1-21)-1c in serial twofold dilutions. Aliquots of 10 μl were withdrawn at different time intervals, diluted in LB and spread onto LB-agar plates. After overnight incubation at 37 °C, the number of CFU was counted. Controls were run without peptide and in the presence of peptide solvent (Luca et al. 2013).

Bactericidal activity was defined as the peptide concentration necessary to cause a reduction in the number of viable bacteria of $\geq 3 \log_{10}$ CFU/ml.

Antibiofilm activity

Biofilm formation was performed by adapting the procedure described in (Ceri et al. 2001; Falciani et al. 2012), using the Calgary Biofilm Device (Innovotech, Innovotech Inc. Edmonton, Canada). Briefly, 96-well plates, each well containing 150 μl of the bacterial inoculum (1×10^7 CFU/ml) in LB medium were sealed with 96 peg-lids on which biofilm cells can build up. Afterwards, plates were placed in an humidified orbital incubator at 35 °C for 20 h under agitation at 125 rpm. Once biofilms were allowed to form, the pegs were rinsed twice with PBS to remove planktonic cells. Each peg-lid was then transferred to a "challenge 96-well microtiter plate", each well containing 200 μl of a twofold serial dilution of peptide in PBS. The "challenge plate" was incubated at 37 °C for 2 h. Peptide activity was evaluated by determining the amount of viable biofilm cells by measuring the reduction of MTT to its insoluble formazan. Briefly, after peptide treatment, the pegs-lid was washed with PBS and used to close another 96-well microtiter plate, each well containing 200 μl of Hank's buffer (136 mM NaCl; 4.2 mM Na_2HPO_4; 4.4 mM KH_2PO_4; 5.4 mM KCl; 4.1 mM $NaHCO_3$, pH 7.2, supplemented with 20 mM D-glucose) containing 1 mg/ml MTT. The plate was incubated at 37 °C for 4 h. Afterwards, 50 μl of 25 % sodium dodecyl sulfate were added to each well to dissolve formazan crystals. Bacterial viability was determined by absorbance measurements at 595 nm and calculated with respect to control cells (bacteria not treated with the peptide) (Mangoni et al. 2005). The percentage of viable cells was calculated according to the equation:

$$\frac{\text{Absorbance}_{\text{sample}} - \text{Absorbance}_{\text{blank}}}{\text{Absorbance}_{\text{control}} - \text{Absorbance}_{\text{blank}}} \times 100$$

where the blank is given by samples without cells and not treated with the peptide.

Peptides' effect on cell viability

The effect of both peptides on the viability of mammalian macrophages and lung epithelial cells was determined by the MTT assay according to (Di Grazia et al. 2014). Lung epithelial cells in DMEM supplemented with 2 mM glutamine (DMEMg) and 2 % FBS or macrophages in DMEMg containing NEAA, sodium pyruvate and 2 % FBS were plated in triplicate wells of a microtiter plate, at 4×10^4 cells/well. After overnight incubation at 37 °C in a 5 % CO_2 atmosphere, the medium was replaced with 100 µl fresh serum-free medium supplemented with each peptide at different concentrations. The plate was incubated for 24 h at 37 °C in a 5 % CO_2 atmosphere. Afterwards, the medium was removed and replaced with Hank's buffer containing 0.5 mg/ml MTT. After 4 h incubation at 37 °C, the formazan crystals were dissolved by adding 100 µl of acidified isopropanol according to (Grieco et al. 2013), and viability was determined by absorbance measurements at 570 nm using a microplate reader (Infinite M200; Tecan, Salzburg, Austria). Cell viability was calculated with respect to the control (cells not treated with peptide). The percentage of viable cells was calculated as described above. LD_{50}, is the lethal peptide dose causing 50 % reduction in the number of viable cells.

Cell migration assay

The ability of both peptides to stimulate migration of lung epithelial cells was studied as follows: A549 cells (4×10^4) suspended in DMEMg and supplemented with 10 % FBS were seeded on each side of an Ibidi culture insert for wound healing assay (Ibidi, Munich, Germany). Inserts were placed into 35-mm dish plates and incubated overnight at 37 °C and 5 % CO_2 to allow cells grow to confluence. Afterwards, inserts were removed to create a cell-free area (pseudo-"wound") of approximately 500 µm; 1 ml DMEMg supplemented with 2 % FBS and containing or not the peptide at different concentrations was added. Cells were allowed to migrate in an appropriate incubator. At 0, 15, 20 and 24 h, fields of the injured area were visualized microscopically under an inverted microscope (Olympus CKX41) at 4× magnification and photographed with a Color View II digital camera. The percentage of cell-covered area at each time was determined by WIMASIS Image Analysis program. Pseudo-"wound" closure assays were also conducted after cells pretreatment with the cell proliferation inhibitor mitomycin C (5 µM) for 90 min (Chieng-Yane et al. 2011; Wang et al. 2012). Furthermore, the involvement of epidermal growth factor receptor (EGFR) in peptide-induced cell migration was analyzed by pretreating cells for 15 min with 0.2 µM AG1478 inhibitor (Tokumaru et al. 2005; Hoq et al. 2011).

Fluorescence studies

Lung epithelial cells (1.5×10^5) were seeded on coverslips (properly put into 35 mm dishes) in DMEMg supplemented with 10 % FBS, at 37 °C and 5 % CO_2. After overnight incubation, cells were washed with PBS and pretreated or not with 0.2 µM AG1478 before adding 10 µM Esc(1-21) or 4 µM Esc(1-21)-1c in DMEMg supplemented with 2 % FBS. For comparison, cells incubated with 0.2 µM AG1478 without any peptide treatment were also included. Cells neither treated with the peptide nor with the inhibitor served as control. After 24 h incubation at 37 °C and 5 % CO_2, cells were washed with PBS and fixed with 3.7 % formaldehyde for 10 min at 4 °C. Afterwards, they were washed with PBS, permeabilized with 0.1 % Triton X-100 in PBS for 10 min at room temperature, washed again and stained with phalloidin-fluorescein isothiocyanate (40 µM in PBS) for 30 min at room temperature to visualize the cytoskeleton. The nuclei were stained by adding 50 µl of Hoechst 33258 (2 µg/ml) for 10 min at room temperature. The coverslips were mounted on slides using buffered glycerol, observed under the fluorescent microscope KOZO OPTICS XJF800 at 20× magnification and photographed with a Color View II digital camera.

Evaluation of Esc(1-21) isomers on the TNF-α release from Raw 264.7 macrophages

Macrophages were cultured overnight in 96-well plates (1×10^5 cells/well) in DMEMg supplemented with sodium pyruvate, NEAA and 10 % FBS. The medium was then removed and replaced with fresh medium containing 10 ng/ml LPS in the presence of 1, 5, 10 and 20 µM peptide. Samples were incubated at 37 °C for 4 h. The medium was then collected and TNF-α concentration was evaluated using a mouse TNF-α enzyme-linked immunosorbent assay kit according to the manufacturer's protocol (eBioscience, Affymetrix, San Diego, CA, USA). Cells that were stimulated with LPS alone and untreated cells served as controls. All experiments were done in triplicates.

Circular dichroism (CD) spectroscopy

CD measurements were performed on an Aviv 202 spectropolarimeter (Applied Photophysics spectropolarimeter, United Kingdom). The spectra were scanned using a thermostatic quartz cuvette with a path length of 1 mm. All measurements were done at 25 °C. The average time recording of each spectrum was 20 s in 1 nm steps in the wavelength range of 190–260 nm. The peptides were scanned at a concentration of 50 µM in 5 mM Hepes, 50 µM of purified *P. aeruginosa* LPS and 10 mg/ml LPC. Average MW of LPS used for calculations is 4 kD.

Table 1 Peptide amount after 5 h and 24 h incubation with human fresh serum at 37 °C

Peptide designation	Peptide sequence[a]	Peptide amount (%)[b]			
		5 h		24 h	
		10 % Serum	30 % Serum	10 % Serum	30 % Serum
Esc-1a(1-21)NH$_2$	Gly-Ile-Phe-Ser-Lys-Leu-Ala-Gly-Lys-Lys-Ile-Lys-Asn-Leu-Leu-Ile-Ser-Gly-Leu-Lys-Gly-NH$_2$	44.4	20.95	22.19	11.5
Esc-1a(1-21)-1cNH$_2$	Gly-Ile-Phe-Ser-Lys-Leu-Ala-Gly-Lys-Lys-Ile-Lys-Asn-***Leu***-Leu-Ile-***Ser***-Gly-Leu-Lys-Gly-NH$_2$	63.34	30.12	45.61	25.46

[a] D-Amino acids are in italics and bold

[b] Peptide amounts were determined by the peak areas of the RP-HPLC relative to those of the control peptide (dissolved in PBS) at 0 min (set as 100 %)

LPS micelles measurements by using dynamic light scattering (DLS)

DLS is a well-known technique used to measure the Brownian motion (diffusion) and the size distribution of particles in solution. Here, we used the DLS machine (802 DLS manufactured by Viscotek) to determine the size of LPS micelles in solution. To estimate the average size of the LPS particles, the measurements were done in wavelength of 830 nm, the detection was performed at 90°, temperature between 22 and 25 °C (the refractive index was measured, respectively) and analyzed by the Software of OMNISIZE (Viscotek). LPS measurement was performed before and after peptides addition. LPS:peptide molar ratio was 1:1 and the solvent was filtered water.

Statistical analyses

Data were collected from three independent experiments. Quantitative data are expressed as the mean ± SEM. Statistical analysis was performed using two-way analysis of variance (ANOVA), with PRISM software (GraphPad, San Diego, CA). Differences were considered to be statistically significant for $p < 0.05$. The levels of statistical significance are indicated in the legend to figures.

Results

Design of Esc(1-21)-1c

Previous studies using CD spectroscopy showed that Esc(1-21) adopts an α-helical structure in phosphatidylethanolamine/phosphatidylglycerol (7:3, v:v) vesicles mimicking the lipid composition of the cytoplasmic membrane of gram-negative bacteria (Epand et al. 2006, 2007). Similar results were found for the shorter analog, Esc-1b(1-18)NH$_2$ (Gly-Ile-Phe-Ser-Lys-Leu-Ala-Gly-Lys–Lys-Leu-Lys-Asn-Leu-Leu-Ile-Ser-Gly-NH$_2$)

(Marcellini et al. 2009; Manzo et al. 2012), which is less active against gram-negative bacteria, e.g., *P. aeruginosa*, and differs from Esc(1-21) by a single amino acid at position 11, and lacks the 3 residues tail Leu-Lys-Gly-NH$_2$ at its carboxyl end.

In order to choose a rational position for incorporating D-amino acids in Esc(1-21), we took advantage of the available structural data on the shorter Esc-1b(1-18)NH$_2$. Solution-state NMR experiments in the presence of anisotropic membrane models, i.e., the negatively charged sodium dodecylsulfate/dodecylphosphocholine detergent micelles, revealed that Esc-1b(1-18)NH$_2$ consists of two helical segments separated by a kink at Gly[8] (Manzo et al. 2014). In addition, it was suggested that the cationic residues located at the N-terminal half of this peptide are important not only for peptide–bacteria binding but also for facilitating a deeper insertion of Esc-1b(1-18)NH$_2$ between the detergent headgroups. Furthermore, in the presence of zwitterionic micelles, which mimic the electrically-neutral membrane of mammalian cells only the C-terminal fragment was expected to fold in a helical conformation (Manzo et al. 2014). Therefore, with the aim of optimizing the biostability of Esc(1-21) without affecting its antimicrobial activity, we synthesized a diastereomer of Esc(1-21), named Esc(1-21)-1c, by replacing two L-amino acids in the C-terminal portion, i.e. L-Leu[14] and L-Ser[17], with the corresponding D-amino acid enantiomers (Table 1). These changes were also expected to decrease the toxicity of the peptide towards mammalian cells, by disturbing the expected C-terminal α-helix which is important for cytotoxicity (see "Discussion").

The diastereomer Esc(1-21)-1c is more stable than the all-L Esc(1-21) in human serum

The stability of both Esc(1-21) and its diastereomer in biological fluids were examined in the presence of 10 or 30 % fresh human serum after 5 and 24 h incubation at 37 °C. The data revealed that the isomer containing

Table 2 Anti-*Pseudomonal* activity of Esc(1-21) isomers

Bacterial strains	Bactericidal activity[a] (µM)	
	Esc(1-21)	Esc(1-21)-1c
P. aeruginosa ATCC 27853	1	4
P. aeruginosa AA11	1	4
P. aeruginosa KK1	1	4
P. aeruginosa TR1	1	4

[a] Bactericidal activity was defined as the lowest peptide concentration that is sufficient to reduce the number of planktonic viable bacteria by $\geq 3 \log_{10}$ CFUs/mL in 30 min. The results are the average of four independent experiments

Table 3 Anti-biofilm activity of Esc(1-21) isomers

Bacterial strains	Anti-biofilm activity[a] (µM)	
	Esc(1-21)	Esc(1-21)-1c
P. aeruginosa ATCC 27853	12.5	12.5
P. aeruginosa AA11	25	12.5
P. aeruginosa KK1	12.5	12.5
P. aeruginosa TR1	25	12.5

[a] Antibiofilm activity was defined as the lowest peptide concentration that is sufficient to cause 95 % reduction in the amount of viable biofilm cells in 2 h. The results are the average of three independent experiments

D-amino acids, after 24 h, was less degraded compared to the wild-type: ~46 and 25 % of peptide in 10 and 30 % serum, respectively (Table 1). In comparison, the non-degraded amount of the wild-type Esc(1-21) after 24 h incubation was only ~22 and 11.5 %, in 10 and 30 % serum, respectively. Mass spectrometry analysis of the samples confirmed the presence of two main peaks, one at 2186 Da, corresponding to the calculated molecular mass of unmodified Esc(1-21)/Esc(1-21)-1c, and one at 495 Da corresponding to the secondary product (data not shown). Note that the majority of naturally occurring AMPs have very short (1-2 h) half-life, mainly because they are degraded by circulating proteases (Noto et al. 2008; Knappe et al. 2010; Nguyen et al. 2010; Falciani et al. 2012).

Esc(1-21)-1c is more active than Esc(1-21) against *P. aeruginosa* biofilms

The antibacterial activity of the two esculentin derivatives against the planktonic form of several strains of *P. aeruginosa* (either reference or clinical isolates from CF patients) was determined in phosphate buffered saline (Table 2). The data indicated that both isomers, at low concentrations, had potent microbicidal activity. The wild-type, at 1 µM, reduced $\geq 3 \log_{10}$ the number of viable bacterial cells within 30 min, compared to the corresponding control (untreated cells). The diastereomer had the same efficacy at a concentration of 4 µM against all the examined bacteria (Table 2). Since *P. aeruginosa* biofilm growing is associated with the persistent chronic infection and colonization of lungs in CF patients, the two peptides were also tested for their ability to kill the sessile form of *P. aeruginosa* strains. As shown in Table 3, Esc(1-21)-1c displayed a higher anti-biofilm activity than the all-L peptide on both the clinical CF isolates AA11 and TR1, giving rise to 95 % reduction in the amount of viable biofilm cells at 12.5 µM compared to 25 µM found for Esc(1-21).

Fig. 1 Peptides' effect on the viability of A549 cells and Raw 264.7 macrophages. A549 cells (**a**) or macrophages (**b**) were plated in wells of a microtiter plate, at 4×10^4 cells/well in the corresponding culture medium (see "Materials and methods"). After overnight incubation at 37 °C in a 5 % CO_2 atmosphere, the medium was replaced with 100 µl fresh medium supplemented with the peptides at different concentrations. After 24 h of peptide treatment, cell viability was determined by the MTT reduction to insoluble formazan. Cell viability is expressed as percentage with respect to the control (cells not treated with the peptide). Data points represent the mean of triplicate samples ± SEM. The level of statistical significance between samples treated with Esc(1-21) and Esc(1-21)-1c are indicated as follows *$p < 0.05$, **$p < 0.01$, ***$p < 0.001$

The diastereomer is significantly less toxic than the all-L peptide against mammalian cells

Esc(1-21) and its diastereomer were analyzed for their effect on the viability of human type II alveolar epithelial cell line (A549 cells) by the MTT assay. They did not significantly reduce the percentage of viable cells at concentrations up to 64 µM (Fig. 1a). The LD_{50} values of the
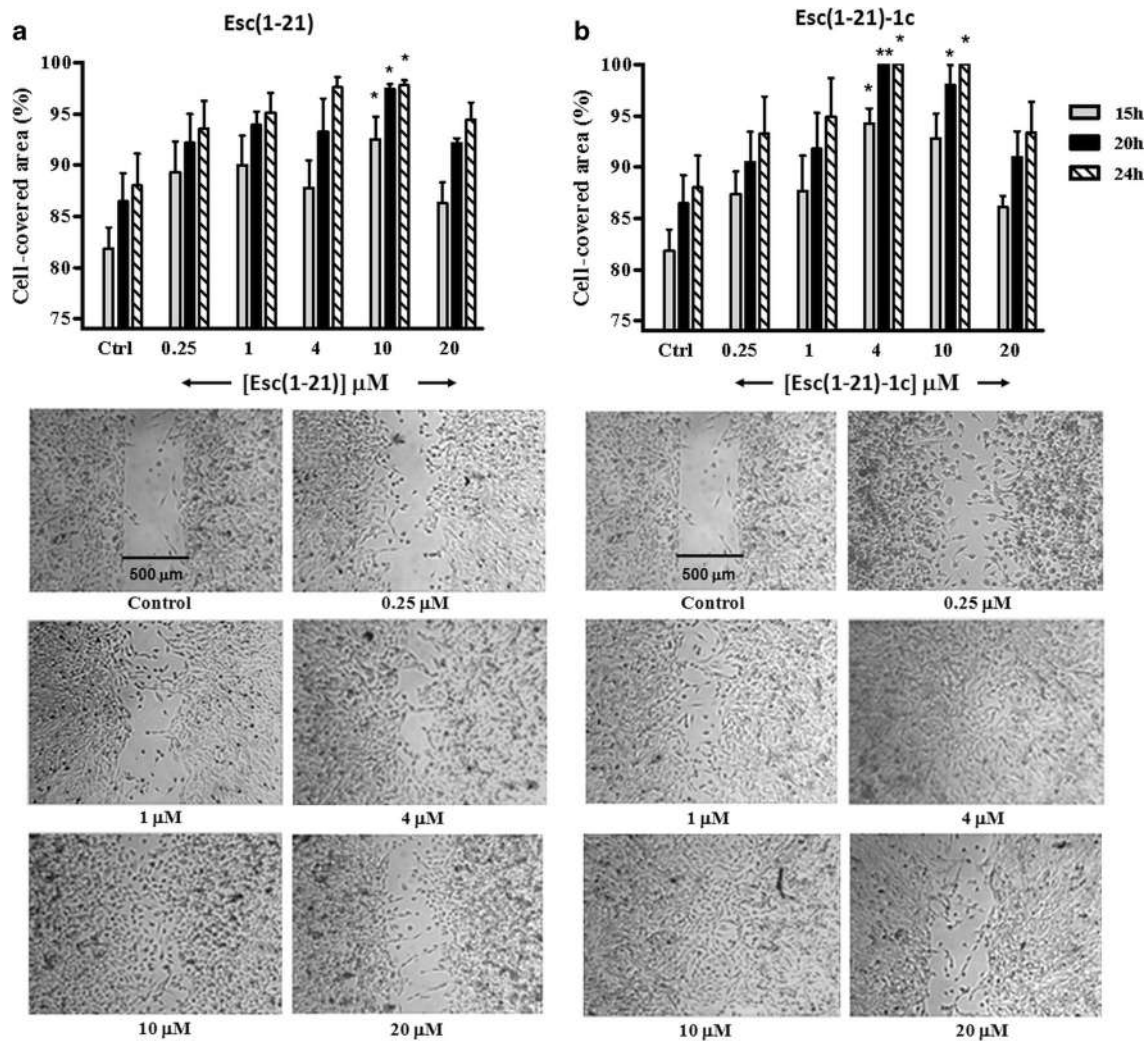
Fig. 2 Effect of Esc(1-21) (*panel a*) and its diastereomer Esc(1-21)-1c (*panel b*) on the closure of a pseudo-"wound" field produced in a monolayer of lung epithelial cells. A549 cells were seeded in each side of an ibidi culture insert and grown to confluence. Afterwards, they were treated or not with the peptide at different concentrations, as indicated. Cells were photographed at the time of insert removal (0 h) and examined for cell migration after 15, 20 and 24 h from peptide addition. The percentage of cell-covered area at each time point is reported on the *y-axis*. Control (Ctrl) are cells not treated with the peptide. All data are the mean of at least three independent experiments ± SEM. The levels of statistical significance between Ctrl and treated samples are indicated as follows *$p < 0.05$, **$p < 0.01$. *Micrographs* show representative results of pseudo-"wound" closure induced after 24 h peptide treatment at different concentrations with respect to the Ctrl sample

peptides were 150 μM and >256 μM for the wild-type and the diastereomer Esc(1-21)-1c, respectively. This difference was even more pronounced against macrophages, since Esc(1-21) had an LD_{50} of ~64 μM and the diastereomer higher than 256 μM (Fig. 1b).

The diastereomeric peptide is more efficient in promoting migration of human lung epithelial cells

It is known that colonization of lung epithelia by *Pseudomonas* leads to tissue damage with impairment of lung functions (Baltimore et al. 1989). Taking into account that

type II pulmonary epithelial cells are responsible for epithelial reparation upon injury (Chuquimia et al. 2013), we studied the peptides' capability to promote migration of A549 cells in an in vitro pseudo-"wound" healing assay, by means of special cell-culture inserts. Both peptides were able to stimulate the closure of a gap produced in a monolayer of A549 cells. The wild-type peptide induced ~98 % coverage of the pseudo-"wound" field within 24 h at a concentration of 10 μM (Fig. 2a). In comparison, the diastereomer Esc(1-21)-1c led to the complete gap closure at 4 μM within 20 h (Fig. 2b).

We further investigated whether the peptide-induced cell migration involved an EGFR-mediated signaling
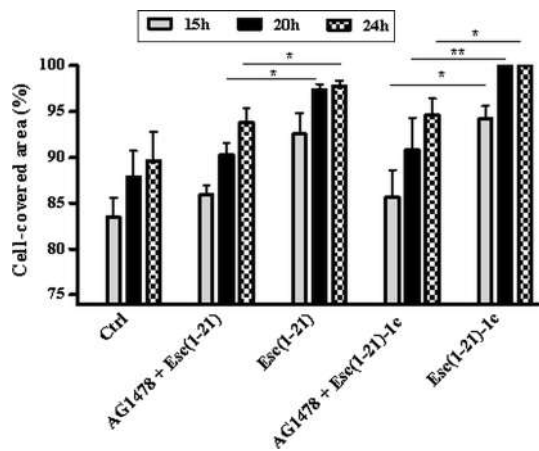
Fig. 3 Effect of AG1478 inhibitor on the peptide-mediated closure of a pseudo-"wound" field produced in a monolayer of A549 cells. After removal of the ibidi culture insert, A549 cells were pre-incubated with 0.2 μM AG1478 for 15 min and subsequently treated with 10 μM Esc(1-21) or 4 μM Esc(1-21)-1c. Some samples were treated with the peptide alone. Cells incubated with medium served as control (Ctrl). Samples were photographed at different time intervals, as indicated in the legend to Fig 2, and the percentage of cell-covered area was calculated and reported on the *y-axis*. All data are the mean of at least three independent experiments ± SEM. The levels of statistical significance between samples pre-treated with AG1478 and subsequently incubated with the peptide and those treated with the peptide alone at the corresponding time intervals are indicated as follows *$p < 0.05$, **$p < 0.01$

pathway, as already found for Esc(1-21) on the immortalized human keratinocytes (HaCaT cells) (Di Grazia et al. 2015). Figure 3 shows that pre-incubation of cells with AG1478, a specifically selective inhibitor of EGFR tyrosine kinase (Osherov and Levitzki 1994; Levitzki and Gazit 1995; Tokumaru et al. 2005; Hoq et al. 2011) resulted in the inhibition of the peptide-induced closure of the pseudo-"wounds". The percentages of cell-covered area in samples treated with the D-amino acids peptide alone were significantly higher than those found when cells were pretreated with AG1478 (Fig. 3), at all time intervals ($p < 0.05$, < 0.01 and < 0.05 after 15, 20 and 24 h, respectively). In the case of Esc(1-21), a significant difference was found only after 20- and 24-h treatment ($p < 0.05$) (Fig. 3). All together, these results clearly emphasize the better efficacy of the diastereomer in promoting the repair of the "wounded" cells monolayer compared to the all-L peptide (for which a higher concentration and a longer time was needed) and the involvement of EGFR in the peptide-induced migration of epithelial cells.

Next, to assess whether the peptide-induced cell migration was accompanied by morphological changes of A549 cells, we used fluorescence microscopy. Both untreated (control) and peptide-treated cells were stained with phalloidin and Hoechst for cytoskeletal and nuclei detection,

respectively. Control A549 cells (Fig. 4a) as wells as those treated with 0.2 μM AG1478 (Fig. 4a') appeared organized into clusters with a regular morphological shape. Differently, cells treated either with Esc(1-21) or Esc(1-21)-1c appeared elongated, polarized and separated one from each other (Fig. 4b, b', respectively), which is consistent with an enhanced cell motility. However, these changes were not identified when the two peptides were added to A549 cells after AG1478 pretreatment (Fig. 4c, c'). These data support the participation of EGFR in the esculentin-elicited migration of alveolar epithelial cells (Fig. 3).

Moreover, to discriminate the contribution of cell migration and proliferation in the peptide-induced recovery of the integrity of A549 monolayers, the pseudo-"wound" healing assay was performed by pretreating cells with the cell proliferation blocker mitomycin C (Chieng-Yane et al. 2011; Wang et al. 2012). As can be seen in Fig. 5, cell proliferation was not essential for the re-epithelialization process, as pretreatment with mitomycin C did not bias the cell migration pattern stimulated by both peptides. Overall, besides the finding of more rapid and efficient re-epithelialization activity of Esc(1-21)-1c compared to the wild-type Esc(1-21), our data indicate that the pseudo-"wound" healing activity primarily depends on the peptide-induced migratory activity of A549 cells.

Both esculentin derivatives neutralize LPS and prevent TNF-α secretion from LPS-activated macrophages

To get insight into additional host-defense properties, we tested Esc(1-21) and its diastereomer for their ability to inhibit the secretion of the pro-inflammatory cytokine TNF-α from murine macrophages after stimulation with LPS (10 ng/ml) from *P. aeruginosa*. The results demonstrated a dose-dependent effect in the inhibition of TNF-α release; 80 and 90 % inhibition at 10 and 20 μM Esc(1-21), respectively, compared to that of LPS alone (Fig. 6). In comparison, a weaker activity was detected with the diastereomer Esc(1-21)-1c; 20 and 30 % inhibition at 10 and 20 μM, respectively (Fig. 6).

Esc(1-21)-1c has less helical content than the all-L peptide in different lipid environments

The secondary structure of the peptides was determined by using CD spectroscopy in several environments: Hepes buffer, LPC, which mimics the zwitterionic nature of the plasma membrane of eukaryotic cells, or LPS (Fig. 7). Both peptides formed β-sheet structure in 5 mM Hepes (aqueous solution), but changed their conformation in LPC and LPS. Whereas Esc(1-21) adopted predominantly α-helix in both LPC and LPS environments, the CD spectra of the diastereomer indicated a loss of most of the α-helical structure.
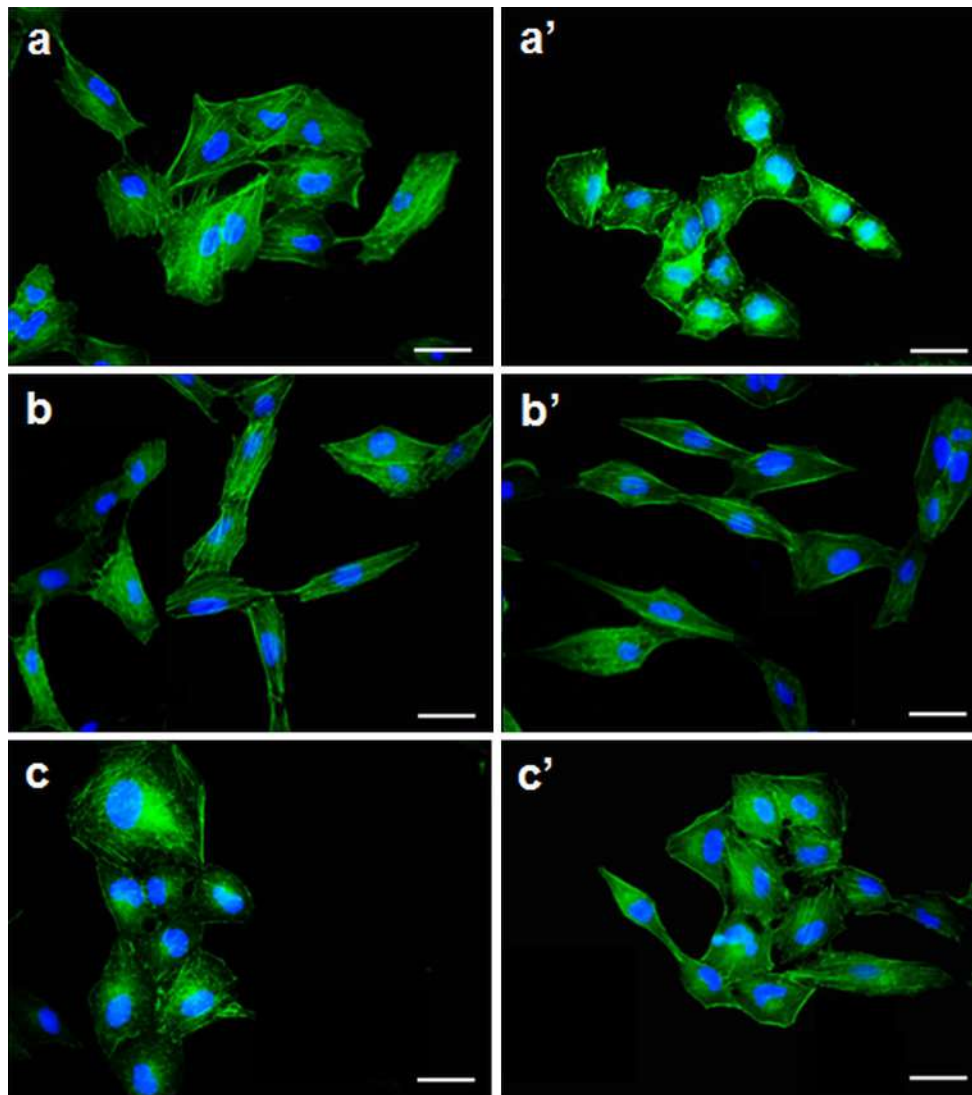
Fig. 4 Effects of Esc(1-21) and Esc(1-21)-1c on the morphology of A549 cells. After fixation in formaldehyde, cells were stained with Hoechst (for nuclei detection) and phalloidin (for cytoskeletal detection). The untreated control cells (**a**) as well as those treated with 0.2 μM AG1478 for 15 min (**a'**) appeared organized in clusters. The Esc(1-21) and Esc(1-21)-1c-treated cells (**b** and **b'** respectively) appeared elongated with a change in their shape and cytoplasmic protrusions. These alterations were not identified in A549 cells pretreated with AG1478 and subsequently exposed to Esc(1-21) and Esc(1-21)-1c (**c** and **c'**, respectively). *Bars* are 20 μm long

This could be the result of the incorporation of D-amino acids that (1) break an α-helical structure, and (2) induce an opposite CD spectra, because CD is chirality dependent.

Esculentin derivatives disassemble LPS aggregates

Light scattering experiments were used to figure out whether the peptides could alter the micelle morphology of LPS (above its critical micelle concentration). The data revealed that LPS from *Pseudomonas* is poly-dispersed in solution with major size-populations having hydrodynamic radius centered at 355 nm (Fig. 8). Incubation of LPS with Esc(1-21) caused a shift of the average size of LPS to a lower value

centered at 67.7 nm, compared to the diastereomer Esc(1-21)-1c which induced a larger LPS mean diameter centered at 116, indicating weaker potency to dissociate LPS aggregates.

Discussion

Previously, we identified a short-length peptide, Esc-1a(1-21)NH$_2$, derived from the frog skin AMP esculentin-1a, with promising in vitro and in vivo anti-*Pseudomonal* activities (Luca et al. 2013). Here, we focused on the immunomodulating properties of this peptide and the effect of incorporation of D-amino acids on both its antimicrobial
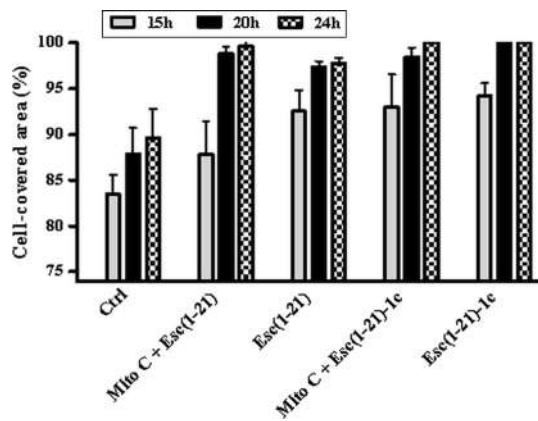
Fig. 5 Effect of mitomycin C on the peptide-mediated closure of a pseudo-"wound" field produced in a monolayer of A549 cells. After removal of the ibidi culture insert, A549 cells were pre-incubated with 5 µM mitomycin (Mito C) for 90 min and subsequently treated with 10 µM Esc(1-21) or 4 µM Esc(1-21)-1c. Some samples were treated with the peptide alone. Cells incubated with medium served as control (Ctrl). Samples were photographed at different time intervals, as indicated in the legend to Fig. 2, and the percentage of cell-covered area was calculated and reported on the *y-axis*. All data are the mean of three independent experiments ± SEM. No statistically significant difference was found between samples pretreated with Mito C and subsequently incubated with the peptide and those treated with the peptide alone, at all time intervals
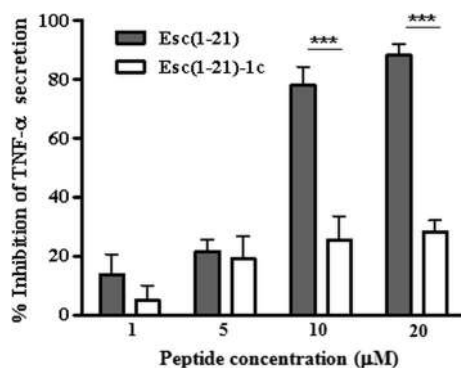
Fig. 6 The effect of peptides on the secretion of TNF-α from murine macrophages. RAW 264.7 macrophages were stimulated with LPS (10 ng/ml) derived from *P. aeruginosa* 10 in the presence of 1, 5, 10 and 20 µM Esc(1-21) or Esc(1-21)-1c for 4 h at 37 °C and 5 % CO_2. The percentage of inhibition of TNF-α release was normalized to that of macrophages stimulated with LPS without peptides (0 % inhibition). All the results are the mean of three independent experiments ± SEM. The level of statistical significance between samples treated with Esc(1-21) and Esc(1-21)-1c is indicated as follows ***$p < 0.001$

and non-antimicrobial activities. Functionally, the D-amino acids containing diastereomer Esc(1-21)-1c retains potent activity against the planktonic form of *P. aeruginosa* and it is more efficient than the all-L peptide against the sessile form of this bacterium, which is very difficult to eradicate.

Furthermore, the diastereomer is significantly less toxic than Esc(1-21) towards both mammalian macrophages and alveolar epithelial cells. In addition, it is endowed with a higher stability in serum and with a higher activity in promoting migration of lung epithelial cells in an in vitro re-epithelialization assay. This suggests better propensity of the diastereomer Esc(1-21)-1c to heal damaged lung tissue. The enhanced stability in serum and lower toxicity to epithelial cells likely justify the diastereomer Esc(1-21)-1c to be a better candidate in future clinical application.

Mode-of-action studies pointed out that as found for Esc(1-21) on HaCaT cells, migration of alveolar epithelial cells induced by both isomers is prevented by AG1478, corroborating the involvement of EGFR in the signaling pathway controlling such an event. Similar results were also described for the frog skin AMPs temporins A and B (Di Grazia et al. 2014) and the cathelicidin LL-37 towards keratinocytes (Tokumaru et al. 2005) or corneal epithelial cells (Huang et al. 2007). It is known that plasma membrane-associated tyrosine kinase receptors, including EGFR, are localized in ordered lipid domain called lipid rafts (Pike et al. 2005) whose alteration may inhibit ligands binding to EGFR and its activation. Due to insertion of α-helical peptides in zwitterionic phospholipid bilayers (see below), the difference in wound healing activity between Esc(1-21) and Esc(1-21)-1c may be explained on the basis of a more pronounced change in the plasma membrane phospholipid organization and a resulting weaker activation of EGFR by the more helical Esc(1-21) compared to its diastereomer.

Importantly, in line with what we lately observed for Esc(1-21) on HaCaT cells (Di Grazia et al. 2015), the gap closure driven by both esculentin isoforms does not appear to be affected by cell proliferation, but rather depends on the cell migration activity. Indeed, cells exposed to mitomycin C before peptide treatment gave the same results as those obtained when the peptide was used alone (Fig. 5).

Esc(1-21)-1c has also the capability to inhibit the release of the pro-inflammatory cytokine TNF-α from macrophages activated by *P. aeruginosa* LPS, albeit to a lesser extent compared to the all-L parental peptide.

To define whether the secondary structure of the two peptides contributes to their different behavior in the toxicity studies and LPS detoxification activity, CD spectroscopy was carried out. We found that Esc(1-21) but not its diastereomer, folds into a predominantly α-helical structure in the presence of LPC. These results are consistent with the higher cytotoxicity of the wild-type Esc(1-21) compared to Esc(1-21)-1c. Indeed, numerous studies conducted with various native AMPs emphasized the importance of an amphipatic α-helical structure for mammalian cell lysis (Pouny et al. 1992; Gazit et al. 1994; Strahilevitz et al. 1994).
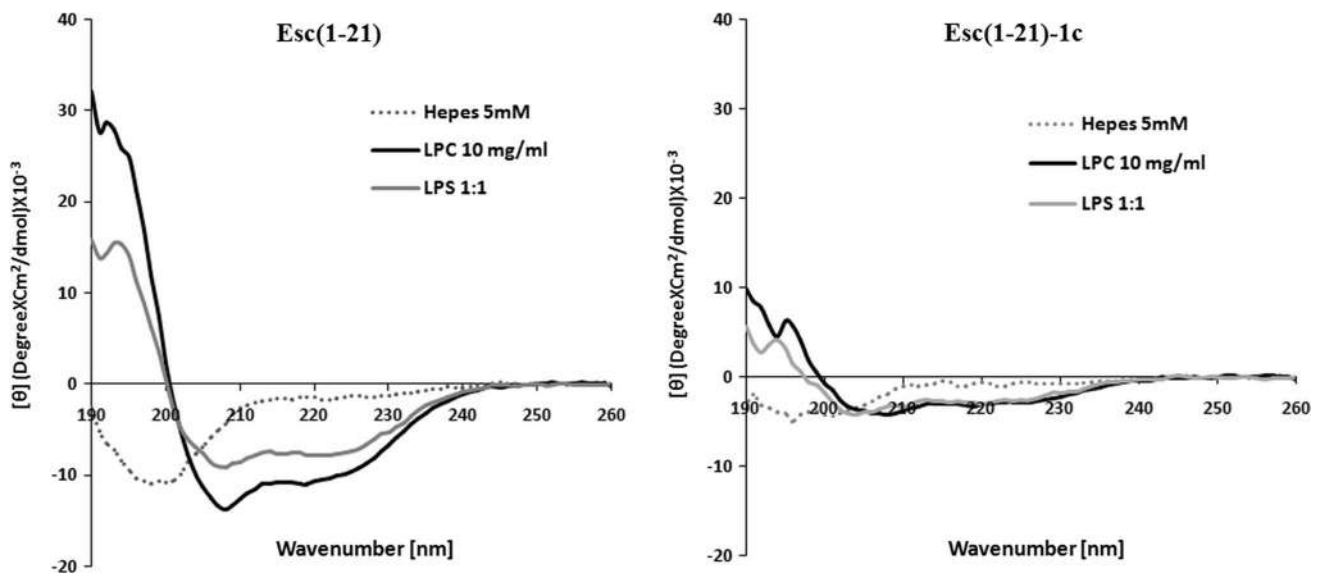
Fig. 7 The effect of LPS and LPC on the structure of Esc(1-21) or Esc(1-21)-1c. Circular dichroism spectra of 50 μM peptide in 5 mM Hepes (*dotted line*), 50 μM of purified *P. aeruginosa* LPS (*grey line*) or 10 mg/ml LPC (*black line*)

Fig. 8 The effect of peptides on the structural organization of LPS micelles. Light scattering of LPS from *P. aeruginosa* 10 in water before and after incubation with Esc(1-21) or Esc(1-21)-1c at equimolar concentration
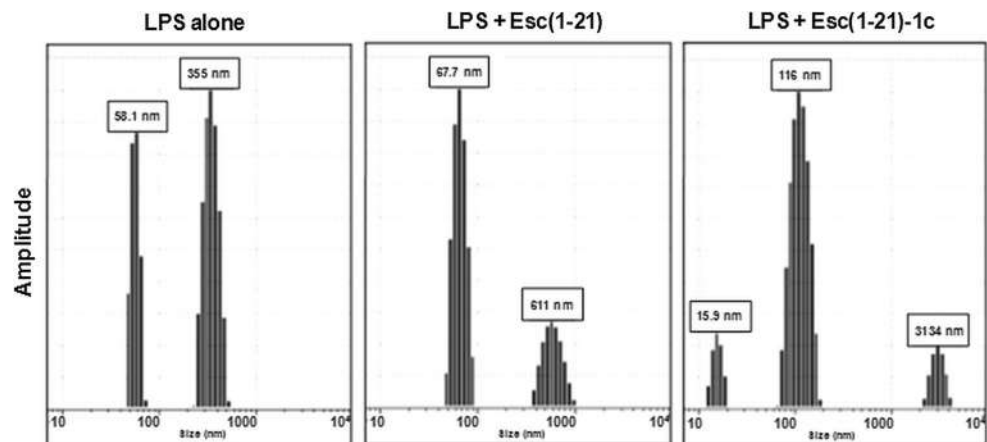
This is likely assisted by a deeper insertion of peptides with a higher helical content into the hydrophobic core of mammalian cell membranes (Carotenuto et al. 2008; Mangoni et al. 2011). Furthermore, our findings are in line with previous reports showing that incorporation of D-amino acids into native AMPs, such as the cytolytic peptides pardaxin (Shai and Oren 1996) and melittin (Oren and Shai 1997) or synthetic peptides causes (1) abrogation of their toxic effect on mammalian cells while retaining antibacterial activity and ability to permeate anionic membranes (Oren et al. 1997), and (2) increases the resistance of diastereomers to serum inactivation (Oren et al. 1997).

Remarkably, LPS covers more than 90 % of the outer membrane in gram-negative bacteria and forms an impermeable barrier preventing the passage of both hydrophobic and hydrophilic molecules (Bhunia et al. 2011; Ghosh et al.

2014). Nevertheless, beside protecting bacteria from their surroundings, LPS can also act as an effector molecule by activating the host's immune response against invading microbial pathogens. Indeed, upon being shed from bacteria as a result of their death or cell division, it forms micelles, which are the active form of the endotoxin (Takayama et al. 1994; Rosenfeld and Shai 2006). However, when LPS is transferred to CD14, e.g., the primary receptor of LPS, which is mainly expressed on macrophages (Schumann et al. 1990), it disaggregates (Tobias and Ulevitch 1993). The LPS-CD14 complex then interacts with the transmembrane protein Toll-like receptor-4 (TLR4) and initiates the intracellular signaling cascade controlling the expression of cytokines, i.e., TNF-α (Rosenfeld et al. 2006b). The possible mechanism of action in which AMPs neutralize LPS by breaking its large micelles into smaller ones has been

proposed by others as well (Rosenfeld et al. 2006a, b; Bhunia et al. 2011). The disaggregated form of LPS can then interfere with its binding to the LPS-binding protein. As a consequence, TLR4 will not be activated and the synthesis of TNF-α will be prevented (Rosenfeld et al. 2006a, b; Mangoni and Shai 2011). Our light scattering analysis highlights the formation of smaller-sized LPS micelles upon addition of the peptides, with a stronger effect in the presence of the all-L Esc(1-21).

Note that peptides characterized by having a well-defined and stabilized structure in both LPS and cytoplasmic membrane and by the capability to disassemble the structural organization of LPS micelles are known to have a potent LPS detoxification activity (Rosenfeld et al. 2008). Therefore, the higher α-helical content of Esc(1-21) in LPS and its stronger efficacy in disrupting LPS aggregates compared to its diastereomer are consistent with its stronger anti-endotoxin activity (Fig. 6). Importantly, by suppressing the secretion of pro-inflammatory cytokines from activated immune cells, these peptides would contribute to a down-regulation of acute inflammatory responses elicited during infection or injury; an advanced benefit of an antimicrobial agent in vivo. The mild anti-inflammatory activity of the diastereomer compared to the wild-type peptide might be an advantage when the host's innate immune response to bacterial infection is at the beginning stage.

Conclusions

In conclusion, we have demonstrated multiple functions for both the wild-type peptide and its diastereomer. Importantly, only two L-to-D-amino acids substitutions in the C-terminal end of Esc(1-21) are sufficient to: (1) significantly reduce its cytotoxic effect towards mammalian cells (e.g., alveolar epithelial cells and macrophages); (2) increase its effectiveness against the biofilm form of *P. aeruginosa*, while maintaining a high activity against the free-living form of this important pathogen; (3) enhance the peptide's biostability; and (4) improve the ability of the peptide to promote migration of lung epithelial cells and presumably its capacity to restore the integrity of the injured lung tissue. To the best of our knowledge, this is the first report showing multiple beneficial effects of D-amino acids incorporation into an AMP. These multiple beneficial properties make the diastereomer a better candidate for future medical preparations against *P. aeruginosa*-induced infections, particularly in CF patients, while offering important findings to assist and optimize the future design of new AMPs exhibiting multiple functions.

References

Akram KM, Samad S, Spiteri MA, Forsyth NR (2013) Mesenchymal stem cells promote alveolar epithelial cell wound repair in vitro through distinct migratory and paracrine mechanisms. Respir Res 14:9

Alba A, Lopez-Abarrategui C, Otero-Gonzalez AJ (2012) Host defense peptides: an alternative as antiinfective and immunomodulatory therapeutics. Biopolymers 98:251–267

Baltimore RS, Christie CD, Smith GJ (1989) Immunohistopathologic localization of *Pseudomonas aeruginosa* in lungs from patients with cystic fibrosis. Implications for the pathogenesis of progressive lung deterioration. Am Rev Respir Dis 140:1650–1661

Bevins CL (2013) Innate immune functions of alpha-defensins in the small intestine. Dig Dis 31:299–304

Bhunia A, Saravanan R, Mohanram H, Mangoni ML, Bhattacharjya S (2011) NMR structures and interactions of temporin-1Tl and temporin-1Tb with lipopolysaccharide micelles: mechanistic insights into outer membrane permeabilization and synergistic activity. J Biol Chem 286:24394–24406

Bjarnsholt T, Jensen PO, Fiandaca MJ, Pedersen J, Hansen CR, Andersen CB, Pressler T, Givskov M, Hoiby N (2009) *Pseudomonas aeruginosa* biofilms in the respiratory tract of cystic fibrosis patients. Pediatr Pulmonol 44:547–558

Boman HG (1995) Peptide antibiotics and their role in innate immunity. Annu Rev Immunol 13:61–92

Bragonzi A, Paroni M, Nonis A, Cramer N, Montanari S, Rejman J, Di Serio C, Doring G, Tummler B (2009) *Pseudomonas aeruginosa* microevolution during cystic fibrosis lung infection establishes clones with adapted virulence. Am J Respir Crit Care Med 180:138–145

Brown KL, Hancock RE (2006) Cationic host defense (antimicrobial) peptides. Curr Opin Immunol 18:24–30

Carotenuto A, Malfi S, Saviello MR, Campiglia P, Gomez-Monterrey I, Mangoni ML, Gaddi LM, Novellino E, Grieco P (2008) A different molecular mechanism underlying antimicrobial and hemolytic actions of temporins A and L. J Med Chem 51:2354–2362

Ceri H, Olson M, Morck D, Storey D, Read R, Buret A, Olson B (2001) The MBEC assay system: multiple equivalent biofilms for antibiotic and biocide susceptibility testing. Methods Enzymol 337:377–385

Chen LF, Chopra T, Kaye KS (2009) Pathogens resistant to antibacterial agents. Infect Dis Clin North Am 23:817–845 **vii**

Chieng-Yane P, Bocquet A, Letienne R, Bourbon T, Sablayrolles S, Perez M, Hatem SN, Lompre AM, Le Grand B, David-Dufilho M (2011) Protease-activated receptor-1 antagonist F 16618 reduces arterial restenosis by down-regulation of tumor necrosis factor alpha and matrix metalloproteinase 7 expression, migration, and

proliferation of vascular smooth muscle cells. J Pharmacol Exp Ther 336:643–651

Chuquimia OD, Petursdottir DH, Periolo N, Fernandez C (2013) Alveolar epithelial cells are critical in protection of the respiratory tract by secretion of factors able to modulate the activity of pulmonary macrophages and directly control bacterial growth. Infect Immun 81:381–389

Cohen J (2002) The immunopathogenesis of sepsis. Nature 420:885–891

Cruz J, Ortiz C, Guzman F, Fernandez-Lafuente R, Torres R (2014) Antimicrobial peptides: promising compounds against pathogenic microorganisms. Curr Med Chem 21:2299–2321

Dempsey CE, Hawrani A, Howe RA, Walsh TR (2010) Amphipathic antimicrobial peptides—from biophysics to therapeutics? Protein Pept Lett 17:1334–1344

Di Grazia A, Cappiello F, Imanishi A, Mastrofrancesco A, Picardo M, Paus R, Mangoni ML (2015) The frog skin-derived antimicrobial peptide esculentin-1a(1-21)NH2 promotes the migration of human HaCaT keratinocytes in an EGF receptor-dependent manner: a novel promoter of human skin wound healing? PLoS One 10:e0128663

Di Grazia A, Luca V, Segev-Zarko LA, Shai Y, Mangoni ML (2014) Temporins A and B stimulate migration of HaCaT keratinocytes and kill intracellular *Staphylococcus aureus*. Antimicrob Agents Chemother 58:2520–2527

Drenkard E, Ausubel FM (2002) *Pseudomonas* biofilm formation and antibiotic resistance are linked to phenotypic variation. Nature 416:740–743

Epand RF, Savage PB, Epand RM (2007) Bacterial lipid composition and the antimicrobial efficacy of cationic steroid compounds (Ceragenins). Biochim Biophys Acta 1768:2500–2509

Epand RF, Schmitt MA, Gellman SH, Epand RM (2006) Role of membrane lipids in the mechanism of bacterial species selective toxicity by two alpha/beta-antimicrobial peptides. Biochim Biophys Acta 1758:1343–1350

Epand RM, Vogel HJ (1999) Diversity of antimicrobial peptides and their mechanisms of action. Biochim Biophys Acta 1462:11–28

Falciani C, Lozzi L, Pollini S, Luca V, Carnicelli V, Brunetti J, Lelli B, Bindi S, Scali S, Di Giulio A, Rossolini GM, Mangoni ML, Bracci L, Pini A (2012) Isomerization of an antimicrobial Peptide broadens antimicrobial spectrum to gram-positive bacterial pathogens. PLoS One 7:e46259

Fjell CD, Hiss JA, Hancock RE, Schneider G (2012) Designing antimicrobial peptides: form follows function. Nat Rev Drug Discov 11:37–51

Gamberi T, Cavalieri D, Magherini F, Mangoni ML, De Filippo C, Borro M, Gentile G, Simmaco M, Modesti A (2007) An integrated analysis of the effects of Esculentin 1-21 on *Saccharomyces cerevisiae*. Biochim Biophys Acta 1774:688–700

Gazit E, Lee WJ, Brey PT, Shai Y (1994) Mode of action of the antibacterial cecropin B2: a spectrofluorometric study. Biochemistry 33:10681–10692

Ghosh A, Datta A, Jana J, Kar RK, Chatterjee C, Chatterjee S, Bhunia A (2014) Sequence context induced antimicrobial activity: insight into lipopolysaccharide permeabilization. Mol Biosyst 10:1596–1612

Giacometti A, Cirioni O, Ghiselli R, Mocchegiani F, Orlando F, Silvestri C, Bozzi A, Di Giulio A, Luzi C, Mangoni ML, Barra D, Saba V, Scalise G, Rinaldi AC (2006) Interaction of antimicrobial peptide temporin L with lipopolysaccharide in vitro and in experimental rat models of septic shock caused by gram-negative bacteria. Antimicrob Agents Chemother 50:2478–2486

Grieco P, Carotenuto A, Auriemma L, Limatola A, Di Maro S, Merlino F, Mangoni ML, Luca V, Di Grazia A, Gatti S, Campiglia P, Gomez-Monterrey I, Novellino E, Catania A (2013) Novel alpha-MSH peptide analogues with broad spectrum antimicrobial activity. PLoS One 8:e61614

Grundmann H, Klugman KP, Walsh T, Ramon-Pardo P, Sigauque B, Khan W, Laxminarayan R, Heddini A, Stelling J (2011) A framework for global surveillance of antibiotic resistance. Drug Resist Updat 14:79–87

Guralp SA, Murgha YE, Rouillard JM, Gulari E (2013) From design to screening: a new antimicrobial peptide discovery pipeline. PLoS One 8:e59305

Hamamoto K, Kida Y, Zhang Y, Shimizu T, Kuwano K (2002) Antimicrobial activity and stability to proteolysis of small linear cationic peptides with D-amino acid substitutions. Microbiol Immunol 46:741–749

Hancock RE, Nijnik A, Philpott DJ (2012) Modulating immunity as a therapy for bacterial infections. Nat Rev Microbiol 10:243–254

Hancock RE, Sahl HG (2006) Antimicrobial and host-defense peptides as new anti-infective therapeutic strategies. Nat Biotechnol 24:1551–1557

Haney EF, Hancock RB (2013) Peptide design for antimicrobial and immunomodulatory applications. Biopolymers 100(572):583

Hoq MI, Niyonsaba F, Ushio H, Aung G, Okumura K, Ogawa H (2011) Human catestatin enhances migration and proliferation of normal human epidermal keratinocytes. J Dermatol Sci 64:108–118

Huang LC, Redfern RL, Narayanan S, Reins RY, McDermott AM (2007) In vitro activity of human beta-defensin 2 against *Pseudomonas aeruginosa* in the presence of tear fluid. Antimicrob Agents Chemother 51:3853–3860

Islas-Rodriguez AE, Marcellini L, Orioni B, Barra D, Stella L, Mangoni ML (2009) Esculentin 1-21: a linear antimicrobial peptide from frog skin with inhibitory effect on bovine mastitis-causing bacteria. J Pept Sci 15:607–614

Jung Kim D, Lee YW, Park MK, Shin JR, Lim KJ, Cho JH, Kim SC (2014) Efficacy of the designer antimicrobial peptide SHAP1 in wound healing and wound infection. Amino Acids 46:2333–2343

Kai-Larsen Y, Gudmundsson GH, Agerberth B (2014) A review of the innate immune defence of the human foetus and newborn, with the emphasis on antimicrobial peptides. Acta Paediatr 103:1000–1008

Kaye KS (2012) Antimicrobial de-escalation strategies in hospitalized patients with pneumonia, intra-abdominal infections, and bacteremia. J Hosp Med 7(Suppl 1):S13–S21

Knappe D, Henklein P, Hoffmann R, Hilpert K (2010) Easy strategy to protect antimicrobial peptides from fast degradation in serum. Antimicrob Agents Chemother 54:4003–4005

Kolar SS, Luca V, Baidouri H, Mannino G, McDermott AM, Mangoni ML (2015) Esculentin-1a(1-21)NH: a frog skin-derived peptide for microbial keratitis. Cell Mol Life Sci 72:617–627

Levitzki A, Gazit A (1995) Tyrosine kinase inhibition: an approach to drug development. Science 267:1782–1788

Li J, Turnidge J, Milne R, Nation RL, Coulthard K (2001) In vitro pharmacodynamic properties of colistin and colistin methanesulfonate against *Pseudomonas aeruginosa* isolates from patients with cystic fibrosis. Antimicrob Agents Chemother 45:781–785

Lohner K, Staudegger E (2001) Are we on the threshold of the post-antibiotic era? In: Lohner K (ed) Development of novel antimicrobial agents: emerging strategies. Horizon Scientific Press, Wymondham, pp 1–15

Luca V, Stringaro A, Colone M, Pini A, Mangoni ML (2013) Esculentin(1-21), an amphibian skin membrane-active peptide with potent activity on both planktonic and biofilm cells of the bacterial pathogen *Pseudomonas aeruginosa*. Cell Mol Life Sci 70:2773–2786

Luca V, Olivi M, Di Grazia A, Palleschi C, Uccelletti D, Mangoni ML (2014) Anti-Candida activity of 1-18 fragment of the frog skin peptide esculentin-1b: in vitro and in vivo studies in a *Caenorhabditis elegans* infection model. Cell Mol Life Sci 71:2535–2546

Macia MD, Rojo-Molinero E, Oliver A (2014) Antimicrobial susceptibility testing in biofilm growing bacteria. Clin Microbiol Infect 20:981–990

Mangoni ML (2006) Temporins, anti-infective peptides with expanding properties. Cell Mol Life Sci 63:1060–1069

Mangoni ML (2011) Host-defense peptides: from biology to therapeutic strategies. Cell Mol Life Sci 68:2157–2159

Mangoni ML, Carotenuto A, Auriemma L, Saviello MR, Campiglia P, Gomez-Monterrey I, Malfi S, Marcellini L, Barra D, Novellino E, Grieco P (2011) Structure-activity relationship, conformational and biological studies of temporin L analogues. J Med Chem 54:1298–1307

Mangoni ML, Marcellini HG, Simmaco M (2007) Biological characterization and modes of action of temporins and bombinins H, multiple forms of short and mildly cationic anti-microbial peptides from amphibian skin. J Pept Sci 13:603–613

Mangoni ML, Saugar JM, Dellisanti M, Barra D, Simmaco M, Rivas L (2005) Temporins, small antimicrobial peptides with leishmanicidal activity. J Biol Chem 280:984–990

Mangoni ML, Shai Y (2011) Short native antimicrobial peptides and engineered ultrashort lipopeptides: similarities and differences in cell specificities and modes of action. Cell Mol Life Sci 68:2267–2280

Mansour SC, Pena OM, Hancock RE (2014) Host defense peptides: front-line immunomodulators. Trends Immunol 35:443–450

Manzo G, Casu M, Rinaldi AC, Montaldo NP, Luganini A, Gribaudo G, Scorciapino MA (2014) Folded structure and insertion depth of the frog-skin antimicrobial Peptide esculentin-1b(1-18) in the presence of differently charged membrane-mimicking micelles. J Nat Prod 77:2410–2417

Manzo G, Sanna R, Casu M, Mignogna G, Mangoni ML, Rinaldi AC, Scorciapino MA (2012) Toward an improved structural model of the frog-skin antimicrobial peptide esculentin-1b(1-18). Biopolymers 97:873–881

Marcellini L, Borro M, Gentile G, Rinaldi AC, Stella L, Aimola P, Barra D, Mangoni ML (2009) Esculentin-1b(1-18)–a membrane-active antimicrobial peptide that synergizes with antibiotics and modifies the expression level of a limited number of proteins in *Escherichia coli*. FEBS J 276:5647–5664

Millar FA, Simmonds NJ, Hodson ME (2009) Trends in pathogens colonising the respiratory tract of adult patients with cystic fibrosis, 1985–2005. J Cyst Fibros 8:386–391

Moreau-Marquis S, Stanton BA, O'Toole GA (2008) *Pseudomonas aeruginosa* biofilm formation in the cystic fibrosis airway. Pulm Pharmacol Ther 21:595–599

Nguyen LT, Chau JK, Perry NA, de Boer L, Zaat SA, Vogel HJ (2010) Serum stabilities of short tryptophan- and arginine-rich antimicrobial peptide analogs. PLoS One 5:e12684

Noto PB, Abbadessa G, Cassone M, Mateo GD, Agelan A, Wade JD, Szabo D, Kocsis B, Nagy K, Rozgonyi F, Otvos L Jr (2008) Alternative stabilities of a proline-rich antibacterial peptide in vitro and in vivo. Protein Sci 17:1249–1255

Oren Z, Hong J, Shai Y (1997) A repertoire of novel antibacterial diastereomeric peptides with selective cytolytic activity. J Biol Chem 272:14643–14649

Oren Z, Shai Y (1997) Selective lysis of bacteria but not mammalian cells by diastereomers of melittin: structure-function study. Biochemistry 36:1826–1835

Osherov N, Levitzki A (1994) Epidermal-growth-factor-dependent activation of the src-family kinases. Eur J Biochem 225:1047–1053

Papo N, Oren Z, Pag U, Sahl HG, Shai Y (2002) The consequence of sequence alteration of an amphipathic alpha-helical antimicrobial peptide and its diastereomers. J Biol Chem 277:33913–33921

Peschel A, Otto M, Jack RW, Kalbacher H, Jung G, Gotz F (1999) Inactivation of the dlt operon in Staphylococcus aureus confers

sensitivity to defensins, protegrins, and other antimicrobial peptides. J Biol Chem 274:8405–8410

Pike LJ, Han X, Gross RW (2005) Epidermal growth factor receptors are localized to lipid rafts that contain a balance of inner and outer leaflet lipids: a shotgun lipidomics study. J Biol Chem 280:26796–26804

Pini A, Falciani C, Mantengoli E, Bindi S, Brunetti J, Iozzi S, Rossolini GM, Bracci L (2010) A novel tetrabranched antimicrobial peptide that neutralizes bacterial lipopolysaccharide and prevents septic shock in vivo. FASEB J 24:1015–1022

Poltorak A, He X, Smirnova I, Liu MY, Van Huffel C, Du X, Birdwell D, Alejos E, Silva M, Galanos C, Freudenberg M, Ricciardi-Castagnoli P, Layton B, Beutler B (1998) Defective LPS signaling in C3H/HeJ and C57BL/10ScCr mice: mutations in Tlr4 gene. Science 282:2085–2088

Pouny Y, Rapaport D, Mor A, Nicolas P, Shai Y (1992) Interaction of antimicrobial dermaseptin and its fluorescently labeled analogues with phospholipid membranes. Biochemistry 31:12416–12423

Pulido D, Nogues MV, Boix E, Torrent M (2012) Lipopolysaccharide neutralization by antimicrobial peptides: a gambit in the innate host defense strategy. J Innate Immun 4:327–336

Rietschel ET, Kirikae T, Schade FU, Mamat U, Schmidt G, Loppnow H, Ulmer AJ, Zahringer U, Seydel U, Di Padova F et al (1994) Bacterial endotoxin: molecular relationships of structure to activity and function. Faseb J 8:217–225

Rosenfeld Y, Barra D, Simmaco M, Shai Y, Mangoni ML (2006a) A synergism between temporins toward gram-negative bacteria overcomes resistance imposed by the lipopolysaccharide protective layer. J Biol Chem 281:28565–28574

Rosenfeld Y, Papo N, Shai Y (2006b) Endotoxin (lipopolysaccharide) neutralization by innate immunity host-defense peptides. Peptide properties and plausible modes of action. J Biol Chem 281:1636–1643

Rosenfeld Y, Sahl HG, Shai Y (2008) Parameters involved in antimicrobial and endotoxin detoxification activities of antimicrobial peptides. Biochemistry 47:6468–6478

Rosenfeld Y, Shai Y (2006) Lipopolysaccharide (Endotoxin)-host defense antibacterial peptides interactions: role in bacterial resistance and prevention of sepsis. Biochim Biophys Acta 1758:1513–1522

Schumann RR, Leong SR, Flaggs GW, Gray PW, Wright SD, Mathison JC, Tobias PS, Ulevitch RJ (1990) Structure and function of lipopolysaccharide binding protein. Science 249:1429–1431

Semple F, Dorin JR (2012) beta-Defensins: multifunctional modulators of infection, inflammation and more? J Innate Immun 4:337–348

Shai Y (2002) Mode of action of membrane active antimicrobial peptides. Biopolymers 66:236–248

Shai Y, Oren Z (1996) Diastereoisomers of cytolysins, a novel class of potent antibacterial peptides. J Biol Chem 271:7305–7308

Strahilevitz J, Mor A, Nicolas P, Shai Y (1994) Spectrum of antimicrobial activity and assembly of dermaseptin-b and its precursor form in phospholipid membranes. Biochemistry 33:10951–10960

Takayama K, Mitchell DH, Din ZZ, Mukerjee P, Li C, Coleman DL (1994) Monomeric Re lipopolysaccharide from *Escherichia coli* is more active than the aggregated form in the Limulus amebocyte lysate assay and in inducing Egr-1 mRNA in murine peritoneal macrophages. J Biol Chem 269:2241–2244

Tobias PS, Ulevitch RJ (1993) Lipopolysaccharide binding protein and CD14 in LPS dependent macrophage activation. Immunobiology 187:227–232

Tokumaru S, Sayama K, Shirakata Y, Komatsuzawa H, Ouhara K, Hanakawa Y, Yahata Y, Dai X, Tohyama M, Nagai H, Yang L, Higashiyama S, Yoshimura A, Sugai M, Hashimoto K (2005)

Induction of keratinocyte migration via transactivation of the epidermal growth factor receptor by the antimicrobial peptide LL-37. J Immunol 175:4662–4668

Uccelletti D, Zanni E, Marcellini L, Palleschi C, Barra D, Mangoni ML (2010) Anti-Pseudomonas activity of frog skin antimicrobial peptides in a *Caenorhabditis elegans* infection model: a plausible mode of action in vitro and in vivo. Antimicrob Agents Chemother 54:3853–3860

Wang YW, Ren JH, Xia K, Wang SH, Yin TF, Xie DH, Li LH (2012) Effect of mitomycin on normal dermal fibroblast and HaCat cell: an in vitro study. J Zhejiang Univ Sci B 13:997–1005

Xiong YQ, Hady WA, Deslandes A, Rey A, Fraisse L, Kristensen HH, Yeaman MR, Bayer AS (2011) Efficacy of NZ2114, a novel plectasin-derived cationic antimicrobial peptide antibiotic, in experimental endocarditis due to methicillin-resistant *Staphylococcus aureus*. Antimicrob Agents Chemother 55:5325–5330

Yeung AT, Gellatly SL, Hancock RE (2011) Multifunctional cationic host defence peptides and their clinical applications. Cell Mol Life Sci 68:2161–2176

RESEARCH ARTICLE

The Frog Skin-Derived Antimicrobial Peptide Esculentin-1a(1-21)NH$_2$ Promotes the Migration of Human HaCaT Keratinocytes in an EGF Receptor-Dependent Manner: A Novel Promoter of Human Skin Wound Healing?

Antonio Di Grazia[1], Floriana Cappiello[1], Akiko Imanishi[2], Arianna Mastrofrancesco[3], Mauro Picardo[3], Ralf Paus[2,4], Maria Luisa Mangoni[1]*

1 Istituto Pasteur-Fondazione Cenci Bolognetti, Department of Biochemical Sciences, Sapienza University of Rome, Rome, Italy, 2 Centre for Dermatology Research, Institute of Inflammation and Repair, University of Manchester, Manchester, United Kingdom, 3 Laboratory of Cutaneous Physiopathology and Integrated Center of Metabolomics Research, San Gallicano Dermatologic Institute, Rome, Italy, 4 Department of Dermatology, University of Münster, Münster, Germany

* marialuisa.mangoni@uniroma1.it

Abstract

One of the many functions of skin is to protect the organism against a wide range of pathogens. Antimicrobial peptides (AMPs) produced by the skin epithelium provide an effective chemical shield against microbial pathogens. However, whereas antibacterial/antifungal activities of AMPs have been extensively characterized, much less is known regarding their wound healing-modulatory properties. By using an *in vitro* re-epithelialisation assay employing special cell-culture inserts, we detected that a derivative of the frog-skin AMP esculentin-1a, named esculentin-1a(1-21)NH$_2$, significantly stimulates migration of immortalized human keratinocytes (HaCaT cells) over a wide range of peptide concentrations (0.025–4 μM), and this notably more efficiently than human cathelicidin (LL-37). This activity is preserved in primary human epidermal keratinocytes. By using appropriate inhibitors and an enzyme-linked immunosorbent assay we found that the peptide-induced cell migration involves activation of the epidermal growth factor receptor and STAT3 protein. These results suggest that esculentin-1a(1-21)NH$_2$ now deserves to be tested in standard wound healing assays as a novel candidate promoter of skin re-epithelialisation. The established ability of esculentin-1a(1-21)NH$_2$ to kill microbes without harming mammalian cells, namely its high anti-*Pseudomonal* activity, makes this AMP a particularly attractive candidate wound healing promoter, especially in the management of chronic, often *Pseudomonas*-infected, skin ulcers.

Introduction

Gene-encoded antimicrobial peptides (AMPs) are produced by all living unicellular and multi-cellular organisms; they serve key roles in innate immune defences and possess a wide spectrum of activities against bacteria, fungi and viruses [1–3]. Despite their enormous structural diversity, most AMPs share a net positive charge at neutral pH, a high content of hydrophobic residues and an amphipathic character [4,5]. In animals, they are predominantly expressed in the skin and the mucosal surfaces (e.g. the mouth, the eyes, the genito-urinary tract and the gut) where they form a chemical barrier between host tissues and the environment [6–8]. In addition, they are also produced by circulating immune cells such as leukocytes [9,10].

The skin is the environmentally most exposed organ and provides first-line defence against penetrating infectious microorganisms. In mammals, including humans, epidermal keratinocytes produce AMPs (e.g., the cathelicidin LL-37 and the beta-defensins hBD2 and hBD3) which are stored along with lipids within secretory granules called lamellar bodies [11–17]. Following skin wounding, infection and inflammation, keratinocyte lamellar bodies release their content of hydrophobic products and AMPs into intercellular spaces forming a chemical barrier against water loss and microbial attack [18–20]. Furthermore, infiltrating immune cells such as neutrophils and natural killer cells also contribute to the pool of AMPs in the skin [21–23].

Apart from their direct antimicrobial activity, mammalian AMPs display additional protective functions which have led to their classification as "host-defence peptides" [24]. These functions include the capability to stimulate the host immune system while suppressing the inflammatory response, as well as the ability to promote tissue repair through stimulation of epithelial cell migration [25–28].

In this respect, frog skin-derived peptides, including AMPs, may be of particular interest [29]. As a stratified squamous epithelium, the epidermis of adult frogs is histologically quite similar to that of humans [30]. Amphibian skin has a tissue repair and a defence system that enables wound healing without scarring [31] and contains a huge arsenal of pharmacological agents, including multiple neuropeptides and AMPs [32]. The AMPs are mainly stored within granules of the dermal glands controlled by the sympathetic nervous system and are secreted in response to stress or physical injury by a holocrine-type mechanism [33–35]. All frog species synthesize a unique set of AMPs, constituting families of 2–100 closely related members [36,37]. Over the past two decades, *in vitro* and *in vivo* experiments have demonstrated that frog-skin AMPs play a crucial role in maintaining the equilibrium of the natural microbial flora and that their synthesis is induced by microorganisms [38–40].

Recently, we have focused on the short variant of the frog-skin AMP esculentin-1a, esculentin-1a(1-21)NH₂ [Esc(1-21), GIFSKLAGKKIKNLLISGLKG-NH₂]. This consists of the first 20 amino acids of esculentin-1a (isolated from the skin of *Pelophylax lessonae/ridibundus*, formerly known as *Rana esculenta*) plus a glycinamide residue at its C-terminus [34,41–43]. This peptide possesses a wide spectrum of antimicrobial activity with demonstrated efficacy against both planktonic and biofilm forms of the Gram-negative bacterium *Pseudomonas aeruginosa*. *P. aeruginosa* is clinically important as a major pathogenic microorganism that causes various types of infections, such as those associated with the lungs, ocular surface, middle ear and skin wounds [44,45]. Mode of action studies have shown that membrane-perturbing activity is the major mechanism responsible for the killing action of Esc(1-21) on both phenotypes of this pathogen, thus limiting the induction of microbial resistance [46]. Resistance to cationic peptides whose mechanism of action is based on non-specific interaction with the anionic phospholipids of the bacterial membrane is considered difficult since it would involve drastic changes of the membrane lipid composition and potentially compromising the pathogen's survival [46]. Note that compared to the extensively studied human skin AMP, LL-37 [47–50], the

frog-skin AMP derived Esc(1-21) peptide may be clinically more attractive, for example due to the ability to preserve antimicrobial activity in biological fluids [51], and to its documented fast killing activity against a major human pathogen associated with chronic skin ulcers, *P. aeruginosa* [46,52]. However, it is as yet unknown whether Esc(1-21) has any wound healing-promoting properties.

As a first screening step towards exploring whether Esc(1-21) peptide is able to promote re-epithelialisation in the human system, we studied its ability to stimulate, *in vitro*, the migratory activity of human immortalized and primary epidermal keratinocytes in a modified scratch assay, and compared the results with those of LL-37. In order to establish whether a stereospecific mechanism based on the interaction with a chiral target was involved, the all-D-enantiomer of Esc(1-21) (containing all amino acid residues in the D configuration) was used. Furthermore, as already found for LL-37 [53], the involvement of the epidermal growth factor receptor (EGFR) and STAT3 protein in the peptide-induced signaling pathway controlling migration of HaCaT cells was also investigated.

Materials and Methods

Materials

Hoechst 33258, 3(4,5-dimethylthiazol-2yl)2,5-diphenyltetrazolium bromide (MTT), AG1478, mitomycin C; phalloidin-fluorescein isothiocyanate, LL-37 were from Sigma-Aldrich (St. Luis, MO); GM6001 was from Calbiochem (Merk Millipore, Germany).

Frog skin peptides

Synthetic all-L and all-D Esc(1-21) peptides as well as the rhodamine-labeled all-L Esc(1-21) were purchased from Selleck Chemicals (Houston, TX, USA). Briefly, each peptide was assembled by step-wise solid-phase synthesis using a standard F-moc strategy and purified by RP-HPLC on a semipreparative C18-bonded silica column (Kromasyl, 5 μm, 100 Å, 25 cm × 4.6 mm) using a gradient of acetonitrile in 0.1% aqueous trifluoroacetic acid (from 25 to 100% in 30 min) at a flow rate of 1.0 ml/min. The product was obtained by lyophilization of the appropriate fraction. Analytical RP-HPLC indicated a purity >98%. The molecular mass was verified by using MALDI-TOF Voyager DE (Applied Biosystems, Carlsbad, CA, USA) as previously described [54].

Cell culture

The extensively characterized human immortalized keratinocyte cell line, HaCaT (ATCC, USA) [55] was used in most assays. Cells were cultured in Dulbecco's modified Eagle's medium (DMEM) supplemented with 10% heat-inactivated fetal bovine serum (FBS), glutamine (4 mM) and 0.05 mg/ml gentamycin, at 37°C and 5% CO$_2$, in 25-cm^2 flasks.

Cultures of primary human epidermal keratinocytes (NHKs), derived from neonatal fore-skins (at passage 4) were maintained in Medium 154 (Invitrogen, Life Sciences, Milan, Italy) supplemented with Human Keratinocyte Growth Supplement (HKGS, Invitrogen) plus antibiotics (100 μg/ml penicillin/streptomycin), 4 mM glutamine and Ca^{2+} (0.07 mM) in a humidified atmosphere containing 5% CO$_2$ at 37°C, as previously described [56]. All treatments were performed in the same medium without HKGS to avoid any interference with the peptide's activity.

Cell toxicity assay

The toxic effect of the investigated peptides on HaCaT cells was evaluated using the MTT colorimetric method [57]. MTT is a tetrazolium salt which is reduced to a formazan product by

mitochondrial reductases giving a purple color. The intensity of the color is directly proportional to the number of metabolically-active cells. Keratinocytes were plated in triplicate wells of a microtiter plate, at 4 x 10^4 cells/well in DMEM supplemented with 4 mM glutamine (DMEMg) and 2% FBS without antibiotic. After overnight incubation at 37°C and 5% CO$_2$ atmosphere, the medium was replaced with 100 µl fresh serum-free DMEMg containing the peptides at different concentrations. The plate was incubated for 2h or 24h at 37°C and 5% CO$_2$ atmosphere. Then, DMEMg was removed and replaced with Hank's buffer (136 mM NaCl; 4.2 mM Na$_2$HPO$_4$; 4.4 mM KH$_2$PO$_4$; 5.4 mM KCl; 4.1 mM NaHCO$_3$, pH 7.2, supplemented with 20 mM D-glucose) containing 0.5 mg/ml MTT. After 4 h incubation, the formazan crystals were dissolved by adding 100 µl of acidified isopropanol according to [57], and absorbance of each well was measured at 570 nm using a microplate reader (Infinite M200; Tecan, Salzburg, Austria).

In vitro cell migration assay

The peptides' ability to stimulate migration of epithelial cells, in vitro, was studied according to a modified scratch assay, as described in [58–60]. Briefly, HaCaT cells (40,000) suspended in DMEMg supplemented with 10% FBS were seeded on each side of an ibidi culture insert for live cell analysis (Ibidi, Munich, Germany). Inserts were placed into wells of a 12-wells plate and incubated at 37°C and 5% CO$_2$ to allow cells grow to confluence. Afterwards, inserts were removed with sterile tweezers to create a cell-free area (pseudo-"wound") of approximately 500 µm, whose re-epithelialisation by migrating HaCaT keratinocytes was quantitatively assessed; 1 ml serum-free DMEMg supplemented or not with the peptide at different concentrations was added. Cells were allowed to migrate in an appropriate incubator.

In the case of NHKs, 35,000 cells suspended in supplemented Medium 154 were seeded on each side of the ibidi culture insert. After overnight incubation at 37°C and 5% CO$_2$ the medium was replaced with fresh medium without HKGS for 6 h. Afterwards, inserts were removed as described above and 1 ml of medium supplemented or not with the peptide at different concentrations was added. Primary keratinocytes were allowed to migrate in an appropriate incubator, as for HaCaT cells. All experiments were run three times in triplicates.

At different time intervals, fields of the pseudo-"wound" area were visualized under an inverted microscope (Olympus CKX41) at x 4 magnification and photographed with a Color View II digital camera. The percentage of cell-covered area at each time was determined by WIMASIS Image Analysis program. The migration speed was evaluated according to WIMASIS' instructions.

Pseudo-"wound" closure assays with HaCaT cells were also conducted by pre-treating these cells with 3 µM mitomycin C [60,61], 25 µM GM6001 [62,63] or 0.2 µM AG1478 inhibitor [53,64] in order to assess the contribution of cell proliferation, metalloproteinase activity or EGFR signaling in the peptide-induced migration of keratinocytes.

Enzyme-linked immunosorbent assay (ELISA)

Phosphorylation of STAT-3 by all-L Esc(1-21) was analyzed by an ELISA assay according to the manufacturer's protocol (Phospho Tyr 705-Stat3 ELISA, RayBiotech, Norcross, GA, USA). Briefly, subconfluent HaCaT keratinocytes (about 1x 10^6 cells in a 6-cm dish plate) were treated or not with 0.25 µM peptide in DMEMg for 20 min. Afterwards, cells were lysed with lysis buffer supplemented with proteases and phosphatases inhibitors. Samples were centrifuged at 12,600 g and the supernatants were added to wells of a microtiter plate coated with anti-STAT3 antibody. After 2.5 h incubation at room temperature, the supernatant was discarded, the wells were washed and biotinylated anti-STAT3 (Tyr 705) antibody was added to each well,

for 1h at room temperature, to detect only phosphorylated STAT3 (Tyr 705). After washing away unbound antibody, horseradish peroxidase conjugated streptavidin was added to each well for 1h. The wells were washed again and a substrate (3,3',5,5'-tetramethylbenzidine) solution was added. Color developed in proportion to the amount of bound phosphorylated STAT3 (Tyr 705). The reaction was stopped after 30 min incubation and the intensity of the color was measured with a microplate reader (Infinite M200; Tecan, Salzburg, Austria) at 450 nm.

Fluorescence microscopy

HaCaT cells (40,000) were seeded on coverslips for 24h in DMEMg supplemented with 10% FBS, at 37°C and 5% CO$_2$. After 24h, cells were washed with phosphate buffered saline (PBS) and treated with rhodamine-labeled Esc(1-21) (4 μM in serum-free DMEMg) at 37°C and 5% CO$_2$. After different time intervals (30 min and 24h), samples were washed with PBS and fixed with 3.7% formaldehyde for 10 min at +4°C. Afterwards, they were washed with PBS and stained with 2 μg/ml Hoechst 33258 for 10 min at room temperature [65]. The coverslips were placed on a glass slide with buffered glycerol and visualized under a fluorescence microscope (Keyence Biozero-8000 Microscope; Keyence Corporation, Osaka, Japan). Hoechst and rhodamine-labeled Esc(1-21) were visualized using laser wavelength of 360 and 560 nm respectively. All images were taken using objective lens of 60X and zoom.

Statistical analyses

Data were collected and pooled from three independent experiments. Quantitative data are expressed as the mean ± SEM. Statistical analysis was performed using Student's *t* test or two-way analysis of variance (ANOVA) with PRISM software (GraphPad, San Diego, CA). Differences were considered to be statistically significant for a p value < 0.05.

Results

Esc(1-21) enantiomers do not exhibit significant toxicity towards HaCaT keratinocytes

In order to assess, first, the toxicity of Esc(1-21) enantiomers, the number of metabolically-active HaCaT cells after a short (2h) and long (24h) treatment interval was studied. Neither peptide showed any marked reduction in the number of metabolically-active keratinocytes after a 2h incubation at concentrations of 2 to 64 μM, and the difference between the two was not statistically significant (Fig 1A). In contrast, after a 24h interval, only the all-L peptide showed slight toxicity at 32 μM and 64 μM (Fig 1B), causing approximately a 20% reduction in the percentage of metabolically-active cells compared to the all-D Esc(1-21) (p<0.001). Note that LL-37 led to complete inhibition of HaCaT cells metabolism at 200 μg/ml (~44 μM) [66]. This shows that only the all-L Esc(1-21) has limited toxicity towards HaCaT cells, but that this is significantly lower than that reported for LL-37 [66].

All-L Esc(1-21), but not its all-D enantiomer, stimulates HaCaT cell migration

To evaluate, next, the ability of different concentrations of both isomers to promote cell migration, an *in vitro* cell migration assay was performed by means of special plastic inserts and a modified scratch assay design [55] to create a 500 μm wide gap within a monolayer of HaCaT cells. The all-L peptide promoted complete coverage of the pseudo-"wound" field in about 9–12h with a bell-shaped dose-response curve (Fig 2A). The optimal concentration allowing
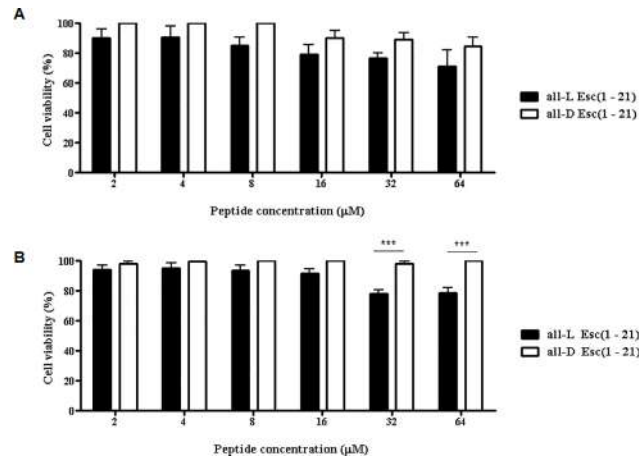
Fig 1. Effect of all-L and all-D Esc(1-21) peptides at different concentrations on the number of metabolically-active HaCaT cells after a short (A) or long (B) term treatment. Cells were plated in wells of a microtiter plate, at 4x10^4 cells/well. After overnight incubation at 37°C in a 5% CO$_2$ atmosphere, the medium was replaced with 100 μl fresh medium supplemented with the peptides at different concentrations. After 2h (A) or 24h (B) of peptide treatment, cell viability was determined by the MTT reduction to insoluble formazan (see Materials and Methods for additional information). Cell viability is expressed as percentage with respect to the vehicle-treated control cells. Data points represent the mean of triplicate samples ± SEM. The level of statistical significance between all-L and all-D peptides is indicated as follows: ***, p<0.001.

doi:10.1371/journal.pone.0128663.g001

gap closure was 0.25 μM (Fig 2A and 2B). In contrast, no statistically significant difference in the cell-covered area was measured between the all-D Esc(1-21)-treated samples and the vehicle (medium)-treated control group (Fig 2B and 2C). That the all-D enantiomer did not significantly promote re-epithelialisation of the pseudo-"wound" area *in vitro* suggests stereospecificity of the mechanism of all-L Esc(1-21)-induced keratinocyte migration.

All-L Esc(1-21) also stimulates "wound" re-epithelialisation by primary human epidermal keratinocytes *in vitro*

As the biological properties of cell lines differ from those of primary cells, the pseudo-"wound" healing activity of all-L Esc(1-21) was also tested on monolayers of primary human epidermal keratinocytes. Importantly, the peptide was found to promote re-epithelialisation of the "wound" gap area within 24h at a concentration range between 4 μM and 10 μM (Fig 3A). The most effective peptide dosage (10 μM) completely restored integrity of the NHK monolayer within 20 h (Fig 3B).

LL-37 stimulates HaCaT cell migration at a narrower concentration range and less efficiently than all-L Esc(1-21)

In order to compare all-L Esc(1-21) with the most extensively investigated human skin AMP, the cells' migratory activity caused by LL-37 was subsequently analyzed (Fig 4A). LL-37 is a well-known human AMP with a demonstrated wound healing effect [67] and ability to promote the migration of several different mammalian cell types, including keratinocytes [68] and corneal epithelial cells [69]. However, LL-37 activities have not previously been evaluated under the present experimental conditions, i.e. using the culture insert scratch assay modification employed here [55].

In agreement with a published report [53], LL-37 was able to stimulate the closure of the pseudo-"wound" field within 12h at an optimal concentration of 0.25 μM (Fig 4A and 4B).
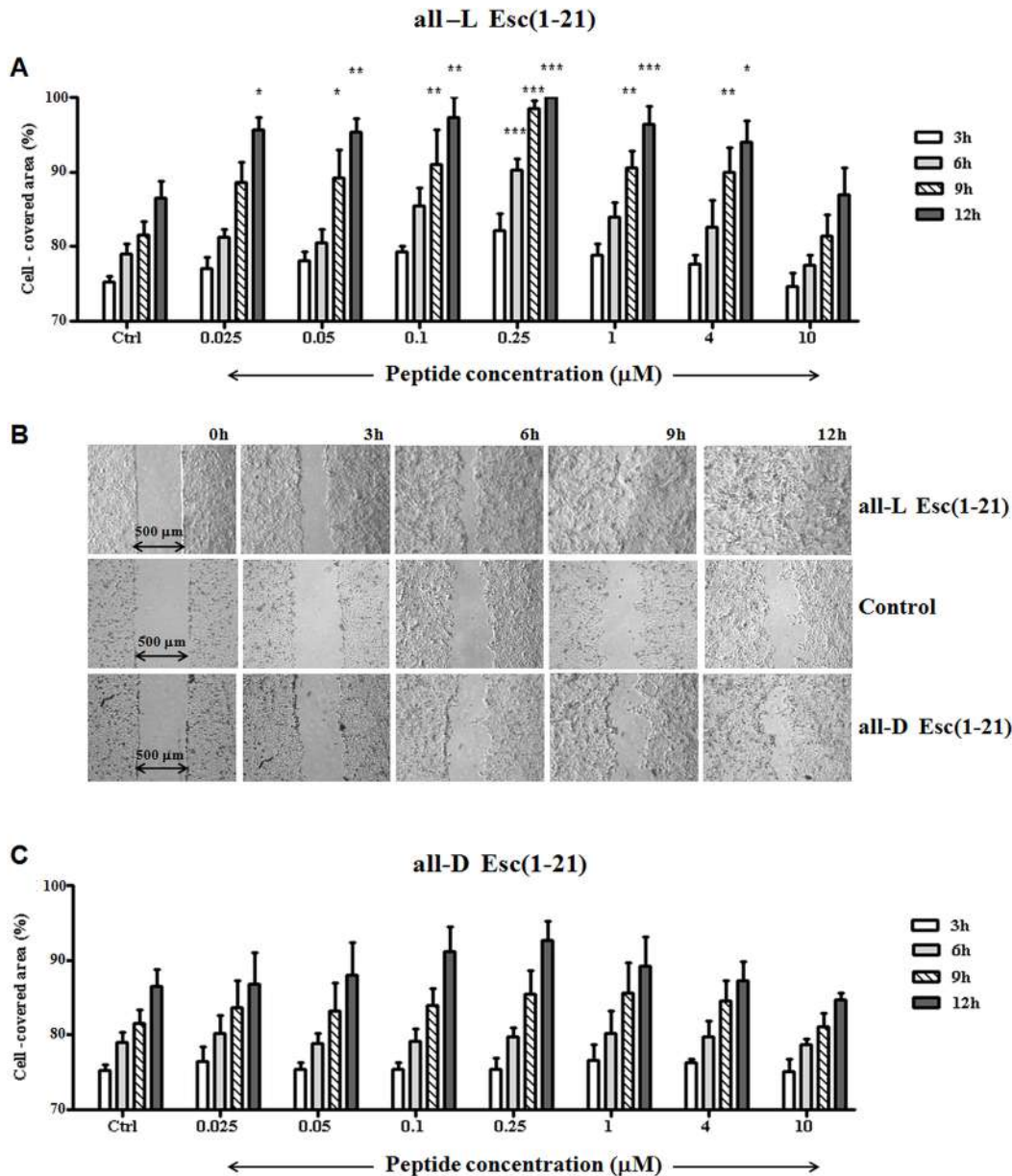
Fig 2. Effect of all-L and all-D Esc(1-21) on the closure of a pseudo-"wound" field produced in a monolayer of HaCaT cells. HaCaT cells were seeded in each side of an ibidi culture insert and grown to confluence. Afterwards, they were treated with all-L (A) or all-D (C) peptide at different concentrations, as indicated. Cells were photographed at the time of insert removal (0 h) and examined for cell migration after 3, 6, 9 and 12h from peptide addition. The percentage of cell-covered area at each time point is reported on the y-axis. Control (Ctrl) is given by vehicle-treated cells. All data are the mean of three independent experiments ± SEM. The levels of statistical significance between Ctrl and peptide-treated samples are indicated as follows: *, $p<0.05$; **, $p<0.01$;***, $p<0.001$. (B): micrographs showing representative results of pseudo-"wound" closure induced upon treatment of keratinocytes with 0.25 μM all-L Esc(1-21) or all-D Esc(1-21) with respect to the Ctrl sample.

doi:10.1371/journal.pone.0128663.g002

Importantly, however, the percentage of the re-epithelialized area calculated at different time intervals following peptide addition was higher for all-L Esc(1-21) (Fig 2A), with a front speed migration equal to 20 μm/h, compared to 17 μm/h estimated for LL-37. No statistically significant difference was obtained between vehicle-treated samples and those incubated with LL-37 at concentrations lower than 0.25 μM (Fig 4A). Furthermore, the cell migration activity was completely inhibited by LL-37 at concentrations of 1 μM and above (Fig 4B). Therefore, under
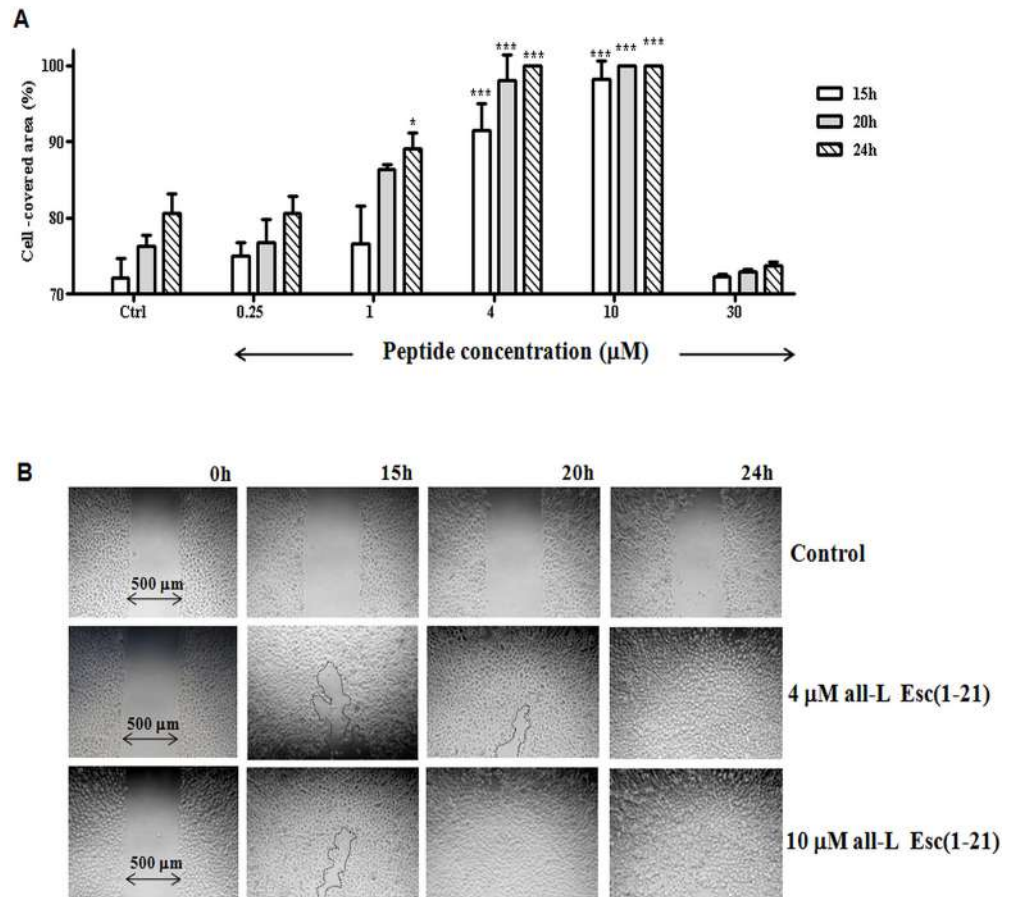
Fig 3. Effect of all-L Esc(1-21) on the closure of a pseudo-"wound" field produced in a monolayer of primary human keratinocytes. (A): two monolayers of primary keratinocytes separated by a defined distance were treated with the peptide at different concentrations, as indicated. Cells were photographed at the time of insert removal (0 h) and examined for cell migration after 15, 20 and 24h from peptide addition. The percentage of cell-covered area at each time point is reported on the y-axis. Control (Ctrl) is given by vehicle-treated cells. All data are the mean of three independent experiments ± SEM. The levels of statistical significance between Ctrl and peptide-treated samples are indicated as follows: *, p<0.5; ***, p<0.001. (B): micrographs showing representative results upon treatment of primary keratinocytes with all-L Esc(1-21) (4 μM and 10 μM) with respect to the Ctrl sample. The black line marks off the cell-free area in the peptide-treated samples after 15 and 20 h. No cell-free area was noted in samples treated with 10 μM peptide after 20 and 24h.

doi:10.1371/journal.pone.0128663.g003

the current assay conditions, LL-37 is less efficient than all-L Esc(1-21) in promoting migration of HaCaT cells *in vitro* and exhibits a narrower "therapeutic" window.

All-L Esc(1-21) primarily promotes keratinocyte migration *in vitro*

Next, we examined potential mechanisms that may underlie the re-epithelialisation-promoting properties of all-L Esc(1-21). In order to abrogate cell proliferation, HaCaT cells were pre-treated with the cell proliferation blocker, mitomycin C. As shown in Fig 5, this did not significantly delay re-epithelialisation of the pseudo-"wound" area in monolayer culture produced by either 0.25 μM all-L Esc(1-21) or LL-37, within 12h. When the activity of mitomycin C was checked independently, it was noted that this treatment switched the morphology of HaCaT cells to a round cell shape, a recognized stop signal for keratinocyte cell division [70], without influencing their viability (data not shown).
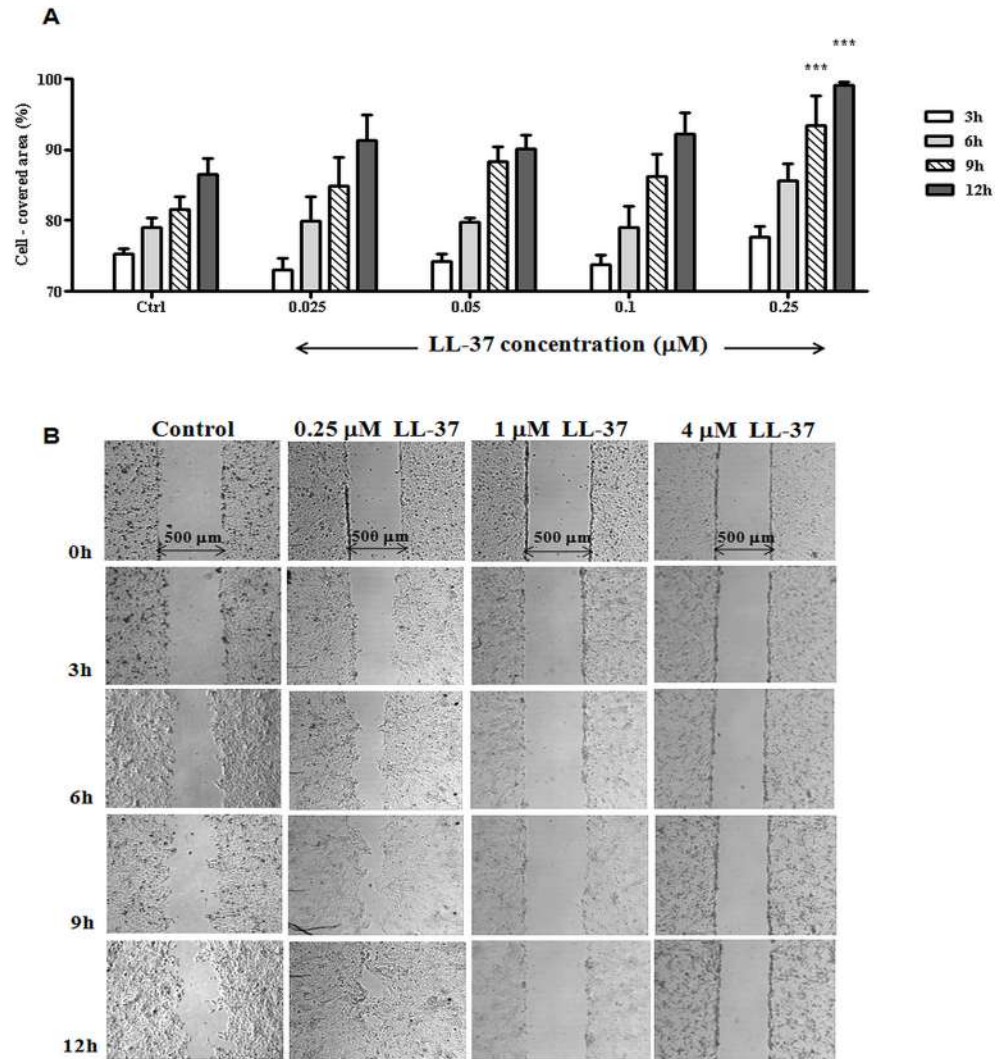
Fig 4. Effect of LL-37 on the closure of a pseudo-"wound" field produced in a monolayer of HaCaT cells. (A): two monolayers of HaCaT cells separated by a defined distance were treated with LL-37 at different concentrations, as indicated. Cells were photographed at the time of insert removal (0 h) and examined for cell migration after 3, 6, 9 and 12h from peptide addition. The percentage of cell-covered area at each time point is reported on the y-axis. Control (Ctrl) is given by vehicle-treated cells. All data are the mean of three independent experiments ± SEM. The level of statistical significance between Ctrl and peptide-treated samples is indicated as follows: ***, $p<0.001$. (B): micrographs showing representative results upon treatment of keratinocytes with LL-37 (0.25 μ M, 1 μ M and 4 μ M) with respect to the Ctrl sample.

doi:10.1371/journal.pone.0128663.g004

Furthermore, compared to vehicle-treated HaCaT cells (Fig 6A), typical morphological changes associated with a migratory phenotype [71,72] were detected in HaCaT cells upon treatment with all-L Esc(1-21). Notably, these became visible through the formation of cytoplasmic protrusions developing into filopodial extensions (Fig 6B), quite similar to the phenotypic effects that have been reported for LL-37 [68]. Overall, these observations suggest that the re-epithelialisation-promoting properties of all-L Esc(1-21) primarily result from its ability to stimulate keratinocyte migration, rather than keratinocyte proliferation.
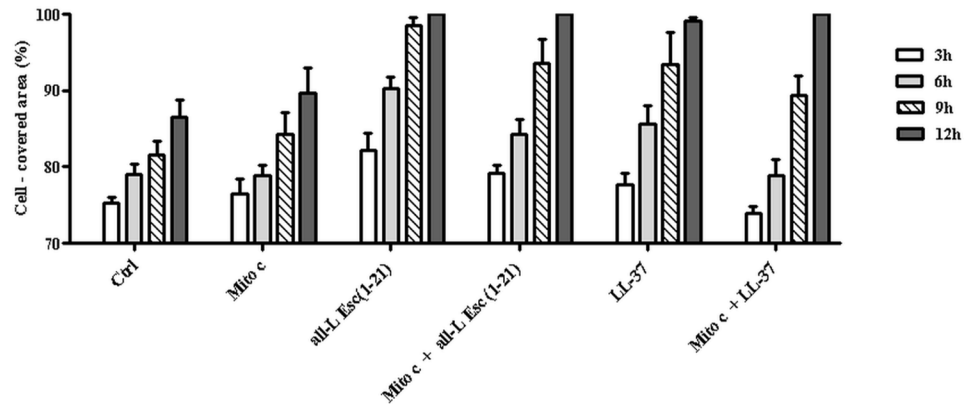
Fig 5. Effect of mitomycin C (Mito) on the peptides-mediated closure of a pseudo-"wound" field produced in a HaCaT cells monolayer. (A) After removal of the ibidi culture insert, HaCaT cell monolayers were pre-incubated or not with 3 µM Mito for 30 min and subsequently treated with 0.25 µM all-L Esc(1-21) or LL-37. Cells incubated with medium served as control (Ctrl). Samples were photographed at different time intervals, as indicated in the legends to Figs 2 and 4, and the percentage of cell-covered area was calculated and reported on the y-axis. All data are the mean of three independent experiments ± SEM. No statistical significance was found between samples treated with the peptide alone or pre-incubated with Mito.
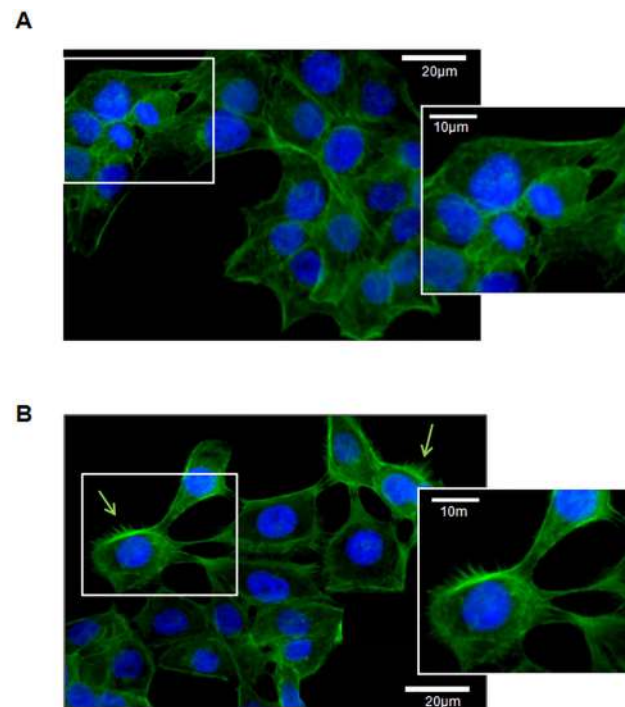
Fig 6. Effect of all-L Esc(1-21) on the phenotype of HaCaT cells. Cells (150,000) were seeded on a glass coverslip and treated or not with 0.25 µM peptide in DMEMg for 12h at 37°C and 5% CO$_2$. Afterwards, samples were washed three times with PBS and fixed with 3.7% formaldehyde for 10 min at +4°C. Then, they were permeabilized with 0.1% Triton X-100 for 10 min at room temperature and stained with phalloidin-fluorescein isothiocyanate (40 µM in PBS) for 30 min at room temperature, to visualize the cytoskeleton. The nuclei were stained by adding 50 µl of Hoechst 33258 (2 µg/ml) for 10 min at room temperature. The coverslips were mounted on slides and observed under a fluorescent microscope (KOZO OPTICS XJF800) at 40 x magnification and photographed with a Color View II digital camera. (A): vehicle-treated control cells; (B) peptide-treated cells. Insets represent the magnification of the image portion indicated by the white frame. rows indicate filopodial formation.
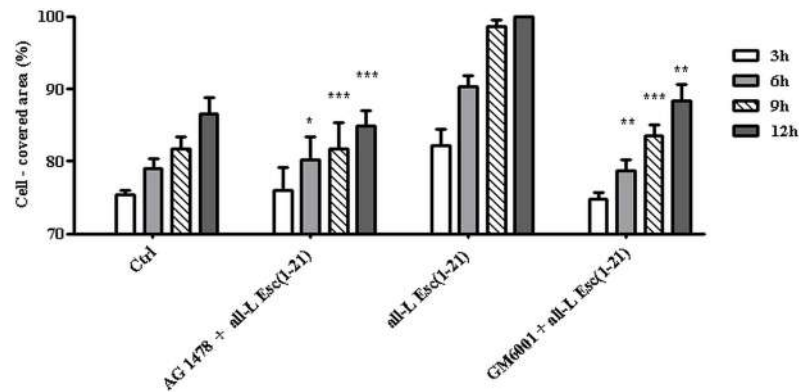
Fig 7. Effect of AG1478 and GM6001 inhibitors on the all-L Esc(1-21)-mediated closure of a pseudo-"wound" field produced in a HaCaT cells monolayer. After removal of the ibidi culture insert, HaCaT cell monolayers were pre-incubated with 0.2 µM AG1478 for 15 min or with 25 µM GM6001 for 30 min and subsequently treated with 0.25 µM all-L Esc(1-21). Cells incubated with medium served as control (Ctrl). Samples were photographed at different time intervals, as indicated in the legend to Fig 2, and the percentage of cell-covered area was calculated and reported on the y-axis. All data are the mean of three independent experiments ± SEM. The levels of statistical significance between inhibitor-pretreated groups and samples treated with the peptide alone are indicated as follows:*, p<0.05; **, p< 0.01; ***, p< 0.001.

doi:10.1371/journal.pone.0128663.g007

All-L Esc(1-21) stimulates migration of HaCaT keratinocytes in a EGFR-dependent manner

To explore whether EGFR played a similar role in the signaling transduction cascade controlling the Esc(1-21)-stimulated migration of cells as it had been reported for LL-37 [53], HaCaT cells were pre-incubated with the tyrosine kinase inhibitor of EGFR, AG1478 [64], and were subsequently exposed to the all-L enantiomer. As illustrated in Fig 7, the peptide-promoted migration of HaCaT cells was significantly impaired by inhibiting EGFR-mediated signaling, suggesting that Esc(1-21)-stimulated re-epithelialisation requires EGFR activation.

Since metalloproteinases have been shown to cleave membrane-anchored EGFR ligands and to be involved in EGFR trans-activation [73], the effect of the metalloproteinase inhibitor GM6001 [62,63] was evaluated on the peptide-induced keratinocyte migration. Pretreatment of HaCaT cells with GM6001 indeed counteracted the Esc(1-21)-stimulated re-epithelialisation of the pseudo-"wound" area in keratinocyte monolayer (Fig 7) indicating a contribution of metalloproteinase activity in the peptide-induced stimulation of keratinocytes migration.

Hereafter, we determined whether the intracellular pathway involving the activation of STAT3 protein that has previously been demonstrated for LL-37 [53], is also implicated in Esc(1-21)-stimulated re-epithelialisation. To this end, an ELISA assay was performed to assess the level of STAT3 phosphorylation at Tyr 705 (active form) [74], after a 20 min incubation of HaCaT cells with the maximally effective concentration of all-L Esc(1-21) (0.25 µM). Keratinocytes treated with 0.25 µM LL-37 were included as a positive control.

This showed that the amount of phospho-STAT3(Tyr 705) was significantly higher in Esc(1-21)-treated cells compared to vehicle-treated controls (p< 0.001) and similar to that induced by LL-37 (Fig 8). This indicates that Esc(1-21)-promoted HaCaT cell migration, again similar to LL-37 [53], also involves STAT3 phosphorylation.

All-L Esc(1-21) efficiently penetrates into the cytoplasm of HaCaT cells

As this may affect the biological activities of this AMP *in vivo*, we finally investigated whether Esc(1-21) remains localized on the surface of cultured keratinocytes or is internalized into the
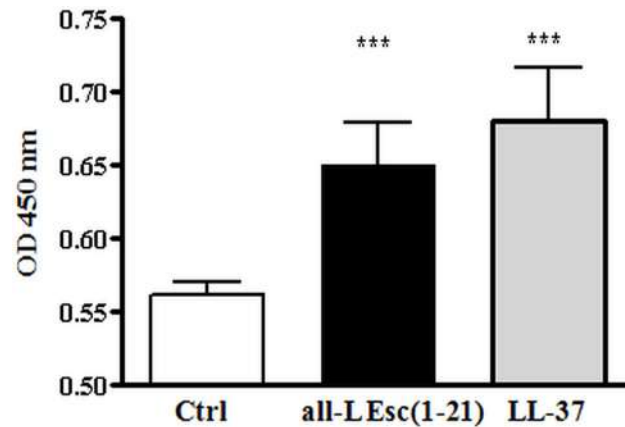
Fig 8. Phosphorylation of STAT3 by all-L Esc(1-21). About 1 x 10⁶ keratinocytes were stimulated with 0.25 µM all-L Esc(1-21) or LL-37 for 20 min. Control (Ctrl) was given by vehicle-treated cells. Cells were harvested into lysis buffer and phospho-STAT3 (Tyr 705) was evaluated by performing an ELISA assay (see Materials and methods). All data are the mean of three independent experiments ± SEM. The level of statistical significance between peptide-treated samples and Ctrl is indicated as follows: ***, $p < 0.001$.

cytoplasm or nucleus. HaCaT cells were exposed to rhodamine-labeled Esc(1-21) and stained with Hoechst 33258 dye so as to permit the differential visualization of the AMP and cell nuclei, respectively, by fluorescence microscopy. This revealed that the fluorescently labelled peptide was distributed inside the HaCaT cells and concentrated mainly at the nuclear periphery within 30 min after administration to the culture medium (Fig 9 left panels), without entering into the nucleus even 24h after its addition to the cells (Fig 9 right panels). Similar results were obtained with another class of amphibian skin AMPs, i.e. the temporins [55], suggesting that after membrane binding and indirect activation of EGFR, Esc(1-21) and likely other frog skin linear peptides are internalized into the keratinocyte cytoplasm.

Discussion

Here, we provide the first evidence that a peptide fragment derived from the frog-skin AMP esculentin-1a, esculentin-1a(1-21)NH₂, promotes the re-epithelialisation of surrogate scratch "wounds" by human keratinocytes *in vitro*, notably both in HaCaT cells and in primary epidermal keratinocytes, and this more effectively and at much lower cell toxicity than the prototypic human skin AMP, LL-37. Importantly, migration of HaCaT cells upon addition of Esc(1-21) occurs over a wider peptide concentration range (from 0.025 to 4 µM) compared to LL-37 which completely loses activity at 1 and 4 µM (Fig 4). Furthermore, although 0.25 µM is the optimal concentration for both AMPs, the cell migration rate induced by Esc(1-21) is higher than that of LL-37.

This introduces Esc(1-21) as a new candidate wound healing promoter. Our study is in general agreement with earlier reports that other frog skin-derived peptides can promote epithelial cells migration [29,55] and wound healing in murine models, namely through the release of transforming growth factor β1 [75]. However, the current study is the first to show that an esculentin-1a-derived peptide promotes keratinocyte migration via an EGFR-dependent signaling pathway.

Mechanistically, we show that the re-epithelialisation promoted by Esc(1-21) is stereospecific, possibly based on a stereoselective interaction with chiral targets, such as proteins [25,76]. Importantly, cell proliferation does not significantly contribute to the re-epithelialisation-promoting effect of Esc(1-21), which appears to be mainly dependent on the stimulation of
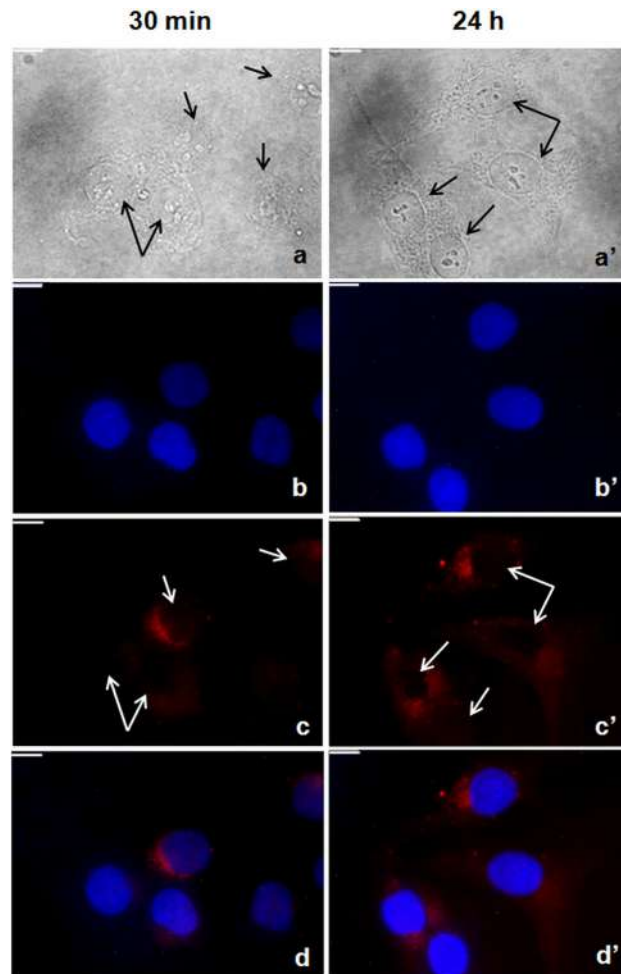
Fig 9. Images of HaCaT cells treated with rhodamine-labeled all-L Esc(1-21) at different times (30 min and 24h). Panels A and A' show bright field images. Black arrows indicate keratinocytes. B and B' show the Hoechst fluorescence signal which indicates the nuclei position. Panels C and C' show the distribution of the rhodamine-labeled Esc(1-21). Red fluorescence is not detectable at the level of nuclei (white arrows), but rather in the cytoplasm and mainly concentrated at the nuclei periphery, already after a short incubation time (C). Panels D and D' show the overlay of the two fluorescent probes. All images are z section images taken from the mid-cell height. All bars indicate 10 µm.

doi:10.1371/journal.pone.0128663.g009

keratinocyte migration. As previously shown for LL-37 [53], the promotion of keratinocyte migration by Esc(1-21) requires activation of an EGFR signaling pathway. Note that erbB4 receptor (another member of the EGFR family), whose activation can be hampered by the EGFR inhibitor employed here (AG1478) [77–79], is not expressed in human keratinocytes and HaCaT cells [80,81]. Our *in vitro* assays have also indicated a contribution of metalloproteinase activity in the Esc(1-21)-induced migration of keratinocytes. This raises the question whether the re-epithelialisation-promoting activities of this AMP require cleavage of membrane-bound EGFR ligands and/or receptor trans-activation by metalloproteinases.

Furthermore, one of the signaling events implicates tyrosine phosphorylation and activation of STAT3 protein [82]. This is in line with the previous demonstration that EGFR-induced cell migration is mediated predominantly by the STAT-pathway in keratinocytes and that STAT3 plays an essential role for skin remodeling and wound healing [82,83].

Yet, multiple additional molecular mechanisms might participate in the enhanced migration of keratinocytes after exposure to Esc(1-21), such as the PI3K/Akt signaling pathway, likely mediated not only through activation of EGFR but also through the induction of G-protein-coupled receptor FPRL-1 [68]. Therefore, additional experiments are needed to clarify the exact intracellular signaling events that govern Esc(1-21)-promoted keratinocyte migration. In this context, it is interesting to note that our data also show that Esc(1-21) quickly translocates into the cytoplasm via yet to be discovered mechanisms, possibly upon interaction with the cell membrane and activation of EGFR; this may trigger further signaling pathways controlling keratinocyte migration and efficient re-epithelialisation. However, it can currently not be excluded that this peptide is also capable of integrating into the cell membrane (without causing cytotoxicity) and to subsequently enter into the cytosol, or that it can be internalized via endocytosis.

The current work also encourages one to re-evaluate the potential overall benefits of frog skin-derived AMPs in clinical medicine [28]. Skin secretions from many species of Anura (frogs and toads), especially those belonging to the Hylidae and Ranidae family, are among the most abundant sources for biologically-active peptides, including AMPs, presently numbering more than a thousand [84]. Esc(1-21) in particular has been recently identified as a derivative of the longer peptide esculentin-1a, with clinically attractive features for a potential new therapeutic agent. Remarkably, Esc(1-21) has the capability to preserve antibacterial activity even at high salt concentrations [46] as well as in the presence of serum and tears [51]. This is in sharp contrast to the properties of the key human AMPs, hBD-2 and LL-37, which completely lose their antimicrobial efficacy at the high ionic strength (e.g., 100 mM monovalent cations) found at many body sites [85], such as the sputum, airway surfaces and serum/plasma [86–90]. Furthermore, their antimicrobial activity is drastically reduced in biological fluids [91].

Although these mammalian AMPs certainly function as powerful microbicidal agents at the high concentration (mg/ml) present in the phagolysosomes of neutrophils, they probably act as immunomodulators at those physiological setting e.g. inflammatory sites, generally containing high levels of mono and bivalent cations, where they are released by degranulation at lower concentrations [47,90]. This would explain the lack of antibacterial activity of these AMPs when tested, *in vitro*, under conditions (i.e. peptide concentrations and culture media) that better mimic those encountered in their natural environment [88,91–94]. In contrast, the estimated concentration of peptides in the skin mucus of resting (non-stressed) frogs is within the concentration range that shows antimicrobial activity in *vitro* [95], supporting the notion that AMPs produced in amphibian skin provide remarkable chemical weapons against skin pathogens [96]. This may be especially important for newly metamorphosed frogs in which the adaptive immune system is still immature [35,97]. Another advantageous feature of Esc(1-21) compared to classical mammalian AMPs is that, given its short sequence, it may be possible to produce this AMP more economically. Finally, we should recall that Esc(1-21) is significantly less cytotoxic than LL-37 toward HaCaT cells, in agreement with literature data showing that human cathelicidins become harmful to mammalian cells, when used at high concentrations [98].

Given the complexity of the recognized individual stages of skin wound healing *in vivo* [99], it is evident that even the re-epithelialisation component of skin wound healing alone can be very incompletely reproduced *in vitro*, i.e. in the absence of fibroblasts, immunocytes, and functional perfusion and innervation. Therefore, the current results need to be followed-up, next, at the preclinical research level in more complex human skin assays, using for example the punch-in-a-punch design of organ-cultured full-thickness human skin [29]. However, the ibidi culture insert system used here [55] provides an objective and highly reproducible initial experimental screening tool for the quantitative evaluation of human keratinocyte migration and its manipulation by candidate wound healing promoters. This simplified *in vitro*-surrogate

assay for re-epithelialisation may be preferable over the classical scratch assay method, where the gap width created with a plastic pipette tip is highly dependent on the pressure applied and where detached cells can easily form clumps at the edges of the scratch, affecting the rate of cell migration, thus giving potentially confounding results.

In summary, here we provide the first evidence that Esc(1-21) significantly and more effectively than LL-37 stimulates human keratinocyte migration in an *in vitro* assay, likely in manner that involves activation of EGFR and STAT3 protein. The established ability of Esc(1-21) to kill microbes without harming mammalian cells, namely its high anti-*Pseudomonal* activity also in physiologically relevant conditions [46,51] makes this short-sized AMP a particularly attractive candidate wound healing promoter, especially in the management of chronic, often *Pseudomonas*-super-infected, human skin ulcers [52,100].

Acknowledgments

Author Contributions

Conceived and designed the experiments: MLM ADG. Performed the experiments: ADG FC AI AM. Analyzed the data: ADG MLM. Contributed reagents/materials/analysis tools: MLM MP RP. Wrote the paper: MLM RP.

References

1. Hancock RE, Diamond G (2000) The role of cationic antimicrobial peptides in innate host defences. Trends Microbiol 8: 402–410. PMID: 10989307

2. Zasloff M (2002) Antimicrobial peptides of multicellular organisms. Nature 415: 389–395. PMID: 11807545

3. Mangoni ML (2011) Host-defense peptides: from biology to therapeutic strategies. Cell Mol Life Sci 68: 2157–2159. doi: 10.1007/s00018-011-0709-3 PMID: 21584810

4. Powers JP, Hancock RE (2003) The relationship between peptide structure and antibacterial activity. Peptides 24: 1681–1691. PMID: 15019199

5. Wang G, Li X, Wang Z (2009) APD2: the updated antimicrobial peptide database and its application in peptide design. Nucleic Acids Res 37: D933–937. doi: 10.1093/nar/gkn823 PMID: 18957441

6. Harder J, Schroder JM (2005) Antimicrobial peptides in human skin. Chem Immunol Allergy 86: 22–41. PMID: 15976486

7. Glaser R, Becker K, von Eiff C, Meyer-Hoffert U, Harder J (2014) Decreased susceptibility of *Staphylococcus aureus* small-colony variants toward human antimicrobial peptides. J Invest Dermatol 134: 2347–2350. doi: 10.1038/jid.2014.176 PMID: 24717245

8. Firat YH, Simanski M, Rademacher F, Schroder L, Brasch J, Harder J (2014) Infection of keratinocytes with *Trichophytum rubrum* induces epidermal growth factor-dependent RNase 7 and human beta-defensin-3 expression. PLoS One 9: e93941. doi: 10.1371/journal.pone.0093941 PMID: 24747887

9. Ganz T, Selsted ME, Szklarek D, Harwig SS, Daher K, Bainton DF, et al. (1985) Defensins. Natural peptide antibiotics of human neutrophils. J Clin Invest 76: 1427–1435. PMID: 2997278

10. Ganz T (2003) Defensins: antimicrobial peptides of innate immunity. Nat Rev Immunol 3: 710–720. PMID: 12949495

11. Ishikawa T, Kanda N, Hau CS, Tada Y, Watanabe S (2009) Histamine induces human beta-defensin-3 production in human keratinocytes. J Dermatol Sci 56: 121–127. doi: 10.1016/j.jdermsci.2009.07.012 PMID: 19734018

12. Feingold KR (2012) Lamellar bodies: the key to cutaneous barrier function. J Invest Dermatol 132: 1951–1953. doi: 10.1038/jid.2012.177 PMID: 22797297

13. Percoco G, Merle C, Jaouen T, Ramdani Y, Benard M, Hillion M, et al. (2013) Antimicrobial peptides and pro-inflammatory cytokines are differentially regulated across epidermal layers following bacterial stimuli. Exp Dermatol 22: 800–806. doi: 10.1111/exd.12259 PMID: 24118337

14. Wittersheim M, Cordes J, Meyer-Hoffert U, Harder J, Hedderich J, Glaser R (2013) Differential expression and in vivo secretion of the antimicrobial peptides psoriasin (S100A7), RNase 7, human beta-defensin-2 and -3 in healthy human skin. Exp Dermatol 22: 364–366. doi: 10.1111/exd.12133 PMID: 23614747

15. Gallo RL (2013) The birth of innate immunity. Exp Dermatol 22: 517. doi: 10.1111/exd.12197 PMID: 23879811

16. Do N, Weindl G, Grohmann L, Salwiczek M, Koksch B, Korting HC, et al. (2014) Cationic membrane-active peptides—anticancer and antifungal activity as well as penetration into human skin. Exp Dermatol 23: 326–331. doi: 10.1111/exd.12384 PMID: 24661024

17. Simanski M, Glaser R, Harder J (2014) Human skin engages different epidermal layers to provide distinct innate defense mechanisms. Exp Dermatol 23: 230–231. doi: 10.1111/exd.12365 PMID: 24612034

18. Braff MH, Zaiou M, Fierer J, Nizet V, Gallo RL (2005) Keratinocyte production of cathelicidin provides direct activity against bacterial skin pathogens. Infect Immun 73: 6771–6781. PMID: 16177355

19. Braff MH, Di Nardo A, Gallo RL (2005) Keratinocytes store the antimicrobial peptide cathelicidin in lamellar bodies. J Invest Dermatol 124: 394–400. PMID: 15675959

20. Aberg KM, Man MQ, Gallo RL, Ganz T, Crumrine D, Brown BE, et al. (2008) Co-regulation and interdependence of the mammalian epidermal permeability and antimicrobial barriers. J Invest Dermatol 128: 917–925. PMID: 17943185

21. Gudmundsson GH, Agerberth B (1999) Neutrophil antibacterial peptides, multifunctional effector molecules in the mammalian immune system. J Immunol Methods 232: 45–54. PMID: 10618508

22. Agerberth B, Charo J, Werr J, Olsson B, Idali F, Lindbom L, et al. (2000) The human antimicrobial and chemotactic peptides LL-37 and alpha-defensins are expressed by specific lymphocyte and monocyte populations. Blood 96: 3086–3093. PMID: 11049988

23. Di Nardo A, Vitiello A, Gallo RL (2003) Cutting edge: mast cell antimicrobial activity is mediated by expression of cathelicidin antimicrobial peptide. J Immunol 170: 2274–2278. PMID: 12594247

24. Yeung AT, Gellatly SL, Hancock RE (2011) Multifunctional cationic host defence peptides and their clinical applications. Cell Mol Life Sci 68: 2161–2176. doi: 10.1007/s00018-011-0710-x PMID: 21573784

25. Oudhoff MJ, Bolscher JG, Nazmi K, Kalay H, van 't Hof W, Amerongen AV, et al. (2008) Histatins are the major wound-closure stimulating factors in human saliva as identified in a cell culture assay. FASEB J 22: 3805–3812. doi: 10.1096/fj.08-112003 PMID: 18650243

26. Semple F, Dorin JR (2012) beta-Defensins: multifunctional modulators of infection, inflammation and more? J Innate Immun 4: 337–348. doi: 10.1159/000336619 PMID: 22441423

27. Haney EF, Hancock RB (2013) Peptide design for antimicrobial and immunomodulatory applications. Biopolymers. 100: 572–583. doi: 10.1002/bip.22250 PMID: 23553602

28. Mansour SC, Pena OM, Hancock RE (2014) Host defense peptides: front-line immunomodulators. Trends Immunol 35: 443–450. doi: 10.1016/j.it.2014.07.004 PMID: 25113635

29. Meier NT, Haslam IS, Pattwell DM, Zhang GY, Emelianov V, Paredes R, et al. (2013) Thyrotropin-releasing hormone (TRH) promotes wound re-epithelialisation in frog and human skin. PLoS One 8: e73596. doi: 10.1371/journal.pone.0073596 PMID: 24023889

30. Haslam IS, Roubos EW, Mangoni ML, Yoshizato K, Vaudry H, Kloepper JE, et al. (2014) From frog integument to human skin: dermatological perspectives from frog skin biology. Biol Rev Camb Philos Soc 89: 618–655. doi: 10.1111/brv.12072 PMID: 24299058

31. Zasloff M (1987) Magainins, a class of antimicrobial peptides from Xenopus skin: isolation, characterization of two active forms, and partial cDNA sequence of a precursor. Proc Natl Acad Sci USA 84: 5449–5453. PMID: 3299384

32. Erspamer V (1994) Bioactive secretions of the amphibian integument. Heatwole H (Ed) Amphibian Biology, Surray Beatty and Sons, Chipping Northon 1: 395–414.

33. Mangoni ML (2006) Temporins, anti-infective peptides with expanding properties. Cell Mol Life Sci 63: 1060–1069. PMID: 16572270

34. Conlon JM, Iwamuro S, King JD (2009) Dermal cytolytic peptides and the system of innate immunity in anurans. Ann NY Acad Sci 1163: 75–82. doi: 10.1111/j.1749-6632.2008.03618.x PMID: 19456329

35. Pask JD, Cary TL, Rollins-Smith LA (2013) Skin peptides protect juvenile leopard frogs (*Rana pipiens*) against chytridiomycosis. J Exp Biol 216: 2908–2916. doi: 10.1242/jeb.084145 PMID: 23580715

36. Conlon JM, Kolodziejek J, Nowotny N (2009) Antimicrobial peptides from the skins of North American frogs. Biochim Biophys Acta 1788: 1556–1563. doi: 10.1016/j.bbamem.2008.09.018 PMID: 18983817

37. Mangoni ML, Shai Y (2009) Temporins and their synergism against Gram-negative bacteria and in lipopolysaccharide detoxification. Biochim Biophys Acta 1788: 1610–1619. doi: 10.1016/j.bbamem.2009.04.021 PMID: 19422786

38. Simmaco M, Mangoni ML, Boman A, Barra D, Boman HG (1998) Experimental infections of *Rana esculenta* with *Aeromonas hydrophila*: a molecular mechanism for the control of the normal flora. Scand J Immunol 48: 357–363. PMID: 9790305

39. Simmaco M, Mignogna G, Barra D (1998) Antimicrobial peptides from amphibian skin: what do they tell us? Biopolymers 47: 435–450. PMID: 10333736

40. Mangoni ML, Miele R, Renda TG, Barra D, Simmaco M (2001) The synthesis of antimicrobial peptides in the skin of *Rana esculenta* is stimulated by microorganisms. FASEB J 15: 1431–1432. PMID: 11387247

41. Simmaco M, Mignogna G, Barra D, Bossa F (1994) Antimicrobial peptides from skin secretions of *Rana esculenta*. Molecular cloning of cDNAs encoding esculentin and brevinins and isolation of new active peptides. J Biol Chem 269: 11956–11961. PMID: 8163497

42. Islas-Rodriguez AE, Marcellini L, Orioni B, Barra D, Stella L, Mangoni ML (2009) Esculentin 1–21: a linear antimicrobial peptide from frog skin with inhibitory effect on bovine mastitis-causing bacteria. J Pept Sci 15: 607–614. doi: 10.1002/psc.1148 PMID: 19507197

43. Uccelletti D, Zanni E, Marcellini L, Palleschi C, Barra D, Mangoni ML (2010) Anti-Pseudomonas activity of frog skin antimicrobial peptides in a *Caenorhabditis elegans* infection model: a plausible mode of action in vitro and in vivo. Antimicrob Agents Chemother 54: 3853–3860. doi: 10.1128/AAC.00154-10 PMID: 20606068

44. Bodey GP, Bolivar R, Fainstein V, Jadeja L (1983) Infections caused by *Pseudomonas aeruginosa*. Rev Infect Dis 5: 279–313. PMID: 6405475

45. Gellatly SL, Hancock RE (2013) *Pseudomonas aeruginosa*: new insights into pathogenesis and host defenses. Pathog Dis 67: 159–173. doi: 10.1111/2049-632X.12033 PMID: 23620179

46. Luca V, Stringaro A, Colone M, Pini A, Mangoni ML (2013) Esculentin(1-21), an amphibian skin membrane-active peptide with potent activity on both planktonic and biofilm cells of the bacterial pathogen *Pseudomonas aeruginosa*. Cell Mol Life Sci 70: 2773–2786. doi: 10.1007/s00018-013-1291-7 PMID: 23503622

47. Bowdish DM, Davidson DJ, Lau YE, Lee K, Scott MG, Hancock RE (2005) Impact of LL-37 on anti-infective immunity. J Leukoc Biol 77: 451–459. PMID: 15569695

48. Schroder JM (2010) The role of keratinocytes in defense against infection. Curr Opin Infect Dis 23: 106–110. doi: 10.1097/QCO.0b013e328335b004 PMID: 20010101

49. Morizane S, Gallo RL (2012) Antimicrobial peptides in the pathogenesis of psoriasis. J Dermatol 39: 225–230. doi: 10.1111/j.1346-8138.2011.01483.x PMID: 22352846

50. Salzer S, Kresse S, Hirai Y, Koglin S, Reinholz M, Ruzicka T, et al. (2014) Cathelicidin peptide LL-37 increases UVB-triggered inflammasome activation: possible implications for rosacea. J Dermatol Sci 76: 173–179. doi: 10.1016/j.jdermsci.2014.09.002 PMID: 25306296

51. Kolar SS, Luca V, Baidouri H, Mannino G, McDermott AM, Mangoni ML (2015) Esculentin-1a(1-21)NH: a frog skin-derived peptide for microbial keratitis. Cell Mol Life Sci. 72: 617–627 doi: 10.1007/s00018-014-1694-0 PMID: 25086859

52. Wolcott RD, Dowd SE (2008) A rapid molecular method for characterising bacterial bioburden in chronic wounds. J Wound Care 17: 513–516. PMID: 19052515

53. Tokumaru S, Sayama K, Shirakata Y, Komatsuzawa H, Ouhara K, Hanakawa Y, et al. (2005) Induction of keratinocyte migration via transactivation of the epidermal growth factor receptor by the antimicrobial peptide LL-37. J Immunol 175: 4662–4668. PMID: 16177113

54. Mangoni ML, Fiocco D, Mignogna G, Barra D, Simmaco M (2003) Functional characterisation of the 1–18 fragment of esculentin-1b, an antimicrobial peptide from *Rana esculenta*. Peptides 24: 1771–1777. PMID: 15019209

55. Di Grazia A, Luca V, Segev-Zarko LA, Shai Y, Mangoni ML (2014) Temporins A and B stimulate migration of HaCaT keratinocytes and kill intracellular *Staphylococcus aureus*. Antimicrob Agents Chemother 58: 2520–2527. doi: 10.1128/AAC.02801-13 PMID: 24514087

56. Mastrofrancesco A, Ottaviani M, Aspite N, Cardinali G, Izzo E, Graupe K, et al. (2010) Azelaic acid modulates the inflammatory response in normal human keratinocytes through PPARgamma activation. Exp Dermatol 19: 813–820. doi: 10.1111/j.1600-0625.2010.01107.x PMID: 20545756

57. Grieco P, Carotenuto A, Auriemma L, Limatola A, Di Maro S, Merlino F, et al. (2013) Novel alpha-MSH peptide analogues with broad spectrum antimicrobial activity. PLoS One 8: e61614. doi: 10.1371/journal.pone.0061614 PMID: 23626703

58. Walter MN, Wright KT, Fuller HR, MacNeil S, Johnson WE (2010) Mesenchymal stem cell-conditioned medium accelerates skin wound healing: an in vitro study of fibroblast and keratinocyte scratch assays. Exp Cell Res 316: 1271–1281. doi: 10.1016/j.yexcr.2010.02.026 PMID: 20206158

59. Hulkower KI, Herber RL (2011) Cell migration and invasion assays as tools for drug discovery. Pharmaceutics 3: 107–124. doi: 10.3390/pharmaceutics3010107 PMID: 24310428

60. Taboubi S, Milanini J, Delamarre E, Parat F, Garrouste F, Pommier G, et al. (2007) G alpha(q/11)-coupled P2Y2 nucleotide receptor inhibits human keratinocyte spreading and migration. FASEB J 21: 4047–4058. PMID: 17609252

61. Arnoux V, Nassour M, L'Helgoualc'h A, Hipskind RA, Savagner P (2008) Erk5 controls Slug expression and keratinocyte activation during wound healing. Mol Biol Cell 19: 4738–4749. doi: 10.1091/mbc.E07-10-1078 PMID: 18716062

62. Stoll SW, Rittie L, Johnson JL, Elder JT (2012) Heparin-binding EGF-like growth factor promotes epithelial-mesenchymal transition in human keratinocytes. J Invest Dermatol 132: 2148–2157. doi: 10.1038/jid.2012.78 PMID: 22592159

63. He YY, Council SE, Feng L, Chignell CF (2008) UVA-induced cell cycle progression is mediated by a disintegrin and metalloprotease/epidermal growth factor receptor/AKT/Cyclin D1 pathways in keratinocytes. Cancer Res 68: 3752–3758. doi: 10.1158/0008-5472.CAN-07-6138 PMID: 18483258

64. Hoq MI, Niyonsaba F, Ushio H, Aung G, Okumura K, Ogawa H (2011) Human catestatin enhances migration and proliferation of normal human epidermal keratinocytes. J Dermatol Sci 64: 108–118. doi: 10.1016/j.jdermsci.2011.08.001 PMID: 21872447

65. Spohn D, Rossler OG, Philipp SE, Raubuch M, Kitajima S, Griesemer D, et al. (2013) Thapsigargin induces expression of activating transcription factor 3 in human keratinocytes involving C2+ ions and c-Jun N-terminal protein kinase. Molecular Pharmacology 78: 865–876.

66. Steinstraesser L, Hirsch T, Schulte M, Kueckelhaus M, Jacobsen F, Mersch EA, et al. (2012) Innate defense regulator peptide 1018 in wound healing and wound infection. PLoS One 7: e39373. doi: 10.1371/journal.pone.0039373 PMID: 22879874

67. Ramos R, Silva JP, Rodrigues AC, Costa R, Guardao L, Schmitt F, et al. (2011) Wound healing activity of the human antimicrobial peptide LL37. Peptides 32: 1469–1476. doi: 10.1016/j.peptides.2011.06.005 PMID: 21693141

68. Carretero M, Escamez MJ, Garcia M, Duarte B, Holguin A, Retamosa L, et al. (2008) In vitro and in vivo wound healing-promoting activities of human cathelicidin LL-37. J Invest Dermatol 128: 223–236. PMID: 17805349

69. Yin J, Yu FS (2010) LL-37 via EGFR transactivation to promote high glucose-attenuated epithelial wound healing in organ-cultured corneas. Invest Ophthalmol Vis Sci 51: 1891–1897. doi: 10.1167/iovs.09-3904 PMID: 19797203

70. Watt FM, Jordan PW, O'Neill CH (1988) Cell shape controls terminal differentiation of human epidermal keratinocytes. Proc Natl Acad Sci U S A 85: 5576–5580. PMID: 2456572

71. Schafer C, Born S, Mohl C, Houben S, Kirchgessner N, Merkel R, et al. (2010) The key feature for early migratory processes: Dependence of adhesion, actin bundles, force generation and transmission on filopodia. Cell Adh Migr 4: 215–225. PMID: 20179423

72. Mattila PK, Lappalainen P (2008) Filopodia: molecular architecture and cellular functions. Nat Rev Mol Cell Biol 9: 446–454. doi: 10.1038/nrm2406 PMID: 18464790

73. Tjabringa GS, Aarbiou J, Ninaber DK, Drijfhout JW, Sorensen OE, Borregaard N, et al. (2003) The antimicrobial peptide LL-37 activates innate immunity at the airway epithelial surface by transactivation of the epidermal growth factor receptor. J Immunol 171: 6690–6696. PMID: 14662872

74. Wen Z, Zhong Z, Darnell JE Jr (1995) Maximal activation of transcription by Stat1 and Stat3 requires both tyrosine and serine phosphorylation. Cell 82: 241–250. PMID: 7543024

75. Liu H, Mu L, Tang J, Shen C, Gao C, Rong M, et al. (2014) A potential wound healing-promoting peptide from frog skin. Int J Biochem Cell Biol 49: 32–41. doi: 10.1016/j.biocel.2014.01.010 PMID: 24441016

76. Wang G (2010) Antimicrobial Peptides, Discovery, Design and Novel Therapeutic Strategies. Advances in Molecular and Cellular Microbiology CABI Oxfordshire, OX10 8DE: 134.

77. Osherov N, Levitzki A (1994) Epidermal-growth-factor-dependent activation of the src-family kinases. Eur J Biochem 225: 1047–1053. PMID: 7525285

78. Levitzki A, Gazit A (1995) Tyrosine kinase inhibition: an approach to drug development. Science 267: 1782–1788. PMID: 7892601

79. Bowers G, Reardon D, Hewitt T, Dent P, Mikkelsen RB, Valerie K, et al. (2001) The relative role of ErbB1-4 receptor tyrosine kinases in radiation signal transduction responses of human carcinoma cells. Oncogene 20: 1388–1397. PMID: 11313882

80. Marques MM, Martinez N, Rodriguez-Garcia I, Alonso A (1999) EGFR family-mediated signal trans-duction in the human keratinocyte cell line HaCaT. Exp Cell Res 252: 432–438. PMID: 10527633

81. De Potter IY, Poumay Y, Squillace KA, Pittelkow MR (2001) Human EGF receptor (HER) family and heregulin members are differentially expressed in epidermal keratinocytes and modulate differentia-tion. Exp Cell Res 271: 315–328. PMID: 11716544

82. Sano S, Itami S, Takeda K, Tarutani M, Yamaguchi Y, Miura H, et al. (1999) Keratinocyte-specific ab-lation of Stat3 exhibits impaired skin remodeling, but does not affect skin morphogenesis. EMBO J 18: 4657–4668. PMID: 10469645

83. Andl CD, Mizushima T, Oyama K, Bowser M, Nakagawa H, Rustgi AK (2004) EGFR-induced cell mi-gration is mediated predominantly by the JAK-STAT pathway in primary esophageal keratinocytes. Am J Physiol Gastrointest Liver Physiol 287: G1227–1237. PMID: 15284024

84. Conlon JM, Mechkarska M, Lukic ML, Flatt PR (2014) Potential therapeutic applications of multifunc-tional host-defense peptides from frog skin as anti-cancer, anti-viral, immunomodulatory, and anti-dia-betic agents. Peptides 57: 67–77. doi: 10.1016/j.peptides.2014.04.019 PMID: 24793775

85. Bals R, Wang X, Zasloff M, Wilson JM (1998) The peptide antibiotic LL-37/hCAP-18 is expressed in epithelia of the human lung where it has broad antimicrobial activity at the airway surface. Proc Natl Acad Sci U S A 95: 9541–9546. PMID: 9689116

86. Turner J, Cho Y, Dinh NN, Waring AJ, Lehrer RI (1998) Activities of LL-37, a cathelin-associated anti-microbial peptide of human neutrophils. Antimicrob Agents Chemother 42: 2206–2214. PMID: 9736536

87. Bals R, Goldman MJ, Wilson JM (1998) Mouse beta-defensin 1 is a salt-sensitive antimicrobial pep-tide present in epithelia of the lung and urogenital tract. Infect Immun 66: 1225–1232. PMID: 9488417

88. Bals R, Wang X, Wu Z, Freeman T, Bafna V, Zasloff M, et al. (1998) Human beta-defensin 2 is a salt-sensitive peptide antibiotic expressed in human lung. J Clin Invest 102: 874–880. PMID: 9727055

89. Garcia JR, Krause A, Schulz S, Rodriguez-Jimenez FJ, Kluver E, Adermann K, et al. (2001) Human beta-defensin 4: a novel inducible peptide with a specific salt-sensitive spectrum of antimicrobial activ-ity. FASEB J 15: 1819–1821. PMID: 11481241

90. Jenssen H, Hamill P, Hancock RE (2006) Peptide antimicrobial agents. Clin Microbiol Rev 19: 491–511. PMID: 16847082

91. Huang LC, Jean D, Proske RJ, Reins RY, McDermott AM (2007) Ocular surface expression and in vitro activity of antimicrobial peptides. Curr Eye Res 32: 595–609. PMID: 17852183

92. Goldman MJ, Anderson GM, Stolzenberg ED, Kari UP, Zasloff M, Wilson JM (1997) Human beta-defensin-1 is a salt-sensitive antibiotic in lung that is inactivated in cystic fibrosis. Cell 88: 553–560. PMID: 9038346

93. Scott MG, Davidson DJ, Gold MR, Bowdish D, Hancock RE (2002) The human antimicrobial peptide LL-37 is a multifunctional modulator of innate immune responses. J Immunol 169: 3883–3891. PMID: 12244186

94. McDermott AM, Rich D, Cullor J, Mannis MJ, Smith W, Reid T, et al. (2006) The in vitro activity of se-lected defensins against an isolate of Pseudomonas in the presence of human tears. Br J Ophthalmol 90: 609–611. PMID: 16622092

95. Ramsey JP, Reinert LK, Harper LK, Woodhams DC, Rollins-Smith LA (2010) Immune defenses against Batrachochytrium dendrobatidis, a fungus linked to global amphibian declines, in the South African clawed frog, Xenopus laevis. Infect Immun 78: 3981–3992. doi: 10.1128/IAI.00402-10 PMID: 20584973

96. Rollins-Smith LA, Reinert LK, O'Leary CJ, Houston LE, Woodhams DC (2005) Antimicrobial Peptide defenses in amphibian skin. Integr Comp Biol 45: 137–142. doi: 10.1093/icb/45.1.137 PMID: 21676754

97. Groner ML, Rollins-Smith LA, Reinert LK, Hempel J, Bier ME, Relyea RA (2014) Interactive effects of competition and predator cues on immune responses of leopard frogs at metamorphosis. J Exp Biol 217: 351–358. doi: 10.1242/jeb.091611 PMID: 24115058

98. Steinstraesser L, Kraneburg UM, Hirsch T, Kesting M, Steinau HU, Jacobsen F, et al. (2009) Host de-fense peptides as effector molecules of the innate immune response: a sledgehammer for drug resis-tance? Int J Mol Sci 10: 3951–3970. doi: 10.3390/ijms10093951 PMID: 19865528

99. Demidova-Rice TN, Hamblin MR, Herman IM (2012) Acute and impaired wound healing: pathophysi-ology and current methods for drug delivery, part 1: normal and chronic wounds: biology, causes, and

approaches to care. Adv Skin Wound Care 25: 304–314. doi: 10.1097/01.ASW.0000416006.55218. d0 PMID: 22713781

100. Percival SL, Hill KE, Williams DW, Hooper SJ, Thomas DW, Costerton JW (2012) A review of the scientific evidence for biofilms in wounds. Wound Repair Regen 20: 647–657. doi: 10.1111/j.1524-475X.2012.00836.x PMID: 22985037